

QC
880
.A46
1974

ATDL-75/17

Environmental Research Laboratories

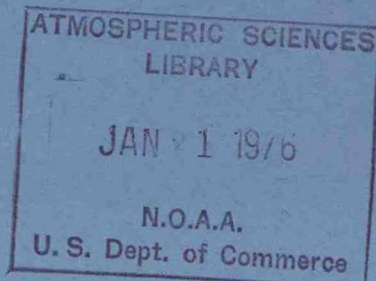
Air Resources

Atmospheric Turbulence and Diffusion Laboratory

Oak Ridge, Tennessee

September 1975

1974 ANNUAL REPORT



U. S. DEPARTMENT OF COMMERCE
NATIONAL OCEANIC AND ATMOSPHERIC ADMINISTRATION

76 0047



NOTICE

This report was prepared as an account of work sponsored by the United States Government. Neither the United States nor the United States Energy Research and Development Administration, nor any of their employees, nor any of their contractors, subcontractors, or their employees, makes any warranty, express or implied, or assumes any legal liability or responsibility for the accuracy, completeness or usefulness of any information, apparatus, product or process disclosed, or represents that its use would not infringe privately owned rights.

This report has been reproduced directly from the best available copy.

Available from the National Technical Information Service, U. S. Department of Commerce, Springfield, Virginia 22161

Price: Paper Copy \$7.60
Microfiche \$2.25 (domestic)
\$3.75 (foreign)

QC

880

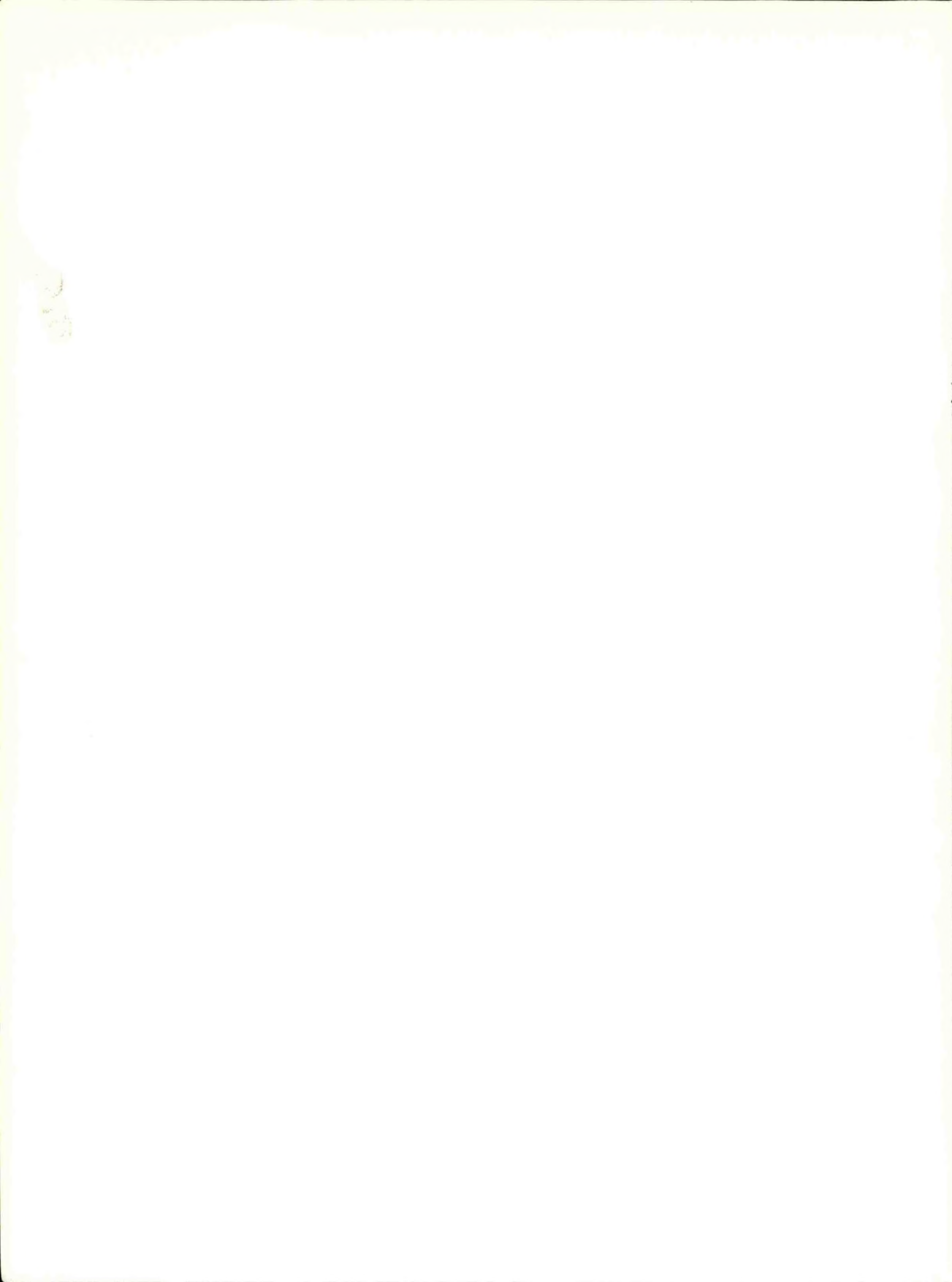
. A46

1974

Foreword

The following is a compilation of research contributions from the National Oceanic and Atmospheric Administration Air Resources Atmospheric Turbulence and Diffusion Laboratory for the calendar year 1974. It was prepared by the Technical Information Center, U. S. Energy Research and Development Administration, Oak Ridge, Tennessee. Subsequent volumes will be issued on an annual basis. The research reported in this document was performed under an agreement between the U. S. Energy Research and Development Administration and the National Oceanic and Atmospheric Administration.

F. A. Gifford
Director
Atmospheric Turbulence
and Diffusion Laboratory



CONTENTS

SUMMARY OF ACTIVITIES AND PLANS - FISCAL YEARS 1975 AND 1976 - Rayford P. Hosker, Jr., and Ruth A. Green	1
METEOROLOGICAL EFFECTS OF THE COOLING TOWERS AT THE OAK RIDGE GASEOUS DIFFUSION PLANT. II. PREDICTIONS OF FOG OCCURRENCE AND DRIFT DEPOSITION - Steven R. Hanna	15
METEOROLOGICAL EFFECTS OF THE MECHANICAL-DRAFT COOLING TOWERS OF THE OAK RIDGE GASEOUS DIFFUSION PLANT - Steven R. Hanna ...	55
RELATING EMISSIONS TO AIR QUALITY IN TENNESSEE - Steven R. Hanna	71
PLUME RISE FROM MULTIPLE SOURCES - Gary A. Briggs	91
MODELLING URBAN AIR POLLUTION - F. A. Gifford and S. R. Hanna ..	111
FURTHER COMPARISON OF URBAN AIR POLLUTION MODELS - F. A. Gifford	117
FOG AND DRIFT DEPOSITION FROM EVAPORATIVE COOLING TOWERS - Steven R. Hanna	127
DIURNAL VARIATION OF VERTICAL THERMAL STRUCTURE IN A PINE PLANTATION - R. P. Hosker, Jr., C. J. Nappo, Jr., and S. R. Hanna	135
CONFERENCE SUMMARY - COOLING TOWER ENVIRONMENT - 1974 - Steven R. Hanna	143
SENSITIVITY OF THE GAUSSIAN PLUME MODEL - F. A. Gifford	145
IAEA-WMO SYMPOSIUM ON THE PHYSICAL BEHAVIOR OF RADIOACTIVE CONTAMINANTS IN THE ATMOSPHERE - R. P. Hosker, Jr.	147
A COMPARISON OF ESTIMATION PROCEDURES FOR OVER-WATER PLUME DISPERSION - R. P. Hosker, Jr.	153
A METHOD FOR EVALUATING THE ACCURACY OF AIR POLLUTION PREDICTION MODELS - Carmen J. Nappo, Jr.	163

RESEARCH NEEDS RELATED TO HYDROMETEOROLOGIC ASPECTS OF FUTURE ENERGY PRODUCTION - Steven R. Hanna	169
A COMPARISON OF THE TRAJECTORIES OF RISING BUOYANT PLUMES WITH THEORETICAL EMPIRICAL MODELS - Gary A. Briggs	181
DESCRIPTION OF THE EASTERN TENNESSEE TRAJECTORY EXPERIMENT (ETTEX) - S. R. Hanna, C. J. Nappo, R. P. Hosker, and G. A. Briggs	185
AVERAGE AEROSOL SCALE HEIGHTS OVER OAK RIDGE, TENNESSEE - Walter M. Culkowski and Searle D. Swisher	213
RESPONSE OF LINTRONIC DOME SOLARIMETERS TO VARYING SOLAR RADIATION FLUX DENSITIES - D. R. Matt and B. A. Hutchison ...	227

Summary of
Activities and Plans
FY 1975 - 1976

Air Resources
Atmospheric Turbulence and Diffusion Laboratory
National Oceanic and Atmospheric Administration
Oak Ridge, Tennessee
September 1975

Rayford P. Hosker, Jr.
and
Ruth A. Green

I. Preface.

A. Scope.

The Atmospheric Turbulence and Diffusion Laboratory (ATDL) in Oak Ridge, Tennessee, is operated for the Energy Research and Development Administration (ERDA) by the National Oceanic and Atmospheric Administration's Air Resources Laboratories, a group of research units generally concerned with problems of environmental pollution and its control. Major funding is from ERDA's Division of Biomedical and Environmental Research. ATDL works closely with various divisions of Holifield (Oak Ridge) National Laboratory (HNL) on environmental projects of joint interest, and also functions as a meteorological consultant and advisor to that laboratory.

The ATDL is organized to perform research studies on atmospheric diffusion, transport, and removal of pollutants, including heat, and moisture with most emphasis on scales up to regional size (up to \sim 200 km). Current research programs include air transport studies, especially for the eastern Tennessee region; air pollution studies, including the meteorological effects of cooling towers and energy centers; research on plume and wake behavior, including effects of buoyancy, active thermal convection, and removal processes; extension of atmospheric transport, diffusion, and effluent removal models to special situations such as over-water and over-forest flows; and study of the role of forest structure on the energy balance and on diffusion.

B. FY1975 Highlights.

A major program completed during FY1975 was the Eastern Tennessee Trajectory Experiment (ETTEX), which was conducted to determine the mesoscale wind field and typical air parcel trajectories over the eastern Tennessee Valley. Other research on atmospheric transport included modifications to the Holifield (Oak Ridge) National Laboratory--ATDL air transport model and major improvements in the ATDL mesoscale planetary boundary layer model.

Research on atmospheric pollution included estimates of the meteorological effects of large power parks, development of a simple photochemical smog model, and comparative evaluations of several urban air pollution models.

Work on plume behavior encompassed theoretical study of dense plumes, calculation of over-water effluent concentrations intercomparison of several dry deposition models, and experiments on the lift-off of a buoyant plume initially trapped in the wake of an obstacle.

Forest meteorological studies were devoted to analysis of solar radiation data obtained within a deciduous forest, analysis of wind and temperature data taken within a pine plantation, and limited smoke diffusion experiments. Instrumentation of a new forest site was begun.

C. FY1976 Highlights.

Atmospheric transport research will make considerable use of ETTEX data for model validation. Regional wind fields will be used to calculate air parcel trajectories, and prediction of the behavior of diffusing effluent clouds will be attempted. Both the HNL-ATDL air transport model and the ATDL mesoscale planetary boundary layer model will also be used for trajectory predictions. A potential flow model for the eastern Tennessee Valley will be developed as a first approximation to flow over rough terrain.

Reviews of current diffusion, plume rise, and urban air pollution models have been completed. Models to predict the rise of multiple plumes, cloud growth, and mixing layer height will be developed. The photochemical smog model will be tested for several U.S. cities. A drone airplane is being constructed to carry out measurements within the mixing layer.

Analysis of the convective diffusion results from ETTEX and of the entrained buoyant plume experiments will be completed. Further intercomparisons of dry deposition models with each other and with field data are underway. Diffusion and deposition calculations using Monte Carlo techniques and based on the statistical theory of turbulence are being initiated. A wind tunnel for near-obstacle flow investigations will be procured. Modeling tank studies of plume rise and spread under calm conditions will begin.

Instrumentation of the new deciduous forest site will be completed. A cooperative program with HNL on sulfur transport to this site is planned. Analysis of the extensive body of forest solar radiation data will continue. Diffusion research is continuing at the pine plantation; additional smoke studies as well as preliminary heat and momentum flux measurements are planned.

II. FY1975 Accomplishments - ATDL.

A. Air Transport Studies.

The Eastern Tennessee Trajectory Experiment (ETTEX), an ATDL experiment, conducted with ARL and TVA assistance, was carried out during a three-week period in July and August. Trajectories of radar-tracked tetroons were determined for several launch times (before dawn, mid-day, early evening) and flight durations of up to 6 hours, for a variety of weather conditions. On 16 occasions, two tetroons were released simultaneously, and about 50 useful tetroon runs were made. A grid of five single-theodolite pilot balloon stations measured vertical wind profiles and surface weather variables over the eastern Tennessee area. Attempts are under way to estimate the regional wind field using these pibal data, together with synoptic information and data obtained from TVA's meteorological sites. Air parcel trajectories calculated from these wind fields will be compared to the tetroon observations. A convective diffusion experiment was also carried out to provide data for a model previously developed to predict the behavior of buoyant plumes imbedded in convective downdrafts. An airplane equipped with an MRI "ε-meter," a fast-response temperature probe, and a vertical accelerometer was flown in patterns near TVA's Bull Run steam plant, while a helicopter sampled SO₂ cross-sections through the plume. Ground sampling of SO₂ was attempted. The object was to simultaneously measure wind, temperature, and eddy diffusivity profiles, vertical velocities on a convective scale, and plume response to these motions. A report describing ETTEX design has been completed, and detailed reports on individual experiments and their results are in preparation.

HNL and ATDL entered into a joint effort to improve the HNL "Air Transport Model." The "Air Transport Model" is part of an overall program to follow the pathways and assess the environmental insult of trace contaminants in the atmosphere. After substantial revision, the model was tested against observed TVA data and produced correlations as high as $r = .90$. An addition to the model now causes it to search for the highest possible one-hour concentration from a matrix of wind sources and wind and stability conditions.

The ATDL mesoscale planetary boundary layer model has been expanded to increase its generality. Incoming solar radiation and atmospheric longwave radiation at the surface are calculated at each time step; also, atmospheric cooling is now calculated. Advection sub-routines are being developed which use the mesoscale model's results to create trajectories of air parcels. Graphic packages have been added to give immediate visual results of the model's forecasts and computed trajectories. A program has been started with HNL's Environmental Sciences Division to incorporate their surface evapotranspiration and sensible heat flux hydrologic models into the ATDL mesoscale model. This will eliminate the constant flux layer assumption from the ATDL model, as well as further extend its generality to include many different surface configurations.

B. Atmospheric Pollution.

Estimates of the meteorological effects of power parks were made. The heat release of proposed power parks is about 100,000 Mw, which is nearly equal to the heat release from the Surtsey volcano, brushfires and a few other natural and manmade phenomena. A major danger of the proposed heat release is the possibility of the concentration of vorticity. Also, there is the possibility of increased rainfall and thunderstorm development. There is little known about the modeling of multiple plumes or clouds.

Observations of smog concentrations in California along a trajectory from Los Angeles to Palm Springs reveal that an oxidant front moves with the sea breeze, passing through Palm Springs in the late evening. In the downtown Los Angeles area, where emissions are high, the oxidant curve peaks near noon. In Pomona and Riverside, where emissions are relatively low but still significant, the oxidant curve peaks near 3 p.m. The delayed peak is due to advection from the downtown area. In Banning and Palm Springs, emissions are insignificant, and oxidant variations are almost entirely due to advection from more populated areas. A simple empirical model was able to explain the observed diurnal variations of oxidant concentrations. More complex numerical models were attempted, but in every case led to too much removal of oxidants at night in Palm Springs.

A method for the comprehensive evaluation of air pollution forecast models has been developed and applied to several urban air pollution models. An immediate result of this study is that models previously considered equal in their ability to predict time-averaged air pollution concentrations are not equal in their ability to predict the spatial and temporal character of observed air pollution patterns.

The vertical aerosol lidar program was completed. It showed a very high correlation (.96) between average monthly aerosol scale heights and monthly solar radiation, indicating that solar radiation data is an excellent indicator of vertical diffusivity in the Oak Ridge area.

Estimates of horizontal dispersion parameters were obtained from the ERDA's Tower Shielding Facility in Oak Ridge for time scales of sixteen to five hundred seventy-six hours. At these time scales horizontal dispersion was found to follow a $t^{.21}$ approximation.

C. Plume Behavior.

Theoretical work was initiated on the behavior of dense gases released near the ground, including the effects of ground friction, ambient turbulence, and ambient stability. Dense plumes, hardly ever studied previously, are of considerable practical importance, for example in connection with the transportation of liquid natural gas, and in certain industrial and radiation accident situations.

Experiments on a small scale on the lift-off of a wake-entrained buoyant plume released at ground level were carried out in the field. Buoyant lift-off occurs following plume downwash, for instance in mechanical draft cooling towers, and also governs certain nuclear reactor accident hazards.

A Gaussian plume model was used for calculations of concentrations over the open sea, using a number of formulations for the required dispersion coefficients. Data taken off the California coast and off Long Island were used for validation. The best prediction of horizontal dispersion was obtained with a theoretical expression due to G. I. Taylor, which utilized observed wind speed and standard deviation of direction as input parameters. Prediction of vertical dispersion was not as satisfactory. A combination of Taylor's expression in the horizontal, and the usual Pasquill-Gifford curves in the vertical, using observed wind variables, provided concentration estimates to within about 15%, in the mean, with a factor of 4 or so accuracy for individual cases. More data, especially on direct observations of the vertical dispersion parameter, would be helpful in refining the technique.

A new dry deposition model suggested by Horst of Battelle's Pacific Northwest Laboratories was investigated and is being programmed for application to comparisons of the relative efficiencies of forests and grassland as scavengers of effluent material. A second model, somewhat similar to Csanady's partial reflection model, is also being developed for the same cases. Both of these models have the advantage of being applicable in stable conditions where the usual Chamberlain model becomes unrealistic. All three models will be compared for daytime conditions; the Horst and partial reflection models will also be compared at night. A serious obstacle to choosing one of these models as "best" is the apparent lack of detailed experimental data for validation purposes; research directed at filling this void is badly needed.

Work continued on the chapters on meteorological effects of energy production, plume rise, and flow and diffusion near obstacles, for the book Meteorology and Power Production.

D. Forest Meteorology.

Analysis of the deciduous forest solar radiation data continued and a major report summarizing the results of this research was completed. Another paper describing a technique for photographic assessment of deciduous forest radiation regimes was also completed. Retrieval of forest energy balance data continued throughout this year and all faulty tapes have now been corrected or discarded as nonretrievable. Installation of equipment at the new Walker Branch Watershed Meteorology site was begun.

Instrumentation on the pine plantation's forest tower has been fully refurbished. Permanent instrumentation for wind speed profile, wind direction, and temperature difference has been installed on the nearby field tower. Data obtained over this open field will be used to categorize the "open country" conditions prevailing during experiments with the forest. A back-log of wind and temperature data from the forest tower is being analyzed. A paper describing some of these results and their significance with regard to diffusion was published. Simultaneous sequential releases of up to 100 smoke puffs were conducted at various times of the day and night within the forest and in the open field. Standard deviations of wind direction in the forest were found to be between 1.0 and 2.5 times the corresponding values in the open field, depending on atmospheric stability. Additional experiments are planned to verify the apparent trends in these data.

II. FY1976 - ATDL.

A. Air Transport Studies.

Air parcel trajectories calculated from the estimated regional wind fields based on ETTEX data are being compared with observed tetraoon behavior. Prediction of mesoscale trajectories of pollutant clouds subject to diffusion will begin. Sensitivity of the results to various diffusion parameters and to the nature of the underlying terrain will be examined.

The HNL-ATDL Air Transport Model is being expanded to include trajectory analysis and chemical changes in vivo. Studies of long-term energy spectra will continue, with insertion into the Air Model as the goal.

The ATDL mesoscale PBL model using the simplifying assumption of zero momentum advection in the planetary boundary layer will be compared with the same model but with momentum advection included. Simulations of pollution transport and diffusion from real and hypothetical sources in the East Tennessee region will be performed.

A potential flow approximation to the regional wind field is being developed and will be compared to the ETTEX results for certain conditions.

B. Atmospheric Pollution.

Reviews of mathematical models of diffusion, models of plume rise and urban diffusion models have been prepared for the American Meteorological Society Workshop on Meteorological and Environmental Assessment, to be held in Boston, September 29-October 3, 1975.

A model for multiple plume rise and cloud growth will be developed, for use in the study of the meteorological effects of power parks.

The ATDL simple photochemical dispersion model is being applied to data from other cities, such as Tampa--St. Petersburg, Florida, and St. Louis, Missouri.

A model to predict the mixing layer height will be developed based on current theories. Results will be compared with measurements made with the TVA acoustic sounder.

A large radio-controlled model airplane is being constructed to carry pressure, temperature, humidity, and acceleration sensors to altitudes up to 2 km; data will be telemetered to the ground for recording. The airplane will be used to determine diurnal variations of vertical temperature and humidity profiles and of mixing layer height, and to investigate horizontal changes in temperature and humidity over terrain discontinuities such as forest edges.

C. Plume and Wake Behavior.

Analysis of the convective diffusion and the entrained buoyant plume lift-off experiments will be completed. Some of the material will be included in the revision of Plume Rise and in the plume rise chapter of Meteorology and Power Production, both of which will be completed. Small-scale field experiments on the lift-off of a buoyant plume initially trapped in the wake of an obstacle will conclude. Similar experiments may be conducted in a wind tunnel to further validate the data.

A dry deposition model developed at Lawrence Livermore Laboratory using the ADPIC technique was compared to the usual Chamberlain-Gaussian model. Rather limited field data indicated that the Gaussian model performed as well as or better than the ADPIC model. Further comparisons with the Horst surface depletion model and with the partial reflection model are planned. A literature search for more data will be completed and used to judge the various models.

Diffusion calculations based on the statistical theory of turbulence are being initiated, following the model suggested by Barr and Watson of Los Alamos Scientific Laboratory. Observed turbulent energy spectra are required for this model, and the calculations use Monte Carlo techniques to obtain the solution. Collaboration with personnel of HNL's Neutron Physics Division, who are skilled in these methods, is anticipated. One advantage of this type of calculation is the physically realistic picture of dry deposition that becomes possible; the probability of removal of a particular surface type can be incorporated into the model via an "accommodation coefficient" like that used in rarefied gas dynamics. Trial computations using this deposition model will begin.

A wind tunnel facility suitable for both routine calibrations of anemometers as well as for investigations of flow near obstacles immersed in a turbulent shear layer will be purchased, installed, tested, and calibrated. Devices to produce a suitable boundary layer flow within the test section will be fabricated and tested. Initial flow visualization studies will begin, using simple building shapes. The chapter on flow near obstacles for Meteorology and Power Production will be completed.

Modeling tank studies, postponed in FY 1975 due to the convective diffusion field experiment, will be carried out to study the effects of various stratifications on the rise and spread of plumes in a quiescent atmosphere.

D. Forest Meteorology.

Installation of equipment at the new Walker Branch Watershed deciduous forest study site will be completed and further studies of deciduous forest energy balances initiated. Assistance is being provided to HNL personnel studying sulfur transport from power plants to this site. Smoke releases to elucidate the flow over this locally complex terrain will be attempted before installing a network of meteorological towers. analysis of forest solar radiation data is continuing and reduction of retrieved energy balance data will begin.

Diffusion research is continuing at the pine plantation. Initial measurements of momentum and heat flux over the forest, possibly in collaboration with Argonne National Laboratory personnel, will be done for several weather conditions and time periods. Results will be compared to those at other sites, including Walker Branch. Additional smoke releases have been carried out in the forest and in the adjacent field; the data are being analyzed.

III. Laboratory Staff.

During FY 1975 the staff of the ATDL numbered 23, 10 of whom were full-time professional scientists, six were full-time technician and administrative personnel, and 7 were part-time workers, mostly students. One professional scientist and one administrative employee will be added in FY 1976. The staff is frequently augmented by visiting scientists from abroad. Several have come via International Atomic Energy Agency-National Research Council Fellowships, to work on problems of nuclear meteorology. Others have been assigned here to work on basic problems of atmospheric diffusion through various programs such as Oak Ridge Associated Universities (ORAU) faculty research fellowships. Also much use of university students at various levels is made, including part-time undergraduate workers, summer fellowship students, "Co-op" students, and part-time graduate students. University students in these various capacities supplied approximately 3 person-years in FY 1975, a substantial fraction (~ 16%) of the ATDL total.

When the ATDL wind tunnel installation is completed, employment of an additional two to three graduate students to collect, reduce, and analyze data is planned; the test programs should be suitable for master's theses in several departments at the University of Tennessee.

IV. Publications in FY1975.

Hosker, R. P., C. J. Nappo, Jr., and S. R. Hanna: "Diurnal Variation of Vertical Thermal Structure in a Pine Plantation." Agricultural Met., 13 (1974), p 259-265.

Hanna, S. R.: "Cooling Tower Environment - 1974." Bulletin of AMS, Vol. 55, No. 6, June 1974, pp 597-598.

Gifford, F. A.: "Sensitivity of the Gaussian Plume Model". Atmos. Environment, Vol. 8, No. 8, August, 1974, pp 870-871.

Hosker, R. P.: "Review of IAEA-WMO Symposium on the Physical Behavior of Radioactive Contaminants in the Atmosphere". Nuclear Safety, Vol. 15-3, May-June, 1974, pp 306-310.

Hosker, R. P.: A Comparison of Estimation Procedures for Over-Water Plume Dispersion. Proceedings of Symp. on Atmos. Dif. and Air Poll., Santa Barbara, California, September 9-13, 1974.

Nappo, C. J.: A Method for Evaluating the Accuracy of Air Pollution Prediction Models. Proceedings of Symp. on Atmos. Dif. and Air Poll., Santa Barbara, California, September 9-13, 1974.

Hanna, S. R.: Research Needs Related to Hydrometeorologic Aspects of Future Energy Production. Workshop on "Research Needs Related to Water for Energy," Indianapolis, Ind., October 20-22, 1974.

Briggs, G. A.: Discussion of D. J. Moore's "A Comparison of the Trajectories of Rising Buoyant Plumes with Theoretical Empirical Models." Atmos. Environment, Vol. 9, pp 455-462, 1975.

Hanna, S. R., C. J. Nappo, Jr., R. P. Hosker, and G. A. Briggs: Description of the Eastern Tennessee Trajectory Experiment (ETTEX). A.M.S. Conference on Regional and Mesoscale Modeling Analysis, and Prediction, Las Vegas, May, 1975.

Culkowski, W. M. and S. D. Swisher: Average Aerosol Scale Heights Over Oak Ridge, Tennessee. Read at 1974 International Laser Radar Conference 6th Conf. on Laser Atmos. Studies.

Hutchison, B.: Ph.D. Dissertation: Photographic Assessment of Deciduous Forest Radiation Regimes. ATDL Cont. #75/3.

Briggs, G. A.: Research Required for Predicting the Behavior of Pressurized Gases Escaping into the Atmosphere. February, 1975, ATDL Cont. # 75/5

Nappo, C. J., Jr.: Time Dependent Mesoscale Wind Fields Over Complex Terrain. Presented at First Conference on Regional and Mesoscale Modeling, Analysis, and Prediction of AMS, Las Vegas, Nevada, May 6-9, 1975.

Hanna, S. R.: Relative Diffusion of Tetroon Pairs During Convective Conditions. Presented at The First Conference on Regional and Mesoscale Modeling, Analysis and Prediction of the AMS, Las Vegas, Nevada, May 6-9, 1975.

Culkowski, W. M.: Validation of a Multisource Dispersion Model for Atmospheric Sulfur Concentrations. Presented at 1974 Fall Meeting of the American Geophysical Union, San Francisco, December 12-17, 1974.

V. Publications in FY1976.

Hanna, S. R. and F. A. Gifford: "Meteorological Effects of Energy Dissipation". To be published in Bulletin of AMS, Vol. 56, No. 10, 1975.

Gifford, F. A.: "A Review of Turbulent Diffusion Typing Schemes." To be published in Nuclear Safety.

Hanna, S. R.: "Modeling Smog Along the Los Angeles-Palm Springs Trajectory." To be published in Advances in Envir. Sci. and Tech.

Gifford, F. A.: Atmospheric Dispersion Models for Environmental Pollution Applications. Presented at AMS Workshop on Meteorology and Environmental Assessment, Boston, Mass., September 29-October 3, 1975.

Hanna, S. R.: Urban Diffusion Problems. Presented at AMS Workshop on Meteorology and Environmental Assessment, Boston, Mass., September 29-October 3, 1975.

Gifford, F. A. and S. R. Hanna: "Part III. Dispersion of Sulfur Dioxide Emissions from Area Sources." To be published in Power Generation Monitoring and Control.

Culkowski, W. M.: Standard Deviation of Wind Direction as a Function of Time; Three Hours to Five Hundred Seventy-Six Hours. ATDL Cont. #75/11, July, 1975.

Hosker, R. P.: Comparison of Two Plume Depletion Estimation Techniques: The ADPIC Method vs. The Gaussian Model. ATDL Cont. #75/12, August, 1975.

Hutchison, B. and D. Matt: "Beam Enrichment of Diffuse Radiation in a Deciduous Forest." To be published in Ag. Met.

Briggs, G. A.: Plume Rise Predictions. To be presented at AMS Workshop on Meteorology and Environmental Assessment, Boston, Mass., September 29-October 3, 1975.

Meteorological Effects of the Cooling Towers
at the Oak Ridge Gaseous Diffusion Plant

II. Predictions of Fog Occurrence and Drift Deposition

By

Steven R. Hanna
Air Resources
Atmospheric Turbulence & Diffusion Laboratory
P. O. Box E
Oak Ridge, Tennessee 37830

Abstract

The frequency of occurrence of fogs and the rate of deposition of chromate due to emissions from the cooling towers at the Oak Ridge Gaseous Diffusion Plant are calculated. Observations of drift deposition agree fairly well with calculated values. A detailed summary of significant findings is given at the end of the report.

1. Introduction

In part I of this report, source parameters of the cooling towers at the Oak Ridge Gaseous Diffusion Plant were described and plume photographs and hygrothermograph records were analyzed. Models of visible plume length were tested with observations. In part II, modelling of fog occurrence and drift deposition is described. The methods used are reviewed and outlined by Hanna (1974). To determine fog occurrence, the Gaussian plume dispersion model is used. To determine drift deposition, the trajectory of drops is calculated, accounting for drop evaporation. The drift deposition model is tested with observed data from April and June 1973 deposition experiments.

2. Fog due to Emissions from Cooling Towers at ORGDP

The water that is emitted from the cooling towers can condense to form fog or clouds. It can intensify an existing fog or clouds. Because latent heat is released in the condensation process, it is not strictly correct to treat the dispersion of water in the same manner as the dispersion of an inert substance such as suspended particles. However, since there is no accepted way to treat the dispersion of a substance which changes phase, the calculations in this report assume that water vapor is dispersed in the same way as an inert substance. The ground level fog concentrations calculated by this method are therefore likely to be too high, since the release of latent heat will cause the plume to rise.

In this section the climatological humidity variations are given and the frequency of occurrence of fog at distances out to 50 km from the towers is calculated.

2.1 Climatology of Moisture in the ORGDP Area.

Weather records at Knoxville have been taken since the late 1800's and are summarized in the Climatic Atlas of the U. S. (Environmental Data Service, 1968). The distribution of relative humidities by season and time of day is given in Figure 1. It is seen that the month with the most humid afternoons is January and the month with the most humid pre-dawn periods is July. However, since the saturation

vapor content or mixing ratio , m , is a strong function of temperature, as shown in Table 1, saturation due to the cooling tower moisture is most likely at cold temperatures.

Table 1
Variation of saturation mixing ratio m (gm water/kg air) with temperature.

T($^{\circ}$ C)	-10	-5	0	5	10	15	20	25	30	35	40
m (gm/kg)	1.84	2.71	3.94	5.64	7.97	11.1	15.4	21.0	28.5	38.3	104.

As stated in the report ORO-99 (Holland, 1953) the average frequency of hours with rain in the Knoxville Area is 10%. From the Airway Meteorological Atlas (U. S. Weather Bureau, 1941), it is seen that the average frequency of hours with dense fog (visibility $< 1/4$ mile) is .7% and with light fog (visibility < 6 miles) is 14%. However, the usual definition of fog (Neuberger, 1957) specifies a visibility less than 1 km. It is not possible to estimate this frequency from the available data.

The joint probability distribution of hourly wind speed, $u(m/s)$, and saturation deficit, Δm (mass water vapor/mass air), given in Table 2, was calculated using 5 years of data from the X-10 meteorological station in Oak Ridge. Saturation deficit, Δm , is defined as the difference between the saturation mixing ratio and the actual mixing ratio.

Table 2
Joint Probability Distribution of Hourly Wind Speed and Saturation Deficit, X-10 Station.

Saturation deficit class (g/kg)	$\Delta m < .5 \frac{g}{kg}$.5 - 1	.5 - 2	2 - 4	4 +	Σ
Wind Speed Class m/s	Effective saturation deficit (g/kg)	0	.75	1.5	3	6
Calm	.5 m/s	.0721	.0347	.0459	.0440	.0435
.5-2 m/s	1.5	.103	.0462	.0660	.0692	.121
2-4.5 m/s	3.0	.0239	.0202	.0362	.0423	.112
4.5-7 m/s	6.0	.00450	.00713	.0136	.0161	.0434
7-10 m/s	8.0	.00147	.00200	.00438	.00416	.0132
10+ m/s	10.0	.000343	.000648	.00149	.00170	.00503
						.00920
	Σ	.206	.111	.167	.177	.339
						1

This distribution is probably very similar to that at the Oak Ridge Gaseous Diffusion Plant, since both sites are in valleys with ridges on either side. The wind rose measured at the Gaseous Diffusion Plant (from Hilsmeier, 1963) is given in Table 3.

Table 3

Wind Rose at Oak Ridge Gaseous Diffusion Plant. A North Wind Blows from the North.

Direction	N	NNE	NE	ENE	E	ESE	SE	SSE
Frequency	2%	9	24	6	4	2	3	2
Direction	S	SSW	SW	WSW	W	WNW	NW	NNW
Frequency	5%	6	12	5	6	5	6	3

The flow is strongly channeled in the NE-SW direction by the ridges in the area (see the map in Hanna and Perry, 1973). In general the Oak Ridge area is relatively humid with relatively light winds compared to the rest of the country, and the local flows are greatly influenced by local topography.

2.2 Source Terms and Diffusion Models.

Since beginning operation twenty years ago, the cooling towers at the Gaseous Diffusion Plant have continuously dissipated heat in the range from about 500 MW to 2000 MW. In this report, it is assumed that the heat dissipated is 1000 MW, corresponding to a total emission of water,

Q , of 4.6×10^5 g/sec (about 80% of the total heat dissipated is in the form of latent heat, as measured by Hanna and Perry, 1973).

The cooling towers can be described as a finite line source about 500 m long. A diagram of the cooling towers is given by Hanna and Perry (1973). Thus the line source strength is about 10^3 g/m sec. However at distances x downwind large compared to the length of the towers, they can be treated as a point source. In this report, we use point source formulas at distances from the source greater than 1 km, and line source formulas at distances from the source less than 1 km. The point source formula is easier to use.

When wind directions are reported in sixteen $22\frac{1}{2}^\circ$ sectors, the average yearly ground level concentration, χ (g./m³), in each sector at a distance x (m) from a point source is given by the equation (see Gifford, 1968),

$$\chi = \sqrt{\frac{2}{\pi}} \frac{Qf}{\sigma_z U \frac{\pi x}{8}} e^{-h^2/2\sigma_z^2} \quad (1)$$

where Q (g/sec) is source strength, f is the fraction of the time that the wind blows towards that sector, h (m) is effective plume height, and σ_z is the vertical dispersion length.

In part I of this report (Hanna and Perry, 1973) it was stated that the plume from these towers downwashes at wind speed, u , greater

than about 3 m/s. In these cases the effective plume height is close to zero. But visual observations suggest that the plume recovers from its initial downwash, and rises slightly beginning at downwind distances, x , of about 100 m. For cases when downwash does not occur, plume rise H can be calculated using Briggs (1969) equation:

$$H = 2.9 (F/us)^{1/3} \quad (2)$$

where $s(\text{sec}^{-2})$ is the stability parameter $(q/T_p)(dT_e/dz + .01^\circ\text{C}/\text{m})$ and $F(\text{m}^4/\text{s}^3)$. proportional to the initial buoyancy flux is defined by:

$$F = w_o r_o^2 \frac{g}{T_{po}} (T_{po} - T_{eo}) \quad (3)$$

In these equations w_o , r_o , T_{po} , and T_{eo} are the initial plume vertical speed, plume radius, plume temperature, and environment temperature, respectively. T_p is the plume temperature and g is the acceleration of gravity. Hanna (1972) showed how equation (2) could be modified to account for the release of latent heat. Effective plume height h is the sum of plume rise H and tower height. Based on visual observations and calculations with Hanna's (1972) modification of equation (2), using known climatological values of U and s , the values of effective plume height in Table 4 were arbitrarily chosen.

Table 4

Effective Plume Heights as a Function of Wind Speed

Wind speed U(m/s)	.5 m/s	1.5	3	6, 8, 10
Effective plume height h(m)	200 m	100	25	12.5

A detailed measurement program should take place to better determine the plume rise at these towers. The straightforward application of equation(2)is complicated by the effects of multiple cells, latent heat, and downwash. Here it is assumed that the buoyancy from all the cells in a block can be added to give an effective buoyancy, but that the buoyancy from the three blocks does not combine. The blocks are separated by 200 m and 50 m.

At distances from the towers less than 1 km, a line source diffusion equation is used. Because of our lack of knowledge about the details of diffusion from such complicated sources, we decided to use the simplest basic formula. A complicated model is not justified until it is verified by an observation program. The sector average concentration due to the towers at short distances is thus given by the formula:

$$x = \sqrt{\frac{2}{\pi}} \frac{Qf}{\sigma_z U \left(\frac{\pi x}{8} + 500m \right)} e^{-h^2/2\sigma_z^2} \quad (4)$$

where now f is defined as the fraction of the time the wind blows towards a sector of width $(\pi x/8 + 500 \text{ m})$ at distance x from the towers.

The concentration, χ , on the plume axis very close to the tower openings is calculated by dividing the source strength, Q_p , by the plume velocity, $(w_o^2 + U^2)^{1/2}$, times the cross-sectional area, A , of the towers. The cross-sectional area equals tower width times tower length. The initial maximum concentration is therefore:

$$\chi = \frac{Q}{(w_o^2 + U^2)^{1/2} A} = \frac{4.6 \times 10^5 \text{ g/sec}}{(w_o^2 + U^2)^{1/2} (20\text{m} \times 500\text{m})} = \frac{46 \text{ g/m}^2 \text{ sec}}{(w_o^2 + U^2)^{1/2} (\text{m/sec})} \quad (5)$$

For an initial tower plume temperature of 100°F , the saturation water vapor content is about 50 g/m^3 . This concentration should be regarded as an upper limit to the calculated concentrations. The maximum concentration will increase if the initial tower plume temperature increases.

In all these calculations, it is assumed that the atmospheric stability is nearly neutral. This assumption is most valid for long term averages or for cloudy, windy days. Briggs (1973) recommends that $\sigma_z(x)$ during these conditions is given by the relation:

$$\sigma_z = .07x / (1 + .0015x)^{.5} \quad (6)$$

The smoothed distributions of dimensionless ground level concentrations calculated using equations (1), (4), and (6) are given in Figure (2)

for various classes of plume rise. As expected, an increase in plume rise greatly lowers the maximum ground concentration.

2.3 Average Annual Ground Level Excess Moisture due to Cooling Tower Operation

First, ground level excess moisture concentrations were calculated for each of the wind speed and plume rise classes in Tables 2 and 4. These values were then weighted by the wind direction and speed class frequency, to give the values in Figure 3, which are the average annual ground level excess moisture concentrations.

From Table 2, it is seen that the average annual saturation deficit (saturation mixing ratio minus actual mixing ratio) in this area is about 2 g/m^3 . This figure is not exceeded on Figure 3. The ratio of average cooling tower excess moisture to average natural saturation deficit in the SW Direction is .4, .13, .06, .03, and .02 at distances from the towers of 1, 2, 5, 10, and 20 km, respectively. The city of Oak Ridge (population 30,000) which is the nearest center of population to the towers is about 10 km to the NE. Here the average contribution at the ground due to the cooling towers is about one percent of the average saturation deficit. However, it is obvious that at some times, when the saturation deficit is low, the excess moisture due to the cooling towers will exceed the saturation deficit and fog will occur.

2.4 Annual Frequency of Ground Level Fog due to Cooling Towers.

Depending on the definition of fog, the natural occurrence of fog and rain in this area is about ten to twenty percent. In this

saturated environment, the cooling tower plume may form a long cloud which releases much latent heat. Consequently, the diffusion of water in this thermodynamic system may not be similar to the diffusion of an inert substance. But, for simplicity of calculations, we will assume that the release of latent heat does not affect the diffusion. The resulting calculated fog frequencies are therefore probably conservative (too high).

Calculations of the ground level concentration of liquid water (excess water due to cooling towers minus saturation deficit) were made for the 30 joint classes of wind speed and saturation deficit listed in Table 2. These results will first be given in terms of hours of extra fog per year and then in terms of visibility.

It is assumed on the basis of known frequencies of rain and fog that the saturation deficit Δm is zero for the class $0 < \Delta m < .5$. These cases are examined separately. For the classes where $\Delta m > .5$ (i.e. no rain or fog) the hours of extra ground fog per year in the area around the towers are given in Figure 4. No extra fog occurs under these conditions farther than 2 km from the towers. At distances of 100 to 200 m from the towers, there is predicted to be about 100 extra hours of fog per year.

Figure 5 contains predictions of the hours per year when existing ground fog and rain is intensified by the cooling tower plumes. This effect extends to great distances from the towers. The maximum number on the figure is 408 hours per year with intensified fog, which occurs at distances 20 to 50 km SW of the towers. These calculations are highly tentative, since thermodynamic effects were not taken into account.

The average predicted fog concentrations and visibilities at certain distances from the towers are listed in Table 5. Visibility, V, is calculated from Trabert's (1905) formula:

$$V(m) = 2 \frac{g}{m^2 \mu m} \frac{D(\mu m)}{\omega(g/m^3)} \quad (7)$$

where D is drop diameter in μm and ω is liquid water content in g/m^3 .

It is assumed that the drop diameter, D, equals 10 μm , typical of continental radiation fogs.

Table 5

Average Fog Concentrations Caused by Cooling Tower Operation and Corresponding Visibilities

x(m)	100	200	500	1000	2000	5000
$\omega(g/m^3)$	5.1	2.9	2.0	1.4	.61	.35
V(m)	4	7	10	15	33	57

Notice that the predicted visibilities are so low that a person could barely see a few meters. These visibilities are surely too low, since we have not accounted for removal. As liquid water concentration increases, droplets come together and are deposited as rain on the surface.

2.5 Occurrence of a Visible Plume Aloft

Another environmental effect of cooling towers is the possibility of an elevated visible plume decreasing the amount of sunlight reaching a station. The length of the visible plume was calculated

for each of the wind speed and saturation deficit classes in Table 2.

For the case $\Delta m < .5$, which occurs 20% of the time, it is assumed that the plume extends indefinitely. This is an effect often observed during naturally foggy or rainy conditions. In Figure 6, the hours per year with a visible plume aloft are plotted. It is seen that in the SW direction at a distance of 1 km from the towers there are about 1500 hrs per year with a visible plume aloft. In Oak Ridge, 10 km to the NE, there are 240 hours per year with a visible plume aloft. Since there is also a natural cloud deck during most of these cases, the cooling tower plume is not very noticeable.

The median visible plume length is calculated to be about 1 km. During the day, the observed visible plume length is only about .2 km (Hanna and Perry, 1973). But we are not able to observe the plume very well in the night, when the plume is the longest. Clearly an extensive observation program is needed to test the model predictions.

3. Drift Deposition

The mechanical draft cooling towers at ORGDP are about 20 years old and release a large amount of drift water, by today's standards. Hanna and Perry's (1973) and Environmental Science Corporation's (1973) measurement of the flux of liquid water from representative cells of these towers are summarized in Part I of this report series. A flux of

about 180 gm/sec of liquid water was observed at a typical cell on the K-31 towers. A total liquid water flux of about 3600 gm/sec was emitted during the period that our experiments were run. A more typical value for the liquid water flux would be about 14000 gm/sec, since usually the towers are dissipating more heat than was the case during the experimental period.

The concentration of sodium dichromate in the cooling water and the drift water is about 20 parts per million. A potential environmental problem is the deposition of chromate on the ground around the towers. In this section of the report, the techniques described by Hanna (1974) are used to estimate the deposition of drift water and chromates.

3.1 Mathematical Model of Drift Deposition.

The mathematical model of drift deposition that we developed accounts for the rise of the plume and entrainment of environmental air into the plume. The drop diameter changes due to differences between its vapor pressure and the vapor pressure of its environment. The model equations are solved numerically on the IBM 360/75 computer at Oak Ridge National Laboratory.

3.1.1 Plume Rise

The drop is assumed to originate from the center of the cooling tower cell opening. While it is in the plume, it experiences (see Briggs, 1969) a plume vertical speed, w , given by the relation:

$$w = \frac{.48 \left[\frac{F_m}{\left(\frac{1}{3} + \frac{U}{w_o} \right)^2 U} + \frac{4F_x}{U^2} \right]}{\left[\frac{F_m}{\left(\frac{1}{3} + \frac{U}{w_o} \right)^2 U^2} + \frac{2F_x^2}{U^3} \right]^{2/3}} \quad (7)$$

where F_m is proportional to the momentum flux:

$$F_m = w_o^2 r_o^2 \quad (8)$$

The vertical motion of the plume ceases at a distance, x^* , given by the equation:

$$x^* = 50m [F(m^4/s^3)]^{5/8}$$

For an individual cell at these particular cooling towers, $F = 25 m^4/s^3$, and the distance x^* at which maximum plume rise is achieved is about 370 m.

Entrainment of environmental air causes the plume radius, R , to increase. The ratio of the volume flux of plume air, $V(z) = UR^2$, at any height to the initial volume flux, $V_o = w_o R_o^2$, is found by Hanna (1972) to equal:

$$\frac{V(z)}{V_o} = \left(1 + .5 \frac{(h-H)}{R_o} \frac{U^{1/2}}{w_o^{1/2}} \right) \quad x \leq x^* \quad (9)$$

$$\frac{V(z,x)}{V_o} = \frac{U(R_o) \left(\frac{w_o}{U} \right)^{1/2} + .5(h(x^*) - H) + C(x - x^*)^2}{w_o R_o^2} \quad x > x^* \quad (10)$$

where C is a constant proportional to the rate of spread of the plume after final rise is achieved at distance x^* .

Since the plume cools rapidly, we make the assumption that the saturation vapor pressure at the drop surface equals the saturation

vapor pressure of a drop at the temperature of the environment. To be strictly correct, the actual temperature of the plume should be used. Furthermore, we assume that the environment temperature and vapor pressure are constant, independent of height.

3.1.2 Drop evaporation

The drop will evaporate at a rate dependent on its diameter, the mass of solute in it, and the saturation and actual vapor pressures of the environment (see Fletcher, 1962, and Fleagle and Businger, 1964)

$$\frac{dD}{dx} = \frac{-8.0 \times 10^{-10}}{UD} [1 + .59 \sqrt{DV_g}] [p_s \frac{e^{\frac{2.0 \times 10^{-7}}{D}} - p_a}{(1+1.3 \frac{M_s}{D^3})}], \quad (11)$$

where $D(\text{cm})$ is drop diameter, $U(\text{cm/s})$ and $V_g(\text{cm/s})$ are wind speed and drop settling speed, $M_s(\text{g})$ is the mass of solute in the drop, and p_s (dynes/cm^2) and p_a (dynes/cm^2) are saturated and actual environmental vapor pressures. Vapor pressure is related to mixing ratio by:

$$p(\text{dynes/cm}^2) = 1.57 \times 10^6 \times m(\text{gm/gm}) \quad (12)$$

As the drop evaporates, its fall speed changes. For small drop sizes, Stokes law is assumed to apply:

$$\begin{aligned} V_g &= 3.2 \times 10^5 D^2 & D < .0093 \text{ cm water drops} \\ V_g &= 8.0 \times 10^5 D^2 & \text{Sodium dichromate particles} \end{aligned} \quad (13)$$

For larger drops, we use the following analytical approximations to the data given by Engelmann (1968, p 212):

$$\begin{aligned}
 V_g &= 6816.D^{1.177} & .0093 \text{ cm} < D < .068 \text{ cm} \\
 V_g &= 2155.D^{.746} & .068 < D < .26 \text{ cm} \\
 V_g &= 1077.D^{.224} & .26 \text{ cm} < D
 \end{aligned} \tag{14}$$

For small drops in a dry environment, the drop evaporates to a particle a few μm in diameter. If this happens, the motion of the particle is governed by diffusion and is treated similar to the diffusion of fog in section 2. The plume of particles dips down relative to the gaseous plume due to the slight settling of the particles. The deposition, $w(\text{g}/\text{m}^2\text{s})$, is then given by the relation $w = V_g \chi_0$. For V_g greater than 1 cm/s, the actual settling speed is used in equation (15). For V_g less than 1 cm/s, it is assumed that dry deposition occurred, and V_g is set equal to 1 cm/s in equation (15). More refined estimates of the dry deposition speed can be made following the recommendations of Van der Hoven (1968).

3.2 Computer Program

The above equations were programmed in Fortran IV for solution on the ORNL, IBM, 360/75 computer. It is assumed that all drops begin their motions at the center of an individual cooling tower cell. A downwind distance interval, Δx , of .5 m is used and calculations are carried out to a distance of 20 km from the towers. The total number of program statements is 95.

Input parameters are the saturated and actual mixing ratios of the environment, the wind speed, the tower height, and the initial momentum flux, buoyancy flux, radius, and vertical speed of the plume. In addition, several initial drop sizes are input.

The output consists of the final size of each drop or particle and the distance from the tower at which it strikes the ground. If the drop does not reach the ground, its final height and sizes are listed. Plume rise is also given.

3.3 Calculation of Chromate Deposition Rates.

The results of the computer program give information on the distance from the tower that a drop of a given size strikes the ground. From these numbers, it is possible to calculate the chromate deposition rate. For example, the program is run for a variety of initial drop diameters. It can be assumed that the drops of a given initial diameter fall uniformly between the point halfway between the points where that drop and the drop of next largest diameter fall, and half way between the points where that drop and the drop of next smallest diameter fall. This concept is illustrated in Figure 7. If long term average deposition rates are desired, the sector averages can be employed, similar to the technique in equation (1). In this case the drops blowing in a given direction on a 16 point wind direction scale fall uniformly within a $22\frac{1}{2}^\circ$ angle centered on that direction. For simplicity, the $22\frac{1}{2}$ sector concept can also be applied to instantaneous deposition. This assumption is most correct for nearly neutral stability.

3.4 Results

Drift deposition rates are summarized for the period in June, 1973, during which observations were made, and for average annual conditions.

3.4.1 Drift Deposition During June, 1973, Experiments.

Measurements of drift deposition during the last week of June, 1973, are plotted on Figure 8. The ATDL (Hanna and Perry, 1973) and ESC (Shofner et al., 1973) observations, made with sensitive paper, were

generally from a location under the center of the visible plume. In contrast the BPNL (Lee et al., 1973) observations were made with a flat plate, and the station locations were fixed. Consequently, the BPNL stations were not often beneath the plume, which meandered about with the variable wind directions during this week.

The calculated drift deposition rates are also given in this figure. Deposition rates are interpolated between the curve for a single cell at x equal to 50 m and the curve for 20 cells at x equal to 500 m. Environmental conditions typical of those during the experiment are assumed:

$$m_s = .0238 \quad m_a = .0138 \quad U = 150 \text{ cm/sec}$$

Input source parameters have already been outlined by Hanna and Perry (1973).

The calculated and observed deposition rates agree fairly well at distances of 10 and 15 m, where it is likely that only one cell influences the deposition. The ESC (Shofner et al., 1973) measurements at distances of 35 and 80 m are about a factor of two greater than the calculated deposition rate, possibly because their sensitive paper was tilted a few degrees from the horizontal.

Since the ESC sensors were moved to insure that they were always beneath the plume, their measurements at these distances are greater than the BPNL (Lee et al., 1973) measurements. The BPNL sensors were beneath the plume only a fraction of the time, and their measured drift deposition rates are an order of magnitude less than the calculated

plume centerline deposition rates. If we assume that the plume blew over the BPNL sensors only 10% of the time, then calculated and observed deposition rates agree within a factor of two. The observations and the model estimates are therefore reconcileable at distances from 10 m to 1500 m from the tower.

3.4.2 Average Annual Drift Deposition

The average annual emission of drift water is about four times the emission assumed for the June, 1973, period. The drift deposition computer model was run for the following combinations of environmental parameters:

Summer day: $m_s = .0238$ $m_e = .0138$ $U = 150 \text{ cm/s}$

Summer night: $m_s = .017$ $m_e = .017$ $U = 50 \text{ cm/s}$

Winter day: $m_s = .0080$ $m_e = .0048$ $U = 250 \text{ cm/s}$

Winter night: $m_s = .0037$ $m_e = .0031$ $U = 100 \text{ cm/s}$

The four calculated values of deposition rate never differ by more than an order of magnitude. The average annual deposition rate at any distance x from the towers, plotted in Figure 8, is assumed to be given by the average of the deposition rate for the above four combinations. The resulting annual deposition rate of chromate in the area within 20 km of the towers is given in Figure 9. Figures are given for each $22\frac{1}{2}^\circ$ wind direction sector at distances greater than 1 km. Closer to the towers, the finite size of the line sources is accounted for by combining sectors. For example, at a distance of 50 m to the east of the tower center, the deposition rate is nearly the same whether the wind is from the west or northwest. The deposition rates close to the towers are listed in Table 6.

Table 6

Average Annual Chromate Deposition Rates ($\mu\text{g}/\text{m}^2\text{s}$) Close to

Cooling Towers

x (m)	East Sector	West Sector
5 m	23.2 $\mu\text{g}/\text{m}^2\text{s}$	26.7
10 m	4.6	5.3
20 m	1.3	1.5
50 m	.23	.27
100 m	.08	.09

There is great variation in calculated deposition rate with distance from the tower. Chromate deposition varies from about 20 $\mu\text{g}/\text{m}^2\text{s}$ near the tower to about $5 \times 10^{-5} \mu\text{g}/\text{m}^2\text{s}$ at a distance of 20 km from the tower. At distances greater than 1 km (i.e., beyond the plant boundary) chromate deposition rate is calculated to be less than about $5 \times 10^{-4} \mu\text{g}/\text{m}^2\text{sec}$, or 80 g/acre yr. The measured concentration of chromate in plants near the towers is being analyzed by F. Taylor of Oak Ridge National Laboratory and will be related to the deposition rates calculated above. These are the only data available to test the model for average annual deposition at this site.

3.5 Limitations

The deposition calculations must be regarded as tentative. In the first place there are no really good validation data for the model. Our method does not account for thermodynamic processes. To be strictly correct, the drops should originate at various locations across the mouth of the tower. In our technique, where all drops are started at the center of

the tower, a critical drop size is found during cases when relative humidity is less than 70%. Drops smaller than this critical size do not fall from the plume, but remain in the plume and eventually evaporate. Drops larger than this critical size fall from the plume and strike the ground within 200 m of the tower. A much more complicated model could be developed, but would not be justified by the current state of the art of the theory and measurement of drift deposition. The figures calculated here are probably accurate within a factor of five or ten.

4. Summary

The main results of this study can be summarized:

4.1 Average wind speed at this site is 2 m/s; average saturation deficit is 2 g/kg. This site has a relatively high potential for environmental problems with cooling tower plumes, due to the relatively low wind speed and saturation deficit.

4.2 The cooling towers are represented as a finite line source, with average total moisture (gaseous plus liquid) output of 4.6×10^5 g/sec. Average drift water output is 1.4×10^4 g/sec.

4.3 Neighboring plumes from the cells in a bank merge after a distance of about 50 m. Plumes from the three banks, initially separated by about 100 m, merge after a distance of about 500 m. Total plume rise averages about 200 m.

4.4 The ratio of average cooling tower excess moisture to average natural saturation deficit (2 g/kg) in the SW direction is .4, .13, .06, .03, and .02 at distances from the towers of 1, 2, 5, 10, and 20 km, respectively.

4.5 When latent heat is released during naturally rainy or foggy conditions, a cloud forms aloft with constant base height. This occurs about ten to twenty per cent of the time.

4.6 When naturally occurring rain or fog is absent, it is predicted that the cooling towers will cause about 100 extra hours of fog per year at distances of 100 to 200 m from the towers. The standard Gaussian plume model is used to make these predictions. No extra fog is predicted to occur under these conditions at distances greater than 2 km from the towers.

4.7 A visible plume aloft is calculated to occur over the city of Oak Ridge, 10 km to the NE, about 240 hours per year. During almost all of this time, a natural cloud deck will also be present.

4.8 Drift deposition is calculated using the Gaussian plume model for drops with diameters less than 200 μg . The trajectory approach is used for larger drops. The variation of vertical speed in the plume and the evaporation of drops are accounted for.

4.9 Predictions of chromate deposition at distances from 10 m to 1500 m from the towers agree fairly well with observations during the June, 1973, experiment.

4.10 Calculated average annual chromate deposition rates vary from about 20 $\mu\text{g}/\text{m}^2$ s at distance of 5 m from the towers to 10^{-4} $\mu\text{g}/\text{m}^2$ s at a distance of 20 km from the towers.

5. Acknowledgements.

This research was performed under an agreement between the National Oceanic and Atmospheric Administration and the Atomic Energy Commission.

W. M. Culkowski of this laboratory calculated the joint distribution functions of wind speed and saturation deficit. S. G. Perry, an Oak Ridge Associated Universities summer trainee at this laboratory, took part in the initial development of the drift deposition model. The cooperation of G. Kidd and T. Shapiro of the Oak Ridge Gaseous Diffusion Plant is gratefully acknowledged.

References

- Briggs, G. A., 1969: Plume Rise, AEC Critical Rev. Series, USAEC-TID-24635, available from Clearinghouse, Springfield, Va., 22151, \$3.00, vi + 81 pp.
- Briggs, G. A., 1973: Diffusion Estimation for Small Emissions, draft of a manuscript to be published in the AEC critical review series, available as ATDL Contribution No. 79, P. O. Box E, Oak Ridge, Tn., 37830, 59 pp.
- Engelmann, R. J., 1968: The calculation of precipitation scavenging, Meteorology and Atomic Energy 1968, edited by D. Slade, USAEC TID-24190, available for \$6.00 from Clearinghouse, Springfield, Va., 22151, pp 208-221.
- Environmental Data Service, 1968: Climatic Atlas of the United States, U. S. Dept. of Commerce, price \$4.25 from Superintendent of Documents, U. S. Government Printing Office, Washington, D. C. 20402, 80 pp.
- Fleagle, R. G. and J. A. Businger, 1963: An Introduction to Atmospheric Physics, Academic Press, Inc., New York, pp 79-108.
- Fletcher, N. H., 1962: The Physics of Rainclouds, Cambridge Univ. Press, 386 pp.
- Gifford, F. A., 1968: An outline of theories of diffusion in the lower layers of the atmosphere, chapter 3 in Meteorology and Atomic Energy 1968, D. Slade, ed., available as TID-24190 for \$6.00 a copy from Clearinghouse, Springfield, Va., 22151, pp 66-105.
- Hanna, S. R., 1972: Rise and condensation of large cooling tower plumes. J. Appl. Meteorol., 11, 793-799.
- Hanna, S. R., 1974: Fog and drift deposition from cooling towers, to be published in Nuclear Safety, March-April 1974 issue.
- Hanna, S. R. and S. G. Perry, 1973: Meteorological Effects of the Cooling Towers at the Oak Ridge Gaseous Diffusion Plant. I. Description of Source Parameters and Analysis of Plume Photographs and Hygrothermograph Records, available as ATDL Contribution No. 86, P. O. Box E, Oak Ridge, Tn. 37830, 30 pp + 10 figs.
- Hilsmeier, W. F., 1963: Supplemental Meteorological Data for Oak Ridge. ORO-199, Division of Technical Information, USAEC, available from ATDL, P. O. Box E, Oak Ridge, Tn. 37830, 57 pp.

Holland, J., 1953: A Meteorological Survey of the Oak Ridge Area, ORO-99, Division of Technical Information, USAEC, 584 pp.

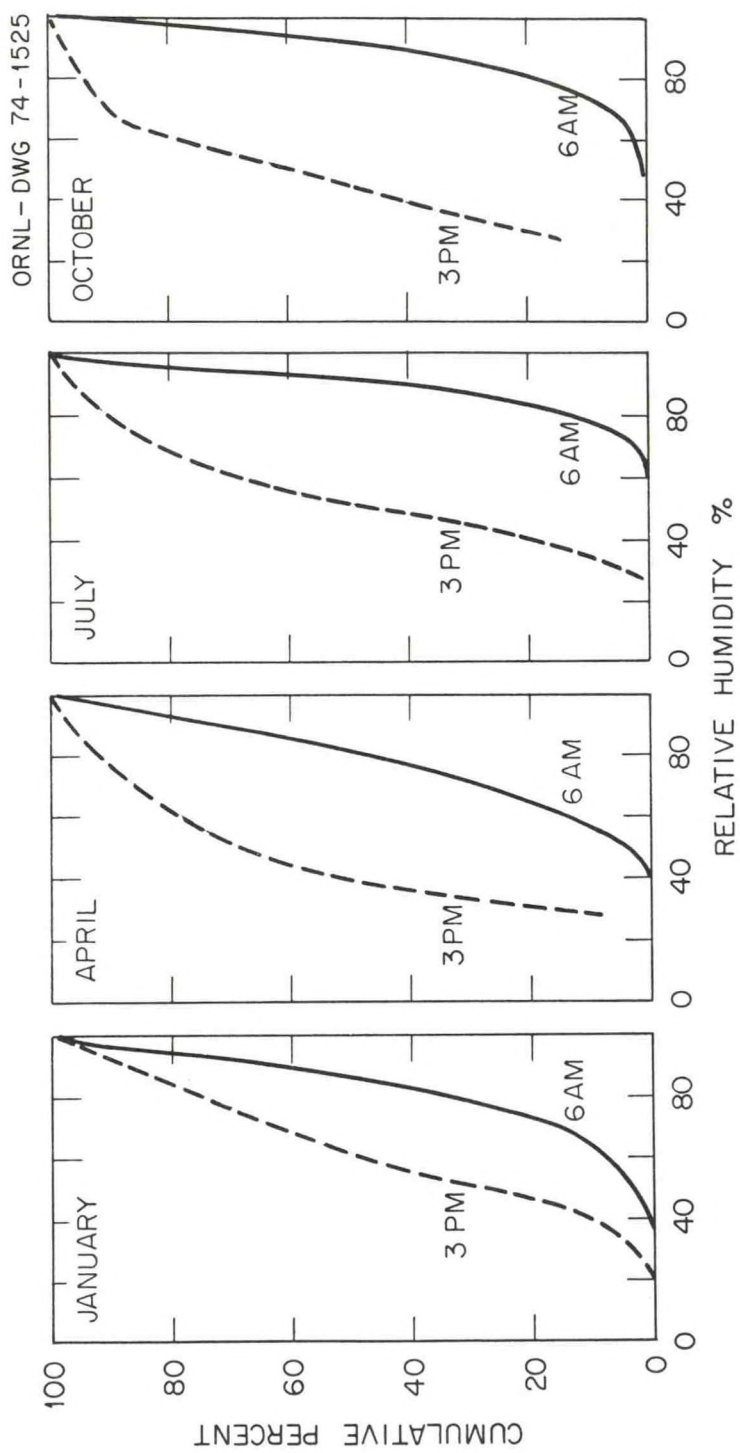
Lee, R. N., J. W. Sloot, and M. A. Wolf, 1973: Measurements of Chromate Resulting from Cooling Tower Drift at the Oak Ridge Gaseous Diffusion Plant, Final Report prepared for Union Carbide Nuclear Co. (AEC Contr. No. AT (45-1)1830) by Battelle Pacific Northwest Lab., Richland, Wa., 99352, 14 pp.

Neuberger, H., 1957: Introduction to Physical Meteorology. The Pennsylvania State University, University Park, Pa., 271 pp.

Shofner, F. M., G. O. Schrecker, and K. R. Wilber, 1973: Characterization of Drift Emissions and Drift Transport for Representative Cells of K-31 and K-33 Cooling Towers. Final Report prepared for Union Carbide Nuclear Co. by Environmental Systems Corp., P. O. Box 2525, Knoxville, Tn., 37901, 66 pp.

U. S. Weather Bureau, 1941: Airway Meteorological Atlas for the United States, U. S. Department of Commerce, W. B. Report No. 1314.

Van der Hoven, I., 1968: Deposition of particles and gases, Meteorology and Atomic Energy 1968, edited by D. Slade, USAEC TID-24190, available for \$6.00 from Clearinghouse, Springfield, Va., 22151, pp 202-208.



Figures 1: Distribution of relative humidity by season and time of day, in Knoxville, Tn. (From Environmental Data Service, 1966).

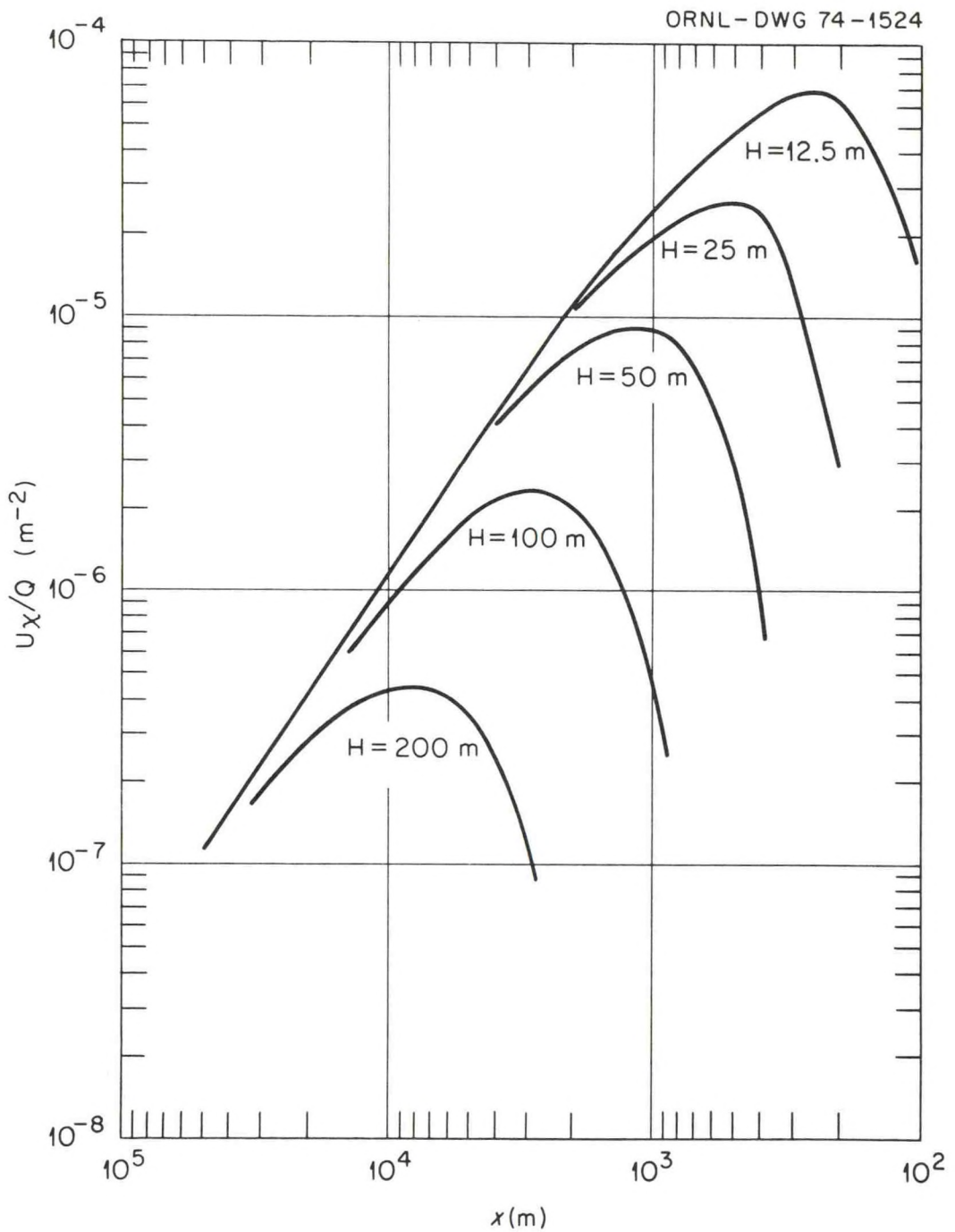


Figure 2: Curves of $\chi U / Q \text{ (m}^{-2}\text{)}$ as a function of downwind distance x , for neutral stability. Sector width is $500\text{m} + \pi x / 8$. Vertical dispersion parameter σ_z equals $.07 x / (1 + .0015x)^{.5}$.

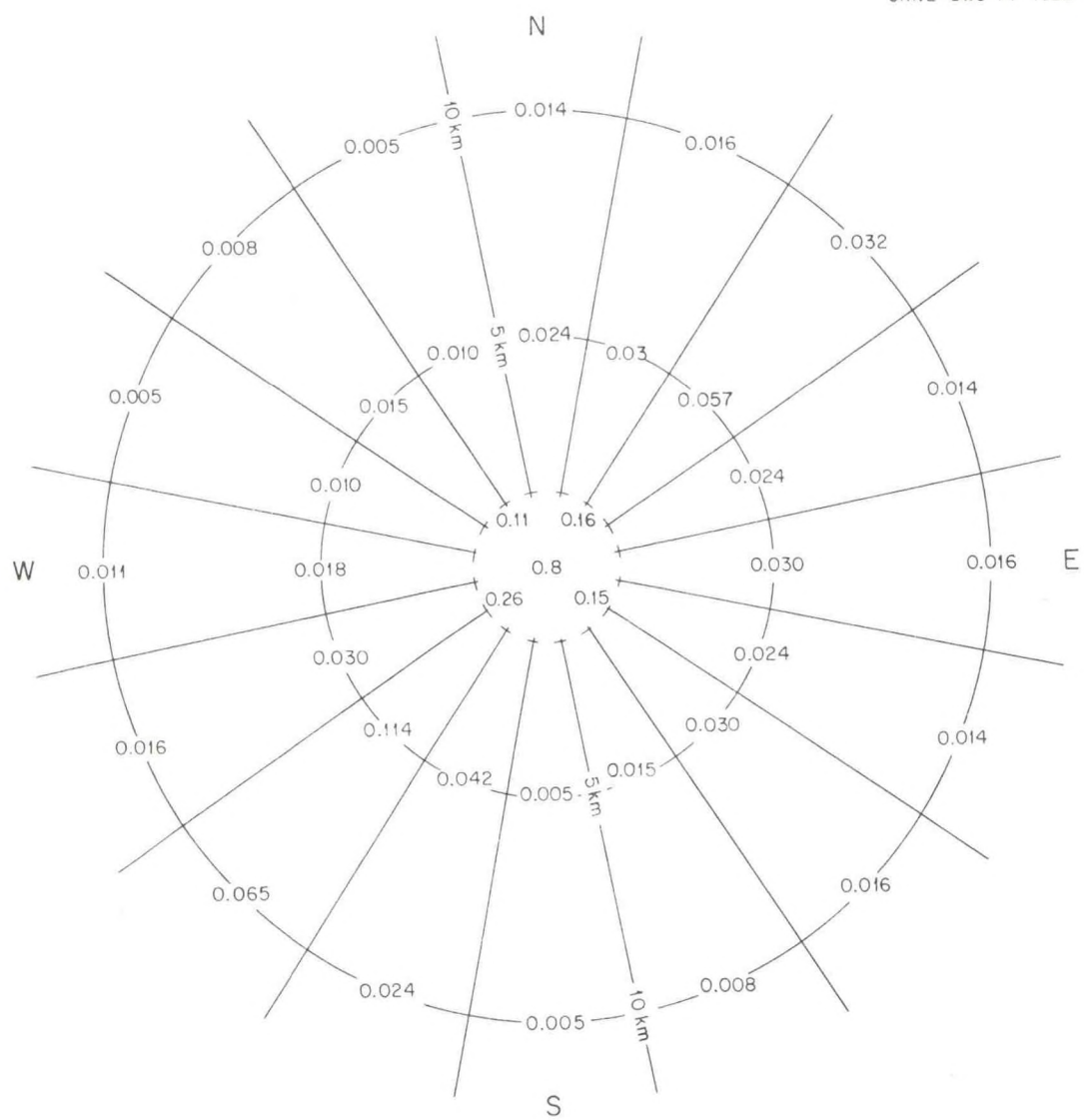


Figure 3: Average annual ground level water concentration (g/m^3) due to cooling towers at ORGDP.

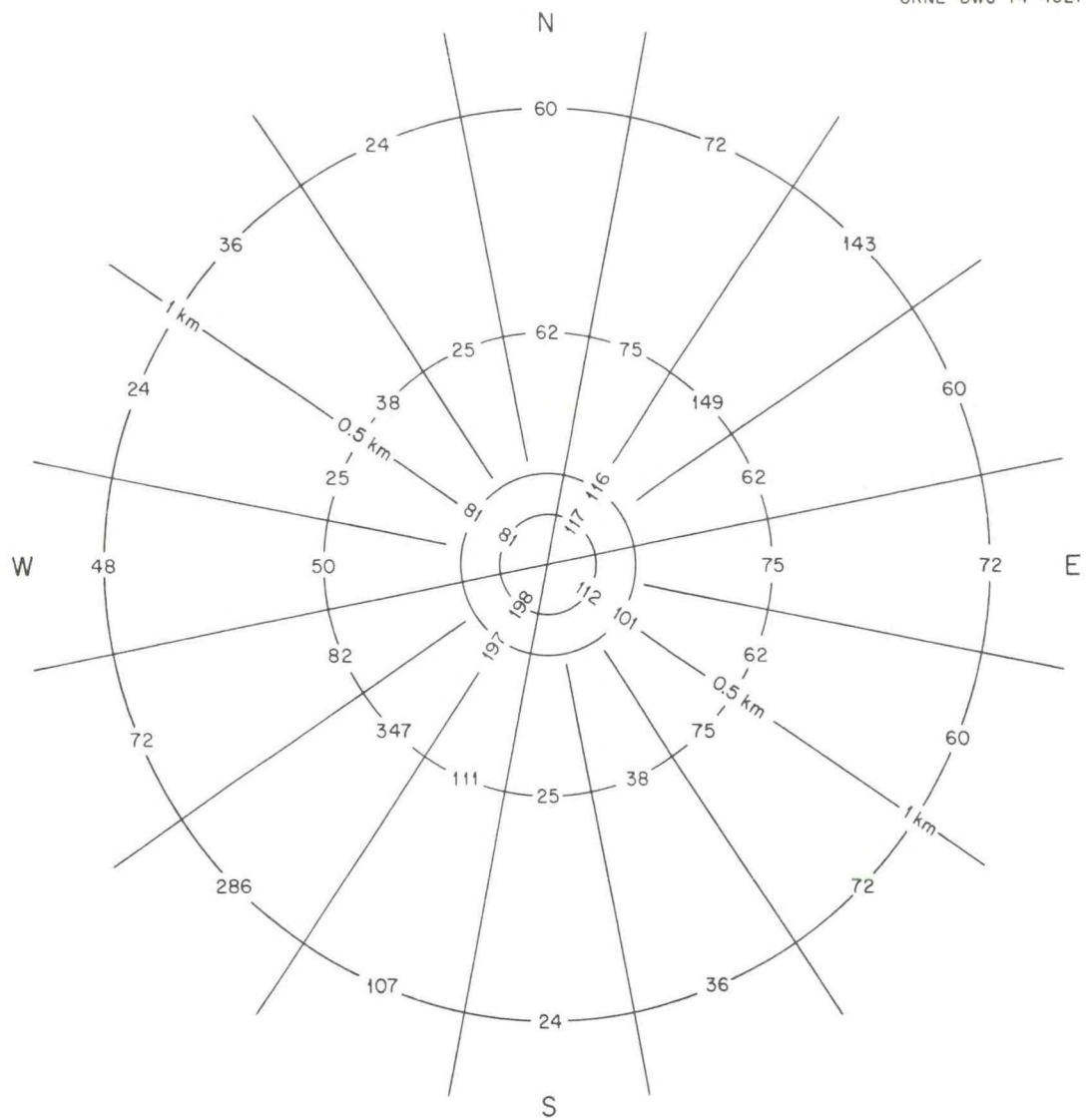


Figure 4a: Extra hours per year of fog caused by cooling tower operation, excluding cases when rain or fog naturally occurs.

ORNL-DWG 74-1520

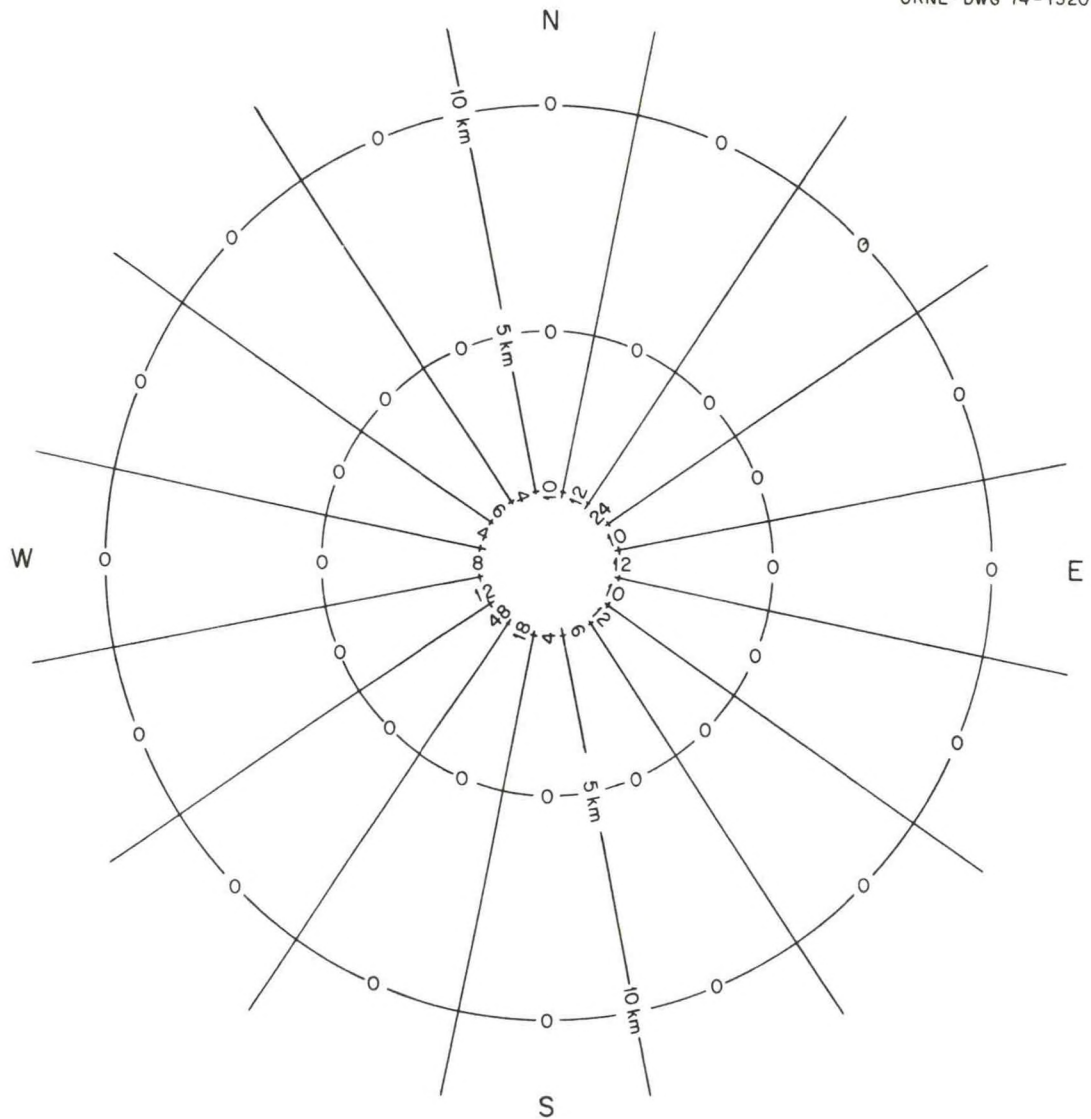


Figure 4b: Same as Figure 4a, but with expanded scale.

ORNL - DWG 74-1519

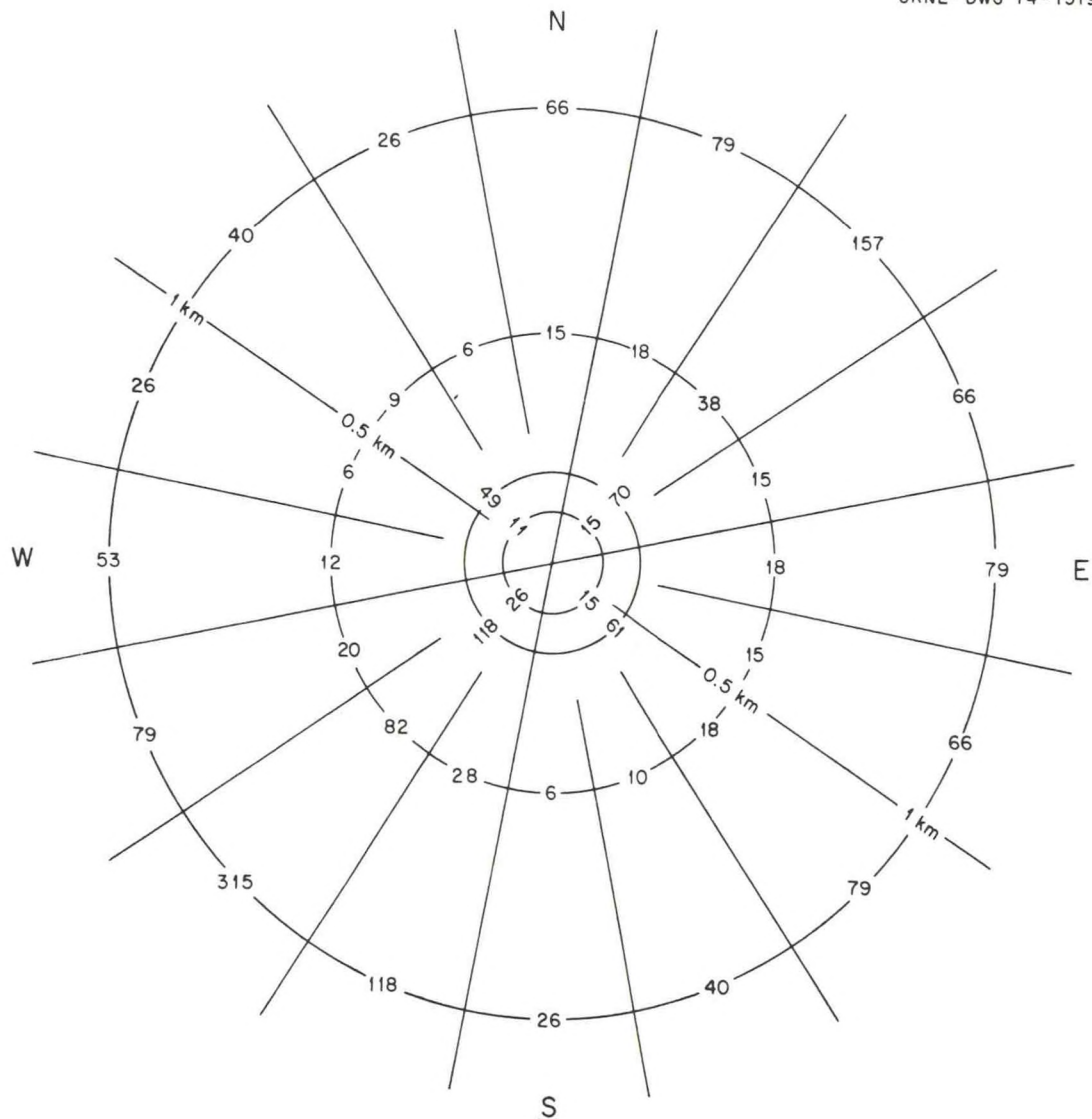


Figure 5a: Hours per year that the cooling tower fog augments naturally-occurring rain or fog.

ORNL-DWG 74-1518

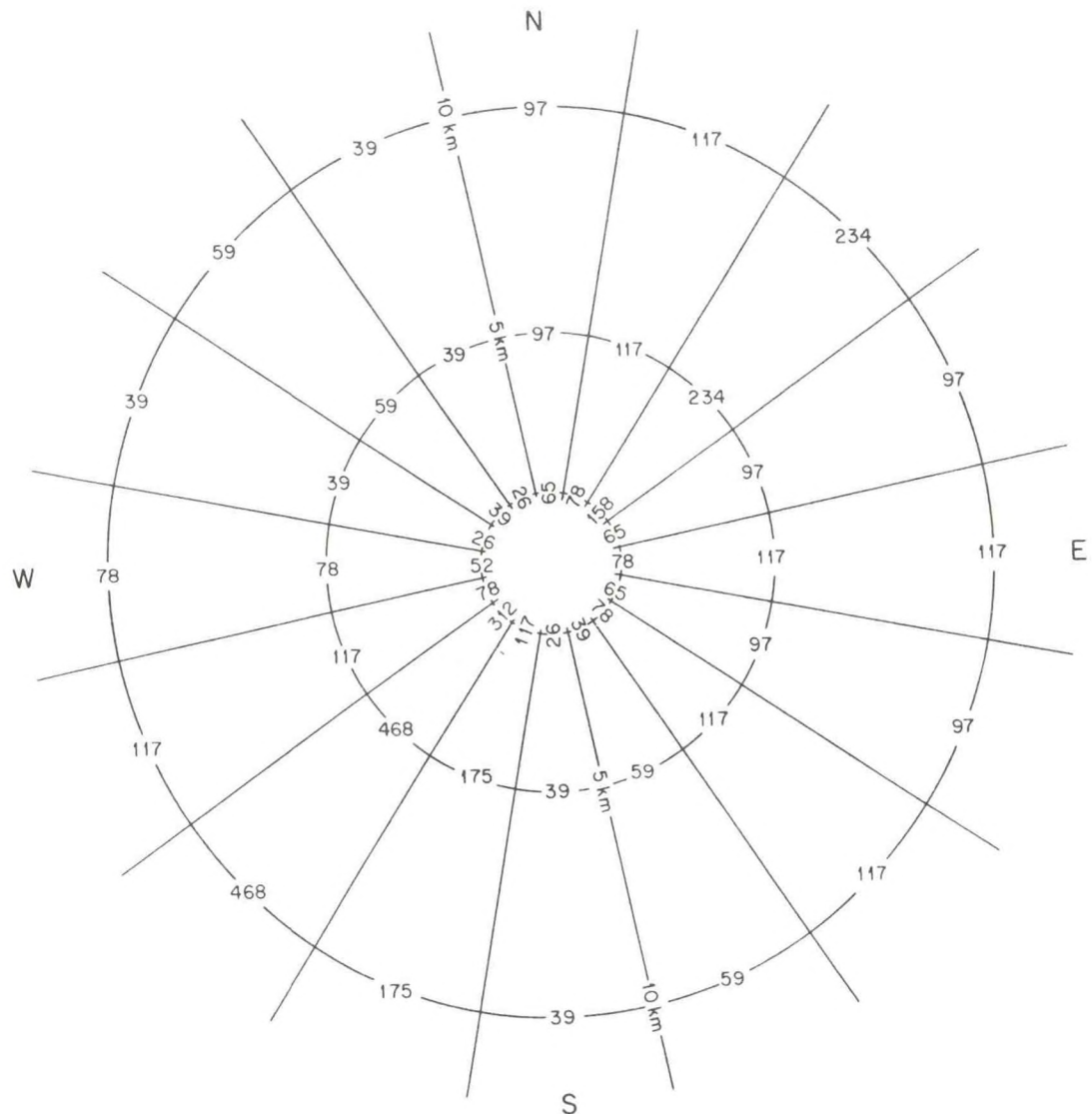


Figure 5b: Same as Figure 5a, but with expanded scale.

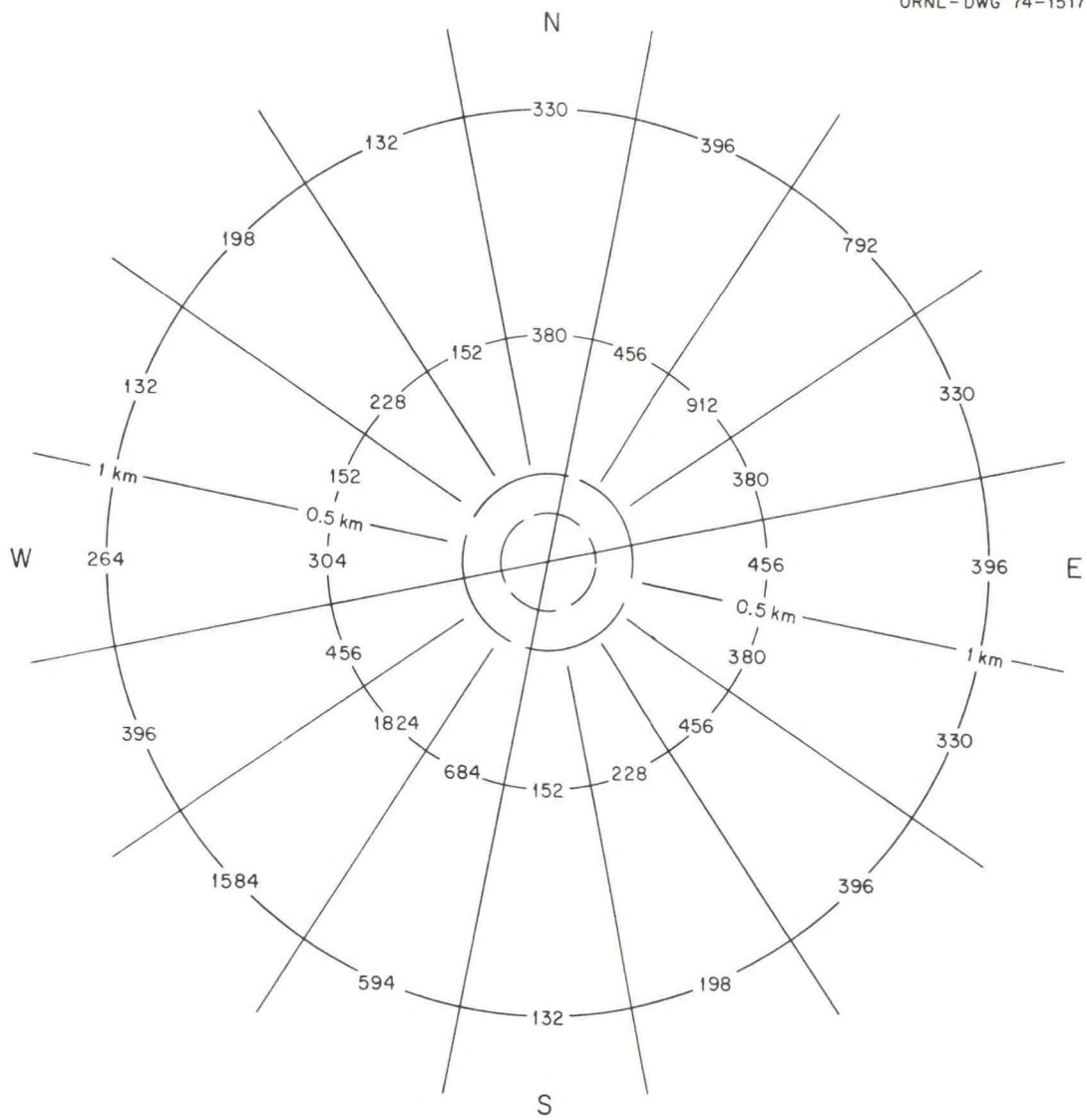


Figure 6a: Hours per year that a visible plume can be seen aloft.

ORNL-DWG 74-1516

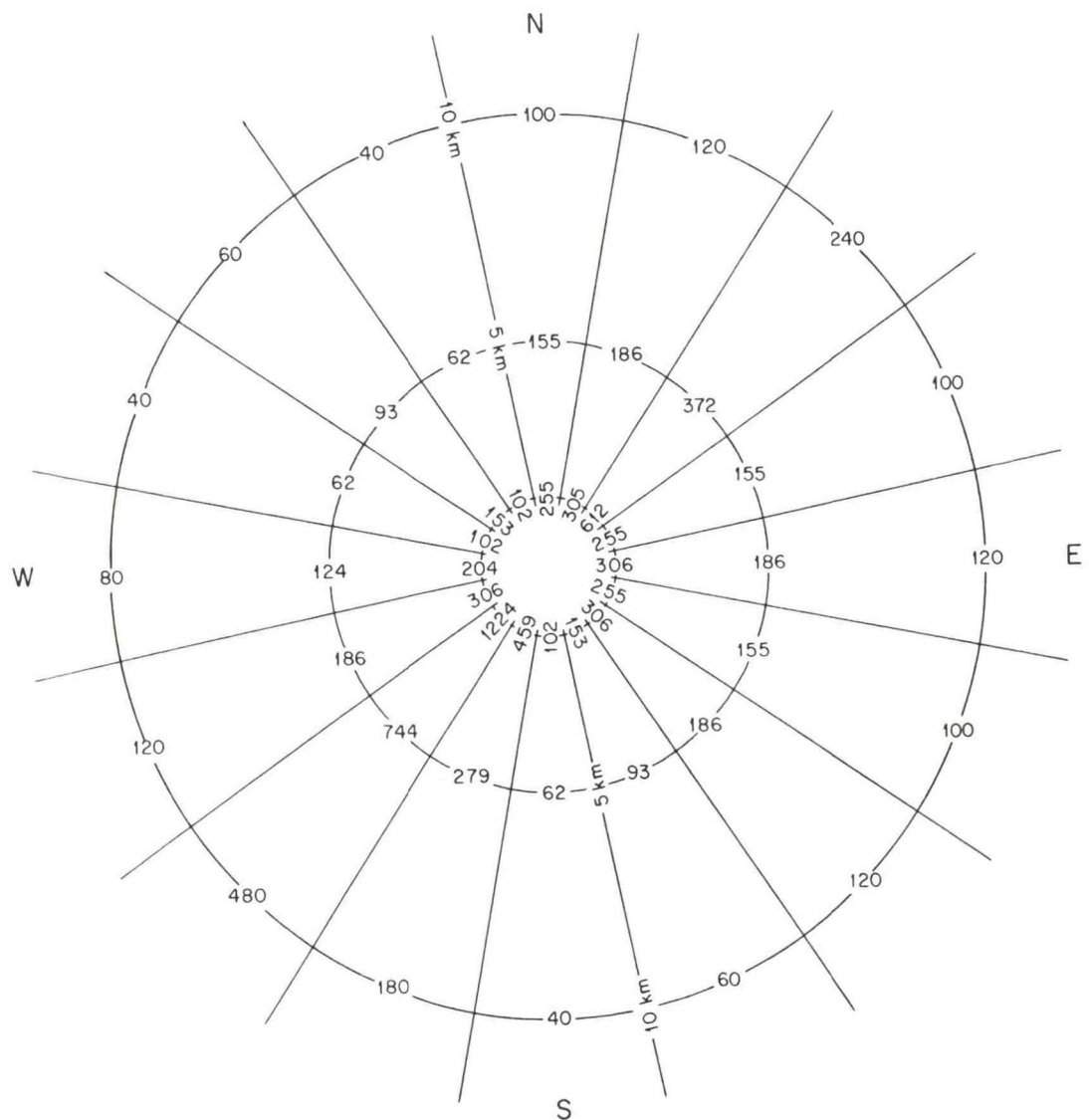


Figure 6b: Same as Figure 6a, but with expanded scale.

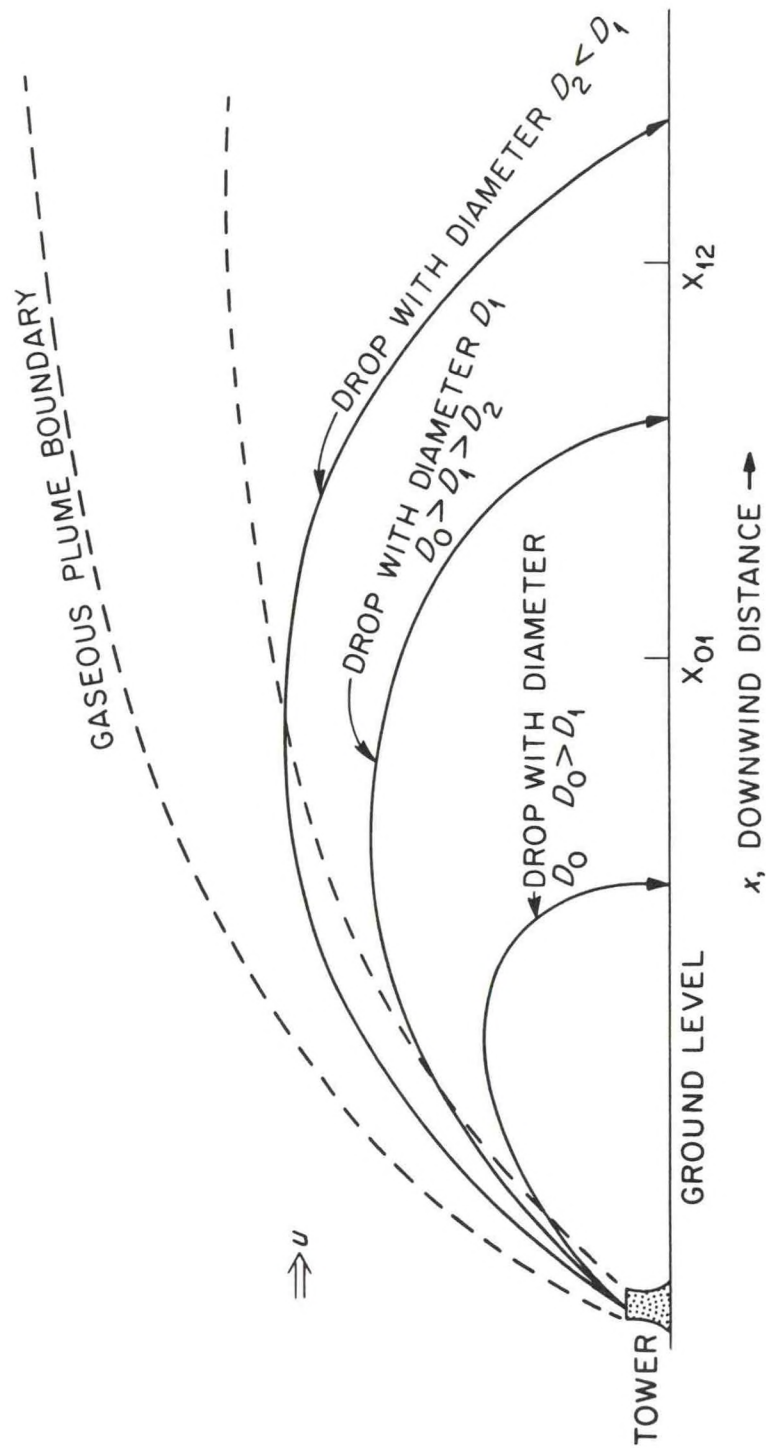


Figure 7: Schematic drawing of drift drop trajectories. Drops with diameter D_1 are assumed to be deposited uniformly between distances x_{01} and x_{12} .

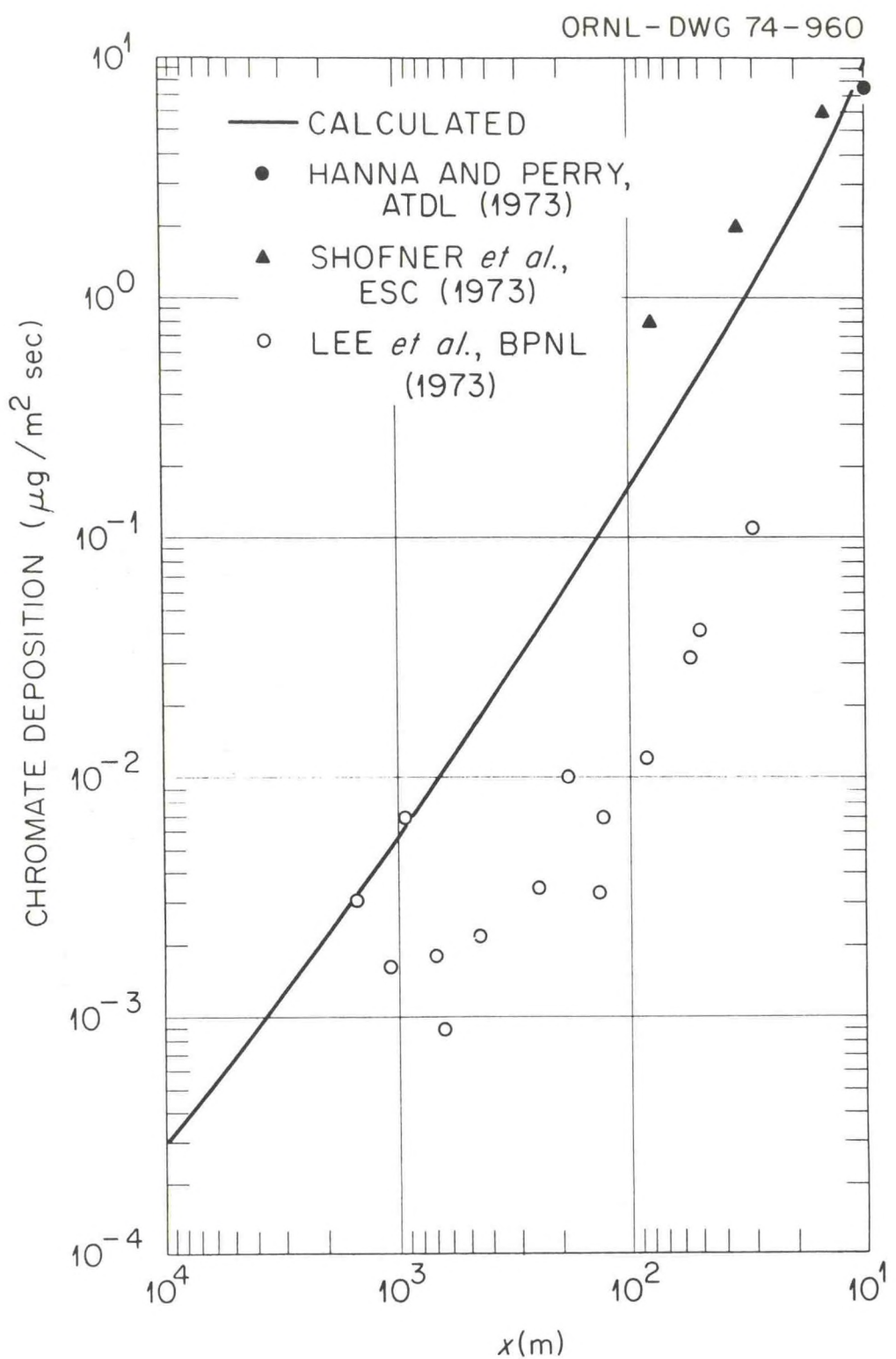


Figure 8: Chromate deposition rate, observed and calculated, during the June 1973 experiment.

ORNL-DWG 74-1514

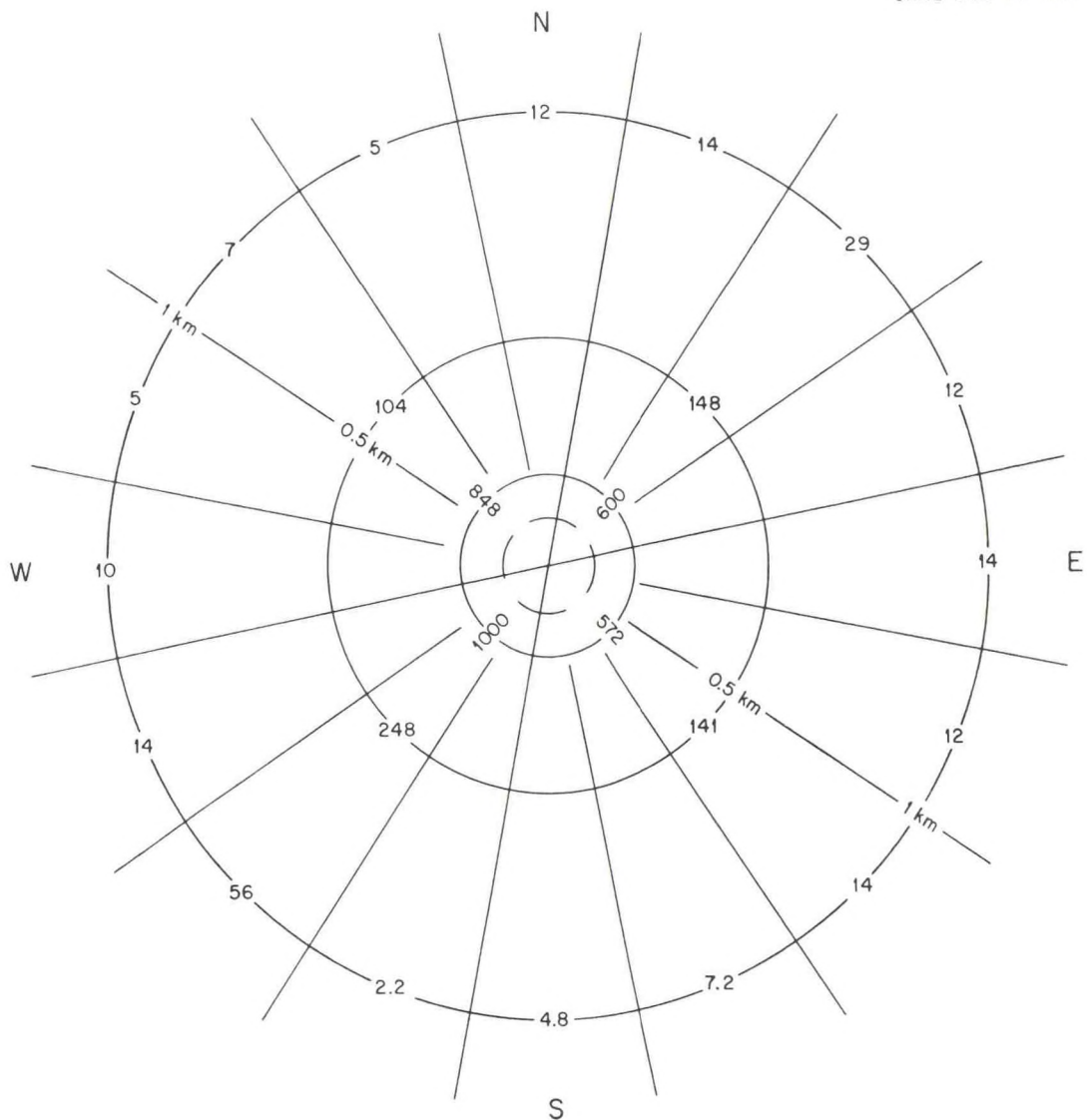


Figure 9a: Annual average deposition rate of chromate, in $10^{-10} \text{ g/m}^2 \text{ sec.}$

ORNL-DWG 74-1515

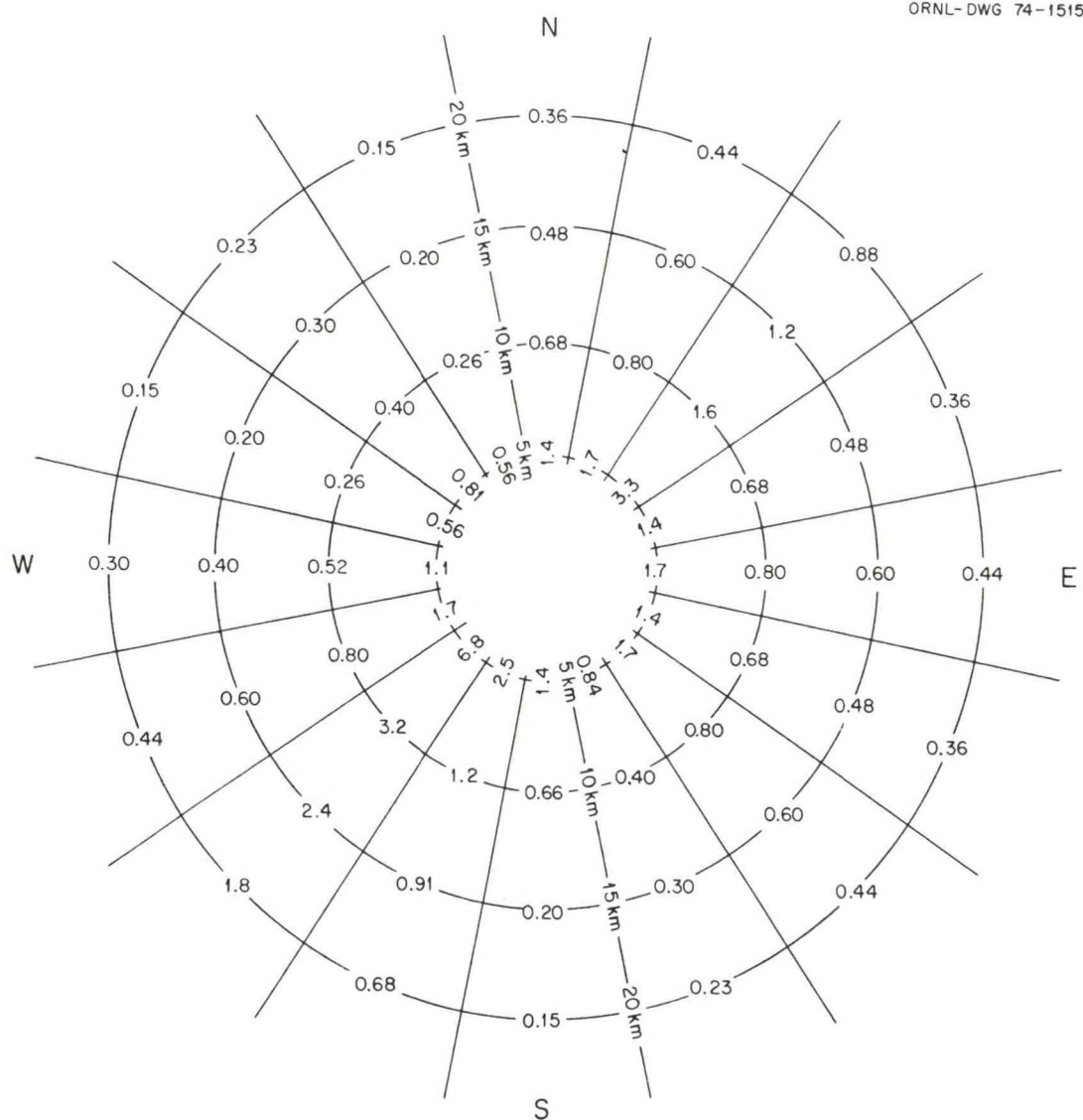


Figure 9b: Annual average deposition rate of chromate, in $10^{-10} \text{ g/m}^2 \text{ sec.}$

COOLING TOWER ENVIRONMENT-1974

Proceedings of a symposium held at the University of Maryland
Adult Education Center March 4-6, 1974

METEOROLOGICAL EFFECTS OF THE MECHANICAL-DRAFT COOLING TOWERS OF THE OAK RIDGE GASEOUS DIFFUSION PLANT

STEVEN R. HANNA

Air Resources Atmospheric Turbulence and Diffusion Laboratory, National Oceanic
and Atmospheric Administration, Oak Ridge, Tennessee

ABSTRACT

The mechanical-draft cooling towers at the Oak Ridge Gaseous Diffusion Plant dissipate about 2000 MW of heat. Downwash occurs about 40% of the time, when wind speeds exceed about 3 m/sec. An elevated cloud forms about 10% of the time. The length of the visible plume, which is typically 100 or 200 m, is satisfactorily modeled if it is assumed that the plumes from all the cells in a cooling-tower bank combine.

The calculation of fog concentration is complicated by the fact that the moisture is not inert but is taking part in the energy exchanges of a thermodynamic system. Calculations of drift deposition agree fairly well with observations.

In 1973 an interdisciplinary study was undertaken of the environmental effects of the mechanical-draft cooling towers at the Oak Ridge Gaseous Diffusion Plant. Some results of this study are presented here (Alkezweeny, Glover, Lee, Sloot, and Wolf, this volume, and Taylor and Mann, this volume). Other results have been presented in lengthier reports.¹⁻⁴ Potential environmental problems are local fogging and deposition of chromate carried from the tower in drift water. The major problem in modeling plume rise and dispersion at this site is how to account for the merging of the individual plumes from the 60 cells. Photographs and deposition measurements are used to estimate the degree of plume merging at various distances from the towers. Models of visible plume length, fog frequency, and drift deposition are compared with observations.

SOURCE PARAMETERS

Figure 1 shows the size and location of the cooling towers. Each bank of towers is about 20 m high. The southernmost (K-31) bank is a crossflow tower

ATDL Contribution File No. 89.

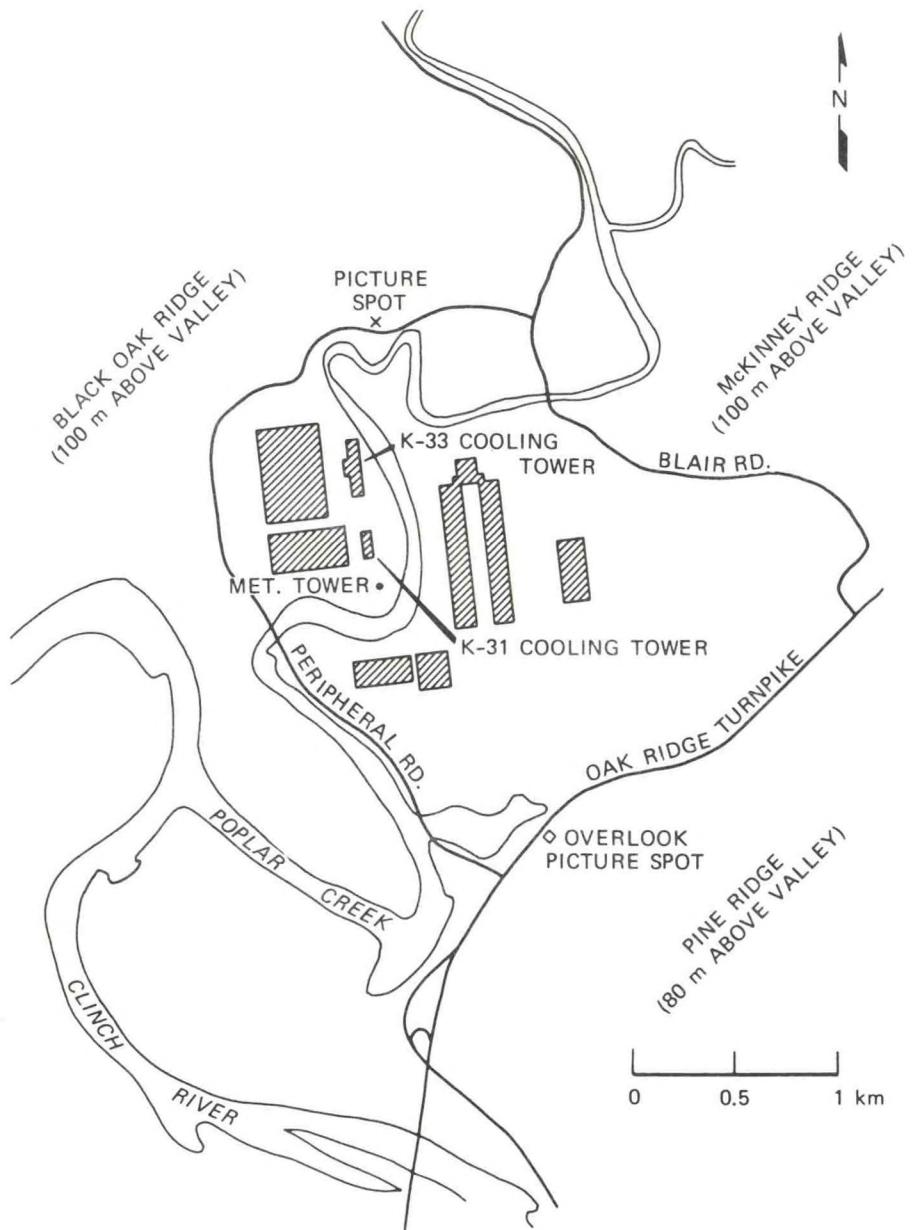


Fig. 1 Map of area around Oak Ridge Gaseous Diffusion Plant cooling towers.

containing 16 cells, and the northernmost (K-33) bank is a counterflow tower split into two sets of 22 cells each. During an intensive observation period in June 1973, the average radial distribution of vertical velocity (shown in Fig. 2) was measured on the K-31 cells. A typical temperature distribution is shown in Fig. 3. From these measurements we can calculate the initial buoyancy flux, F , and volume flux, V , as defined by Briggs:⁵

$$V = w_0 R_0^2 = 330 \text{ m}^3/\text{sec} \quad (1)$$

$$F = \frac{g}{T_{p0}} V(T_{p0} - T_{e0}) = 25 \text{ m}^4/\text{sec}^3 \quad (2)$$

where g is the acceleration of gravity and w_0 , R_0 , T_{p0} , and T_{e0} are the initial plume vertical speed, plume radius, plume temperature, and environmental temperature, respectively. At the time of these experiments, the total heat dissipation was only about 250 MW, which is a fraction of its normal value.¹ From our measurements, total volume flux was about $2600 \text{ m}^3/\text{sec}$ at the K-31 tower and about $2000 \text{ m}^3/\text{sec}$ at the K-33 tower. Total buoyancy flux was about

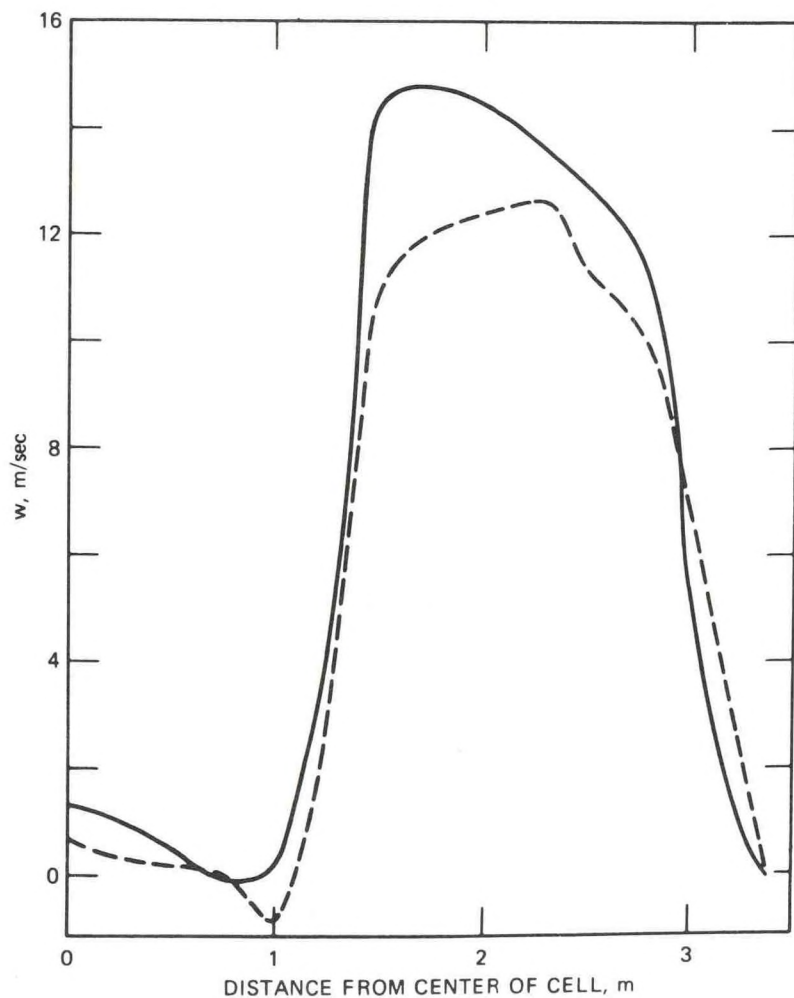


Fig. 2 Average updraft speed measured at the mouth of cell 6 of the K-31 cooling tower during the period June 25-June 29, 1973. —, Atmospheric Turbulence and Diffusion Laboratory. ---, Environmental Systems Corporation.

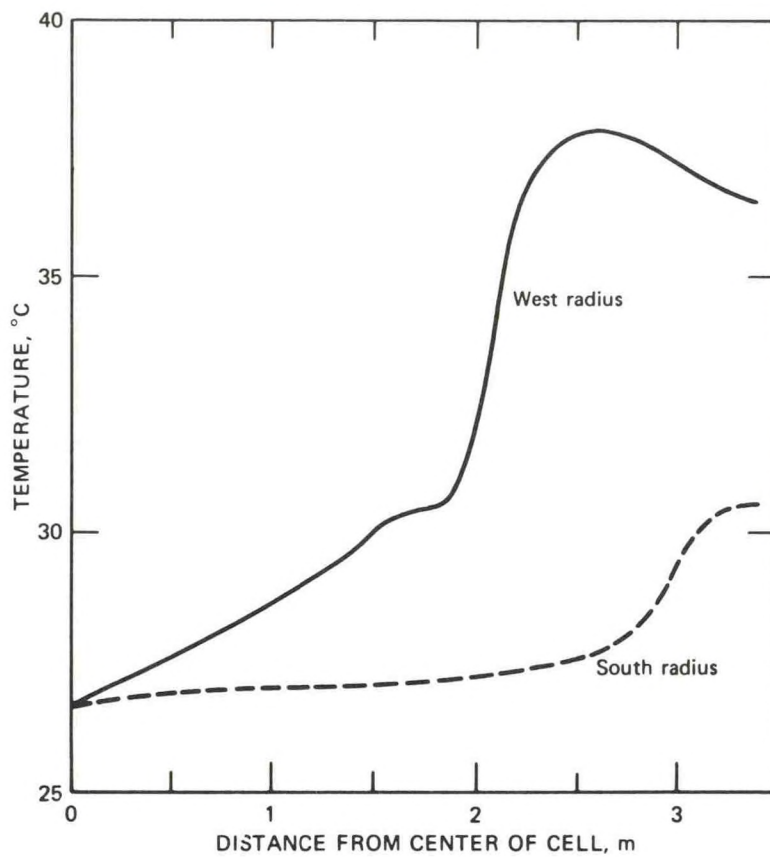


Fig. 3 Temperature distribution along west and south radii of cell 2 of the K-31 cooling tower at 10:00 a.m., June 27, 1973. Ambient temperature, 22°C; relative humidity, 83%; calm winds.

200 m⁴/sec³ at the K-31 tower and about 150 m⁴/sec³ at the K-33 tower. The energy released by latent heat was measured to be about five times the buoyancy flux.

A sensitive-paper technique devised by Engelmann⁶ was used to measure the size and flux of drift droplets. Our technique, which is most accurate for drops with diameters greater than about 500 μm, complements the concurrent measurements taken by Shofner, Schrecker, and Wilber,³ who could detect drops with diameters less than about 1000 μm. The composite drop-size spectrum is given in Fig. 4. Total drift flux from each cell of the K-31 tower is measured to be about 170 g/sec, giving a drift rate, or ratio of drift flux to circulating-water flux, of about 0.1%. This drift rate is high when compared with the rate at most modern towers. But these towers are about 20 years old and employ older, less efficient, drift eliminators. Total drift-water flux from the towers during the June experiment was about 2000 g/sec. Since the concentration of sodium dichromate in the drift water is 20 ppm, the flux of sodium dichromate to the air was about 0.04 g/sec.

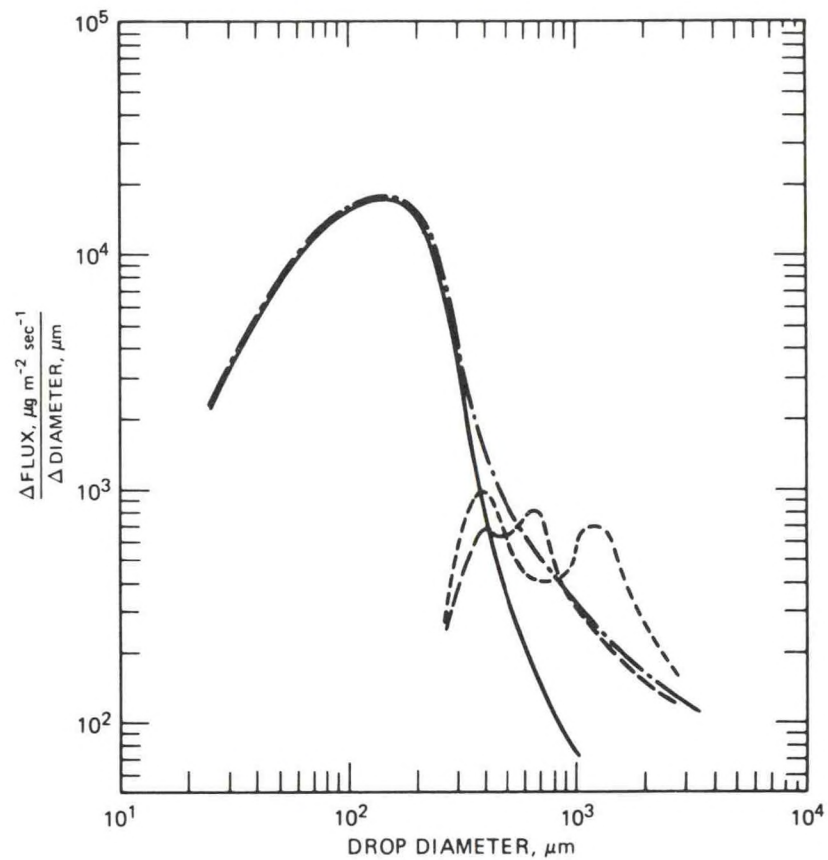


Fig. 4 Liquid-water flux per unit drop diameter, K-31 cooling tower. Week of June 25–29, 1973. —, Environmental Systems Corporation (ESC), average of all positions, diameter 1, cell 6. - - -, Atmospheric Turbulence and Diffusion Laboratory (ATDL), cell 6. - - - , ATDL, average over all cells. - - ., best fit to ESC and ATDL results.

DOWNWASH FREQUENCY

Two techniques were used to measure the frequency of downwash. In the first the plumes were photographed almost daily for a period of 4 months. In the second hygrothermographs were set in standard shelters 10 m east and west of the K-31 cooling tower. When downwash occurs, it causes an increase in temperature and humidity at the hygrothermograph that the plume touches. Wind speed and direction are measured at a height of 20 m on a pole located in a field about 100 m south of the K-31 tower.

Downwash is observed on the photographs about 65% of the time. In general, downwash is observed on the photographs when the wind speed exceeds about 3 m/sec. However, when the wind direction is within $\pm 10^\circ$ of the axis of the towers, downwash is not observed even for wind speeds as high as 5 m/sec. In this case, as suggested by Reisman,⁷ the towers present less of an obstacle to the wind and the plumes merge more easily.

During extreme downwash conditions, temperature differences as great as 3°C and relative humidity differences as great as 50% are observed between the hygrothermographs on either side of the tower. Downwash frequencies of about 40% are observed during the daytime and of about 30% during the nighttime. The frequency estimated from the hygrothermographs is lower than that estimated from the photographs since the plume sometimes downwashes on the photographs but does not quite descend to the level of the weather shelters.

Briggs⁸ suggests the following downwash criterion: if the product $4(w_0/U - 1.5)R_0$ is less than 1.5 times the building height, then downwash occurs; the parameter U is the wind speed. Thus the theoretical critical wind speed is about 2.4 m/sec, which is close to the observed critical wind speed of 3 m/sec. Currently we are studying the criterion for lift-off of a plume that has been brought to the ground by downwash. It appears that these plumes have sufficient buoyancy to continue rising once they escape the tower cavity region, which extends about 100 m downwind of the towers.

CLOUD DEVELOPMENT

From the photographs it is concluded that cloud development is initiated by the cooling-tower plumes about 10% of the time. On a cold afternoon (-5°C) in January, with nearly calm conditions, a cumulus cloud of 0.5 km depth was initiated at a height of 0.5 km. On rainy days the cooling towers form a stratus cloud that extends to the horizon. We are studying rainfall records from the Oak Ridge area to determine whether the presence of the towers has significantly increased local rainfall. On one occasion⁹ a light snowfall extending many kilometers downwind of the towers was reported.

VISIBLE PLUME LENGTH

The end of the visible plume is the point where the flux of excess water in the plume, $V_0 m_0$, is just equal to the flux of water necessary to saturate the plume, $V(m_s - m_e)$. The difference $(m_s - m_e)$ is commonly known as the saturation deficit. The parameters m_0 , m_s , and m_e are the initial, saturation, and environmental mixing ratios (grams of water per gram of air), respectively. The ratio of volume flux at height z to initial volume flux is given by Hanna:¹⁰

$$\frac{V}{V_0} = \left[1 + 0.5 \frac{z}{R_0} \left(\frac{U}{w_0} \right)^{1/2} \right]^2 \quad (\text{windy}) \quad (3)$$

$$\frac{V}{V_0} = \left(1 + 0.2 \frac{z}{R_0} \right)^2 \quad (\text{calm}) \quad (4)$$

Thus we obtain the following equations for the height and length of the visible plume under conditions of no downwash:

Windy:

$$\text{height } h' = 2 R_0 \left(\frac{w_0}{U} \right)^{\frac{1}{2}} \left[\left(\frac{m_0}{m_s - m_e} \right)^{\frac{1}{2}} - 1 \right] \quad (5)$$

$$\text{length } l' = 1.7 \frac{R_0^{\frac{3}{4}} U^{\frac{3}{4}} w_0^{\frac{3}{4}}}{F^{\frac{1}{2}}} \left| \left(\frac{m_0}{m_s - m_e} \right)^{\frac{1}{2}} - 1 \right|^{\frac{3}{2}} \quad (6)$$

Calm:

$$\text{height } h' = 5.0 R_0 \left[\left(\frac{m_0}{m_s - m_e} \right)^{\frac{1}{2}} - 1 \right] \quad (7)$$

Since it is assumed that environment conditions are constant with height, then these formulas should be applied only during well-mixed conditions at heights less than about 200 m.

First calculations with these formulas, using the radius and buoyancy flux of a single cell, yielded plume lengths and heights that were far too short. Clearly the cell plumes were merging. The photographs show that generally neighboring cell plumes merge by a distance of about 20 m from the tower. Plumes from the three banks of cells do not merge until they are several hundred meters from the tower. Consequently the predicted visible plume lengths and heights in Table 1 are calculated by assuming that the 16 cells of the K-31 tower combine. The effective buoyancy flux is then $400 \text{ m}^4/\text{sec}^3$ and the effective radius is $(16)^{\frac{1}{2}} \times R_0 = 13.6 \text{ m}$. Cases when downwash occurs are not considered in this table.

Good correlation is obtained in Table 1 between observed and calculated visible plume lengths and heights. The ratio of calculated to observed plume heights is 0.86. However, the ratio of calculated to observed plume length is 0.49. Apparently the plumes are merging in such a way that the actual visible plume length is greater than expected.

As another test, the purely empirical formulas

$$l' = \frac{a}{U(m_s - m_e)} \quad (8)$$

$$h' = \frac{b}{U(m_s - m_e)} \quad (9)$$

were compared with observations. The data in Figs. 5 and 6 suggest that, with a equal to $1.5 \text{ m}^2/\text{sec}$ and b equal to $1.0 \text{ m}^2/\text{sec}$, these formulas simulate the observations fairly well. Correlation coefficients between observed and calcu-

TABLE 1
CALCULATED AND OBSERVED VISIBLE PLUME LENGTH AND HEIGHT

Date	Observed plume length (l'_0), m	Calculated plume length (l'_c), m	Observed plume height (h'_0), m	Calculated plume height (h'_c), m
Dec. 29, 1972	Calm		150	90
Jan. 10, 1973	500	200	200	290
Jan. 11, 1973	Calm		200	210
Jan. 31, 1973	Calm		175	135
Feb. 1, 1973	250	100	200	155
Feb. 5, 1973	125	70	100	105
Feb. 6, 1973	100	40	75	80
Feb. 7, 1973	200	60	200	145
Feb. 26, 1973	Calm		75	81
Mar. 9, 1973	Calm		75	65
Mar. 12, 1973	Calm		50	35
Mar. 20, 1973	500	400	500	400
Apr. 8, 1973	150	70	100	105
Apr. 19, 1973	100	65	100	100
Apr. 26, 1973	1500	1450	500	330
May 10, 1973	Calm		400	240
May 17, 1973	700	430	500	680
$r(\text{obs.}, \text{calc.}) = 0.98$		$r(\text{obs.}, \text{calc.}) = 0.87$		
$l'_c/l'_0 = 0.49$		$h'_c/h'_0 = 0.86$		

lated values are 0.46 for visible plume length and 0.66 for visible plume height. The cases in which downwash occurs are included in this comparison. These empirical formulas work fairly well for this site and these conditions but should not be used at other sites.

FOG OCCURRENCE

Calculations were made of the extra hours per year that fog occurred owing to emissions of water from the cooling towers. At a dissipation rate of 1000 MW, there are 4.6×10^5 gps of water vapor emitted to the atmosphere. The Gaussian plume model, as integrated for a finite line source,¹¹ was applied to this problem.² During otherwise clear weather approximately 300 extra hours of fog per year were calculated to occur at distances less than 3 km from the towers in the direction of the dominant wind. However, there are several reasons why this figure is probably much too high. First, because of plume lift-off, a plume that initially suffers downwash may rise to heights of several hundred meters. Consequently our assumption that effective plume rise is 10 m during downwash

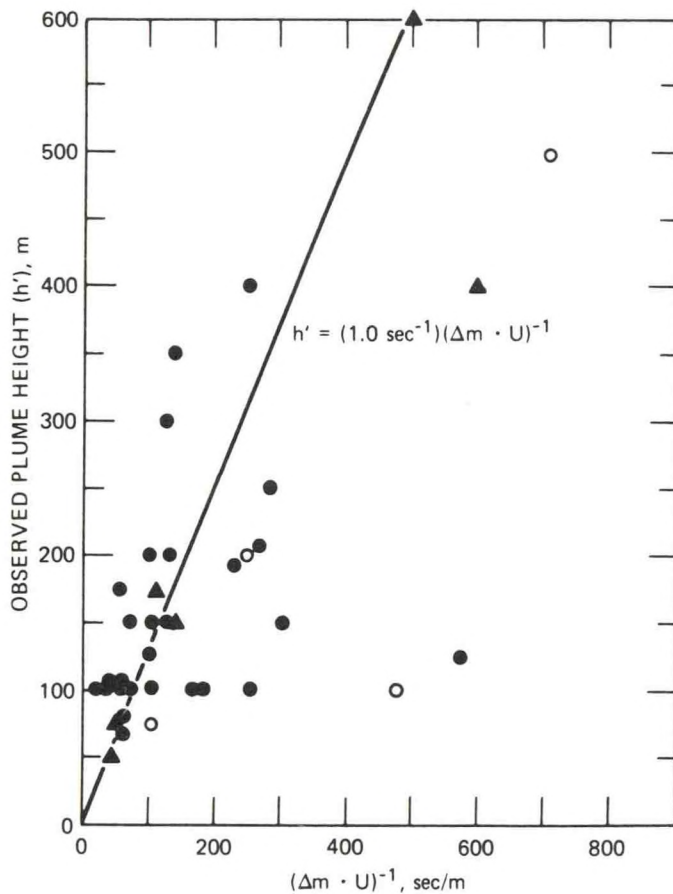


Fig. 5 Observed visible plume height as a function of $(\Delta m \cdot U)^{-1}$. ●, with downwash the correlation coefficient is 0.27. ○, with no downwash (windy) the correlation coefficient is 0.75. ▲, with no downwash (vertical plume) the correlation coefficient is 0.90. For all points the correlation coefficient is 0.66.

conditions will lead to overestimates of ground-fog occurrence. Second, when condensation occurs in a plume, latent heat is released and the plume follows the thermodynamic laws of cloud physics. Thus the Gaussian plume model, which assumes that the substance being modeled is inert, is no longer valid. On a typical day when the plume is visible for great distances, it looks like a long, narrow stratus cloud with a well-defined constant cloud base. Third, we have never observed the visible plume at the ground at distances greater than 0.5 km from the towers.

A good model for the dispersion of water should take into account thermodynamic processes. The Gaussian plume dispersion model will lead to calculations of fog occurrence which are too great. A cooling-tower plume provides modelers of cumulus clouds with an excellent controlled experiment since input heat and moisture fluxes are known accurately.

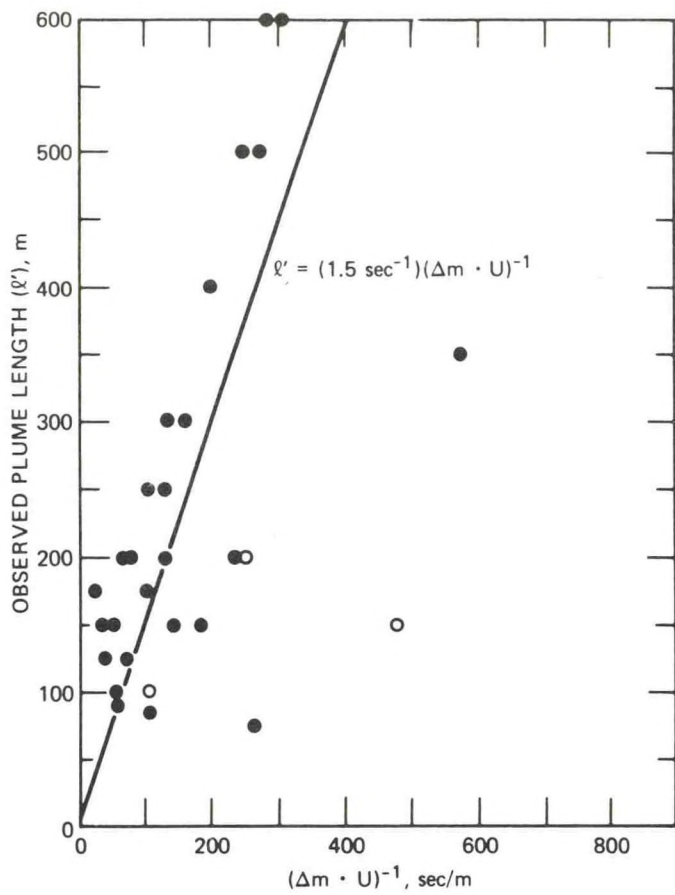


Fig. 6 Observed visible plume length as a function of $(\Delta m \cdot U)^{-1}$. ●, with downwash the correlation coefficient is 0.54. ○, with no downwash the correlation coefficient is 0.39. For all points the correlation coefficient is 0.46.

DRIFT DEPOSITION

During the last week of June 1973, measurements of drift deposition around the towers were taken by three groups.^{1,3,4} We used sensitive paper to detect drift deposition at a distance of 10 m from the towers. This technique is limited to drop sizes greater than about 500 μm , but close to the towers this limitation is not significant since only the largest drops fall out so close to the tower. Chromate deposition rate is calculated by multiplying the water deposition rate by the concentration of chromate.

Shofner et al.³ of Environmental Systems Corporation (ESC) measured drift deposition by the same method at distances of 15, 35, and 80 m from the towers. Their sensitive paper can detect smaller drops than ours, however. Lee, Sloot, and Wolf⁴ of Battelle, Pacific Northwest Laboratories (BPNL), measured dry chromate deposition at distances out to 1500 m from the tower.

Unfortunately the wind did not cooperate very well during this experiment, and the Battelle instruments were not often beneath the cooling-tower plume. The deposition measurements are given in Fig. 7.

A model of drift deposition was developed for comparison with the observations. It is assumed that the deposition rate out to distances of 50 m from the towers is due to emissions from a single cell (water flux, 170 gps) and that the deposition rate at distances greater than 500 m is a result of the merging of the plumes from all cells (water flux, 20×170 gps). The drop-size spectrum in Fig. 4 is divided into 14 regions, with calculations made for the median drop size in each range.

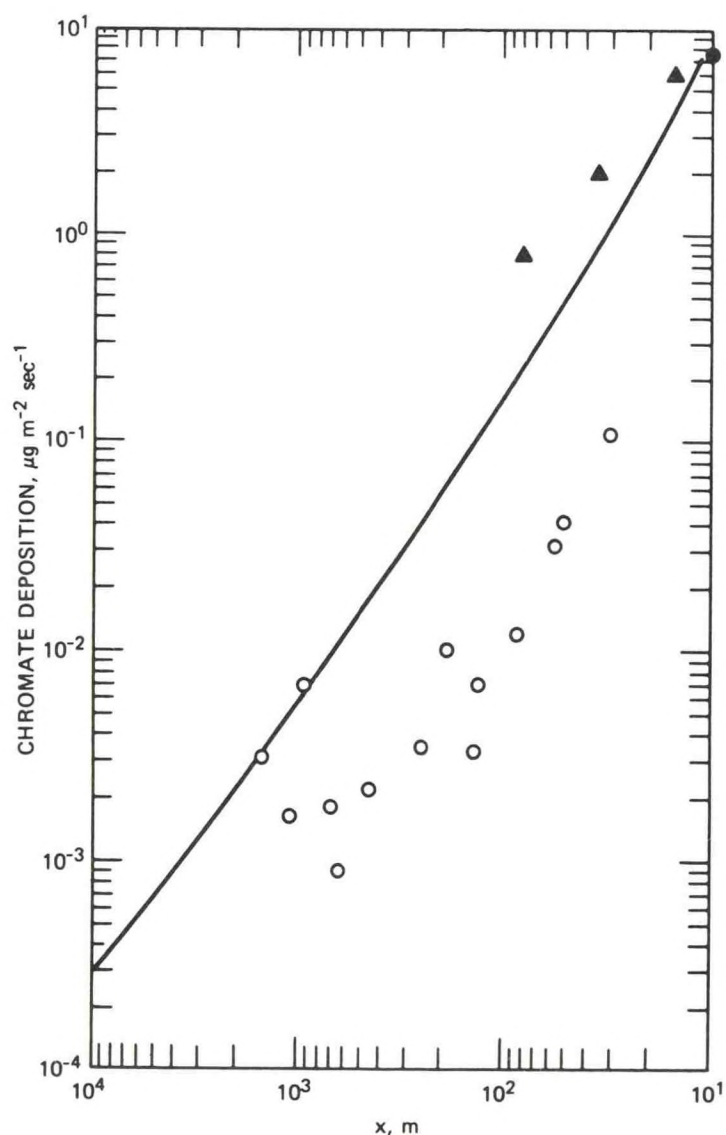


Fig. 7 Calculated drift-deposition rates. —, calculated. ●, Hanna and Perry.¹ ▲, Shofner, Schrecker, and Wilber.³ ○, Lee, Sloot, and Wolf.⁴

As recommended in the review by Hanna^{1,2} of methods for calculating drift deposition, if the final drop diameter is less than 200 μm , the drops are assumed to diffuse according to the Gaussian plume model,^{1,1} with the drop plume descending relative to the gaseous plume at a speed equal to the gravitational settling speed of the drops. To estimate settling speeds, Stokes' law is used for drops or particles with diameters less than 50 μm , and the table given by Engelmann^{1,3} is used for larger drops. Deposition rate for these smaller drops equals the concentration of chromate at the ground times the settling speed or the dry deposition speed, 1 cm/sec, whichever is larger.

Drops with diameters larger than 200 μm are assumed to start at the center of the cell opening and then follow a trajectory determined by their settling speed, the vertical speed of the plume, and the wind speed. While the drop is in the plume, it experiences a plume vertical speed given by⁵

$$w = \frac{0.48 \left[\frac{F_m}{(1/3 + U/w_0)^2 U} + \frac{4Fx}{U^2} \right]}{\left[\frac{F_m x}{(1/3 + U/w_0)^2 U^2} + \frac{2Fx^2}{U^3} \right]^{1/2}} \quad (10)$$

where F_m is proportional to the momentum flux:

$$F_m = w_0^2 R_0^2 \quad (11)$$

The vertical motion of the plume ceases at a distance, x^* , given by the equation

$$x^* = 50 F^{5/8} \quad (12)$$

where x^* is in meters and F is in m^4/sec^3

Entrainment of environmental air causes the plume radius, R , to increase. The ratio of the volume flux of plume air, $V(z) = UR^2$, at any height to the initial volume flux, $V_0 = w_0 R_0^2$, is given by Eq. 3 for $x < x^*$ and by the following equation for $x > x^*$.

$$\frac{V}{V_0} = \frac{U[R_0(w_0/U)^{1/2} + 0.5Z + C(x - x^*)]^2}{w_0 R_0^2} \quad (x > x^*) \quad (13)$$

where C is a constant proportional to the rate of plume spread after final rise, Z , is achieved at distance x^* .

The drop will evaporate at a rate dependent on its diameter, the mass of solute in it, and the saturation and actual vapor pressure of the environment.^{1,4,15}

$$\frac{dD}{dx} = \frac{-7 \times 10^{-10}}{UD} [1 + 0.59(DV_g)^{1/2}] \left(\frac{p_s e^{2.0 \times 10^{-7}/D}}{1 + 1.3 M_s/D^3} - p_e \right) \quad (14)$$

where D = drop diameter, cm

U = wind speed, cm/sec

V_g = drop settling speed, cm/sec

M_s = mass of solute in the drop, g

p_s = saturated environmental vapor pressure, dynes/cm²

p_e = actual environmental vapor pressure, dynes/cm²

It is assumed that the plume temperature equals the environmental temperature. Vapor pressure is related to the mixing ratio by

$$p = 1.57 \times 10^{-6} \times m \quad (15)$$

where p is in dynes/cm² and m is in g/g. Owing to entrainment, the vapor pressure, p_p , in the plume gradually decreases from a saturated value to the value in the air around the plume. Equations 3 and 13 are used to calculate the entrainment.

Using the above techniques, we can calculate the distance from the tower at which the median-size drop of each drop size range strikes the ground. Constant wind speed and direction are assumed. Deposition is assumed to occur uniformly in a $22\frac{1}{2}^\circ$ sector bounded by the distances halfway between the distances at which the drops strike the ground. One of the drawbacks of this method is that it is difficult to determine the area over which the drops of a given size range are deposited.

Another drawback is the assumption that all drops originate from the center of the cell. As a result, if the relative humidity is less than about 70%, there is a definite critical drop size. Drops above the critical size fall from the plume and strike the ground less than 100 m from the tower. Drops below the critical size remain in the plume and evaporate, and the resulting dry particles do not strike the ground within 50 km of the towers. To improve on this assumption, we should calculate several trajectories for a drop of a given size, varying the position of the beginning point of each trajectory across the cell mouth. Probably a more serious drawback, however, is that we do not know the rate at which the plumes merge with downwind distance.

Figure 7 gives the calculated drift-deposition rates. Deposition rates are interpolated between the curve for a single cell at x equal to 50 m and the curve for 20 cells at x equal to 500 m. Environmental conditions typical of those during the June experiment are assumed: $m_s = 0.0238$, $m_e = 0.0138$, and $U = 150$ cm/sec. Input source parameters have already been outlined in this paper and in the more complete reports.^{1,2}

The calculated and observed deposition rates agree fairly well at distances of 10 and 15 m, where it is likely that only one cell influences the deposition. The ESC (Ref. 3) measurements at distances of 35 and 80 m are about a factor of 2 greater than the calculated deposition rate, possibly because their sensitive paper was tilted a few degrees from the horizontal.

Since the ESC sensors were moved to ensure that they were always beneath the plume, their measurements at these distances are greater than the BPNL (Ref. 4) measurements, which were taken from positions fixed during the week-long experiment. Owing to the variability of the wind, the BPNL sensors were beneath the plume only a fraction of the time. Consequently their measured drift-deposition rates are an order of magnitude less than the calculated plume center-line deposition rates. If we assume that the plume blew over the BPNL sensors only 10% of the time, then calculated and observed deposition rates agree within a factor of 2. The observations and the model estimates are therefore reconcilable at distances from 10 to 1500 m from the tower. The model is now being used to calculate average annual deposition rates for comparison with measurements by Taylor and Mann (this volume) of chromate accumulation in vegetation and soil near the towers.

FURTHER COMMENTS

It must be stressed that calculations of fog concentration and drift deposition from cooling towers are highly tentative. Irregular source geometries and thermodynamic processes make the usual diffusion and trajectory calculations uncertain. Extensive measurements of diffusion and drift deposition from cooling towers, including detailed measurements of source terms and environmental parameters, are necessary before these calculations are regarded as firm bases for legal decisions.

ACKNOWLEDGMENTS

This research was performed under an agreement between the National Oceanic and Atmospheric Administration and the U. S. Atomic Energy Commission. The assistance of G. A. Briggs, W. M. Culkowski, and S. G. Perry of this laboratory is greatly appreciated. The experiment would not have been possible without the efforts of G. Kidd and T. Shapiro of the Oak Ridge Gaseous Diffusion Plant.

REFERENCES

1. S. R. Hanna and S. G. Perry, Meteorological Effects of the Cooling Towers at the Oak Ridge Gaseous Diffusion Plant. I. Description of Source Parameters and Analysis of Plume Photographs and Hygrothermograph Records, ATDL Contribution No. 86, Atmospheric Turbulence and Diffusion Laboratory, 1973.
2. S. R. Hanna, Meteorological Effects of the Cooling Towers at the Oak Ridge Gaseous Diffusion Plant. II. Fog Occurrence and Drift Deposition, ATDL Contribution No. 88, Atmospheric Turbulence and Diffusion Laboratory, 1974.
3. F. M. Shofner, G. O. Schrecker, and K. R. Wilber, Characterization of Drift Emissions and Drift Transport for Representative Cells of K-31 and K-33 Cooling Towers, Final Report Prepared for Union Carbide Nuclear Company by Environmental Systems Corporation, 1973.

4. R. N. Lee, J. W. Sloot, and M. A. Wolf, Measurements of Chromate Resulting from Cooling Tower Drift at the Oak Ridge Gaseous Diffusion Plant, Final Report Prepared for Union Carbide Nuclear Company by Battelle, Pacific Northwest Laboratories, 1973.
5. G. A. Briggs, Plume Rise, AEC Critical Review Series, Report TID-24635, 1969.
6. R. J. Engelmann, The Hanford Raindrop Sampler and Selected Spectra, USAEC Report HW-73119, General Electric Company, Hanford Atomic Products Operation, 1962.
7. J. I. Reisman, A Study of Cooling Tower Recirculation, Presented at *Winter Annual Meeting of American Society of Mechanical Engineers*, New York, Nov. 26–30, 1972, American Society of Mechanical Engineers, New York.
8. G. A. Briggs, Diffusion Estimation for Small Emissions, ATDL Contribution No. 79, Atmospheric Turbulence and Diffusion Laboratory, 1974.
9. W. M. Culkowski, An Anomalous Snow at Oak Ridge, Tennessee, *Mon. Weather Rev.*, 90(5): 194-196 (May 1962).
10. S. R. Hanna, Rise and Condensation of Large Cooling Tower Plumes, *J. Appl. Meteorol.*, 11: 793-799 (1972).
11. F. A. Gifford, Jr., An Outline of Theories of Diffusion in the Lower Layers of the Atmosphere, in *Meteorology and Atomic Energy—1968*, D. H. Slade (Ed.), USAEC Report TID-24190, pp. 66-105, July 1968.
12. S. R. Hanna, Fog and Drift Deposition from Evaporative Cooling Towers, *Nucl. Safety*, 15(2): 190-196 (March–April 1974).
13. R. J. Engelmann, The Calculation of Precipitation Scavenging, in *Meteorology and Atomic Energy—1968*, D. H. Slade (Ed.), USAEC Report TID-24190, pp. 208-221, July 1968.
14. N. H. Fletcher, *The Physics of Rainclouds*, Cambridge University Press, New York, 1962.
15. R. G. Fleagle and J. A. Businger, *An Introduction to Atmospheric Physics*, pp. 79-108, Academic Press, Inc., New York, 1963.

DISCUSSION

Slinn: Steve, three questions: First, in your Gaussian plume model, in addition to tower height and the settling term, did you account for the plume's trajectory, $h = h(x)$, for example, using the " $\frac{2}{3}$ law"? Second, you stated that you have seen plumes coast along underneath a stratus deck without spreading as much as you expected, but what about the point of view: if there was a stratus deck, then the atmosphere was probably quite stable and therefore the σ 's would be small? Third, where did you let the drops break free from the plume?

Hanna: The drops are all assumed to start their travel on the axis of the plume, which is rising according to the $\frac{2}{3}$ law, and break out of the plume when they settle a distance equal to the plume radius. The atmosphere beneath a stratus deck is usually well mixed.

Hales: In response to Slinn's question, the lapse rate within a stratus cloud typically is saturated adiabatic. The lapse rate below a stratus cloud typically is unsaturated adiabatic. Thus a stratus cloud is typically in and above neutral (i.e., dry and saturated adiabatic) lapse rates. Typically the stratus cloud is capped by an inversion. Some such inversions may be very small.

Manning: At the time of the early photographs, where the plumes settled to the ground in the downwash, was any ice present? Were any agricultural effects measured or detected from the chromate fallout?

Hanna: Icing was not observed. Agricultural effects are reported by Taylor et al. (this volume).

Overcamp: What techniques were used to measure the drift deposition by the three research groups?

Hanna: Drift deposition was measured by our group and by Environmental Systems Corporation using droplet imprints on sensitive paper exposed to the drift in a horizontal position for several seconds. Knowing the water deposition and the concentration of chromate in the water, we could estimate the chromate deposition. Battelle collected the chromate deposited on a plate and estimated the total amount of drift deposition by chemical analysis.

Shapiro: Snowfall reported as the contribution of the Oak Ridge Gaseous Diffusion Plant towers was observed only once during a period of 30 years of operation. Icing of plant roads in the vicinity of the towers has not occurred, although freezing temperatures are experienced in winter.

Has there been any attempt to distinguish whether large droplets visually observed at the top of the tower are actually drift (contain salts) or are actually condensate drops that have blown off structural members?

Hanna: The chemistry group at the Gaseous Diffusion Plant attempted unsuccessfully to find chromate in the residue left on the sensitive paper by single drift drops. Possibly the lack of success is due to the fact that at 20 ppm concentration only about 10^{-11} g of chromate would be left on the paper by a 100- μm -diameter drift drop.

Gifford: The snowfall observed near the Oak Ridge Gaseous Diffusion Plant was reported by Culkowski [*Mon. Weather Rev.*, **90**: 914-916 (May 1962)]. Fortunately, as it turns out we used the word "anomalous" in the title, though at the time I confidently expected this to occur once or twice every winter. The snowfall was about a mile wide and 16 miles long, and in spots it was nearly an inch deep. As far as we know, it has not happened again, at least to this degree. We should probably try to figure out why—though at the time nothing especially unusual seemed to be going on meteorologically.

Carson: How do the operating conditions (water temperature, approach range, etc.) of the Oak Ridge towers compare with those of nuclear power plants?

How are such things as plume rise, downwash, etc., affected by these differences?

Shapiro: I believe that I can answer Carson's question. Cooling-tower operation at the AEC diffusion plants differs from normal power plants in two significant ways:

1. At diffusion plants the water temperatures are higher than for power cycles by about 25° F.

2. The water contains water-treatment chemicals, such as zinc and chromium, for corrosion inhibition which are generally not necessary under power-generating conditions.

RELATING EMISSIONS TO AIR QUALITY IN TENNESSEE

by

Steven R. Hanna
Air Resources

Atmospheric Turbulence and Diffusion Laboratory
National Oceanic and Atmospheric Administration
Post Office Box E
Oak Ridge, Tennessee 37830

March 1974

Abstract

Average annual emissions of suspended particles, SO_2 , and CO from each of the 95 counties in Tennessee during 1970 are compared with observed air quality. Due to the location of air monitoring instruments close to large local sources, the readings of these instruments are found to be usually not representative of regional air quality. In order to adequately test regional dispersion models in Tennessee, it is necessary to install additional air monitoring stations that are not influenced by large local sources.

The variations of county pollutant concentrations across the state are generally within a factor of three, while the variations of county pollutant emissions are generally over several orders of magnitude. The wind speed therefore strongly controls the day-to-day background level of air pollution in the state.

To be published as a chapter in the 1975 edition of Industrial Air Pollution Control, edited by K. Noll and published by Ann Arbor Science Publishers.

1. Introduction

When modeling diffusion on regional scales (length scales greater than about 10 km), it is necessary to account for topography and changing meteorological conditions along the trajectory of the pollutant. Many sources and receptors are usually included in the model. We are currently developing a regional diffusion model which will be solved numerically on a large digital computer. This model will first be used to estimate diffusion in the Tennessee valley. However, at the same time that the model is being developed, it is necessary to study existing emissions and air quality data. Hopefully, certain patterns between emissions and air quality will be revealed.

In this report, data from the 95 counties in Tennessee are analyzed. These data were collected by the state in 1970 in order to comply with federal regulations and develop the Air Pollution Control Implementation Plan (1972). Average annual emissions of suspended particles, SO_2 , CO, NO_x , and hydrocarbons are published. In the four major metropolitan areas (Memphis-Shelby Co., Nashville-Davidson Co., Chattanooga-Hamilton Co., and Knoxville-Knox Co.), more detailed emissions and air quality were obtained. Air quality data for suspended particles and SO_2 were collected in about one third of the counties. In almost all cases, air monitoring instruments were intentionally located near the pollution sources. Consequently, there are very few stations which represent rural areas. In 1970, only a handful of CO, NO_x , hydrocarbon, and ozone data were collected.

More data are currently being collected, but is not in a form suitable for analysis. The 95 counties are listed in Table 1, along with their areas and populations, and suspended particle emissions.

We have developed a simple urban dispersion model (Hanna, 1972, Gifford and Hanna, 1973) which states that concentration, $x(\mu\text{g}/\text{m}^3)$, is directly proportional to area emissions, $Q(\text{g}/\text{m}^2 \text{sec})$, and inversely proportional to wind speed, $U(\text{m}/\text{s})$:

$$x = C \frac{Q}{U} \quad (1)$$

where C is a dimensionless parameter, roughly equal to the region length divided by the depth of the pollutant cloud. This formula is intended for use in urban areas, but can be applied to regional data in order to determine rough relationships between emissions and air quality. The Tennessee data are used to work backwards in equation (1) and estimate the parameter C . The correlation between published emissions, Q , and concentrations, x , is also studied.

2. Suspended Particles Data Analysis

Suspended particles are studied first because there are more data available for this pollutant. Furthermore, chemical transformations are generally unimportant since most suspended particles are inert. Dry deposition and precipitation washout are the main

mechanisms for removal of suspended particles from the atmosphere. The emissions data for suspended particles are listed in Table 1. So that the data can be compared on a common basis, emissions per unit area are given. Emissions per capita are calculated and listed in the table in order to determine whether it is possible to estimate suspended particles emissions as a function of population. The emissions rate for each county is plotted as a function of population in Figure 1. There is a great deal of scatter among the data. For counties with populations less than 10,000, the relation

$$\text{Emissions} = 8 \times 10^{-4} \text{ g/sec} \times \text{population}$$

is accurate within about a factor of two. But for counties with populations in the middle of the range no such relationship is valid, since emissions are dependent on the type of industry in the county rather than on the population. For example, among counties with populations of about 30,000, emissions range over three orders of magnitude. In the four metropolitan areas, however, the relation

$$\text{Emissions} = 3 \times 10^{-2} \text{ g/sec} \times \text{population}$$

is accurate within about a factor of three. Apparently the degree of industrialization in large Tennessee cities is fairly uniform.

The map of Tennessee in Figure 2 contains the county by county emissions and air quality data for suspended particles. It is seen that the Tennessee valley region in the eastern part of the state has the highest emissions per unit area. Average emissions over the state are $.17 \text{ g/km}^2 \text{ sec}$. Observed annual average suspended particle concentrations for some counties are also given on the figure. In the counties where there was more than one monitoring station, the number given is the average over all the stations. It is interesting that while the county emissions vary over three orders of magnitude, the observed concentrations vary only by a factor of three, from $50 \mu\text{g/m}^3$ to $154 \mu\text{g/m}^3$. The small variation in concentrations is partly due to the continual presence of a "background" amount of suspended particles, whose origin is natural and man-made sources upwind of the region. The annual average background of suspended particles in Roane County was found by Hanna (1973) to equal about $40 \mu\text{g/m}^3$, which agrees reasonably well with the minimum observed in this study. Two stations in suburban Davidson County registered annual average suspended particle concentration of about $40 \mu\text{g/m}^3$.

Emissions and air quality are not well correlated in Figure 3, which suggests that the air monitoring stations were not situated so that their measurements would represent the regional average. Instead, most of the monitoring stations were intentionally located close to large pollution sources. Consequently the three highest

concentrations were recorded in counties with very low total emissions. To record a truly representative regional average using a single monitor, it is necessary to locate the monitor far enough from large point sources that they do not strongly influence the measurement.

If it is assumed that the background concentration of suspended particles is $40 \mu\text{g}/\text{m}^3$, then the average contribution to the suspended particle concentration due to sources in the region is about $50 \mu\text{g}/\text{m}^3$. Thus the dimensionless parameter C in equation (1) can be calculated to equal

$$C = \frac{\chi U}{Q} = \frac{5 \times 10^{-5} \text{ g}/\text{m}^3 \times 3 \text{ m/s}}{1.7 \times 10^{-7} \text{ g}/\text{m}^2 \text{s}} = 880 .$$

In urban areas, Gifford and Hanna (1973) find that C equals about 220. If we interpret C as the ratio of the region length to the depth of the pollution cloud, and assume that the depth of the pollution cloud is about 1 km, then the region length is about 880 km. This is roughly the length of Tennessee along the dominant wind direction.

3. Carbon Monoxide Data Analysis

Carbon Monoxide (CO), which is the most inert of the three substances studied in this report, is emitted mainly from cars and trucks. Tennessee emissions of CO during 1970 averaged $.63 \text{ g}/\text{km}^2 \text{ sec}$ and were more evenly distributed than emissions of suspended particles. County CO emissions plotted in Figure 4

vary by a factor of only about 20 and are better correlated with population than suspended particle emissions. Again, the Tennessee valley region has significantly higher emission rates than the rest of the state. The only two available 1970 measurements of CO concentration are in Memphis (1.6 ppm) and Nashville (1.5 ppm). Since these air quality data are taken near highways in large cities, they are not representative of the region. Using equation (1) and assuming that C equals 880, it is possible to predict the expected annual average contribution of Tennessee to the total concentration of CO:

$$x = 880 \frac{Q}{U} = 880 \frac{.62 \times 10^{-6} \text{ g/m}^2 \text{ s}}{3 \text{ m/s}} = 182 \frac{\text{ug}}{\text{m}^3}$$

or .15 ppm

The background concentration of CO is approximately equal to this value (see Air Quality Criteria for CO, 1970). Thus the total regional CO concentration is expected to be about .3 ppm.

4. Sulfur Dioxide Data Analysis

Chemical transformations to sulfates cause sulfur dioxide (SO_2) to be a non-conservative pollutant. Its average annual emission rate over Tennessee is $.37 \text{ g/km}^2 \text{ s}$. About two-thirds of the SO_2 emissions in Tennessee is from the TVA power plants, whose tall stacks and buoyant plume rise cause the pollution to be discharged at an effective height of from 200 to 500 m above the surface. These power plants were designed so that local, ground-level

air quality criteria for SO_2 are not exceeded. However, the great amounts of SO_2 emitted by these plants contribute to the gross flux of SO_2 over the state.

County emissions and air quality observations of SO_2 are listed in Figure 5. The heaviest SO_2 emissions are from the Tennessee valley. The highest (by far) annual SO_2 concentration is $240 \mu\text{g}/\text{m}^3$ in Copperhill in Polk County. This monitor is located too close to a large smelter to be of use in estimating a regional average. With the exception of this figure, the average SO_2 concentration in Tennessee is $21 \mu\text{g}/\text{m}^3$. As is true for suspended particles and CO, the air quality monitors were usually placed in towns or close to large sources, so that the resulting observations are not representative of regions. Consequently there is poor correlation between observed concentrations and emissions. Instrumental errors may also contribute to this lack of correlation. For example, it is difficult to believe that the lowest SO_2 concentration ($10 \mu\text{g}/\text{m}^3$) would occur in Shelby County, in which Memphis is located.

From these data, the parameter C is calculated to have the value:

$$C = \frac{XU}{Q} = \frac{21 \times 10^{-6} \text{ g}/\text{m}^3 \times 3 \text{ m/s}}{.37 \times 10^{-6} \text{ g}/\text{m}^2 \text{ s}} = 170 .$$

This number is about a factor of five less than the value for C calculated for suspended particles. Gifford and Hanna (1973) found the same difference using pollution data from many urban areas, and attributed part of the difference to the fact that SO_2 is

generally emitted much higher in the atmosphere than suspended particles. Consequently ground level concentrations of SO_2 are relatively low. Chemical transformations further remove SO_2 relative to suspended particles.

Removal by dry deposition and precipitation washout is also important. Hanna (1973) developed the following rough approximation for accounting for deposition and washout:

$$\chi = C \frac{Q}{U} / \left(1 + C \frac{V_d}{U} + \frac{\Lambda \Delta x}{U} \right), \quad (2)$$

where V_d (m/s) is the dry deposition speed, $\Lambda(\text{s}^{-1})$ is the washout coefficient, and Δx is the region length. Letting C , Δx , and V_d equal 880, 800 km, and .001 m/s, respectively, we find that dry deposition can decrease the flux of pollutant over Tennessee by about 25%. During rainy periods, it can be assumed that Λ equals 10^{-4} s^{-1} , and consequently about 95% of the flux of pollutant over Tennessee is carried to the surface by rain.

5. Further Comments

While the emissions data for NO_x and hydrocarbons are fairly complete, there are very few air quality measurements of these substances. A revised emissions inventory is currently being compiled, and there are now more extensive and more accurate air monitoring instruments in operation. However, it is clear from this study that the air monitoring instruments do not represent regional air quality, defined as the average ground level pollutant concentration over a county. Instead, the monitoring instruments were usually placed

in the largest town in the county, close to major pollution sources. A few instruments should be located in rural or suburban areas, or at least sufficiently far from major sources that they do not dominate the reading at that station.

The annual average concentrations of SO_2 and suspended particles, reported on Figures 2 and 5, do not vary much across the state. Thus, from equation (1), the wind speed governs the general level of air pollution in a region on a day to day basis. The main use of a regional diffusion model would be to account for perturbations on this background due to local sources.

Acknowledgements: The assistance of D. Neeley and B. Barnard of the Tennessee Division of Air Pollution Control is greatly appreciated. This research was performed under an agreement between the National Oceanic and Atmospheric Administration and the U. S. Atomic Energy Commission.

References:

1. Air Pollution Control Implementation Plan, 1972, Tennessee Department of Public Health, Div. of Air Poll. Control, Cordell Hull Bldg., Nashville, Tenn. 37219.
2. Air Quality Criteria for Carbon Monoxide, 1970, NAPCA Publ. No. AP-62 (\$1.50), from Supt. of Documents, U. S. Govt. Printing Office, Washington, D. C. 20402.
3. Gifford, F. A., Jr. and S. R. Hanna, 1973: Modeling urban air pollution. Atmos. Envir. 7, 131-136.

4. Hanna, S. R., 1972: A simple model of calculating dispersion from urban area sources. J. Air Poll. Control Assoc., 21, 774-777.
5. Hanna, S. R., 1973: Application of a simple dispersion model to a rural industrial region. Presented at the Third Ann. Indust. Air Poll. Control. Conf., March 29-30, Knoxville, Tenn., 14 pp.

Table 1

1970 Suspended Particles Emission for the Counties of Tennessee

County	Area (km ²)	Population	Suspended Particle Emissions (g/s)	Emissions per capita (mg/s person)	Emission per unit area (g/s km ²)
Anderson	858	60,300	160	2.65	.186
Blount	1472	63,744	99.0	1.56	.0672
Bradley	856	50,686	16.3	0.317	.019
Campbell	1154	26,045	35.9	1.38	.031
Carter	891	43,259	354	8.18	.397
Claiborne	1137	19,420	11.1	5.73	.00976
Cocke	1085	25,283	22.8	0.893	.0210
Grainger	722	13,948	7.34	0.518	.0102
Greene	1570	47,630	22.0	0.461	.0140
Hamblen	397	38,696	380	9.82	.957
Hancock	589	6,719	3.80	0.576	.00645
Hawkins	1229	33,757	2466	72.6	2.00
Jefferson	702	24,940	13.9	0.547	.0198
Johnson	750	11,569	6.74	0.576	.00899
Loudon	606	24,266	16.4	0.691	.0271
McMinn	1106	35,462	53.0	1.50	.0479
Meigs	488	5,219	6.91	1.32	.0142
Monroe	1690	23,475	51.6	2.19	.0305
Polk	1110	11,669	34.4	2.94	.0310
Phea	798	17,202	11.0	0.63	.0138
Roane	897	38,881	581	14.9	.648
Sevier	1530	28,241	11.5	0.403	.00752
Sullivan	1060	127,329	1634	12.8	1.54
Unicoi	473	15,254	7.20	0.461	.0152
Union	543	9,072	4.38	0.490	.00807
Washington	827	73,924	53.8	0.720	.0651
Bledsoe	1033	7,643	5.64	0.749	.00546
Coffee	1110	32,572	61.8	1.90	.0557
Cumberland	1738	20,733	21.7	1.04	.0125
Fentress	1275	12,593	32.9	2.62	.0258
Franklin	1416	27,289	218	8.01	.154
Grundy	917	10,631	6.62	0.634	.0072

Table 1 (continued)

County	Area (km ²)	Population	Suspended Particle Emissions (g/s)	Emissions per capita (mg/s person)	Emission per unit area (g/s km ²)
Marion	1295	20,577	873	42.3	.674
Morgan	1380	13,619	17.2	1.27	.0125
Overton	1128	14,866	13.9	0.922	.0123
Pickett	404	3,774	2.45	0.662	.00606
Putnam	1037	35,487	18.3	0.518	.0176
Scott	1392	14,762	14.4	0.979	.0103
Sequatchie	699	6,331	7.11	1.12	.0102
Van Buren	651	3,758	7.03	1.87	.0108
Warren	1124	26,972	26.4	0.979	.0235
White	978	16,355	124	7.57	.127
Bedford	1233	25,039	7.2	0.288	.00589
Cannon	695	8,467	22.5	2.65	.0324
Cheatham	781	13,199	6.85	0.518	.00878
Clay	596	6,624	12.7	1.93	.0213
DeKalb	711	11,151	62.0	5.56	.0872
Dickson	1241	21,977	24.6	1.12	.0198
Giles	1585	22,138	21.2	0.950	.0134
Hickman	1562	12,096	4.09	0.346	.00262
Houston	514	5,853	3.28	0.547	.00638
Humphreys	1358	13,560	3661	279.	2.70
Jackson	817	8,141	3.83	0.461	.00469
Lawrence	1623	29,097	5.67	0.196	.00349
Lewis	730	6,761	2.59	0.374	.00355
Lincoln	1485	24,318	12.9	0.518	.00869
Macon	778	12,315	37.1	3.02	.0477
Marshall	965	17,319	28.1	1.61	.0291
Maury	1582	44,028	1318	29.7	.833
Montgomery	1381	62,721	17.8	0.288	.0129
Moore	317	3,568	2.48	0.691	.0078
Perry	1051	5,238	4.58	0.864	.00436
Robertson	1219	29,102	155	5.33	.127
Rutherford	1566	59,428	26.3	0.432	.0168
Smith	817	12,509	48.4	3.89	.0592

Table 1 (continued)

County	Area (km ²)	Population	Suspended Particle Emissions (g/s)	Emissions per capita (mg/s person)	Emission per unit area (g/s km ²)
Stewart	1204	7,319	7.63	1.04	.00634
Sumner	1367	56,284	248	4.41	.181
Trousdale	292	5,155	3.11	0.605	.0107
Wayne	1892	12,365	5.56	0.461	.00293
Williamson	1520	34,423	9.59	0.276	.00631
Wilson	1452	36,999	30.1	0.806	.0207
Benton	1002	12,126	27.5	2.28	.0274
Carroll	1526	25,741	9.87	0.374	.00647
Chester	730	9,927	4.26	0.432	.00583
Crockett	689	14,402	8.84	0.605	.0128
Decatur	863	9,457	3.66	0.374	.0042
Dyer	1355	30,427	12.5	0.403	.00923
Fayette	1802	22,692	10.3	0.461	.00572
Gibson	1554	47,871	57.9	1.21	.0373
Hardeman	1680	22,435	13.3	0.605	.00792
Hardin	1502	18,212	45.4	2.51	.0302
Haywood	1330	19,596	8.96	0.461	.00674
Henderson	1319	17,360	7.49	0.432	.00568
Henry	1452	23,749	231	9.73	.159
Lake	428	8,091	5.52	0.691	.0129
Lauderdale	1220	20,271	8.35	0.403	.00684
Madison	1435	65,774	36.9	0.547	.0257
McNairy	1457	18,369	7.92	0.432	.00544
Obion	1424	29,936	10.3	0.346	.00723
Tipton	1175	28,001	15.6	0.547	.0133
Weakley	1474	28,827	40.3	1.41	.0273
Shelby	1930	722,111	1460	0.0576	.756
Davidson	1300	447,877	754	0.0490	.580
Hamilton	1408	254,236	478	0.0547	.339
Knox	1300	276,293	1385	0.150	1.07

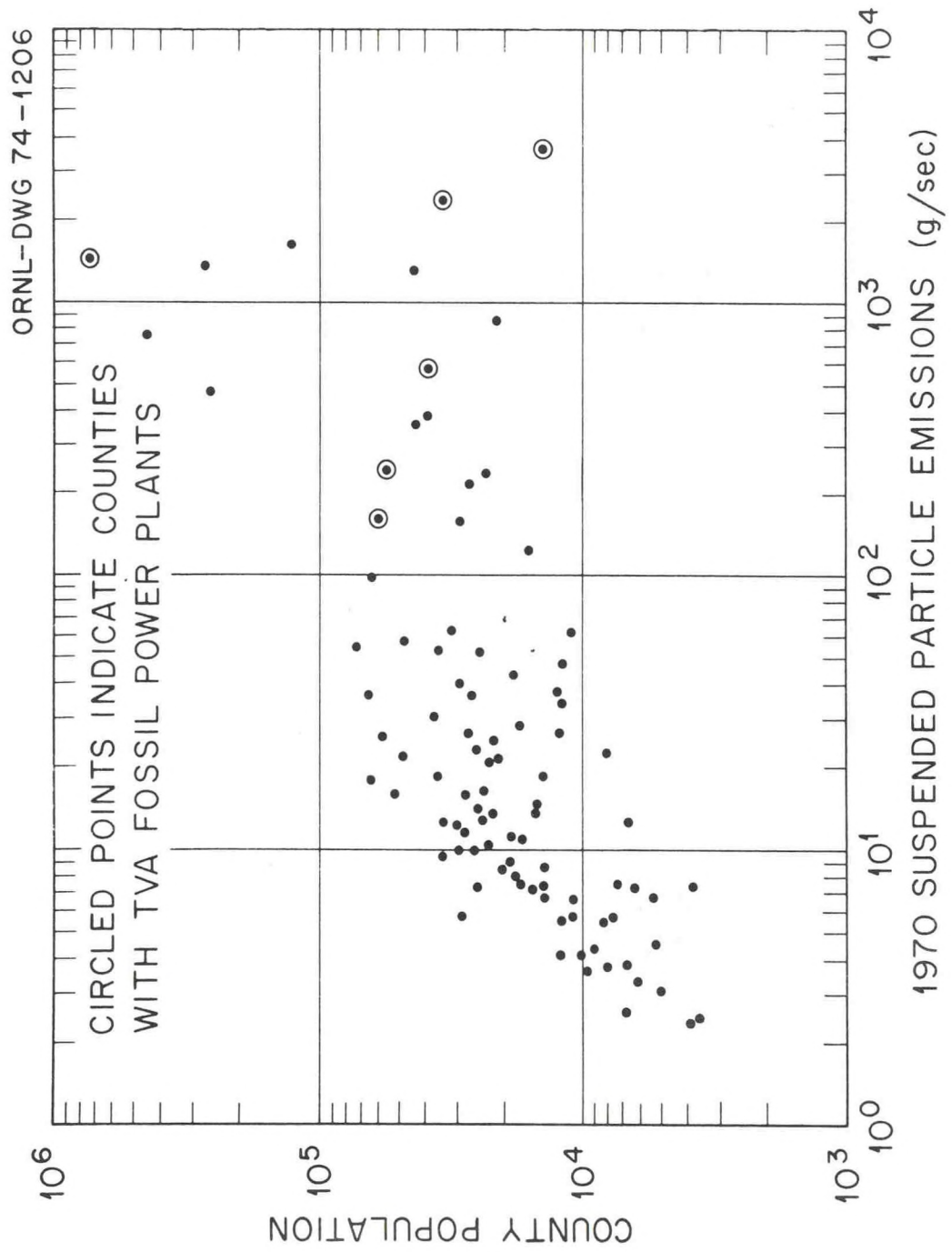


Figure 1: County emission rates (g/s) of suspended particles as a function of population (1970 data).

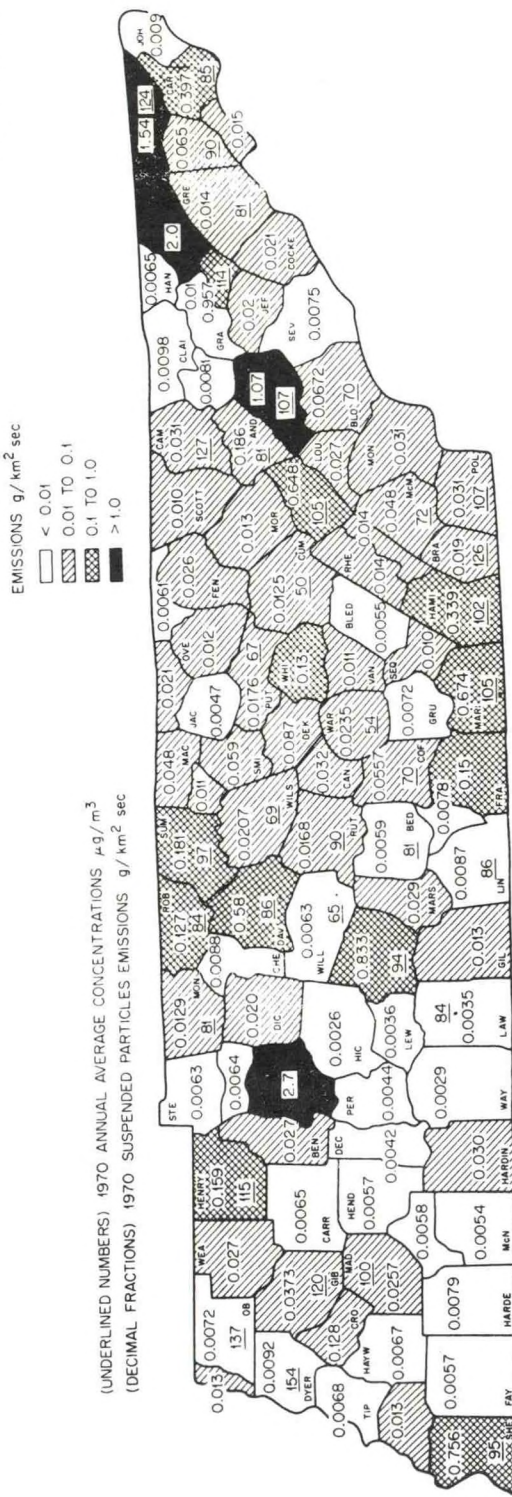


Figure 2: County emission rates ($\text{g}/\text{km}^2 \text{ s}$) and air quality data ($\mu\text{g}/\text{m}^3$) for suspended particles (1970 data).

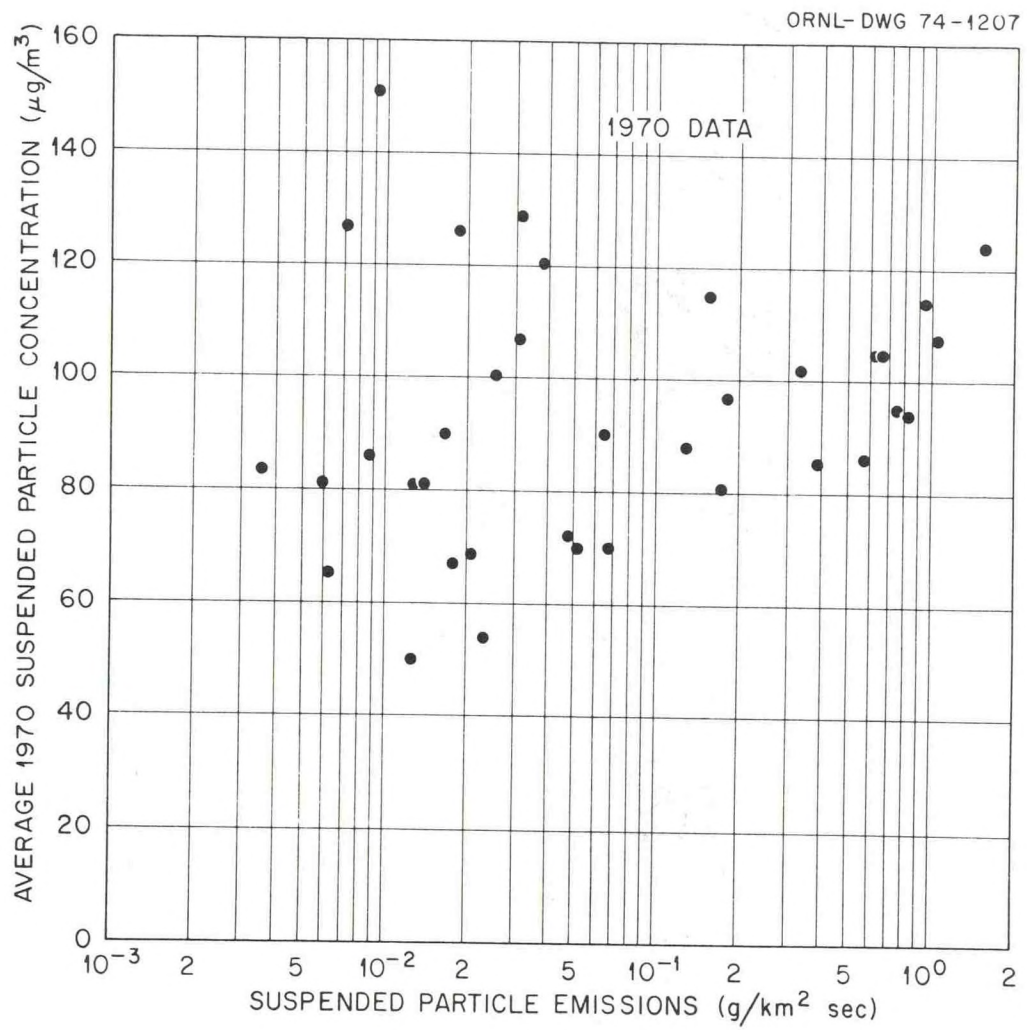


Figure 3: County emission rates ($\text{g}/\text{km}^2 \text{ s}$) as a function of air quality ($\mu\text{g}/\text{m}^3$) for suspended particles (1970 data).

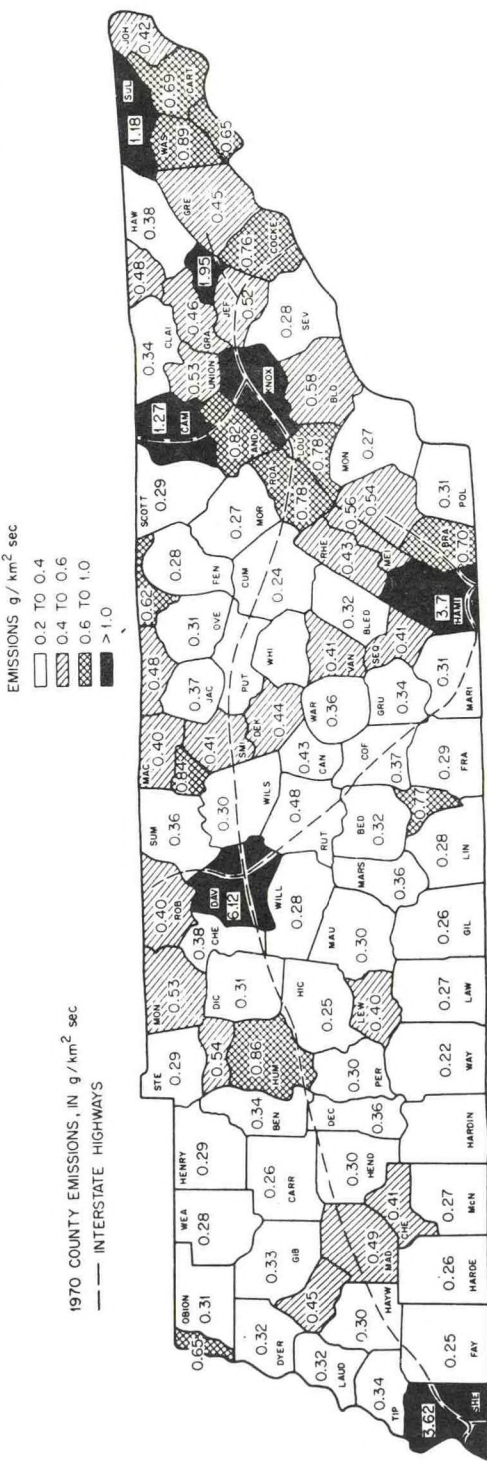


Figure 4: County emission rates (g/km² s) of carbon monoxide (1970 data).

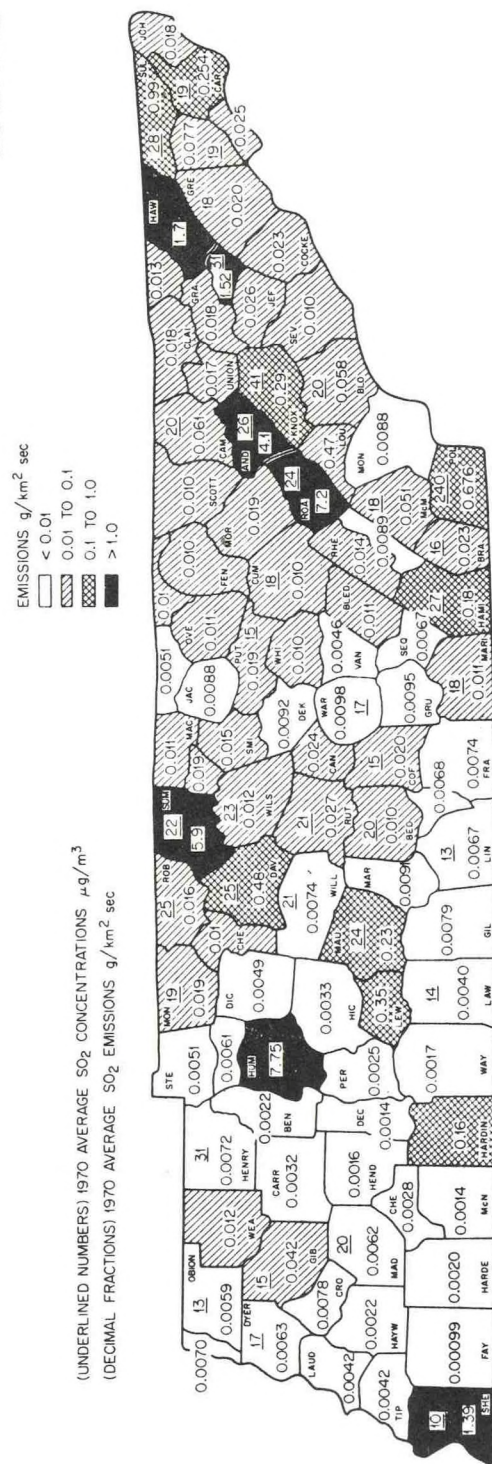


Figure 5: County emission rates ($\text{g/km}^2 \text{ s}$) and air quality data ($\mu\text{g/m}^3$) for SO_2 (1970 data).

COOLING TOWER ENVIRONMENT-1974

Proceedings of a symposium held at the University of Maryland
Adult Education Center March 4-6, 1974

PLUME RISE FROM MULTIPLE SOURCES

GARY A. BRIGGS

Air Resources Atmospheric Turbulence and Diffusion Laboratory,
National Oceanic and Atmospheric Administration, Oak Ridge, Tennessee

ABSTRACT

A simple enhancement factor for plume rise from multiple sources is proposed and tested against plume-rise observations. For bent-over buoyant plumes, this results in the recommendation that multiple-source rise be calculated as $[(N + S)/(1 + S)]^{1/3}$ times the single-source rise, Δh_1 , where N is the number of sources and $S = 6$ (total width of source configuration/ $N^{1/3} \Delta h_1$) $^{3/2}$. For calm conditions a crude but simple method is suggested for predicting the height of plume merger and subsequent behavior which is based on the geometry and velocity variations of a single buoyant plume. Finally, it is suggested that large clusters of buoyant sources might occasionally give rise to concentrated vortices either within the source configuration or just downwind of it.

In spite of extensive literature on the subject of plume rise,¹ many questions of practical consequence are still unanswered. One of these is the question of plume rise at large distances downwind in neutral conditions, where the few available data show no leveling; one can "fit" a linear, a power-law, or an asymptotic exponential curve to these data, depending on which data are selected, how they are weighted, and, to some extent, on one's personal prejudices. On the other hand, there are several special cases for which simple power-law approximations have been confirmed both by full-scale observations of plume rise and by physical modeling; this holds especially for buoyant plumes in the close-in rising stage, where wind velocity is the only atmospheric variable of consequence, and for final rise in stable conditions.²

One inadequately answered question is whether single-source plume rise is augmented by the presence of nearby plumes. This question is of decreasing importance to the tall stack problem since the trend has been to combine as much effluent as possible into one or two tall stacks, which assures the

ATDL Contribution File No. 91.

maximum possible plume rise. However, large cooling towers are frequently paired, and clusters of up to 30 towers are being considered. Even with plume rise depending only on the $\frac{1}{3}$ power of buoyancy flux, it is possible that the plume from such a cluster will combine and rise three times as high as the plume from a single tower isolated from the cluster.

A GENERAL APPROACH

Obviously, if the sources are very close to each other, the plumes will combine, and, if they are very far apart, the plumes will rise separately. It seems reasonable to assume that the resultant rise will be the single-source rise times some function of the number of sources and the ratio of spacing between the sources to the single-source rise (this assumes sources of approximately equal magnitude):

$$\Delta h_N = \Delta h_1 f(N, s/\Delta h_1) \quad (1)$$

where Δh_N is the rise from N sources and s is the center-to-center spacing between the sources. An alternative that suggests itself in the case of a line of sources is to replace s with the spacing perpendicular to the wind direction, s_d (s_d is zero if the wind is parallel to the line of sources). As previously noted,³ at one TVA power plant greater rise enhancement was observed when the wind was parallel to the line of three stacks.

The rise enhancement is not necessarily a monotonically decreasing function of $s/\Delta h_1$. As can be visualized with the help of Fig. 1, in between the uncombined stage of rise ($\Delta h < s$) and the fully combined stage ($\Delta h \gg s$) is an intermediate stage where the double-vortex flows associated with isolated bent-over plumes⁴ may interact in a complex way, possibly causing increased entrainment and decreased plume rise. However, this is a transient stage, and, given the normal scatter observed in the behavior of turbulent plumes even in quiescent surroundings,⁵ it is likely that the rise enhancement will appear to be a monotonic function anyway.

It was decided to try fitting data from multiple sources to a simple monotonic function of $s/\Delta h_1$ that has the correct asymptotes, namely,

$$E_N = \frac{\Delta h_N}{\Delta h_1} = \left(\frac{N + S}{1 + S} \right)^n \quad (2)$$

where E_N will be called the "enhancement factor," S is a nondimensional spacing factor, and Δh_1 is proportional to the n th power of source strength.

Several possibilities were tried for S , the most obvious of which was $S \propto s/\Delta h_1$. The other possibilities were based on the notion that, if one has a line of evenly spaced sources and $N \rightarrow \infty$, the number of effectively combined plumes would be proportional to the resultant rise divided by the spacing:

$$E_N^{1/n} = \frac{N + S}{1 + S} \propto \frac{E_N \Delta h_1}{S} \quad (3)$$

This assumption leads to $E_N \propto (\Delta h_1 / S)^{n/(1-n)}$, which in turn leads to $S \propto N(s/\Delta h_1)^{1/(1-n)}$ if $N \gg S$ and $S \gg 1$, i.e., if the number of effectively combined plumes is much less than N but much greater than 1. An alternative formulation, equally valid when $N \gg 1$, is

$$S \propto \left[\frac{(N - 1)s}{N^n \Delta h_1} \right]^{1/(1-n)} \quad (4)$$

In this case S^{1-n} has a simple interpretation; it is the ratio of total line width to the total possible rise if all the plumes combined. This has the advantage of being easily applied to a cluster, as well as a line, by merely using the largest dimension across the cluster in place of the total line width.

These formulations assume that $n < 1$. If $n \geq 1$, it would be possible for E_N to "jump" from $E = 1$ to $E = N^n$ below some critical value of $s/\Delta h_1$. For a large $[(N)^{1/2} \gg 1]$ homogeneous two-dimensional array of sources, the term on the right side of Eq. 3 would be squared, which results in an equation similar to Eq. 4 except that the exponent becomes $2/(1 - 2n)$. This leads to similar behavior of the rise enhancement except for a more abrupt rise as $s/\Delta h_1$ decreases, with a jump in E_N if $n \geq 1/2$.

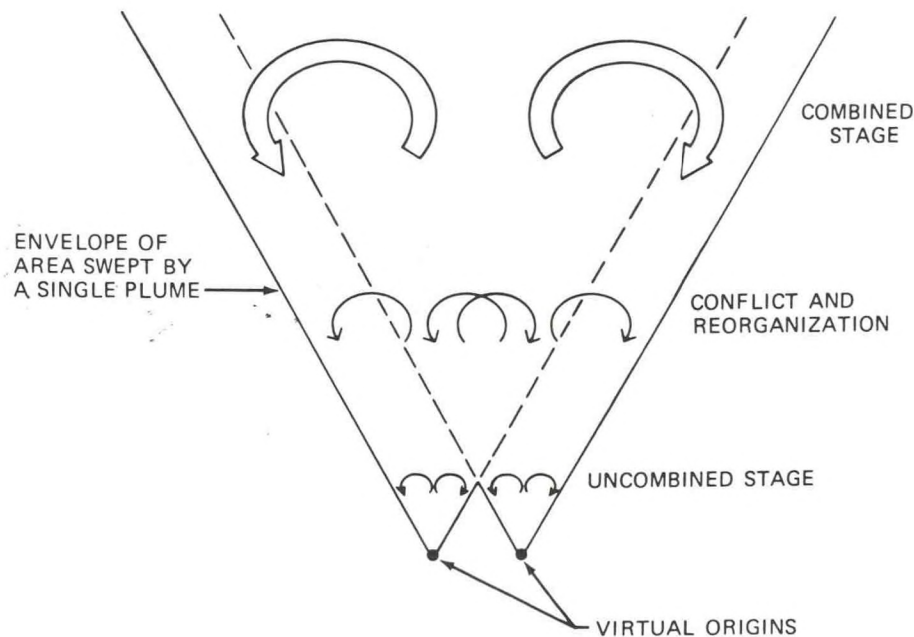


Fig. 1 Cross sections of two adjacent bent-over plumes showing geometry of flow at three distinctly different stages of rise.

APPLICATION TO BUOYANT BENT-OVER PLUMES

The best data available to test the above approach are extensive observations made by the Tennessee Valley Authority (TVA) in 1963 to 1965 (Ref. 6). These include many observations with one or two stacks operating (at two sites both $N = 1$ and $N = 2$ cases are available) and some observations with lines of three, four, eight, and nine stacks operating. These plumes are buoyancy dominated beyond a distance of about 5 sec times the wind speed and in the great majority of cases are bent over ($x > \Delta h$, where x is the distance downwind of the stack). Therefore I undertook a comparison of these data with two well-proven formulas for buoyant bent-over plumes,² namely,

$$\Delta h_1 = C_1 F^{1/3} u^{-1} x^{2/3} \quad (5)$$

and

$$\Delta h_1 = C_2 \left(\frac{F}{uG} \right)^{1/3} \quad (6)$$

where C_1 and C_2 = dimensionless constants

u = mean wind speed at plume height

F = flux of buoyant force in the plume divided by π times the ambient density ρ

G = restoring acceleration per unit vertical adiabatic displacement in stable air

More specifically,

$$G = \frac{g}{T} \frac{\partial \theta}{\partial z} = \frac{g}{T} \left(\frac{\partial T}{\partial z} + \frac{1^\circ C}{100 \text{ m}} \right) \quad (7)$$

where g is gravity, T is the ambient absolute temperature, and $\partial \theta / \partial z$ is the ambient potential temperature gradient. Experience has shown that best results obtain when $\partial \theta / \partial z$ is averaged between the source height and the top of the plume. For the isothermal case ($\partial T / \partial z = 0$), $G^{-1} \approx 3000 \text{ sec}^2$. Also, for plumes in which buoyancy is due to sensible heat flux, Q_H , we can write

$$F = \frac{g Q_H}{\pi c_p \rho T} \quad (8)$$

$$\approx 8.9 \frac{m^4}{sec^3} Q_H / (MW)$$

$$\approx 3.7 \frac{m^4}{sec^3} Q_H / (10^5 \text{ cal/sec})$$

where c_p is the specific heat capacity of air. The approximations are for sea level; F is inversely proportional to ambient pressure.

Reported values of C_1 range from 1.2 to 2.6 and values of C_2 range from 1.8 to 3.1 when applied to the plume center line.² The wide range is due partly to different measurement techniques, to greatly different scales of sources, and in some cases to extraneous local effects. Since the apparent enhancement factor E_N is going to depend directly on what is accepted as the correct single-source values of C_1 and C_2 , it seems most appropriate to establish them on the basis of the same data set, especially since it includes many single-stack experiments.

The distance $x = 1000$ ft was chosen to test Eq. 5, the " $\frac{2}{3}$ law," because this distance is well into the buoyancy-dominated region of rise, is well short of the distance at which atmospheric turbulence might diminish the rise, and is well represented by the available data. To limit the extent of stability effects, I omitted periods in which $1000 \text{ ft} > 2uG^{-\frac{1}{2}}$ since the $\frac{2}{3}$ law rise is diminished by more than 10% in such cases.⁷ On the other hand, since experiments² have substantiated the theoretical prediction that a buoyant plume reaches its maximum rise at $x = \pi uG^{-\frac{1}{2}}$, I chose $x = 4uG^{-\frac{1}{2}}$ as the "standard distance" for testing the prediction of Eq. 6. Beyond this distance the number of available data diminished rapidly. Some of the periods of observation were suitable for testing both formulas, containing data as far as $x = 6000$ ft or more. In most cases, however, the distance $x = 4uG^{-\frac{1}{2}}$ was not reached, the stratification being close to neutral ($G \rightarrow 0$). Consequently, fewer data were available to test Eq. 6.

Some additional periods to test Eq. 6 for three and four stacks were found in some 1957 observations made at the Colbert power plant by TVA (Ref. 8). In these observations the plume top and bottom elevations were determined by SO_2 sampling with a helicopter at $\frac{1}{2}$, $\frac{3}{4}$, 1, and 2 miles downwind and in some cases at further distances. In this analysis the average of the rises at these four distances was used except in two cases; in one case there was no determination at $\frac{3}{4}$ mile and in another the $\frac{1}{2}$ -mile value was less than $4uG^{-\frac{1}{2}}$.

Few plume-rise data are free of extraneous effects, and in some cases the data do not make sense if these effects are ignored. For instance, on the one day at the Widows Creek power plant when the winds came from the southeast quadrant, the observed values of C_1 were much lower than those observed on the other three days. However, there is an unusual topographic feature at this site, namely, a plateau escarpment 900 ft above grade about 7000 ft to the southeast (the plateau runs southwest-northeast). In wind tunnels the cavity region of such drops is observed to end at roughly 10 times the height of the drop downwind with pronounced subsidence in this area. It seems likely that the plume was imbedded in such an area of terrain-induced subsidence on this day, so these three periods were eliminated. Some form of downwash is also suspected at the Shawnee plant since the observed values of C_1 are very low except when the wind speed is less than 12 fps. This suspicion is reinforced by the fact that in most of these cases the bottom of the plume was observed to drop below the stack top, i.e., the reported plume depth was greater than twice the

center-line rise. This plant is situated in very flat terrain, and the stacks are $2\frac{1}{2}$ times the building height; but it may be that the line of ten stacks itself forms a vigorous wake (the stacks average 19 ft in outside diameter and are spaced 83 ft apart). Periods were omitted when the ratio of plume depth to center-line rise ≥ 1.6 to eliminate such cases of likely downwash (the median value at $x = 1000$ ft for single plumes was 0.85, with an average deviation of $\pm 22\%$). Since the bottom of a plume is more susceptible to stack- or building-induced downwash than the top, as a further precaution the rise of the plume top above stack height was used in this analysis instead of the center-line rise; in fact, comparison showed that the scatter resulting in observed values of C_1 and C_2 was less or unchanged in every case.

In addition, three periods were eliminated from the comparison with Eq. 6 because the measured temperature profiles did not extend to the top of the plume (Gallatin, 3/18/64, and Shawnee, 4/10/65). This left only one suitable period of data at Shawnee, with nine stacks operating and the stratification only slightly stable. Unfortunately the observed value of C_2 was a little less than the average for single stacks; so the nine-stack data seemed altogether inadequate for the present purpose.

When the data were compiled by TVA, they were divided into periods mostly ranging from 30- to 180-min duration, averaging about 90 min; the period length chosen depended on the relative constancy of meteorological conditions and the temporal spacing of helicopter soundings to measure temperature profiles and pibal releases to measure wind profiles. Within these periods the number of photographs of the plume at the distances specified above ranged from zero to more than 30. It was arbitrarily decided that four or more observations (photographs) at that distance would be required for a period to be used in this analysis in order that it be adequately represented.

With such a range of period duration and number of observations per period, how to weight the data was problematic. The more periods, the more likely that the wide range of possible meteorological conditions will be well represented. The longer the period duration, the better it is represented by temperature profiles (usually one per hour) and wind profiles (usually two per hour). The larger the number of observations per period, the better the plume rise is represented. There is also the question of whether to use average or median plume rises. The former is more commonly employed, but, in a nonlinear relation, the average of the function is not necessarily the function of the average argument; it probably is not. On the other hand, if the relation is monotonic, the median of the function is given by the function of the median argument. Perhaps more clearly we can write: average $\chi(\Delta h) \neq \chi(\text{average } \Delta h)$, but median $\chi(\Delta h) = \chi(\text{median } \Delta h)$, provided the relation is monotonic. This condition is satisfied in the case of Gaussian plume-diffusion models provided that χ is the ground concentration at any point. Furthermore, when the number of data are few, the median is less affected by an anomalous datum, although it may be more erratic if the distribution of values is bimodal.

The criticality of the weighting technique employed is illustrated by Tables 1 and 2. Reading down any column, we find the expected trend of plume rise with the number of stacks and the spacing factor. Reading across any row, however, we note large disparities in observed values of $\Delta h_N/\Delta h_1$, depending on which kind of average or median is used. In general, median values are lower than average values in the case of the $2/3$ law (Eq. 5), indicating that anomalous rises tend to be higher than expected; it may be that the measured wind speeds are too high in these cases owing to inadequate sampling. The same is true for the stable rise formula (Eq. 6) for one stack, except that wind speed is not such a strong determining factor in this case. Curiously, the two "high rise" periods here are also the two periods of the greatest wind-direction shear (105° and 170°). The median and the average rises compared with the predictions of Eq. 6 are in good agreement for $N > 1$, but unfortunately substantial differences appear when these rises are divided by the single-stack rise computed by the two methods. This emphasizes the importance of obtaining good base values of C_1 and C_2 for single sources for comparison with multiple-source values. Unfortunately only 10 periods were suitable for determining C_2 . The value of C_1 was determined from 53 periods and shows good agreement between the average values and the median values.

Table 3 shows the resulting values of $s/\Delta h^*$ and the observed values of the dimensionless spacing factor S calculated by two different methods [$\Delta h^* = F^{1/6} u^{-1} x^{2/3}$ or $(F/us)^{1/6}$ was used to nondimensionalize data for each period]. The values designated (av.) were calculated by using the average of averages of $s/\Delta h^*$, $\Delta h_N/\Delta h^*$, and $\Delta h_1/\Delta h^* = C_1$ or C_2 . The values designated (med.) were calculated by using the median of medians for the same quantities. Such values are shown for $(\Delta h_N/\Delta h^*) \div C_1$ and C_2 in the last two columns of Tables 1 and 2. The value of S was calculated from the relation $S = (N - E_N^3)/(E_N^3 - 1)$, with $E_N = (\Delta h_N/\Delta h^*) \div C_1$ or C_2 . It is readily seen that the type of calculation used makes little difference with regard to $s/\Delta h^*$ but greatly affects S , particularly in the stable case.

Finally, both estimates of S were used to develop optimum approximations of S based on N and $s/\Delta h_1$ [for the latter, $(s/\Delta h^*) \div C_1$ or C_2 was used]. Three formulas were tried in each case:

$$S = S_1 \frac{s}{\Delta h_1} \quad (9)$$

$$S = S_2 N \left(\frac{s}{\Delta h_1} \right)^{2/3} \quad (10)$$

$$S = S_3 \left[\frac{(N - 1)s}{N^{1/6} \Delta h_1} \right]^{2/3} \quad (11)$$

as discussed earlier (in Eqs. 5 and 6, $n = 1/3$). Optimum values of S_1 , S_2 , and S_3 were computed from the above formulas and the values of S , $s/\Delta h^*$, C_1 , and C_2

TABLE 1
MULTIPLE-SOURCE RISE COMPARED TO $\Delta h_1 = C_1 F^{\frac{1}{3}} u^{-1} x^{\frac{2}{3}}$ *

Number of stacks	Number of periods	Range of $s \div$ $F^{\frac{1}{3}} u^{-1} x^{\frac{2}{3}}$	Averages by			Medians by			Average of averages	Median of medians
			Periods	Dura- tions	Observa- tions	Periods	Dura- tions	Observa- tions		
1	53	(2.11)	(2.20)	(2.18)	(2.14)	(2.17)	(2.14)	(2.16)	(2.14)	(2.14)
2	13	0.94 to 1.30	1.17	1.11	1.12	1.10	1.06	1.08	1.13	1.08
2	13	0.29 to 0.87	1.29	1.22	1.16	1.21	1.19	1.15	1.22	1.21
3	5	0.35 to 0.58	1.53	1.46	1.47	1.43	1.41	1.43	1.48	1.43
9	3	0.26 to 0.29	1.62	1.51	1.51	1.49	1.49	1.51	1.55	1.51

*Values of C_1 are in parentheses.

TABLE 2
MULTIPLE-SOURCE RISE COMPARED TO $\Delta h_1 = C_2 (F/u s)^{\frac{1}{3}}$ *

Number of stacks	Number of periods	Range of $s \div$ $(F/u s)^{\frac{1}{3}}$	Averages by			Medians by			Average of averages	Median of medians
			Periods	Dura- tions	Observa- tions	Periods	Dura- tions	Observa- tions		
1	10	(4.30)	(4.66)	(4.23)	(3.96)	(4.70)	(3.81)	(4.40)	(3.96)	(3.96)
2	10	0.40 to 0.99	1.15	1.05	1.14	1.25	1.01	1.25	1.12	1.20
3	4	0.70 to 0.91	1.24	1.17	1.29	1.39	1.17	1.45	1.23	1.39
3†	4	0.66 to 0.79	1.13	1.04	1.15	1.27	1.07	1.32	1.10	1.27
4†	4	0.51 to 0.59	1.32	1.22	1.34	1.43	1.21	1.49	1.29	1.43

*Values of C_2 are in parentheses.

†1957 data (by SO₂ sampling).

TABLE 3
NONDIMENSIONAL SPACING FACTORS

Equation	Number of stacks	s/Δh*(av.)	s/Δh*(med.)	S(av.)	S(med.)
5	2	1.16	1.18	1.22	2.90
5	2	0.66	0.70	0.21	0.33
5	3	0.46	0.46	0($E_N > N^{1/3}$)	0.04
5	9	0.26	0.26	1.95	2.28
6	2	0.68	0.64	1.59	0.39
6	3	0.76	0.70	1.31	0.19
6	3†	0.72	0.725	4.79	0.91
6	4†	0.55	0.55	1.58	0.55

†1957 data (by SO₂ sampling).

shown in Tables 1 to 3. Within each group the S_i values ranged considerably; so an overall "optimum" value was chosen using a weighted geometric average. The weighting factor was the number of periods per subgroup times -d(ln E_N)/d(ln S) at the observed S value, as calculated from Eq. 2. This derivative indicates in a rough way the sensitivity of the plume-rise prediction to a compromised value of S, deviating from the specific optimum.

Table 4 shows how well these "optimum" estimates of S predict the average or median plume rise ($\Delta h_N/\Delta h^*$) for each subgroup of data. It is interesting to note that the use of medians instead of averages improves the performance of all three estimates for S for both plume-rise equations. For the data compared with plume-rise Eq. 5, for S Eq. 10 works better than Eq. 9, and Eq. 11 works best of all. For the data compared with Eq. 6, all three estimates for S perform about the same. Another interesting feature of the calculations with medians is that the optimum values of S₁, S₂, and S₃ turn out to be about the same with either plume-rise formula, in contrast to the calculations using averages. This is a very desirable result since it permits a "universal" approximation for the nondimensional spacing factor, namely, Eq. 11 with S₃ = 6:

$$S = 6 \left[\frac{(N-1)s}{N^{1/3} \Delta h_1} \right]^{1/2} \quad (12)$$

(see the last column of Table 4). This seems the best choice since Eq. 11 clearly works best for the $2/3$ law of rise, has a simple interpretation, and is easily adapted to clustered sources as well as line sources. For n = $1/3$ this estimate for S can be readily substituted in Eq. 2 to get the enhancement factor over single-stack plume rise.

TABLE 4
ERROR IN PREDICTING $\Delta h_N/\Delta h^*$ FOR VARIOUS
ESTIMATES OF S

Plume-rise equation	Number of stacks	Using averages			Using medians			Medians, Eq. 11
		Eq. 9	Eq. 10	Eq. 11	Eq. 9	Eq. 10	Eq. 11	
$S_1 = 3.19 \quad S_2 = 1.83 \quad S_3 = 4.00 \quad S_1 = 5.08 \quad S_2 = 2.80 \quad S_3 = 6.50 \quad S_3 = 6$								
5	2	-2%	-1%	+1%	0%	+1%	+2%	+3%
5	2	-7%	-4%	-3%	-8%	-5%	-4%	-4%
5	3	-13%	-11%	-12%	-13%	-11%	-12%	-12%
5	9	+22%	+16%	+7%	+20%	+12%	+2%	+3%
$S_1 = 12.2 \quad S_2 = 11.2 \quad S_3 = 22.6 \quad S_1 = 3.08 \quad S_2 = 2.72 \quad S_3 = 5.52 \quad S_3 = 6$								
6	2	-1%	+1%	+3%	-1%	0%	+1%	+1%
6	3	-4%	-5%	-6%	-5%	-6%	-6%	-7%
6	3†	+7%	+6%	+6%	+4%	+3%	+2%	+1%
6	4†	0%	-2%	-5%	+2%	0%	-2%	-3%

†1957 data (by SO₂ sampling).

To adapt Eq. 12 to clustered sources, one can simply replace $(N - 1)s$ by the greatest distance across the cluster. This seems a fairly safe procedure since this equation is not based on a wind-direction-dependent spacing factor, such as s_d . The data fairly indiscriminately include cases of wind parallel, perpendicular, and diagonal to the line of stacks. Since Eq. 12 is valid whether the plumes overlap each other vertically or flow together side by side, it seems likely to work satisfactorily in mixed cases, although it is possible that very different types of plume interaction could occur. As a factor of conservatism, the coefficient $S_3 = 6$ does more severely underpredict than overpredict rises in Table 4.

Incidentally I did make similar calculations with the directional spacing s_d . In comparisons with Eq. 5, it worked much better than s for the three- and nine-stack data but did poorly for the two-stack data (the highest values of $\Delta h_2/\Delta h^*$ tended to occur with the larger values of $s_d/\Delta h^*$, contrary to expectations). In comparisons with Eq. 6, s_d again worked poorly for the two-stack data, although $s_d/\Delta h^*$ was remarkably well correlated with $\Delta h_3/\Delta h^*$, as was previously noted.³ In view of these mixed results, the limited applicability of s_d (to lines of sources only), and the presence of large wind-direction shears with height at times, the emphasis in this paper is on s instead of s_d .

One may be tempted to further generalize Eq. 12 for other values of n , such as might apply for final rise in neutral or unstable conditions, by putting S_3

inside the parentheses, changing the exponent to $1/(1 - n)$, and replacing $N^{1/3}$ with N^n . This would give $S^{1-n} \approx 15$ times the maximum horizontal dimension of the source configuration divided by the rise for the fully combined plumes. It seems intuitively reasonable that substantial combination will occur if the rise is 15 times the total source diameter, but still I would not recommend this procedure since it is too speculative. It would be safer to just apply Eq. 12 at the distance where the $2/3$ law rise terminates for a single source (see Ref. 7) and use

$$E_N = \frac{\Delta h_N}{\Delta h_1} = \left(\frac{N + S}{1 + S} \right)^{1/3} \quad (13)$$

as for the $2/3$ law. The termination distance is probably extended when the plumes combine in neutral and unstable conditions, but no data exist to confirm this. The termination distance in stable conditions does not depend on the source strength, which is why n is the same for Eqs. 5 and 6.

TECHNIQUE FOR BUOYANT VERTICAL PLUMES

The generalized approach described earlier could also be used to predict multiple-source rise in nearly calm conditions, when buoyant plumes rise vertically until they reach a limiting height in stable air. For rise in uniformly stratified stable air, one would use Eqs. 2 and 4, with $n = 1/4$, since the tops of single plumes are found at

$$h_1 = 5F^{1/4}G^{-3/8} \quad (14)$$

(Ref. 1). Unfortunately no data are on hand to test this approach for vertical plumes. Furthermore, any results for bent-over plumes cannot be adapted to vertical plumes because the geometry of the flow is quite different; e.g., in the rising stage the plume radius $R \approx 0.5z$ for a bent-over plume and $\approx 0.1z$ for a vertical plume, where z is the height above the virtual point source.¹

There is a simple alternative approach, however, based on what is known about single-plume vertical-velocity profiles. According to laboratory measurements on buoyant vertical plumes,⁹ the vertical velocity is given by

$$w = 6.9 \left(\frac{F}{z} \right)^{1/3} e^{-9.6(r/z)^2}$$

where r is the distance off-axis. This gives a volume flux $0.226F^{1/3}z^{4/3}$, and the effective plume radius is at least $R = (96)^{-1/2}z \approx 0.1z$ (this is for a top-hat profile with the vertical velocity anywhere within the plume equal to the measured axial velocity). If N sources were clustered in an area of maximum dimension (center to center) D , the plumes would have to combine at

$z \leq (96)^{1/2}(D/2)/(N)^{1/2} = 5D/(N)^{1/2}$ or else the total plume cross-sectional area would exceed $(\pi/4)D^2$. If the effect of inflow velocity at the circumference when the peripheral plumes bend toward the center is considered, plume merger occurs at less than $z = 4D/(N)^{1/2}$ (this was done by assuming horizontal inflow, differentiating the volume flux to get entrainment rate at each level, assuming conservation of entrained radial momentum for the peripheral plumes, and assuming the axial value for vertical velocity). This result suggests that plume merger always occurs if the rise exceeds $2.8D$ (for a “cluster” of 2 sources) and if the rise exceeds even $1D$ when $N \geq 16$.

If the single-source rise exceeds the plume-merger height calculated above, we could treat the sources as a single one, but there is no ready model for handling the dynamics of the transition region. One crude way to handle this would be to consider the plumes to be separate below the height of merger z_m and to be one plume above $z = z_m$, with a source strength (NF) and a virtual point-source height at $z = [1 - (N)^{1/2}] z_m$, i.e., below the actual source height. This results in the same total cross-sectional area of the plume(s) at $z = z_m$ and a disparity in the axial velocities equal to $N^{1/6}$. This disparity would diminish above $z = z_m$ as the plume adjusts to being unified. Of course, if this technique results in less total rise than that for a single plume, which can happen if $n < 1/2$, then it would be more realistic to use the single-source rise.

MULTIPLE-SOURCE BEHAVIOR WITH VORTICITY

There is an interesting, and possibly important, question about the behavior of the rising plume from a multiple source in the presence of vorticity. Under the right combination of large-scale horizontal vorticity and vertical driving force (such as buoyancy), one or more areas of concentrated vorticity can develop.

The exact mechanism of vortex formation is complex and not fully understood but can be described roughly as follows: In an area of steady-state rotation, in the absence of friction the centripetal acceleration of a fluid is just balanced by a radial pressure gradient. If such an area of rotation with a vertical axis is located over a horizontal surface, the centripetal acceleration is zero at the surface since friction causes the velocity to approach zero there. The radial pressure gradient then induces a horizontal inflow near the surface until it is balanced by frictional forces. This horizontal convergence can be maintained if some continuous removal mechanism is available, such as suction from above or a continuous supply of buoyancy. Unless overwhelmed by turbulent friction, the angular momentum of converging fluid tends to be conserved, which leads to a concentration of vorticity and greatly increased tangential velocity near the surface around the center of the inflow.

This general phenomenon occurs with a wide range of scales and intensities in nature. The hurricane develops from large-scale vorticity due to the earth's rotation and maintains itself with buoyancy generated by latent heat release

from convective showers around the eye wall. Tornadoes may be induced by "suction" from low pressure created aloft in the "tornado cyclone," which again may derive from vertical instability created by latent heat release. In contrast, dust devils feed on buoyancy generated by dry heat that is most intense at the ground. Their vorticity may derive from topographically induced eddies, surface-roughness inhomogeneity, mechanical shear, or convective eddies. Such convective eddies are present throughout any day that is not heavily overcast, with vertical and horizontal scales of the order of 1 km and velocities of the order of 1 m/sec. Waterspouts may generate in a similar fashion, with most of the buoyancy due to the lower molecular weight of water vapor rather than to dry heat. Vortices have also been observed dangling from smoke plumes from volcanoes.¹⁰ In the case of the Surtsey volcano, wind speeds of the order of 90 m/sec were estimated in one of the vortices.¹⁰ The vortex field could derive from either the wake of the volcano or the wake produced by the plume itself.

Concentrated vortices have also been produced in the atmosphere by man's activities. In France a multiple source consisting of 100 oil burners generated dust devils near the burners "with intensities equal to small tornadoes."^{11,12} This array, producing a total of 700 MW of heat, was built as an experiment to artificially induce cumulus convection. "Fire whirlwinds" have occurred over fire-bombed cities, over large oil fires, and over natural and intentional timber burns.¹⁰ One timber burn produced a 1200-ft-diameter whirl which lifted 30-in. by 30-ft logs.¹³ Similar vortices (though less intense) have been produced by relatively modest burns of less than 100 acres¹⁴ and by experimental bonfires releasing only 100 MW of heat.¹⁰ Interestingly, I have not seen any vortex phenomena reported for a compact source of heat, such as a chimney plume or a cooling-tower plume.

The conditions necessary for the formation of concentrated vortices are poorly defined by present knowledge. The best presently available tool for exploring these conditions is physical modeling. A number of laboratory experiments on vortices have been performed over smooth plates (see, for instance, Refs. 15 to 19). Fitzjarald¹⁵ used particularly simple boundary conditions, namely, a uniformly heated circular plate surrounded by Plexiglas vanes tilted uniformly with respect to the local tangent. Depending on the relative temperature elevation of the plate and the degree of tilt, five qualitatively different flow regimes were observed. The type of flow regime depends generally on the ratio of buoyancy-induced velocity to tangential velocity at the periphery of the heated region. When this ratio is large, a pure plume (no vortex) develops, and, when this ratio is low, pure swirl develops. Well-formed vortices are generated at intermediate values. It is difficult to apply the results of a smooth-plate (laminar-boundary-layer) experiment directly to the atmosphere. One interpretation of the above experiment, however, is that natural convection is likely to produce vortices (namely, "dust devils"), but a single cooling tower or chimney plume is much too buoyancy-dominated to do so. However, a large ($\sim 1 \text{ km}^2$) multiple source might sometimes produce a

vortex; if it does, the vortex velocities are likely to be about three times those occurring in natural dust devils (see the appendix).

The smooth-plate laboratory studies on vortices beg many questions about their applicability to multiple-buoyancy-source behavior in a field of vorticity. For instance, what are the effects of ground roughness, the "spottiness" of the buoyancy source, the source structure, the above-ground heat release, and the presence of a "lid"? These questions could be at least partially answered by performing similar laboratory experiments with models simulating prototype geometry. The "dangling vortices" observed on the downwind side of the Surtsey plume, to my knowledge, have not been modeled; however, since the phenomenon is more likely to have off-site effects, it would be prudent to model a large multiple source in a low-wind-speed (atmospheric-boundary-layer) wind tunnel as well as for the zero crosswind case. In either case it is important to scale the imposed velocities (either the tangential velocity of imposed circulation or the crosswind velocity) to the scale velocity for buoyancy, $(F/R)^{1/3}$ (F is the total buoyancy flux parameter for the complex of sources and R is the complex radius). In other words, characteristic Froude numbers must be the same in model and prototype.

SUMMARY AND RECOMMENDATIONS

It seems reasonable to expect enhanced plume rise over that of a single source when two or more sources are in close proximity. A simple enhancement factor was postulated which had the correct asymptotes for large spacing ($E_N = 1$, no enhancement) and very close spacing ($E_N = N^n$, where N is the number of sources and the single-source rise Δh_1 is proportional to the single-source strength to the n th power). This was compared with TVA observations of plume rise from lines of stacks ($N = 1, 2, 3, 4$, and 9) for three different assumed forms of the nondimensional spacing factor and for two different plume-rise equations:

$$\Delta h_1 = C_1 F^{1/3} u^{-1} x^{2/3} \quad (5)$$

and

$$\Delta h_1 = C_2 \left(\frac{F}{uG} \right)^{1/3} \quad (6)$$

The $2/3$ law (Eq. 5) was applied at $x = 1000$ ft when 1000 ft was less than $2uG^{-1/2}$, and the stable rise law (Eq. 6) was applied at $x = 4uG^{-1/2}$. A few periods of observations were excluded because of strong reason to suspect downwash or because of too few plume photographs (less than four).

The nondimensionalized observed rises, and hence the observed values of $E_N = \Delta h_N / \Delta h_1$, varied significantly, depending on whether the data were

weighted by number of periods, number of photographs, or duration of periods and also depending on whether averages or medians were employed. Medians resulted in the best ordering of data and also in nearly the same optimum nondimensional spacing factor for both plume-rise formulas. Recommended is

$$E_N = \left(\frac{N + S}{1 + S} \right)^{\frac{1}{3}} \quad (13)$$

with

$$S = 6 \left[\frac{(N - 1)s}{N^{\frac{1}{3}} \Delta h_1} \right]^{\frac{1}{2}} \quad (12)$$

where s is the spacing between adjacent sources.

Although this empirical enhancement was developed by using line-source data, it is suggested that it could be conservatively applied to clusters of sources by replacing $(N - 1)s$ with the maximum diameter of the cluster. For "final" rise in neutral conditions, for which no adequate data exist, the above formulas can again be recommended since $n = \frac{1}{3}$ is conservative for this case.

No suitable data from multiple sources were found for calm conditions, but, from basic knowledge of the geometry and dynamics of buoyant point-source plumes, one can infer that plume merger will occur at a height $z_m \approx 4 D/(N)^{\frac{1}{3}}$, where D is the diameter of a cluster of sources. The characteristics of the merged plume could be roughly predicted by assuming a single combined source at a virtual origin $z = [1 - (N)^{\frac{1}{3}}] z_m$.

Finally, it is suggested that large clusters of buoyant sources, in the presence of vorticity fields due to natural convection or due to the wake of the source and plume itself, may be capable of producing concentrated vortices. Certainly they would release as much energy as many natural sources that have produced strong vortices, and many concentrated vortices have been observed to develop over man-made area sources of heat as well. The results of one smooth-plate laboratory experiment, if applicable to multiple sources of buoyancy in the real atmosphere, imply that a large source of that type could occasionally produce a vortex on the scale of a large dust devil and with velocities about three times those in dust devils. Certainly such an extrapolation is not conclusive, but accurate modeling of specific source configurations in the presence of a vorticity field is strongly recommended when any substantial jump in source size is proposed.

APPENDIX: AN INTERPRETATION OF A CONVECTIVE VORTEX EXPERIMENT

To apply the results of Fitzjarald's experiment¹⁵ to multiple sources of buoyancy (rather than a uniformly heated surface), we must estimate the total

heat flux removed from the plate by the flow. Only the plate temperature excess, ΔT_p , the tangential velocity, V_∞ , at the periphery ($R = 50$ cm), and the vane tilt angle, θ , are reported. We assume an inflow velocity at the periphery $U_\infty = V_\infty \cot \theta$. Outside the vortex a constant inflow angle = θ can be assumed with a local velocity $V = V_\infty \csc \theta (R/r)$; this satisfies both conservation of angular momentum and continuity. Outside the vortex the flow appears laminar; so a rough estimate of the local heat-transfer rate can be made by using the rate for uniform, laminar flow over a flat plate using $(R - r) \sec \theta$ for the travel distance and the local total velocity in place of the velocity at infinity.²⁰ The resulting total F equals $1.322g(\Delta T_p/T)(U_\infty \nu R)^{1/2}R$, where ν is the kinematic viscosity. When we define a characteristic buoyant velocity $V_B = (F/R)^{1/4}$, we discover that the observed inflow velocity U_∞ equals $0.6V_B$ with only 6% average deviation, i.e., it depends mostly on the buoyancy flux calculated above and not on the inflow angle. Thus $V_\infty/V_B \doteq 0.6 \tan \theta$ in this experiment.

The observed flow regimes depended strongly on $\tan \theta$ and much less strongly on ΔT_p (Ref. 15, Fig. 12). Since it is difficult to specify any equivalent flat plate ΔT_p for a multiple source, I will interpret the results for variations of $\tan \theta \doteq 1.7V_\infty/V_B$ only, evaluated at average $\Delta T_p \approx 40^\circ\text{C}$. When the ratio V_∞/V_B is less than 0.15, there is no significant vortex. Above this value and below 0.35, a one-cell (all upward motion) vortex forms. Above 0.35 a two-cell vortex (inner core of subsiding air) with much stronger circulation forms, but above 0.6 this two-cell vortex becomes more turbulent and diffuse. When V_∞/V_B exceeds 0.9, the whole flow swirls, with no concentration of vorticity. At smaller values of ΔT_p , these transition values of V_∞/V_B shift downward, being proportional to $\Delta T_p^{1/2}$.

To apply this result to phenomena in the mixing layer of the atmosphere, we need to estimate possible values of V_∞ available from natural convection. This requires multiple-point field data. In lieu of this I used the results of a numerical experiment by Deardorff²¹ to estimate that the maximum possible $V_\infty \approx 0.8(Hz_i)^{1/4}$, where z_i is the height of the mixing layer (usually of the order of 1 km) and $H = gH_0/(c_p \rho T)$, where H_0 is the average sensible heat flux at the ground (note that H is defined similarly to F ; for an area of radius R , $F = HR^2$). For a strongly convective day ($H = 10^{-2} \text{ m}^2/\text{sec}^3$ and $z_i = 10^3 \text{ m}$), the maximum $V_\infty \approx 1.7 \text{ m/sec}$. This occurs on a scale $2R \approx z_i$, about 1 km. On much smaller scales the maximum $V_\infty \approx 6(Hz_i)^{1/4}(R/z_i)$.

Now apply these estimates to three very different kinds of sources:

1. A large cooling tower with $R = 25$ m, a total heat rejection of 2000 MW, and a sensible heat rejection of 400 MW. With sensible heat only (no condensation), we have $F = 3500 \text{ m}^4/\text{sec}^3$, $V_B = (F/R)^{1/4} = 5.2 \text{ m/sec}$. On a strongly convective day, $H = 10^{-2} \text{ m}^2/\text{sec}^3$ and $z_i = 10^3 \text{ m}$; so $V_\infty \leq 6(10)^{1/4}(25/10^3) \text{ m/sec} = 0.32 \text{ m/sec}$ and $V_\infty/V_B \leq 0.06$. Thus such sources would not be expected to produce a vortex. This is even more true of smaller cooling towers and hot plumes from stacks since presumably the available V_∞ is smaller with smaller radius.

2. Twenty (20) of the above towers clustered over an area with $R = 500$ m. With sensible heat only, $F = 71,000 \text{ m}^4/\text{sec}^3$, $V_B = 5.2 \text{ m/sec}$ again, and $V_\infty/V_B \leq 1.7/5.2 = 0.33$. Vortices, especially the single-cell type, are possible on this scale owing to the larger available V_∞ .

3. Strong natural convection on the same scale as in item 2. $F = HR^2 = 2500 \text{ m}^4/\text{sec}^3$, $V_B = 1.7 \text{ m/sec}$, $V_\infty/V_B \leq 1.7/1.7 = 1.0$. All types of vortices are possible, depending on the magnitude of V_∞ . Scales smaller than z_i are probably favored since V_∞/V_B becomes smaller for them. The threshold for dust-devil formation is the scale $R \approx (0.15/6)z_i(HR)^{1/4}/(Hz_i)^{1/4} = 0.004z_i \approx 4\text{m}$, which is quite small.

Thus a very large multiple buoyant source in a field of natural convection may occasionally produce a vortex on the scale of a large dust devil. However, if velocities in such vortices scale roughly to V_B , the velocities in a vortex produced by the source in example 2 above would be about three times those of a large natural dust devil.

ACKNOWLEDGMENTS

This research was performed under an agreement between the U. S. Atomic Energy Commission and the National Oceanic and Atmospheric Administration.

REFERENCES

1. G. A. Briggs, Plume Rise, AEC Critical Review Series, TID-25075, November 1969.
2. G. A. Briggs, Discussion of Chimney Plumes in Neutral and Stable Surroundings, *Atmos. Environ.*, 6: 507-510(1972).
3. G. A. Briggs, Plume Rise, AEC Critical Review Series, TID-25075, pp. 55-56, November 1969.
4. G. A. Briggs, Plume Rise, AEC Critical Review Series, TID-25075, pp. 8-9, November 1969.
5. R. S. Richards, Experiment on the Motions of Isolated Cylindrical Thermals Through Unstratified Surroundings, *Int. J. Air Water Pollut.*, 7: 17-34(1963).
6. S. B. Carpenter, F. W. Thomas, and F. E. Gartrell, Full-Scale Study of Plume Rise at Large Electric Generating Stations, Tennessee Valley Authority, Muscle Shoals, Ala., 1968 (additional data were obtained in the form of computer printout by personal communication).
7. G. A. Briggs, Some Recent Analyses of Plume Rise Observation, in *Proceedings of the Second International Clean Air Congress*, Washington, D. C., Dec. 6-11, 1970, pp. 1029-1032, H. M. Englund and W. T. Beery (Eds.), Academic Press, Inc., New York, 1971.
8. F. E. Gartrell, F. W. Thomas, and S. B. Carpenter, Full Scale Study of Dispersion of Stack Gases, Tennessee Valley Authority, Chattanooga, Tenn., 1964.
9. H. Rouse, C. S. Yih, and H. W. Humphreys, Gravitational Convection from a Boundary Source, *Tellus*, 4: 201-210(1952).
10. S. Thorarinsson and B. Vonnegut, Whirlwinds Produced by the Eruption of Surtsey Volcano, *Bull. Amer. Meteorol. Soc.*, 45: 440-444(1964).

11. J. Dessens, Man-Made Thunderstorms, *Discovery*, **25**:40-43 (1964).
12. J. Dessens, Man-Made Tornadoes, *Nature*, **193**: 13-14 (1962).
13. H. E. Graham, Fire Whirlwinds, *Bull. Amer. Meteorol. Soc.*, **36**: 99-102 (1955).
14. D. A. Haines and G. H. Updike, Fire Whirlwind Formation over Flat Terrain, U. S. Department of Agriculture, Forest Service Research Paper NC-71, 1971.
15. D. E. Fitzjarald, A Laboratory Simulation of Convective Vortices, *J. Atmos. Sci.*, **30**: 894-895 (1973).
16. C. A. Wan and C. C. Chung, Measurement of Velocity Field in a Simulated Tornado-Like Vortex Using a Three-Dimensional Velocity Probe, *J. Atmos. Sci.*, **29**: 116-127 (1972).
17. N. B. Ward, The Exploration of Certain Features of Tornado Dynamics Using a Laboratory Model, *J. Atmos. Sci.*, **29**: 1194-1204 (1972).
18. B. R. Morton, The Strength of Vortex and Swirling Core Flows, *J. Fluid Mech.*, **38**: 315-333 (1969).
19. B. R. Morton, Geophysical Vortices, in *Progress in Aeronautical Sciences*, Vol. 7, Chap. 6, Pergamon Press, Inc., Oxford, London, Edinburgh, N. Y., Paris, Frankfurt, 1966.
20. W. H. Giedt, *Principles of Engineering Heat Transfer*, D. Van Nostrand Co., Princeton, Toronto, London, New York, 1957 (see Eq. 7.38).
21. J. W. Deardorff, Numerical Investigation of Neutral and Unstable Planetary Boundary Layers, *J. Atmos. Sci.*, **29**: 91-115 (1972) (see especially Fig. 22).

DISCUSSION

Muschett: Are the percentages of errors to be interpreted as standard errors, average errors, or neither?

Briggs: They are average errors for a whole group of a particular number of sources.

Kennedy: Your starting point for this analysis is an assumed function for Δh ?

Briggs: Yes, it is assumed, but there is a body of data to support it.

Kennedy: Did you work backward to quantify the entrainment coefficient that is implicit in your analyses to see how this is affected as the aspect ratio. For example, for the large circular plume, the vortices have a great influence on entrainment. But this effect would be more limited for the slot plume.

Briggs: These are not quite slot plumes. I did not try to work backward to calculate entrainment coefficients, because I think it is hopeless to get that much from these data. There is a great deal of scatter which these simplified tables do not show.

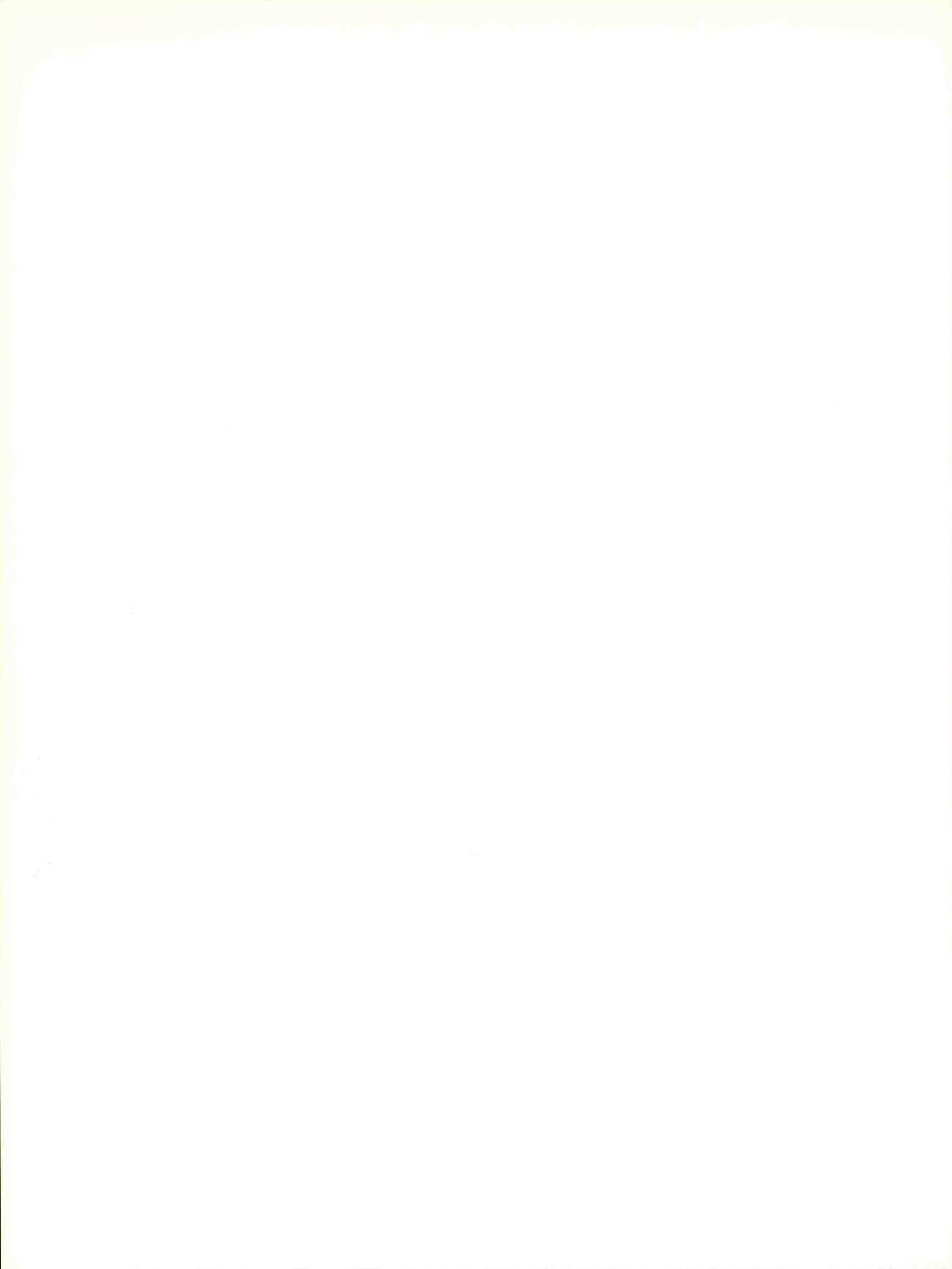
Slinn: Gary, I know that a lot of people will be interested in reading your paper carefully because an estimate of the plume rise from multiple sources is badly needed. But, when the combined power production in a concentrated region is tens of thousands of megawatts, there are probably more significant topics to address than plume rise, and your comments about the possibility of concentrating mesoscale vorticity into a smaller space scale is rather unsettling to say the least. Can you give us the benefit of any other ball-park estimates that you or other members of your group might have made for this problem concerned, for example, with possible updraft velocities, cloud formation, etc.?

Briggs: For a very large complex of cooling towers, say 20 or 30 2000-MW towers concentrated on a 1-km² area, the total heat flux is 30 to 100 times the maximum natural sensible heat flux from such an area. This certainly is strong enough a "thermal" to frequently initiate small convective showers in humid conditions. Using the methods suggested in my paper for vertical buoyant plumes, we find that such a source would entrain roughly 10⁷ m³/sec of ambient air from a 1-km-deep mixing layer. If the air is just moderately humid (dew point, 53°F), this amounts to 10⁵ kg/sec of water entrained (100 tons a second!), about four times the amount evaporated by the towers. If the water is spread over 100 km², this gives a precipitation rate of about 0.45 cm/hr, i.e., over 4 in. a day. Given very humid conditions or a deeper mixing layer, you can double these figures. Thus the amount of latent heat "organized" by such a source can easily be an order of magnitude larger than the source value itself, up to the range of a large thunderstorm.

Plumes from such a source will merge at roughly 700 m above the tops of the cooling towers and will have a vertical velocity of 10 to 20 m/sec at the top of the mixing layer, depending on the mixing-layer height and on whether or not condensation occurs. With this much "punch" the plume can penetrate 1 or 2 km above the top of the mixing layer and on many occasions will condense—even on days when no natural condensation occurs. Should condensation occur after entrainment of moderately humid air in the mixing layer, the total buoyancy can easily be boosted 25 times the original owing to sensible heat of the cooling-tower plumes, boosting the total rise to about 6 km (20,000 ft). This assumes normal atmospheric stability aloft (approximately wet adiabatic) and a saturated environment.

Should an ordinary vortex like the commonly observed dust devil or fire whirlwind develop, the experiment discussed in the appendix of my paper suggests maximum tangential and vertical velocities roughly 10 times the buoyant scale velocity, V_B. For the large complex of cooling towers, these velocities would be of the order of 50 to 60 m/sec.

It seems quite likely that there sometimes occurs unstable ambient-temperature and moisture stratifications for which such a source could "trigger" a much greater release of energy, but I consider this area to be outside the competence of our group.



DISCUSSIONS

MODELLING URBAN AIR POLLUTION*

In the paper "Modelling urban air pollution" Hameed makes an important observation about urban air pollution models, one to which we heartily subscribe. He says, "If the proposed model cannot forecast the specific parameters better than persistence then the model is of questionable value". Hanna (1973a) earlier made the same point in nearly the same words, in saying that, "If a new model is not any more accurate than a simple model such as persistence, then the new model is not useful as an applied model". Unfortunately, the remainder of Hameed's paper is based on a quite distorted application of the simple urban pollution model recommended by Gifford and Hanna (1971, 1973). Hameed compares our model, quite unfavorably, with Randerson's (1970) model of air pollution in Nashville. The main objections to this comparison are the following.

1. Hameed bases his comparison on an evaluation of our parameter, c , equation (3) in his paper, that uses values of the vertical atmospheric dispersion parameter typical of average meteorological conditions over a city. But, as emphasized by Gifford and Hanna (1973), this stability assumption is strictly valid only for long-term average concentration conditions and for an inert contaminant, like particulates. For SO_2 we pointed out in this reference that it is necessary to divide c by $225/50 = 4.5$, to compensate for removal or other processes affecting SO_2 ground concentrations. (The case of a reacting system has subsequently been discussed by Hanna (1973b).) When the concentration values calculated by Hameed from our equation are corrected by this factor, they are seen to have quite reasonable levels, essentially nullifying the comments in his Section 3 and most of his conclusions. The revised Table I included here provides these corrected values.

2. In spite of the rather good agreement of the average concentration levels with observed data shown by this corrected application of our method, however, we ourselves would not use it in practice for an application like Nashville, i.e. for a shortterm (2 h) concentration prediction. Randerson's solution to the Nashville problem was an initial value calculation, based on observed values of the concentrations at time zero. Where initial values are available, we too have always based short-term urban concentration estimates on these, rather than the application of our model that Hameed suggests. This was the procedure used for short-term estimates by Gifford and Hanna (1971, 1973), Hanna (1971, 1972, 1973) and Gifford (1972, 1973). Our model works best, as pointed out by Gifford and Hanna (1971) and Hanna (1971), for long-term averaged concentration values. The reason is that short-term air pollution concentrations are strongly affected by various factors, including the completely unknown short-term variability of the source strengths, which make them very uncertain objects for any model.

To minimize this source of uncertainty it seems to us to be clearly preferable to make use of, rather than to ignore, the given, known initial concentration values. We do not look on doing this as in any sense a failure, or shortcoming of our method. Indeed we consider it to be part of normal procedure. We have always operated on this basis and would view Hameed's suggested application, which ignores the given concentration values, as foolhardy—something like trying to make a local short-term weather forecast without looking out the window.

It follows, if in addition the wind speed, stability conditions, and source strengths, the variables in our model, are also constant during the given 2-h period, that our method results in an estimate of concentration levels and pattern that is identical with the assumption of persistence, under these special conditions. This lies behind Hanna's remark quoted above.

It is interesting to note from Table I that the result of following our usual procedure (i.e. assuming persistence) in this particular case leads to a higher area pattern correlation (0.93 compared with 0.81) but a larger relative error of the concentration level (-0.53 compared with 0.23). In fact Nashville SO_2 concentrations actually increased slightly during the forecast period (18:00-20:00 h CST), while maintaining much the same areal pattern. Since a slight decrease in wind and increase in vertical stability are normal for this time of day, this is consistent with the physics of our model. That a correct direct application of our method, Hameed's equations (2 and 3) corrected for SO_2 , gives the smallest relative error (i.e. the closest concentration level) of all the methods considered (0.23) is, we believe, somewhat fortuitous. It supports in general the basic idea of what we recommend; but we would not always expect such good agreement in such an application unless wind speed and stability changes could be included directly. We would be very interested to determine the effects of variation of any of the variables of our model on the 2-h Nashville results. As is so often the case, unfortunately, no data have been reported.

3. Hameed refers to a single application of Randerson's model. Actually Randerson (1970), with admirable candor, reported the results of two distinct applications, to the same Nashville data set, of the same numerical urban diffusion model. In the first of these, all the tall stack SO_2 sources in Nashville were included at the upper boundary of the model, i.e. at or near the point corresponding to their actual physical height. Based on this natural arrangement of the sources, the resulting ground level concentration pattern, after 2 h of model time (and 15 min of digital computer time), was calculated to have a fairly sizeable negative correlation with the observed values. The concentration levels for this calculation averaged about four times those values included as Randerson's model predictions in Hameed's Table I.

* HAMEED S. (1974) *Atmospheric Environment* 8, 555-561.

Discussions

Table 1. Comparison of observed concentrations of SO_2 in Nashville with predictions of several theoretical models. Concentrations are expressed in ppbm (1 ppbm equals $2.7 \times 10^{-5} \text{ g m}^{-3}$ of SO_2). For an explanation of differences from Hamed's Table 1, see text

Observation station	Initial concentration (obs.)	Observed final concentration	Randerson—I model (conc.)	Randerson—II model (conc.)	Equation (1)* (conc.)	Gifford and Hanna model (conc.)	Multicell model (conc.)	Persistence (conc.)
19	3.5	5.8	50	5.1	0.22	10.0	4.0	3.5
48	5.8	13.6	5	6.5	0.23	11.1	7.3	5.8
52	0.0	2.9	30.5	0.4	0.19	6.2	3.2	0.0
56	2.0	6.9	8.5	0.9	0.015	0.8	5.9	2.0
60	14	20.9	16.5	14.0	0.40	18.7	6.8	14
82	5.5	13.2	6.7	4.2	0.35	15.3	3.6	5.5
90	3.5	4.1	6.0	2.7	0.15	7.1	2.9	3.5
Correlation coefficient		-0.34	0.89	0.74	0.81	0.70	0.93	
Mean relative error		2.36	-0.53	-0.97	0.23	-0.36	-0.53	

* In Hamed's paper.

Discussions

To correct this problem, Randerson arbitrarily relocated the strong point sources, which represent 16 per cent of the total number of sources but probably 75 per cent or more of the total SO₂ emissions in Nashville. Instead of placing them at the top model boundary, at a point approximating their actual physical location, he placed them at the surface in his second run, "reapportioning their output among the neighboring area sources". As a result, his pattern correlation increased from -0.34 to 0.89 using exactly the same model. The various concentration values for these cases are included in Table 1, as Randerson—I and Randerson—II. The latter is the only case that Hameed mentions.

Our point is not that such a retroactive, arbitrary, and physically unrealistic modification of a model is necessarily incorrect. Maybe this is the only adjustment that can be made to Randerson's scheme that will permit it to work reasonably well. Of course, in the absence of any further data comparison to verify this point, there is just no way to tell. Perhaps an entirely different adjustment would have to be made for a different source set-up in some other city. It isn't possible to say.

Hameed says of such complex models that, "a model in which an effort is made to systematically consider the various physical and chemical processes...allows us to analyze the reasons for the short-comings of the model and the methods by which they may be corrected". As a broad generalization this statement would be hard to argue with, but it certainly doesn't apply to Randerson's model. Hameed further goes on to say that a "sophisticated", i.e. a complex model, presumably one such as Randerson's, "can be depended upon to predict pollution concentration to within a factor of, say, 2 on the average". This is an astonishing statement. We know of no secure basis for it in the literature, certainly none involving extensive comparisons with data. It is certainly not supported by Hameed's example. Based on Randerson's own analysis, his method is seen to give results varying by a large factor in concentration depending on where you decide to assume the elevated point sources are located. Hameed has either used the wrong example or drawn the wrong conclusion.

4. This leads us to make a comment about the word "sophisticated" which, as used by Hameed as well as others in characterizing urban pollution models, has a distinctly pejorative connotation with respect to the simple models that we study. Gifford (1973) pointed out that "simple" is the opposite not of "sophisticated" but of "complex". The antonym of "sophisticated" is "naive". Simple urban pollution models are not necessarily naive, and may in fact represent the essence of sophistication. Conversely complex models can be, as we believe is amply apparent from the above discussion, quite naive.

5. Hameed included in his Table 1 some results of an application to the Nashville data of his "multi-cell" model, details of which have not yet been published. Based on his concentration values the magnitude of the relative error figure that he gives for his model should be increased by about 10 per cent, from -0.33 to -0.36. Also the corresponding error figure for persistence should be reduced, from -0.56 to -0.53. These numerical corrections have been incorporated into our Table 1.

6. Hameed makes the point in his Section 4, that Q/u and X are not well correlated for the gross annual SO_x and particle pollution data from 29 U.S. cities listed in Table 1 of Gifford and Hanna (1973). This is quite true and is one reason why we did not use these data for this purpose. We were on the contrary trying, using these data, to establish the value of the parameter c in the relation, $X = cQ/u$, which equation we had previously derived by other logic. At the time, these data represented the main published information on air pollution concentrations. To a considerable extent this is still true. Our opinion is that much, perhaps most of the large city-to-city variability in c determined from this information is due to uncertainty in estimating the true pollution source area A , as opposed to the given, standard metropolitan statistical areas. The resulting large, non-meteorological uncertainty in area source strength Q primarily reflects political, social, and economic influences which we could only hope averaged out. The excellent agreement of the average c 's determined this way with values we had previously calculated gave us confidence that this was so.

Parenthetically, looking at Hameed's Fig. 1 leads us to remark that if one really for some reason wishes to apply our formula at the limit of very low air-concentration, i.e. to the problem of non-pollution, then background must certainly be taken into account. Our formula was only presented as a method for accounting for the effect on ambient air quality of given urban pollution sources. This seemed so obvious to us as not to have required any special explanation. In the light of Hameed's criticism we see that we were wrong about this, and that no methodology, however simple, can be made entirely foolproof.

7. Finally, lest all the above be misinterpreted as a general denunciation of complex urban pollution models on our part, we must take issue with another of Hameed's statements. He says that, based on our studies using simple models, we "concluded that efforts to develop more sophisticated models for simulating pollution dispersion are not necessary". (By "sophisticated" Hameed means what we intend by the word "complex" as explained above.) We have never said or implied this and we don't believe it. The statement simply isn't true. Hanna (1973a) discussed the roles of both simple and complex models in the analysis and estimation of urban air pollution. Complex models are clearly necessary for the detailed study of many difficult problems in the physics and chemistry of urban pollution. On the other hand, applied pollution studies of all kinds require the simplest possible models that can successfully explain the particular problem involved.

What we do claim and have repeatedly emphasized is that if a complex urban pollution model can not estimate observed conditions better than a simple model like persistence, a box-model, or our scheme, then it is not useful in applied studies and its development for this purpose is not only unnecessary but unprofitable.

Discussions

In conclusion we wish to draw attention to what could well be called Panofsky's law. Recalling Parkinson's well-known law of bureaucratic growth, Erwin Panofsky (1962) pointed out that "The equally ceaseless growth of scholarly literature...is dominated by the somewhat analogous rule that the more research (R) is done on a smaller number of subjects (S), the more our understanding (U) seems to diminish: $U = S/R^2$. If A writes four pages about a given problem, it takes B sixteen to refute him, and C needs sixty-four to restore—more or less—the status quo". We do not especially enjoy playing the part of C , and apologize to readers for the length of our comments. But we felt it necessary in this instance to try to restore—more or less—the status quo.

ERL/NOAA,
Oakridge,
Tennessee, U.S.A.

F. A. GIFFORD
S. R. HANNA

REFERENCES

- Gifford F. and Hanna S. R. (1971) Urban air pollution modelling. *Proc. 2nd Int. Clean Air Congress* (Edited by Englund H. M. and Beery W. T.) pp. 1146–1151.
- Gifford F. and Hanna S. R. (1973) Modelling urban air pollution. *Atmospheric Environment* **7**, 131–136.
- Gifford F. (1972) Application of a simple urban pollution model. *Proc. Conf. on Urban Environment*, pp. 62–63. American Meteor. Soc., Philadelphia.
- Gifford F. (1973) The simple ATDL urban air pollution model. *Proc. 4th Meeting of the Expert Panel on Air Pollution Modelling*, Chap. XVI. NATO-COCMS Pub. No. 30.
- Hanna S. R. (1971) Simple methods of calculating dispersion from urban area sources. *J. Air Pollut. Control Ass.* **21**, 774–777.
- Hanna S. R. (1972) A simple model for the analysis of photochemical smog. *Proc. Conf. on Urban Environment*, pp. 120–123. American Meteor. Soc., Philadelphia.
- Hanna S. R. (1973a) Urban air pollution models—Why? *Proc. Nordic Symp. on Urban Air Poll. Modelling*, 3–5 October 1973. Vedbaek, Denmark.
- Hanna S. R. (1973b) A simple model for the analysis of chemically reactive pollutants. *Atmospheric Environment* **7**, 803–817.
- Hameed S. (1974) Modelling urban air pollution. *Atmospheric Environment* **8**, 555–561.
- Panofsky E. (1962) Virgo and Victrix. A note on Dürer's Nemesis, Chap. 2 In *Prints* (Edited by Zigrosser C.), Holt, Rinehart & Winston, New York.
- Randerson D. (1970) A numerical experiment in simulating the transport of sulfur dioxide through the atmosphere. *Atmospheric Environment* **4**, 615–632.

AUTHOR'S REPLY

Gifford and Hanna suggest that the predictions of their model agree with observations if multiplied by the factor $50/225 = 1/4.5$. They obtain this factor from the equations $X = 50(Q/u)$ and $X = 225(Q/u)$, which they have proposed for SO_x and particulates, respectively. It is shown in Section (4) of (I) that these linear relationships between X and (Q/u) are not supported by the data used by Gifford and Hanna to deduce them. It is therefore difficult to see any justification for using these relations to obtain the factor $1/4.5$.

One may also consider the removal rate of SO_2 to investigate if SO_2 decays rapidly enough to justify a loss factor of $1/4.5$. For concentrations of the order 10 ppm, a value of 4.5 h (Randerson, see I) for half-life of SO_2 is realistic according to present estimates. To obtain a removal factor of $1/4.5$ would require a half-life of less than an hour which is realistic only for conditions in stack plumes (Weber, 1971). Also, a multi-cell calculation of the same dispersion problem by the present author (see I) and a calculation of the same dispersion event using an Integral Method (Lebedeff and Hameed, 1975) without any removal mechanisms, both yielded results in good agreement with observations. It is clear, therefore, that the assumption of a large removal factor is not necessary to explain the observations. It may also be noted that use of the factor $1/4.5$ has not been indicated in the calculation by Gifford and Hanna for SO_2 dispersion in Bremen (Gifford and Hanna, 1971).

With regard to Section 7 of Gifford and Hanna's comments, I regret that I misunderstood the implication of their papers to be "that efforts to develop more sophisticated models for simulating pollution dispersion are not necessary". I agree with them in the conclusion that a simple model is to be preferred if its results are consistently as good as those of a more detailed model. It should be possible, and is certainly desirable, to make simplifications in dispersion modelling, depending upon the physical parameters important for the situation being modelled. However, it is necessary to understand, and adhere to, the physical conditions under which a simple method approximates the solution of the fundamental transport equations which describe dispersion of contaminants in the atmosphere.

Institute for Space Studies,
N.A.S.A., New York 10025, U.S.A.

S. HAMEED

Discussions

REFERENCES

- Gifford F. A. and Hanna S. R. (1971) Urban air pollution modelling. *Proc. 2nd International Clean Air Congress* (Edited by Englund H. M. and Beery W. T.), pp. 1146-1151.
- Lebedeff S. A. and Hameed S. (1975) Study of atmospheric transport over area sources by an integral method. Submitted to *Atmospheric Environment*.
- Weber E. (1971) Determination of the life time of SO₂ by simultaneous CO₂ and SO₂ monitoring. *Proc. 2nd International Clean Air Congress* (Edited by Englund H. M. and Beery W. T.), pp. 477-481.
-

Chapter 38

FURTHER COMPARISON OF URBAN AIR POLLUTION MODELS

by

F. A. Gifford

Atmospheric Turbulence a Diffusion Laboratory,
National Oceanic and Atmospheric Administration, U. S. A.

5th Meeting NATO/CCMS Expert Panel
on Air Pollution Modeling

Danish Atomic Energy Commission Research Establishment Risø
Roskilde, Denmark

4-6, June, 1974

Comparisons of the ATDL simple urban diffusion model with the outputs of other models and with urban pollution data, described in a previous report to this group (Gifford, 1973), have continued. Some recent results will be summarized briefly below. The derivation of our model was given in some detail in the reference.

The comparisons reported previously consisted of pairs of correlations of the output of the simple model and other models with data. Many urban pollution models have been applied to Los Angeles County pollution data because the available data from several limited observational periods there are quite complete. A problem with model-data comparisons of this type is that it isn't clear exactly in what sense the correlation coefficients involving a number of models can legitimately be compared with one another. In particular space correlations for different arrays of sampling locations are strongly influenced by the particular sampling pattern involved. Thus it is desirable, in order to compare many models on a common basis, to work as much as possible from the same data base.

Problems of this kind have influenced a study by Nappo (1974) in which a number of urban models, applied to the same Los Angeles air pollution problem, are being compared. Figures 1 and 2 display some preliminary results from this study. The pollutant is in each

case carbon monoxide. In addition to the ATDL simple model and various other published modeling results, persistence has also been included. In Figure 1, for each model, the plotted point indicates two correlations: 1) the correlation of the predicted with the observed time pattern of CO concentration, for data that have been averaged over all the eight CO sampling stations in Los Angeles County; and 2) the correlation of the predicted with the observed space pattern of CO concentration, for data that have been averaged over the (12 hour) time period at each station. The basic concentration, source strength, and wind data are those previously presented and discussed by Hanna (1973a).

In Figure 2 another statistic based on the same data and space and time averaging is presented for each model. This is the standard deviation of the ratio of the predicted to the observed concentration values at each station for each hour.

In my previous report to you (Gifford, 1973) I presented a series of correlations which indicated a generally favorable level of performance of our simple model, compared to various other, more complex models. Correlations of either space or time concentration patterns for the simple model were generally as high as or a bit higher than those for the complex models. For the particular Los Angeles CO-pollution data set, however, Figures 1 and 2 seem to show a more complicated picture. The simple model (ATDL-1) provides, in Figure 1, a reasonably high correlation, $\overline{R(t)}^S$, of the space-averaged time-

concentration pattern, as high as most of the other models. The corresponding space-correlation, $\overline{R(s)}^t$, of the time-averaged values is however rather low in this case, both in absolute value and relative to that of other models. Of course these models in almost all cases represent years of development and adjustment involving the same data. In no case (except for the predictions of the simple ATDL model and of persistence) could these results be accepted as defining the final model performance level without verification on independent data. But it seems unlikely that future, independent testing would modify radically the pattern of results in Figure 1.

The situation displayed in Figure 2 is of even more concern. It appears that the detailed, hour-by-hour predictions of the simple model for each station exhibit considerably more variability than do all other models, including persistence. Mr. Nappo has proposed what is probably the correct interpretation. Examination of the data (see Hanna, 1973) show that the excessive variability and "over-prediction" exhibited by the simple model almost always occurred when the observed wind speeds were low. This happened mainly at locations (Burbank, West L. A., Reseda) that the surface wind field analysis (see Roth, 1971) indicated to be near areas of horizontal convergence which, of course, the simple model does not consider.

The remedy is a simple one. If the wind speeds for each hour are first averaged over all stations prior to forming the time-

pattern statistics, and for each station are first averaged over all the hours prior to forming the space-pattern statistics, the points labeled ATDL-2 on Figures 1 and 2 are obtained by application of the simple model. This modification results in a much more satisfactory performance level and is in fact a more reasonable interpretation of the transport wind speed, u , that is the required input to our model.

In discussion during the previous meeting of this group, Dr. Olsson suggested that the performance of a simple model such as ours, applied to a short-period pollution forecast, could be improved by including a correction to account for the diurnal march of stability. This is accomplished in our model simply by modifying the stability-dependent parameter c . To check on this suggestion, the time-concentration pattern of the previous version of our model (ATDL-2) was arbitrarily modified. (The space-pattern statistics are of course not affected). The modification consisted in (arbitrarily) reducing the value of c by 50% between 0800 hrs. and 1200 hrs. and then increasing it slightly after 1300 hrs. The results appear in Figures 1 and 2 as the points labeled ATDL-3. These are seen to provide a considerable improvement over the previous space-averaged time-pattern statistics, just as Dr. Olsson supposed would be the case.

Of course it would be desirable, in the first place, to introduce the diurnal stability influence on c on some basis related to the observed micrometeorological fields and to its definition, for which

see Gifford (1973). Then too, of course, this and the previous modification should be verified on independent data (as should, also, the developmental results of all the other urban models). Nevertheless it is interesting that such simple, reasonable adjustments of the ATDL model result in sizeable improvements in data correlation. As to the future, we plan to continue model-data comparisons in an attempt to define an optimum regional-scale transport and diffusion model which we need for many applications. At the same time we are continuing development of the chemical-reaction model described by (Hanna, 1973b).

Acknowledgement

This research was performed under an agreement between the Atomic Energy Commission and the National Oceanic and Atmospheric Administration.

References:

- Gifford, F. (1973) The simple ATDL urban air pollution model. Proc. 4th Meeting of the expert panel on air pollution modeling, NATO-COCMS Pub. No. 30, Ch. XVI.
- Hanna, S. R. (1973a) Urban air pollution models - Why? Proc. Nordic Symp. on Urban Air Poll. Modeling, 3-5 Oct. 1973, Vedbaek, Denmark.
- Hanna, S. R. (1973b) A simple model for the analysis of chemically reactive pollutants. Atmos. Env., 7, 803-817.
- Nappo, C. (1974) A method for evaluating the accuracy of air pollution prediction models. Paper to be presented at the Symp. on Atmos. Diffusion and Air Poll., Am. Meteor. Soc., Santa Barbara. Sept. 9-13, 1974.

Eschenroeder, A. Q., J. R. Martinez and R. A. Nordsieck (1972)
Evaluation of a diffusion model for photochemical smog simulation.
Final Rpt. No. 68-02-0336 for the Environmental Protection Agency.
General Res. Corp., Santa Barbara, Cal.

Lamb, R. G. and M. Neiburger (1971) An interim version of a generalized urban air pollution model. Atmos. Environ., No. 4, Vol. 5, 239-264.

Pandolfo, J. P. and C. A. Jacobs (1973) Tests of an urban meteorological-pollutant model using CO validation data in the Los Angeles metropolitan area. Vol. 1, EPA Rpt. No. R4-730-025A, The Center for the Environ. and Man, Inc., Hartford, Conn.

Reynolds, S. D., M. K. Liu, T. A. Hecht, P. M. Roth, and J. H. Seinfeld (1973) Further development and evaluation of a simulation model for estimating ground level concentrations of photochemical pollutants. Final Rpt., EPA Contract 68-02-0339, Systems Applications, Inc., Beverly Hills, Cal.

Roth, P. M., S. D. Reynolds, P. J. W. Roberts, and J. H. Seinfeld (1971) Development of a simulation model for estimating ground level concentrations of photochemical pollutants. Final Rpt. 71-SAL-21, Sys. Applications, Inc., Beverly Hills, Cal.

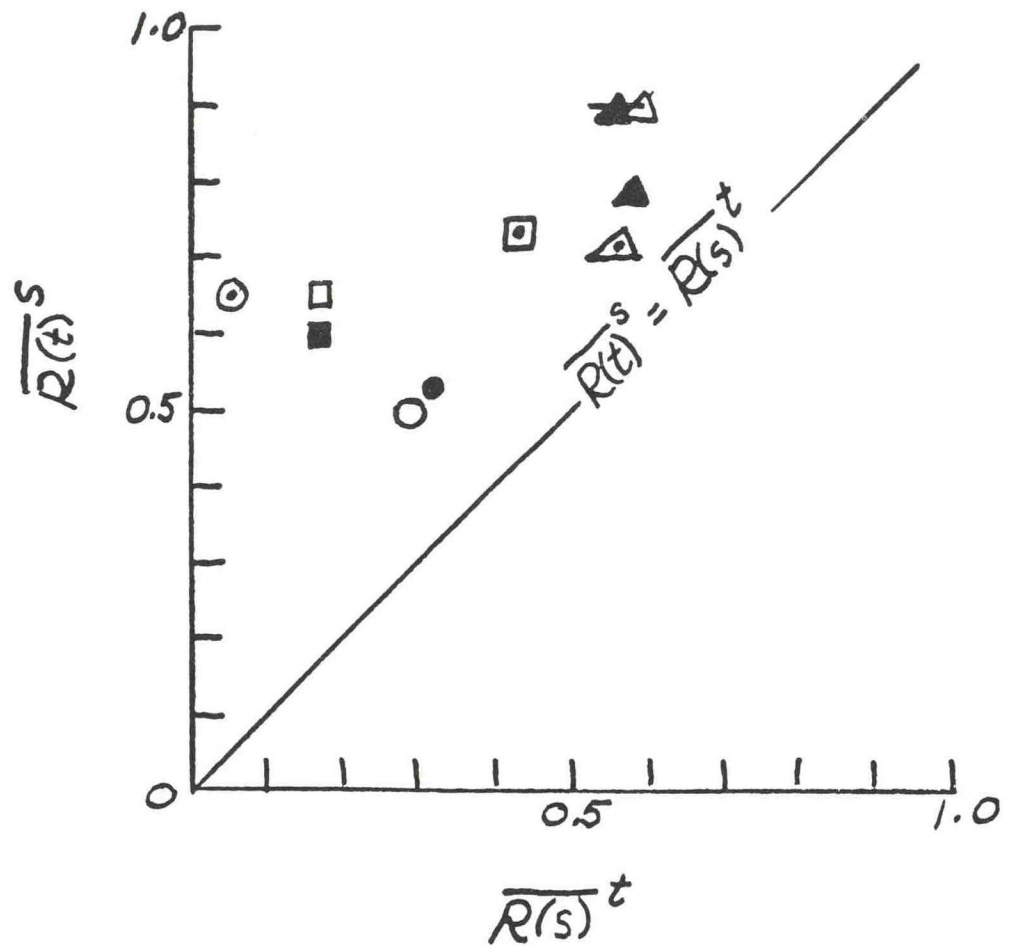
Sklarew, R. C., A. J. Fabrick, and J. E. Prager (1971) A particle-in-cell method for numerical solution of the atmospheric diffusion equation, and applications to air pollution problems. Final Rpt. 3SR-844, Systems, Science and Software, La Jolla, Cal.

Figures:

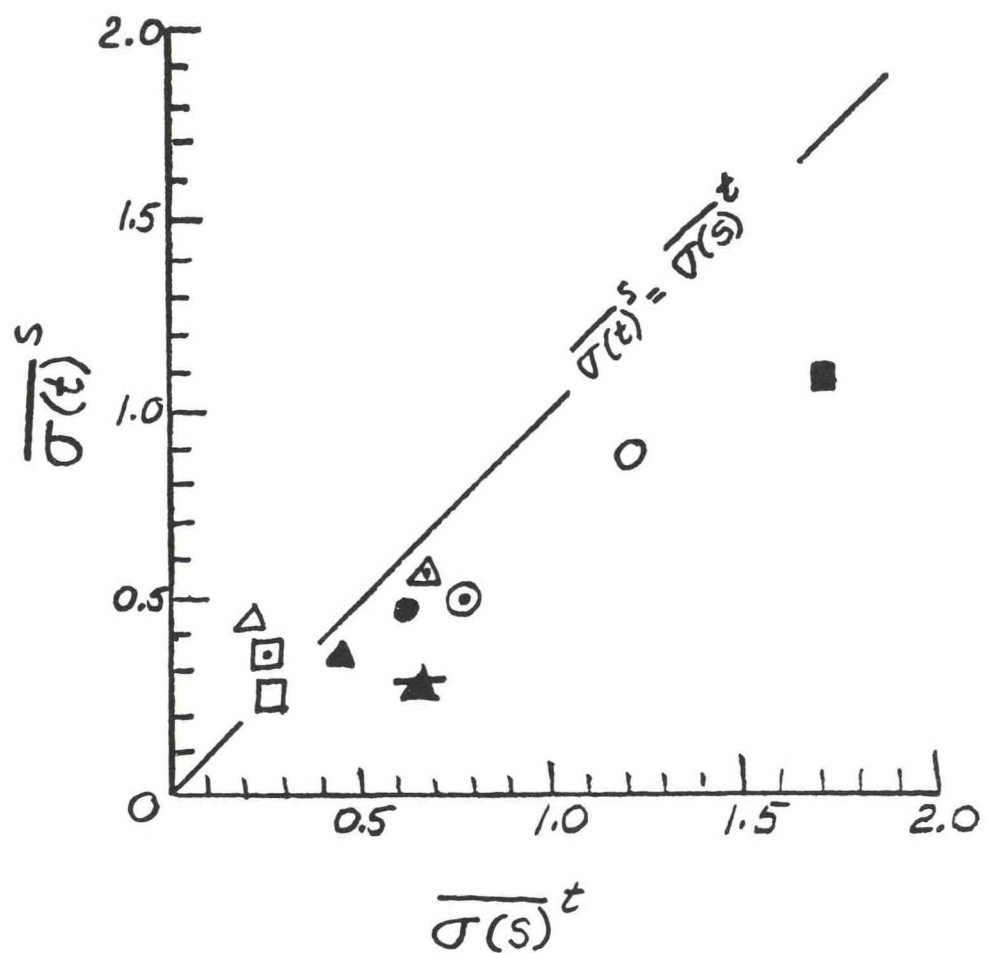
Figure 1. Correlations, for the indicated models, of observed vs. predicted concentrations for Los Angeles carbon monoxide air pollution data; $\overline{R(t)}^S$ refers to time-pattern correlations of space-averaged data; $\overline{R(s)}^T$ refers to space-pattern correlations of time-averaged data.

Figure 2. Standard deviations, for the indicated models, of the ratio of predicted to observed carbon monoxide concentrations at Los Angeles air pollution monitors; $\sigma(t)^S$ refers to space-averaged data and $\sigma(s)^T$ refers to time-averaged data.

- Roth et al. (1971)
- ▲ Reynolds et al. (1973)
- ATDL - I
- Pandolfo and Jacobs (1973)
- Sklarew et al. (1972)
- △ Lamb and Neiburger (1971)
- ▲ ATDL - II
- Eschenroeder et al. (1972)
- 24 Hour Persistence
- ATDL - III



- Roth et al. (1971)
- ▲ Reynolds et al. (1973)
- ATDL - I
- Pandolfo and Jacobs (1973)
- Sklarew et al. (1972)
- △ Lamb and Neiburger (1971)
- ▲ ATDL - II
- Eschenroeder et al. (1972)
- 24 Hour Persistence
- ★ ATDL - III



Fog and Drift Deposition from Evaporative Cooling Towers

By Steven R. Hanna*

Abstract: Methods of determining fog and drift deposition due to emissions from evaporative cooling towers are reviewed and formulas suggested that can be used as a basis for calculations. The Gaussian plume formula is recommended for calculating fog concentrations from which visibility can be estimated. For drift droplets with diameters greater than 200 μm , deposition is calculated by ballistics methods, knowing the environmental wind speed and relative humidity and the vertical velocity of the plume and the droplet. Evaporation of the droplets is accounted for. Drift droplets with diameters less than 200 μm are assumed to be dispersed according to the Gaussian plume formula, with the plume tilted downward to account for the settling speed of the droplet.

There is currently much concern about the environmental effects of evaporative cooling towers. Many are in operation, and many more are being planned for large power-generating stations and other industrial plants. These towers operate by passing air over warm water, which evaporates and thus dissipates excess heat. A thorough discussion of cooling-tower operating characteristics is given in the review by Aynsley and Carson.¹

The environmental problems due to evaporative cooling towers that are of greatest concern at this time

are fog and drift deposition, both of which are most apparent to an observer at the ground. Fog (drop diameter $\approx 10 \mu\text{m}$) is defined as water drops formed in the atmosphere by condensation and thus is relatively free of impurities. Drift is defined as water drops formed by the splashing apart of the circulating cooling water in the tower. The drift droplets are then carried aloft by the air stream. If the cooling water contains chemicals, the drift droplets contain roughly the same concentrations of these chemicals and could affect vegetation, animals, and structures downwind of the cooling tower. In a tower that uses salt water for cooling, the drift water is salty whereas the fog is relatively pure. Several researchers²⁻⁷ during the past 3 years have devised analytical methods for calculating drift deposition or fog potential. These methods are based in some cases on quite different assumptions, and some are geared to application at a specific site. Many of the more important recent papers on the subject of fog and drift deposition are reviewed here, and some formulas that can be used as a basis for calculations are suggested.

SOURCE CHARACTERISTICS

The two types of evaporative cooling towers in common use are natural-draft and mechanical-draft towers. A power station in the 1000-MW(e) range may use from 1 to 3 natural-draft towers or 10 to 30 mechanical-draft towers. Mechanical-draft tower cells are generally grouped into lines of about 10. As its

*Steven R. Hanna received the B.S., M.S., and Ph.D. degrees in meteorology from the Pennsylvania State University in 1964, 1966, and 1967, respectively. Since 1967 he has worked as a Research Meteorologist at the Air Resources Atmospheric Turbulence and Diffusion Laboratory of the National Oceanic and Atmospheric Administration in Oak Ridge, Tenn.

name implies, the natural-draft tower does not use fans to move air but relies on its large size (150 m tall, 60 m top diameter) to create a density difference that forces a vertical speed of about 5 m/sec. In contrast, shorter (20 m) and narrower (10 m) mechanical-draft towers rely on fans to force the air over the warm water at a speed of about 10 m/sec. In both types of towers, the air is saturated and is at a temperature averaging from 10 to 30°C above ambient when it leaves the towers. The flux of latent heat is three to five times the flux of sensible heat. Usually fog (water concentration about 1 g/m³) is also visible in the effluent.

Recent measurements show that the amount of drift emitted at cooling towers is much less than had previously been expected.^{1-3,5} Typical measured values for drift loss at modern towers range from 0.001 to 0.01% of the circulating-water flow. At a 1000-MW(e) power station, these values correspond to drift fluxes ranging from 2 to 20 gal/min (120 to 1200 g/sec). Since the total flux of excess water (drift drops, fog drops, and excess vapor) is typically about 5×10^5 g/sec, it is clear that the flux of water vapor is several orders of magnitude larger than the flux of liquid water (drift plus fog).

Most of the smaller drift drops (diameter 100 to 500 μm) originate from splashing in the tower packing material; some of the larger drift drops (>500 μm) may form by being blown off structural members in the upper part of the tower. Thus the droplet-size distribution can be multimodal and is certainly strongly dependent on the type of drift eliminators, the fan speed, and other physical characteristics of the tower. The few reported measurements of drop-size distribution^{1-3,5} suggest that the mass of the drops emitted by modern towers is fairly evenly distributed in the drop-diameter range from 50 to 300 μm. At some of the older mechanical-draft towers where outdated drift eliminators are in use, drift droplets with diameters up to 0.5 cm can be observed. Owing to the cube dependence of mass on diameter, it is easy to reduce the total mass of drift emission substantially by capturing a few large drops.

CALCULATION OF FOG CONCENTRATIONS

Ground fog downwind of the cooling tower can be created by the dispersion of water, which can be calculated in the same way as the dispersion of any other substance, such as suspended particles.⁸ The Gaussian plume model for a point source can be recommended. According to this model, the hourly

average concentration χ of water in the plume is given by

$$\chi = \frac{Q}{2\pi U\sigma_y\sigma_z} \exp\left(-\frac{y^2}{2\sigma_y^2}\right) \times \left\{ \exp\left[-\frac{(z-h)^2}{2\sigma_z^2}\right] + \exp\left[-\frac{(z+h)^2}{2\sigma_z^2}\right] \right\} \quad (1)$$

where source strength Q (g/sec) is the total flux of excess water from the tower and the parameters σ_y , σ_z , U , y , z , and h are, respectively, the horizontal and vertical dispersion lengths, the wind speed, crosswind distance from the plume axis, height above ground, and the effective source height. The second exponential term involving z accounts for the reflection of the plume from the ground. If it is necessary to calculate yearly averages, the formula for ground-level concentration of χ along a 22½° arc at a distance x from the source is

$$\chi = \left(\frac{2}{\pi}\right)^{\frac{1}{2}} \frac{fQ}{U\sigma_z(\pi x/8)} \exp\left(-\frac{h^2}{2\sigma_z^2}\right) \quad (2)$$

where f is the frequency with which the wind blows toward a given sector.⁸ It is assumed that there are 16 wind-direction sectors. Graphs of σ_z and σ_y as a function of stability and downwind distance were given by Gifford.⁸ Effective source height h is the sum of stack height h_s and plume rise H , which can be estimated from initial plume characteristics and environmental conditions using the plume-rise theory of Briggs⁹ as modified for cooling-tower plumes by Hanna.¹⁰

In a stable atmosphere with the wind blowing at a speed greater than about 1 m/sec and the visible cooling-tower plume evaporating a short distance from the tower, plume rise H is estimated using

$$H = 2.9(F/U_s)^{\frac{1}{2}} \quad (3)$$

where the initial buoyancy flux F and the stability parameter s are defined by

$$F = \frac{g}{T_p} w R^2 (T_p - T_a) \quad (4)$$

and

$$s = \frac{g}{T_a} \left(\frac{dT_a}{dz} \right) + 0.01^\circ \text{K/m} \quad (5)$$

where g = acceleration of gravity

w = initial vertical speed of the air at the tower opening

R = tower-opening radius

T_p = absolute temperature of the plume air

T_a = absolute temperature of the ambient air

Since the atmosphere is usually slightly stable and the wind is usually blowing, this formula applies to most cases of interest. The reader is referred to Briggs⁹ for plume-rise formulas applying to calm or neutral cases.

If the atmosphere is nearly saturated and the plume remains visible for several hundred meters downwind of the tower, much of the latent heat in the plume has probably been released and should be included in the initial buoyancy flux F . This is done by adding the latent heat flux, $(gL/c_p T_p)wR^2 (m_p - m_a)$, to the sensible heat flux calculated from Eq. 4 and substituting the resulting total heat flux for F in Eq. 3 in order to calculate plume rise. The symbols L , c_p , m_p , and m_a are, respectively, the latent heat of vaporization of water, the specific heat of air at constant pressure, and the water-vapor mixing ratios (grams of water/grams of air) of the plume air and the ambient air. In cases where only part of the latent heat is released, an iterative procedure described by Hanna¹⁰ can be used to estimate plume rise.

Owing to aerodynamic downwash, the effective source height h of the plume from a mechanical-draft cooling tower is zero when the wind speed exceeds the vertical speed of the plume at the tower opening.¹⁰ However, for natural-draft towers, the plume very rarely washes down to the ground.¹¹

At distances of less than about 1 km from a bank of mechanical-draft towers, the towers should be treated as a finite line source rather than a point source. Gifford⁸ gives equations and references for finite line sources. Generally these equations result from integration with respect to y of Eq. 1.

Roffman et al.⁶ and England, Enscher, and Taft¹² are analyzing the dispersion of water from cooling towers by solving the diffusion equation, which requires the specification of an eddy diffusivity, K . We hope this approach will work better than the simple, unmodified Gaussian plume model in areas where there are significant terrain variations or nonuniform flow and stability patterns. However, the Gaussian plume model has been used in most of the published studies that calculate fog concentrations and frequencies.^{3,7,13-16} In most cases the results are expressed in terms of the excess number of hours of fog per season caused by the cooling tower. Fog is assumed to form at

a point where the concentration of water caused by the cooling tower is sufficient to saturate the air. Typically, a few dozen extra hours of fog per year are caused by a 1000-MW(e) power plant during the winter at a distance of 10 km from the plant.

The length of the visible plume can be calculated^{17,18} on the basis of the characteristics of the Gaussian plume model. We can see from Eq. 1 that, if X is the visible length of the plume at its axis, then the plume will be visible at the ground only at distances x from the source such that the following condition is satisfied:

$$\sigma_y(X) \sigma_z(X) > \sigma_y(x) \sigma_z(x) e^{h^2/2\sigma_z^2(x)} \quad (6)$$

A nomogram for determining conditions of plume visibility at the ground for source heights of 50 and 100 m and neutral and very stable conditions is given by Hanna and Swisher.¹⁸

Recently it has become important to also determine visibility in the fog caused by evaporative cooling towers. Even if the air is not saturated, increases in water-vapor content can decrease visibility owing to the absorption of water vapor by condensation nuclei. As reported by Neuberger,¹⁹ Junge observed a linear decrease in visibility from 40 to 10 miles as relative humidity increased from 70 to 90%. This process depends strongly on the concentration of condensation nuclei in the air, which depends on the nearness of the air mass to such natural or man-made sources of nuclei as seashores or steel mills.

By definition, fog occurs when visibility is less than 1 km. The amount of liquid water in fog varies within wide limits. A dense sea fog, with visibility less than 30 m, has a liquid-water content of about 3 g/m³. A light valley fog, with visibility of about 1 km, has a liquid-water content¹⁹ of about 0.02 g/m³. An equation for expressing visibility, V (m), in terms of droplet-size distribution and liquid-water content, ω (g/m³), was first derived by Trabert:²⁰

$$V = \frac{\alpha \sum n_D D^3}{\omega \sum n_D D^2} \approx \beta \frac{D}{\omega} \quad (7)$$

where the parameters α and β are constants and n_D is the number of drops of diameter D (μm). The simplification is valid if drop-size spectra have similar shapes. On the basis of observations,²¹ the constant β has the approximate value $2 \text{ g}/(\text{m}^2)(\mu\text{m})$. Thus the visibility increases as liquid-water content decreases or as average drop size increases.

For comparison, the observed parameters²¹ of inland (radiation) and coastal (advection) fogs are listed in Table 1. To assess the annual environmental impact of fogs caused by cooling towers, we must

Table 1 Physical Fog Models

Fog parameters at the surface	Radiation (inland) fog	Advection (coastal) fog
Average drop diameter, μm	10	20
Typical drop-size range, μm	4 to 36	6 to 64
Liquid-water content, g/m^3	0.11	0.17
Droplet concentration, cm^{-3}	200	40
Vertical depth of fog, m		
Typical	100	200
Severe	300	600
Horizontal visibility, m	100	300

acquire joint distribution functions of source strength, wind speed and direction, stability, and environmental saturation deficit (saturation water-mixing ratio minus actual water-mixing ratio). After the concentrations of fog are calculated using Eq. 2, Table 1 and Eq. 7 can be used to determine the visibility in the fog, assuming that cooling-tower fogs have parameters in this range. A measuring program should be carried out to determine whether it is valid to assume that the characteristic parameters of cooling-tower fogs are in the range of those of natural fogs.

A related problem is the extent of the visible plume aloft and its shadowing effect. Bogh et al.²² evaluated the centerline concentration of fog in the plume, using Eqs. 1 or 2 to determine the frequency of occurrence of visible plumes of various lengths. They found that the plume caused less than 1% reduction in sunshine near the plant.

CALCULATION OF DRIFT DEPOSITION

Since the settling speed of fog droplets is less than a few centimeters per second, it is assumed in the preceding calculations that they do not appreciably settle to the ground. However, since drift droplets settle at a speed of roughly 1 m/sec, their deposition on the ground must be accounted for. The effect of surface deposition of drift water droplets in the region around the cooling towers could be good or bad, depending on whether additional rain is beneficial or detrimental to plant and animal life in the vicinity. The amount of additional rain and ice due to drift from

typical towers has been calculated and observed to be insignificant, except in the area within a few hundred meters of the tower.^{23,24} Icing of roads, trees, and power lines is also observed to be insignificant except in the immediate area of the tower. The major problem with drift deposition occurs when seawater is used for cooling or when such substances as chromium are used as biocides or rust inhibitors. There is a potential problem, for example, at the Chalk Point, Md., power plant, where seawater will be used for cooling and tobacco is grown on the farms in the area. The state of Maryland is sponsoring a major research program²⁵ to determine the environmental effects of the cooling towers at Chalk Point. A study is also under way of the effects of using chromium in the cooling towers at the Oak Ridge, Tenn., Gaseous Diffusion Plant. In both these studies, observed drift deposition will be compared with the predictions of models, using observed source and meteorological parameters as input.

The terminal fall speeds V_g of drift droplets are in the range¹⁹ given in Table 2. Typical turbulent fluctuations of vertical wind speed are 0.10 to 1.0 m/sec.

Table 2 Terminal Fall Speeds of Pure-Water Drops

Diameter, μm	50	100	200	400	600
Fall speed V_g , m/sec	0.01	0.25	0.70	1.6	2.5

Drops with terminal fall speeds greater than the turbulent fluctuations fall through the turbulence and are not greatly dispersed by it. As Van der Hoven²⁶ recommends, for terminal fall speeds greater than about 1 m/sec, the effect of turbulent diffusion on the ground deposition pattern can be neglected. The problem then becomes that of calculating drop trajectories, using the appropriate fall speed of each drop and the wind velocity. For terminal fall speeds less than 1 m/sec, either the Gaussian plume model or the diffusion equation can be used to calculate the diffusion and subsequent deposition of the drops. In this case, the droplet plume descends at speed V_g relative to the gaseous plume.

Various combinations of the trajectory and diffusion techniques for calculating drift deposition have appeared in the literature. For example, Hosler, Pena, and Pena⁴ use the trajectory technique. Roffman and Grimble² solve the diffusion equation analytically, accounting for both trajectories and diffusion. Wistrom and Ovard⁵ use the method described above; i.e., the trajectory technique for drops with diameters greater than 200 μm and the Gaussian plume technique for

drops with diameters less than 200 μm . There are many uncertainties in all models due to our imperfect knowledge of the source and of the diffusion parameters and to the lack of a validation experiment.

If the drift droplets pass through a portion of the atmosphere that is unsaturated, they evaporate either to an equilibrium drop solution or to a salt particle. In an unsaturated environment a drop will lose mass at the rate⁵

$$\frac{dm}{dt} = \frac{-2\pi\delta M(p_0 - p_a)D}{RT} \left[1 + \frac{0.276 (\text{Re})^{\frac{1}{4}}}{(\delta/\nu)^{\frac{1}{4}}} \right] \quad (8)$$

where m = mass, g

t = time, sec

R = gas constant, 8.31×10^7 ergs/(mole)(°K)

T = absolute temperature of drop, °K

M = molecular weight of water, 18 g/mole

δ = diffusion coefficient of water vapor, ~ 0.24 cm^2/sec

p_0 = vapor pressure at drop surface, dynes/cm²

p_a = vapor pressure in ambient air, dynes/cm²

D = drop diameter, cm

ν = kinematic viscosity of air, ~ 0.18 cm^2/sec

$\text{Re} = DV_g/\nu$, droplet Reynolds number

The vapor pressure at the drop surface p_0 is related to the vapor pressure p_p over a plane surface of water by the formula⁴

$$p_0 = p_p [\exp(4sM/\rho_w DRT)] \times \left[1 + \frac{im_s M}{M_0 [(1/6)\pi D^3 \rho_w - m_s]} \right]^{-1} \quad (9)$$

where s = surface tension of liquid, ~ 70 dynes/cm for water at room temperature

ρ_w = water density, g/cm³

m_s = mass of solute, g

M_0 = molecular weight of solute

i = van't Hoff factor (usually equal to about 2.0 for sea salt).²

The changes in size of the drop due to evaporation can be calculated using Eqs. 8 and 9. As the drop becomes smaller, its fall speed decreases. For drops less than 200 μ in diameter, the deposition $W[\text{g}/(\text{cm}^2)(\text{sec})]$ at the surface is given by the product of the mass concentration $\chi(\text{g}/\text{cm}^3)$ and the drop fall speed V_g near the surface:

$$W = V_g \chi \quad (10)$$

The above-mentioned calculations are simplified in practice by the use of graphical solutions or nomograms. Hosler et al.⁴ make efficient use of nomograms in their development of methods to estimate the rate of salt deposition due to the use of seawater in cooling towers. They give nomograms for cases of (1) no evaporation of drops, (2) evaporation to saturated solution, and (3) evaporation to dry salt. In each nomogram the distance from the tower at which the drop will strike the ground is given as functions of the droplet size, salt concentrations in the droplet, wind speed, and maximum height reached by the drops. The maximum height reached by the drops is calculated from the equation of motion of the drop, assuming a linear variation with height of the vertical-speed distribution in the plume. The droplets rise to a height h_p and then fall out of the plume. Hosler et al.⁴ could have been more accurate had they used the equation of Briggs⁹ for the vertical speed w_p in the plume:

$$w_p = 1.06 F^{\frac{1}{4}} x^{-\frac{1}{4}} \quad (11)$$

where the symbols are the same as in Eqs. 3 and 4.

The distance h_e that the drops must fall to reach equilibrium size is then calculated by Hosler et al.,⁴ employing methods equivalent to the use of Table 2 and Eqs. 8 and 9. They make the approximation that if the equilibrium distance h_e is less than the maximum droplet height h_p and the relative humidity is less than an arbitrary number, which they select as 50%, evaporation is complete.

Once the distance from the tower at which the drop will strike the ground is known, for the drop sizes that bracket a size range within which the mass flux is known, then it can be assumed that the mass is deposited uniformly on the ground between those two distances, x_1 and x_2 . For constant wind direction, the crosswind variation of deposition from the plume axis can be calculated by assuming that the crosswind distribution is Gaussian and using values of $\sigma_y(x)$ suggested, for example, by Gifford.⁸ For variable wind direction, usually reported at 16 points around the compass, it can be assumed that the deposition in any sector is uniform in the area bounded by the 22½° wind-direction sector and the distances x_1 and x_2 .

Because of the possibility of drop evaporation, the problem of calculating drift deposition is more difficult than that of calculating the deposition of inert particles or aerosols. As the drop evaporates, its fall speed decreases, so that the usual ballistics equations do not apply. Consequently the solution must be obtained by means of computer models or detailed nomograms.

Roffman and Grimble² solved the formidable problem of obtaining an analytical solution to the diffusion equation for drift drops. They did not assume that the plume had Gaussian form but instead relied on the flux-gradient hypothesis of the diffusion equation. They used an empirical form of Eq. 8 for drop evaporation and obtained the drift deposition in terms of Hermite polynomials. However, this mathematically elegant solution is dependent on the assumptions that the vertical and crosswind turbulent diffusivities K_z and K_y are constants; K_z is known to be a linear function of height up to heights of about 100 m. Since all droplets must pass through this layer on their way to the ground, it is important to determine the errors introduced by assuming constant K_z . Their method permits the assessment of the relative importance, as a function of droplet size and atmospheric stability, of turbulence and gravitational settling on the deposition rate. For a typical large cooling tower and typical drift-droplet mass-size distribution, it was found that "under well mixed atmospheric conditions the diffusion mechanism is dominant over gravity forces while under stable atmospheric conditions the gravity forces are dominant over the diffusion," in terms of relative importance in the deposition process.

Whenever any of these models is used to calculate salt deposition rates, it is usually found that the deposition rate is a small fraction of the natural deposition rate.¹⁻⁴ Where seawater is used for cooling, there is usually a high natural salt deposition rate due to advection from the nearby ocean or bay. However, because of the frequent occurrence of downwash from mechanical-draft cooling towers, the resulting salt deposition rate from mechanical-draft towers can be higher than the natural rate in the area within a few hundred meters of these towers. We are not yet sure whether deposition of chromium, etc., due to emissions from inland towers, has significant environmental effects.

SUMMARY

It is recommended that the Gaussian plume model, as discussed by Gifford,⁸ be used to calculate the concentration and frequency of occurrence of ground-level fogs. Visibility can be estimated from the liquid-water content²¹ and average drop size of the fog using Trabert's equation.²⁰

The calculation of drift deposition is complicated because the drops may partially evaporate and thus change their settling speed as they fall through unsaturated air. Methods for calculating the rate of

evaporation of drops as a function of their size, the amount of solute, and the ambient mixing ratio have been given.^{4,5} Drops with diameters less than 200 μm are assumed to be dispersed according to the Gaussian plume model, whereas drops with diameters greater than 200 μm are assumed to fall through the turbulence along a trajectory determined by the ambient wind vector and the drop fall speed.

Models of drift deposition^{2,12} which employ the diffusion equation and diffusivities K_y and K_z may ultimately provide the best estimates of deposition in complex terrain or when the wind vector changes with time; i.e., when the "straight-line," unmodified Gaussian plume model may not apply. However, solutions have been obtained only for constant K_y and K_z at this time.

REFERENCES

1. E. Aynsley and J. E. Carson, Environmental Effects of Water Cooling for Power Plants: A Status Report, USAEC Report ANL/ES-20, Argonne National Laboratory, 1973.
2. A. Roffman and R. E. Grimble, Predictions of Drift Deposition from Saltwater Cooling Towers, presented at the Annual Meeting of the Cooling Tower Institute, Jan. 29-31, 1973, Houston, Tex., 17 pp.; available from Westinghouse Environmental Systems Department, Monroeville Mall, Monroeville, Pa. 15146.
3. Attachment 5, Forked River Nuclear Station, Unit 1, Natural Draft Saltwater Cooling Tower, Assessment of Environmental Effects, Jersey Central Power & Light Co., January 1972.
4. C. L. Hosler, J. Pena, and R. Pena, Determination of Salt Deposition Rates from Drift from Evaporative Cooling Towers, Department of Meteorology, The Pennsylvania State University, University Park, Pa. 16802, May 1972.
5. K. Wistrom and J. C. Ovard, Cooling-Tower Drift, Its Measurement, Control, and Environmental Effects, presented at the Annual Meeting of the Cooling Tower Institute, Jan. 29-31, 1973, Houston, Tex., 22 pp.; available from Ecodyne Cooling Products Co., P.O. Box 1267, Santa Rosa, Calif. 95403.
6. A. Roffman et al., The State of the Art of Saltwater Cooling Towers for Steam Electric Generating Plants, USAEC Report WASH-1244, Westinghouse Electric Corp., February 1973.
7. P. M. Altomare, The Application of Meteorology in Determining the Environmental Effects of Evaporative Heat Dissipation Systems, presented at 64th Annual Meeting of the Air Pollution Control Association, Atlantic City, N. J., June 27-July 1, 1971.
8. F. A. Gifford, Jr., An Outline of Theories of Diffusion in the Lower Layers of the Atmosphere, in Meteorology and Atomic Energy—1968, D. H. Slade (Ed.), USAEC Report TID-24190, pp. 65-116, July 1968.
9. G. A. Briggs, Plume Rise, AEC Critical Review Series, USAEC Report TID-25075, 1969.
10. S. R. Hanna, Rise and Condensation of Large-Cooling-Tower Plumes, *J. Appl. Meteorol.*, 11: 793-799 (1972).

11. T. J. Overcamp and D. P. Hoult, Precipitation in the Wake of Cooling Towers, *Atmos. Environ.*, 5: 751-765 (1971).
12. W. G. England, L. H. Ensheher, and J. R. Taft, Cooling Tower Plumes: Defined and Traced by Means of Computer Simulation Models, presented at the Annual Meeting of the Cooling Tower Institute, Jan. 29-31, 1973, Houston, Tex., 42 pp., available from Systems, Science, and Software, La Jolla, Calif. 92037.
13. R. K. Woodruff et al., Final Report on a Meteorological Evaluation of the Effects of the Proposed Cooling Towers at the Hanford Number Two "C" Site on Surrounding Areas, prepared by Battelle Pacific Northwest Laboratories, Richland, Wash. 99352, under contract No. BR-2808-7 to Burns and Roe, Inc., Hempstead, N. Y., September 1971.
14. J. R. Coleman et al., Environmental Effects of Cooling Tower Operation at the Trojan Site, prepared by NUS Corp., 2351 Research Boulevard, Rockville, Md. 20850, for Portland General Electric Co., January 1969.
15. G. E. Collins, C. R. Case, and C. J. Mule, Cooling-Tower Effects (Fogging), Vermont Yankee Generating Station, prepared by The Research Corp. of New England, 210 Washington Street, Hartford, Conn. 06106, Project 5189, August 1971.
16. EG&G, Inc., Potential Environmental Modifications Produced by Large Evaporative Cooling Towers, U. S. Water Quality Office, Water Pollution Control Research Series, 16130-DNH-01/71, 1971.
17. H. R. A. Wessels and J. A. Wisse, A Method for Calculating the Size of Cooling-Tower Plumes, *Atmos. Environ.*, 5: 743-750 (1971).
18. S. R. Hanna and S. D. Swisher, Discussion of a Method for Calculating the Size of Cooling-Tower Plumes, *Atmos. Environ.*, 6: 587-588 (1972).
19. H. H. Neuberger, *Introduction to Physical Meteorology*, College of Mineral Industries, The Pennsylvania State University, University Park, Pa. 16802, 1957.
20. W. Trabert, Die Extinction des Lichtes in Einem Trüben Medium (Schweite in Wolken), *Meteorol. Z.*, 18: 518-520 (1901).
21. R. J. Pilić, A Review of Project Fog Drops, presented at Symposium on Progress of NASA Research on Warm Fog Properties and Modification Concepts, 1969, Report NASA-SP-212, pp. 1-23, 1969.
22. P. Bogh et al., A New Method of Assessing the Environmental Influence of Cooling Towers as First Applied to the Kaiseraugst and Leibstadt Nuclear Power Plants, presented at International Nuclear Industrial Fair, Oct. 16-21, 1972, Basel, Switzerland, Available from Nuclex 72, CH-4021 Basel/Schweiz.
23. F. A. Huff et al., Effect of Cooling-Tower Effluents on Atmospheric Conditions in Northwestern Illinois, *Illinois State Water Survey, Circular 100*, 1971 (PB-197562).
24. S. R. Hanna and S. D. Swisher, Meteorological Effects of the Heat and Moisture Produced by Man, *Nucl. Safety*, 12(2): 114-122 (March-April 1971).
25. J. Pell, Maryland Initiates Brackish-Water Cooling-Tower Study at Chalk Point, *Record of the Maryland Power Plant Siting Act*, 1, August 1972.
26. I. Van der Hoven, Deposition of Particles and Gases, in Meteorology and Atomic Energy - 1968, D. H. Slade (Ed.), USAEC Report TID-24190, pp. 202-208, July 1968.

DIURNAL VARIATION OF VERTICAL THERMAL STRUCTURE IN A PINE PLANTATION

R. P. HOSKER JR., C. J. NAPPO JR. and S. R. HANNA

Air Resources Atmospheric Turbulence and Diffusion Laboratory, NOAA, Oak Ridge, Tenn. (U.S.A.)

(Received December 3, 1973; accepted March 25, 1974)

ABSTRACT

Hosker Jr., R. P., Nappo Jr., C. J. and Hanna, S. R., 1974. Diurnal variation of vertical thermal structure in a pine plantation. *Agric. Meteorol.*, 13: 259–265.

Initial observations of the diurnal variation of the vertical thermal structure of a loblolly pine plantation are presented. Results obtained in other forests are qualitatively confirmed. On a clear day a very unstable temperature gradient occurs above the trees, while a strong inversion ($\sim 8^{\circ}\text{C}$) develops below the crowns. At night the sub-crown region becomes weakly unstable, but the atmospheric layer above the trees is then stable. On a rainy day, the strength of the temperature inversion beneath the tree crowns is less than 1°C . The position of the daytime temperature maximum in the tree-tops responds to the solar elevation, eventually descending about 2 m to the region of maximum foliage density as the sun's rays penetrate deeper into the tree crowns.

INTRODUCTION

The Atmospheric Turbulence and Diffusion Laboratory (ATDL) in Oak Ridge, Tennessee, is beginning an intensive investigation of diffusion, deposition and turbulence within and above a forest canopy. As a first step, an examination of the thermal structure within and above a pine plantation has begun. In this note the site and instrumentation are described and some initial results are presented.

SITE AND INSTRUMENT DESCRIPTION

The ATDL field site (Fig. 1) is on the Clinch River flood plain about 3.5 km southwest of the Oak Ridge National Laboratory. The topography is typical of the eastern Tennessee valley region, and consists of broad flat valleys between parallel ridges which lie in a mostly southwest–northeast direction. The forest under study is a plantation of loblolly pines. The stand is about 25 years old, with a mean tree height of about 17 m and a tree spacing of

ATDL Contribution File No. 95.

about 3 m. On the basis of wind profiles obtained from a 37 m tower in this forest, the displacement height and roughness length were estimated to be about 14 m and 1 m, respectively.

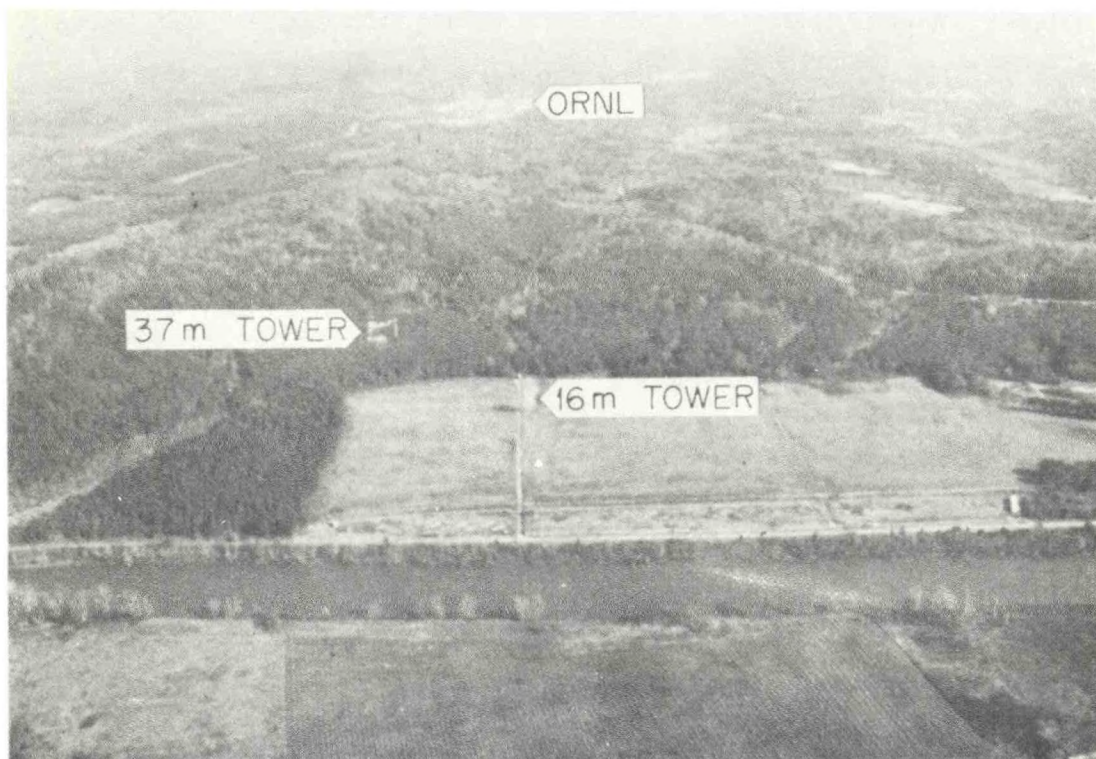


Fig.1. Aerial view, looking north-northeast, of pine plantation and surroundings. Instrumented 37 m forest tower is visible to left of center. Strong winds are most often from southwest. Smoke is being emitted from both towers in this photo.

The tree density is on the order of 1600 trees/ha. The breast-height diameter is about 16 cm, and is normally distributed with a standard deviation of about 4.1 cm. The leaf needle surface area index for the plantation, as determined in late summer, is about 8; this value is in reasonable agreement with data obtained in a loblolly pine plantation near Duke University, where this index was found to vary between 5.2 and 9.7 over the 30 week growing season (Knoerr, 1973). This forest is in need of thinning since the trees are currently very densely packed. When the initial set of experiments is completed, therefore, the forest will be thinned; the experiments will then be repeated to explicitly exhibit the effect of density on the results.

The planted area is fairly flat, and is bounded on the west by a ridge about 80 m above the forest floor, and to the east by lower hills about 50 m above the forest floor. To the southeast is an extensive grass field with a sharp boundary at the forest. Climatological wind data taken near this site show that the flow is across the field and over the forest edge about 40% of the time. It is observed that for strong winds, the flow is usually from the southwest, suggesting channeling by the surrounding ridges.

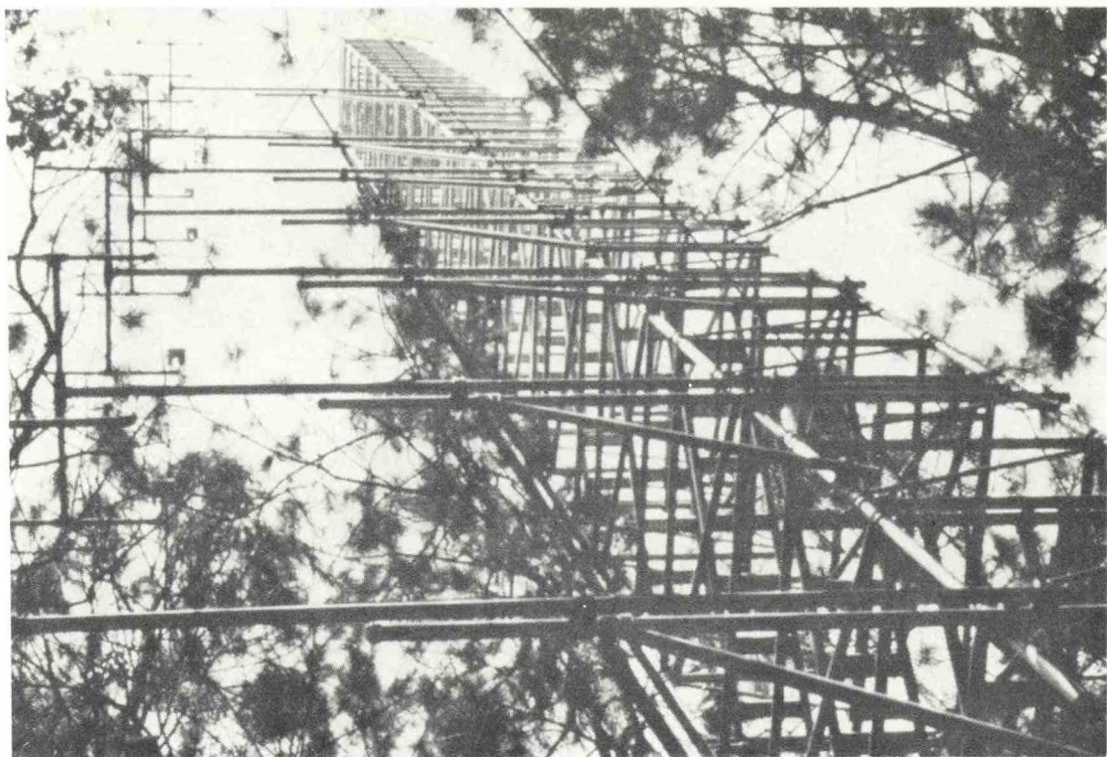


Fig.2. View of 37 m tower and instrument array. Note proximity of trees; no clearing was made for the tower.

Two towers are now on the site, a 16 m triangular tower in the field, and a 37 m walk-up tower in the forest. The forest tower, pictured in Fig.2, was erected with as little disturbance to the trees as possible. This tower is instrumented at ten levels (heights are given in Table I) with shielded bead therm-

TABLE I

Heights of the instruments

Height (m)	Thermistor	Hygrograph	Anemometer	Vane
37.7	x	x	x	x
24.2	x	x	x	
18.7	x	x	x	
16.5	x	x	x	
14.3	x			
12.0	x			
9.4	x	x		
6.9	x			
4.7	x	x		
1.2	x			

istors*. The lowest level is just above the forest floor and the highest is at the tower top. The upper three levels are above the canopy, with the fourth roughly at tree top level; these four stations are also instrumented with low-threshold cup anemometers**. Thermistor accuracy has been checked to within $\pm 0.2^\circ\text{C}$, while the anemometers, with a threshold of about 0.3 m/sec, are accurate to within $\pm 2\%$. Both the thermistors and the anemometers are mounted on 3 m booms extending in a southwest direction from the face of the tower.

The sensor outputs are translated in a near-by shelter and recorded on a 24-channel sequential sampling strip chart recorder. Each sensor is sampled every 75 sec.

RESULTS AND DISCUSSION

Experimental runs are being made for periods of one to two days, in a variety of weather conditions. Fifteen minute averages are determined from the recorded data, and time-height cross-sections of the thermal structure (isotherms) are drawn by computer. One aim of this work is to eventually produce a climatology of the diurnal thermal structure which will be of use in diffusion and deposition estimates and in analysis of turbulent structure.

Clear weather case

For the case of clear skies and light winds, four periods appear within the diurnal cycle, regardless of season. These periods are: morning heating, mid-day slow warming, afternoon—evening cooling, and nocturnal steady cooling. The periods may be described according to the events occurring above, within, and below the crown. A number of cases have been analyzed, and the case of October 3—4, 1972 has been chosen as a typical clear weather illustration (Fig.3a). The observed structure is similar to the results reported by Geiger (1965), and by Raynor (1971), among others.

Morning heating begins at sunrise with nearly isothermal conditions, and is characterized by steady heating above and below the crown. A temperature maximum, which first appears high in the crown, descends as the sun rises in the sky. By late morning (10h30 in Fig.3a), the height of the temperature maximum corresponds roughly to the height of maximum foliage density, where it then remains. Below the crown the temperature gradients become increasingly stable, while above the forest the atmosphere becomes unstable.

The mid-day period is distinguished by a fixed vertical position of the temperature maximum, although slow heating of the entire crown region may continue. Strong stable temperature gradients occur below this maximum,

* WeatherMeasure custom-built air temperature profile measuring system.

** WeatherMeasure model W1034, WeatherMeasure Corp., Sacramento, Calif. 95841.

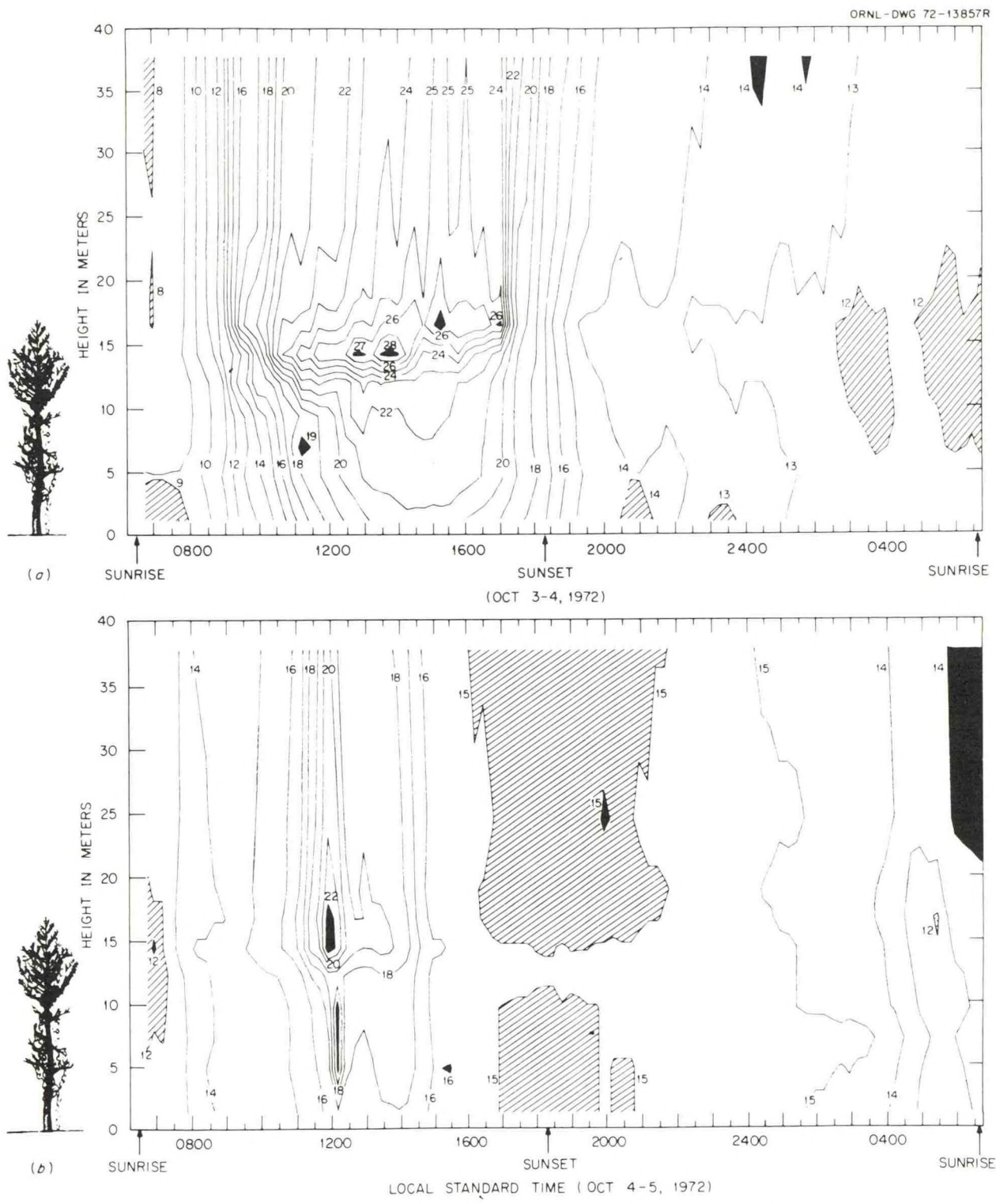


Fig. 3. Diurnal temperature behavior in a dense loblolly pine plantation. Isotherm temperature in $^{\circ}\text{C}$. Hatched areas denote cold spots; blackened areas denote warm spots. A scale "typical tree" is shown for each case. a. Fair weather case. b. Mostly heavy overcast with intermittent rain.

reaching 8°C in this example, while unstable gradients (~2°C between tree-tops and tower top) continue above. Cooler air can be found near the forest floor all day. Bergen (1971), in his study of a lodgepole pine forest, did not observe a period in which the temperature maximum remained at the same height for such an extended interval. In his investigation, the temperature maximum steadily penetrated the crown until it reached a minimum height, and then almost immediately began to rise back toward tree top level. The different behavior found in the present study can probably be attributed to the very dense interlocking foliage of the loblolly pine plantation.

The afternoon—evening cooling begins here with a sudden decrease in crown temperature and ends at sunset when a weak temperature minimum begins to appear in the crown with a temperature maximum below. As also reported by Geiger (1965), this evening cooling is much more rapid than the morning heating, although the rate diminishes near sunset.

Nocturnal steady cooling exists after sunset at all levels, with the crown cooling at the greatest rate. The result is that the crown temperature minimum continues to strengthen until shortly before sunrise. The cooler areas at the forest floor (about 21h00 and 01h00, in Fig.3a) occurred during calm conditions, and are believed to be due to cold air drainage from the nearby ridges. During the night, a weakly unstable temperature gradient occurs beneath the tree-tops, while a stable gradient appears above.

The observed clear-weather temperature structure is of some importance with regard to diffusion in forested regions. During the day, when the above-canopy flow is unstable, the air below the maximum temperature zone is quite stable; the opposite is true at night. Consequently, the diffusion of material from within the forest canopy to the free atmosphere above should be strongly inhibited, except during the isothermal periods around sunrise and sunset. This supposition is approximately verified by the behavior of sub-canopy smoke releases, which have been observed to float about within the forest as easily distinguishable, very slowly dispersing puffs for periods of up to 20 min. Occasionally, however, a puff is ejected upward from the forest at an apparently random location. Such behavior has also been observed by Oliver (1973) in a pine forest in England. The mechanism for this “chimney effect” is presently unknown.

Overcast case

To contrast with the behavior just described as typical for clear skies and light winds, a case is presented for which the weather conditions were primarily overcast, with frequent periods of rain (Fig.3b). This example extends from sunrise October 4 to sunrise October 5, 1972.

Here, light rain and heavy cloud cover create near-isothermal near-steady conditions throughout the normal morning heating period. Observed breaks in the overcast between 11h00 and 12h15 apparently account for the rapid above-canopy and upper-crown heating. A temperature maximum is quickly

established in the central portion of the crown, with strong stable gradients in the lower crown. The thermal structure at these levels is similar to that usually occurring during the mid-day period. The breaks in the overcast disappear, and by 14h30 rain has begun with near-isothermal cooling as a result. Moderate to heavy rain between 15h00 and 22h00 results in a nearly isothermal temperature profile except within the central crown, which persists as a warm spot until the rain ends. The crown is normally a cold spot at night. After the rain ends, about 22h15, conditions become similar to the normal late nocturnal state, with the canopy region becoming somewhat cooler than the air above.

FUTURE WORK

Runs such as those described here are continuing. Mean wind speed measurements above and within the canopy and over the field are being made. Six hygrographs in aspirated shelters have recently been placed on the forest tower. Their heights are given in Table I. Fast-response temperature difference systems will soon be installed on the forest and field towers. On the forest tower, temperature difference will be measured between 37.7 m and the zero plane displacement of the forest canopy (about 14 m). On the field tower, temperature difference will be measured between 16 m and the ground. Correlations between temperature gradients on the forest and on the field towers will be determined. Turbulence within and above the canopy will be examined with a sonic anemometer, and pilot deposition studies will begin within the next year.

ACKNOWLEDGEMENTS

The authors thank Steven D. Ferris, an Oak Ridge Associated Universities summer trainee from Cornell University who performed many of the forest structure measurements.

This work was performed under an agreement between the U.S. Atomic Energy Commission and the National Oceanic and Atmospheric Administration.

REFERENCES

- Bergen, J. D., 1971. Vertical profiles of windspeed in a pine stand. *Forest Sci.*, 17:314—321.
Geiger, R., 1965. *The Climate Near the Ground*. Harvard Univ. Press, Cambridge, Mass., 482 pp.
Knoerr, K., 1973. Material presented at 2nd annual U.S.I.B.P. Eastern Deciduous Forest Biome Information Meeting, Duke University, Durham, N.C., March 18—21.
Oliver, H. R., 1973. Smoke trails in a pine forest. *Weather*, 28:345—347.
Raynor, G. S., 1971. Wind and temperature structure in a coniferous forest and a contiguous field. *Forest Sci.*, 17:351—363.

conference summary

cooling tower environment—1974

The symposium "Cooling Tower Environment—1974," sponsored by the U.S. Atomic Energy Commission and the State of Maryland, was held 4–6 March 1974 at the University of Maryland. The purpose of the symposium was to bring together the persons currently doing research on cooling towers in order to establish the state of the art of our knowledge. The 30 invited papers and the accompanying discussion by the 150 attendees at the symposium will be published about November 1974 by the AEC Technical Information Center. The titles and authors of the papers are listed below:

Engineering and Technology Session

The role of environmental, economic, and social considerations in selecting a cooling system for a steam electric generating plant. A. Roffman (Westinghouse).

Optimum design of dry-wet combination cooling towers for power plants. V. C. Patel, T. E. Croley, II, and M. S. Cheng (University of Iowa).

Plume recirculation and interference in mechanical draft cooling towers. J. F. Kennedy (University of Iowa) and H. Fordyce (The Marley Company).

Drift management in the Chalk Point cooling tower. J. D. Holmberg (The Marley Company).

The Chalk Point cooling tower project. J. Pell (State of Maryland).

Plume Rise Session

Some observations on cooling tower plume behavior at the Paradise steam plant. P. R. Slawson (University of Waterloo), J. H. Coleman and J. W. Frey (Tennessee Valley Authority).

Plume rise from multiple sources. G. Briggs (National Oceanic and Atmospheric Administration).

A three dimensional steady-state simulation of a moist buoyant plume. J. Taft (Systems, Science, and Software).

Recent C.E.G.B. research on environmental effects of wet cooling towers. D. J. Moore (Central Electricity Research Laboratory, Leatherhead).

Meteorological consequences of thermal discharges from nuclear power plants—research needs. J. Carson (Argonne National Laboratories).

Visible Plume and Fog Frequency Session

Meteorological influences of atmospheric cooling systems as projected in Switzerland. A. Junod (Swiss Meteorologi-

cal Institute), R. J. Hopkirk (Electro-Watt), D. Schneiter (Swiss Meteorological Institute), and D. Haschke (Swiss Federal Institute for Reactor Research).

Experience with combined wind tunnel/plume model analysis of cooling tower environmental impact. P. Bøgh (Motor Columbus, Baden, Switzerland).

Meteorological effects of the mechanical draft cooling towers of the Oak Ridge gaseous diffusion plant. S. R. Hanna (National Oceanic and Atmospheric Administration, Oak Ridge).

Mechanical draft cooling tower visible plume behavior: Measurements, models, predictions. J. H. Meyer, T. W. Eagles, L. C. Kohlenstein, J. A. Kagan, and W. D. Stanbro (The Johns Hopkins University).

Ecological Effects Session

Airborne sea salt-techniques for experimentation and its effects on vegetation. B. Moser (Rutgers University).

Sodium and chloride concentrations in native vegetation near Chalk Point, Maryland. C. R. Curtis, H. G. Gauch, R. Sik (University of Maryland).

*Effects of salt sprays on the yield and nutrient balance of corn (*Zea mays*, L.) and Soybeans (*Glycine max.*, L.).* C. L. Mulchi and J. A. Armbruster (University of Maryland).

Some terrestrial environmental considerations relative to cooling tower systems for tower generating facilities. P. Edmonds, R. Maxwell, and H. Roffman (Westinghouse).

Environmental effects of chromium and zinc in cooling water drift. F. G. Taylor, Jr., L. K. Mann, R. C. Dahlman, and F. L. Miller (Oak Ridge National Laboratory).

Thresholds for injury to plants from salt drift from cooling towers. P. Freudenthal (Consolidated Edison).

Drift Deposition Session

Measurement and interpretation of drift particle data. F. Shofner, T. Carlson, and R. Webb (Environmental Systems Corporation).

Prediction and measurement of airborne particulate concentrations from cooling device sources and in the ambient atmosphere. G. Schrecker, K. Wilber, F. Shofner, and C. Thomas (Environmental Systems Corporation).

An analytical search for the stochastic-dominating process in the drift deposition problem. W. G. N. Slinn (Battelle Pacific Northwest Laboratory).

A test program on environment effects of salt water mechanical cooling devices. C. D. Henderson and S. H. Dowdell (Florida Power and Light Company).

The Forked River program—a case study in salt water cooling. J. Devine (General Public Utilities Service Corp.).

Measurements of drift from a mechanical draft cooling tower. A. Alkezweeny, D. Glover, R. Lee, J. Sloot, and M. Wolf (Battelle Pacific Northwest Laboratory).

Influence of the choice of the plume diffusion formula on the salt deposition rate calculation. J. A. Pena and C. L. Hosler (Pennsylvania State University).

Drift deposition rates from wet cooling systems. A. Roffman and R. E. Grimble (Westinghouse).

A mathematical transport model for salt distribution from a salt water-natural draft cooling tower. S. M. Laskowski (Pickard, Lowe, and Associates, Washington).

A drift deposition model for natural draft cooling towers. G. W. Israel and T. I. Overcamp (University of Maryland).

Some of the major points brought up in the papers and the discussion are:

1) Cooling tower manufacturers look forward to guaranteeing drift rates as low as 0.001% (ratio of flux of circulating water splashed out of the top of the tower to the total flux of circulating water in the tower) (Holmberg, Shofner *et al.*).

2) Dry-wet combination cooling towers are becoming technically and economically feasible (Patel *et al.*).

3) Current procedures for selecting cooling systems do not adequately account for environmental, economic, and social considerations. A method for quantitatively evaluating all of these effects is proposed by Roffman.

4) Wind tunnel studies suggest that recirculation rates of up to 5% occur with blocky mechanical draft towers but that this rate is considerably reduced if the wind direction is within 5% of the tower axis (Kennedy *et al.*). At hyperbolic towers, recirculation is insignificant, but slight downwash occurs which should be taken into account in plume rise models (Bøgh; Junod *et al.*).

5) TVA measurements of cooling tower plumes and stack plumes are used to develop models of visible plume

length and plume rise from multiple sources (Slawson *et al.*; Briggs).

6) In Switzerland, shadowing due to the cooling tower and its plume may be of importance (Junod *et al.*). The analysis, however, shows an insignificant reduction in sunshine.

7) A summary of British cooling tower experience by Moore points out that fogging and drift deposition due to cooling tower emissions are not major problems in that area.

8) Large experimental programs on cooling tower drift deposition are planned at Chalk Point, Md., and Turkey Point, Fla. (Pell, Henderson, *et al.*).

9) Current drift deposition measurements are not adequate for validating models (Pena and Hosler, Carson). Measurements at the Oak Ridge Gaseous Diffusion Plant are useful, but the mechanical draft cooling towers (Hanna, Alkezweeny, *et al.*) there are out of date and not representative of the current technology.

10) Drift deposition models are accurate only within an order of magnitude (Pena and Hosler; Roffman *et al.*; Israel *et al.*). Major problems include determining the point at which a drift droplet breaks away from the plume, and estimating the turbulent dispersion of a drop settling at a speed of about 1 m/s (Slinn).

11) Several studies of the effects of natural or laboratory salt spray on vegetation are underway (Moser; Curtis *et al.*; Mulchi *et al.*; Edmonds *et al.*; Freudenthal), but so far there have been no such field studies at the site of an operating salt water cooling tower. Such data are greatly needed (Carson). The study by Taylor *et al.* of the effects of chromium drift on vegetation shows that high chromium concentrations are evident in plants within 500 m of mechanical draft towers, but that levels approach background at greater distances.

12) The general consensus of the people at the symposium was that models had been carried as far as possible in the absence of detailed verification. What is needed now is validation data.

Symposium chairmen were S. R. Hanna of the Atmospheric Turbulence and Diffusion Laboratory, NOAA, P.O. Box E, Oak Ridge, Tenn. 37830, and J. Pell of the Bureau of Air Quality Control, 610 N. Howard Street, Baltimore, Md. 21201. Orders for copies of the proceedings volume available as CONF 740302 (cost \$13.60), to be published late in 1974, should be sent to the National Technical Information Service, U.S. Department of Commerce, Springfield, Va. 22151.

DISCUSSIONS

SENSITIVITY OF THE GAUSSIAN PLUME MODEL*

This technical note, by Bohac, Derrick and Sosebee, suggests several comments. In the first place the version of the Gaussian plume model given as their equation (1) was not proposed by Sutton (1953) as these authors state, although this is a minor quibble. Sutton's plume equation was of the Gaussian type, but employed theoretically formulated S.D., as did Roberts' earlier work and for that matter diffusion studies dating back to Einstein, if not to Fick. The method of combining observational diffusion data with a Gaussian plume equation that now is in such widespread use was developed by Pasquill (1961). Cramer (1957) had previously proposed the Gaussian equation as a convenient interpolation formula for diffusion data, which he fitted to power laws to determine sigmas. As far as I know the first person to introduce the mixing depth into a Gaussian diffusion formula was Holland (1953).

It is perhaps more important to point out that the "sensitivity" of the Gaussian formulation, that is the wide concentration variation that occurs depending on whether or not a plume is present over any particular ground point at any particular time, is also commonly observed in nature. Real plumes exhibit exactly this same variability, because atmospheric turbulence controls their behavior. Sensitivity is not a mathematical property exclusively of Gaussian models, either. A uniform, or "top-hat" plume model exhibits this sensitivity in an even more exaggerated form. Yet for strongly buoyant plumes such a model is perhaps a more realistic approximation to actual plume distributions than the Gaussian model, at least as far as several stack heights downwind.

The rapid variation of ground concentration with distance, and the general sensitivity of concentrations to distance from the plume's axis and variation in the assumed parameters of the Gaussian formula, facts all more or less well-known, seem to come as an unpleasant surprise to many new users of plume formulas. On the contrary these properties should be obvious both from the mathematical form of the equation and from casual observation of real plumes. In highlighting these sensitivity properties to a new and growing clientele, the authors have performed a useful service. Fortunately the most common application of plume formulas is to determine the maximum ground concentration value, irrespective of its exact location. This application is not particularly a sensitive one.

Finally it should be emphasized that the great merit of the Gaussian plume approach, as originated by Pasquill and Cramer and modified for plume buoyancy effects by Briggs (1969) and others, is that it incorporates the available observational data on plume behavior to the maximum possible extent. Properly applied, it will give the best available estimates of plume dispersion. It can of course be misused, by being extrapolated out of the range of the experimental conditions, or through use of parameter values derived from inappropriate experiments. For instance σ -values derived from non-buoyant, passive-tracer diffusion experiments for which the sources were near the ground have frequently been applied to estimate plumes from strongly buoyant sources located high above the ground. This is not however a fault of the Gaussian equation; no formula is foolproof.

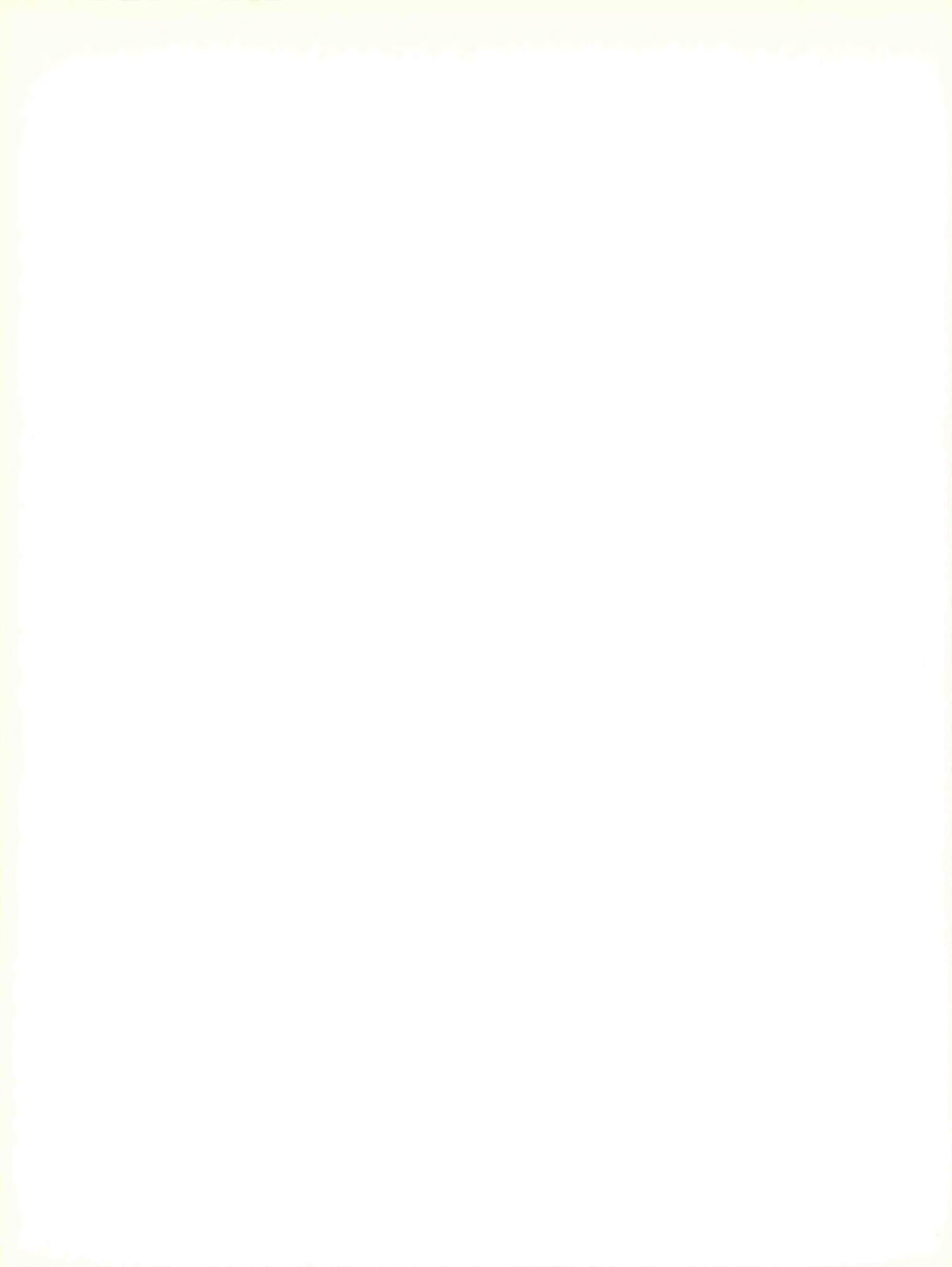
ERL/NOAA, Oakridge, Tennessee, U.S.A.

F. A. GIFFORD

REFERENCES

- Cramer H. K. (1957) A practical method for estimating the dispersal of atmospheric contaminants. *Proc. of the 1st Nat. Conf. on Applied Meteor.*, pp. C-33-C-55, Am. Meteor. Soc., Oct. 1957.
Holland J. Z. (1953) A meteorological survey of the Oak Ridge area. U.S. AEC Report ORO-99, Oak Ridge, Tennessee.
Pasquill F. (1961) The estimation of the dispersion of windborne material. *Meteor. Mag.* **90**, 33-49.
Sutton O. G. (1953) *Micrometeorology*. McGraw-Hill, New York.

* BOHAC R. L., DERRICK W. R. and SOSEBEE J. B. (1974) *Atmospheric Environment* **8**, 291-293.



Consequences of Effluent Release

Edited by J. C. Hart

IAEA-WMO Symposium on the Physical Behavior of Radioactive Contaminants in the Atmosphere

By R. P. Hosker, Jr.*

Abstract: This article is a review of a symposium on the behavior of radioactive atmospheric contaminants; the symposium was held in Vienna, Nov. 12–16, 1973. Theoretical and experimental reports on local, regional, and global dispersion of effluents are discussed, as are the production and environmental impact of the effluents.

The International Atomic Energy Agency (IAEA) and the World Meteorological Organization (WMO) jointly convened a symposium on the physical behavior of radioactive contaminants in the atmosphere, in Vienna, Austria, Nov. 12–16, 1973. This was the latest in a recent series of symposiums dedicated to the study of the release of radioactive materials in the atmosphere and their subsequent behavior in the environment.^{1–4}

The 109 scientists who attended the symposium represented 25 countries and 6 international organizations. Thirty-five papers were presented during eight technical sessions, as listed in Table 1. The meeting concluded with a panel discussion. Since the IAEA will soon publish the complete proceedings of this symposium (IAEA-SM-181), only a brief description of the

various sessions and the topics covered will be attempted here.

The symposium opened with two invited papers. Vogt of Germany reviewed briefly the gradient and statistical methods of diffusion modeling, compared the various systems of diffusion categories and parameters, and discussed dose calculations, local and regional dispersion, computer models, and population exposures. Reiter of Colorado State University considered the scales of atmospheric motion, planetary-boundary-layer flow problems, sources and sinks of effluents, global circulation patterns and resultant transport, and the atmospheric residence times of contaminants.

LOCAL BEHAVIOR OF EFFLUENTS

Sessions II and III were concerned with experiments on local behavior of effluents. König et al. compared the results of diffusion tests at Karlsruhe Nuclear Research Center with those computed from a standard Gaussian plume model. Michael, Raynor, and Brown reported experiments showing that dispersion over water can be much less than that over land. Laser et al. estimated that present-day containment techniques would lead to undesirably high concentration values for certain effluents from large nuclear fuel-reprocessing plants and discussed new techniques to reduce such emissions. Vohra reported that embryo condensation nuclei result from very small amounts of ionizing radiation when certain trace gases such as SO₂ are present in the atmosphere. He suggested that this may be important in assessing the climatic impact of nuclear facilities located in industrialized areas. Gyllan-

*Rayford P. Hosker, Jr., is a physical scientist with the Air Resources Atmospheric Turbulence and Diffusion Laboratory of the National Oceanic and Atmospheric Administration (NOAA) in Oak Ridge, Tenn. He received the B.S. degree from Boston College, the M.S. degree from the University of Minnesota, and the Ph.D. degree from Northwestern University. Before joining NOAA in 1971, he did postdoctoral work at the von Karman Institute for Fluid Dynamics in Belgium. His research interests include diffusion modeling, forest meteorology, and atmospheric flow near buildings and other obstacles.

Table 1 Agenda: IAEA-WMO Symposium on the Physical Behavior of Radioactive Contaminants in the Atmosphere

Paper No. (SM-181/)	Title	Author	Country
Session I Introductory Papers			
39	Dispersion of Airborne Radioactivity Released from Nuclear Installations and Population Exposure in the Local and Regional Environment	K. J. Vogt	Germany
40	Dispersion of Radioactive Material on Small, Meso-, and Global Scales	E. R. Reiter	United States
Session II Local Behavior, Experimental			
4	Experiments Conducted at the Karlsruhe Nuclear Research Center To Determine Diffusion in the Atmosphere by Means of Various Tracers	L. A. König, K. Nester, H. Schüttelkopf, and M. Winter	Germany
5	Atmospheric Diffusion from an Off-shore Site	P. Michael, G. S. Raynor, and R. M. Brown	United States
23	Emission of Radioactive Aerosols from Reprocessing Plants	M. Laser, H. Beaujean, P. Filss, E. Merz, and H. Vygen	Germany
1	Possible Role of Radioactive Releases from Multiple Nuclear Facilities in the Nucleation Processes in the Atmosphere	K. G. Vohra	India
2	Concentration Statistics Based on Experimental Data of Atmospheric Diffusion	Ch. Gyllander and U. Widemo	Sweden
Session III Local Behavior, Experimental			
11	Influence de la Durée d'Exposition sur l'Evaluation des Coefficients de Diffusion Atmosphérique	J. M. Brun, J. Hugon, and R. G. Le Quinio	France
12	Comparaison par Une Méthode de Traçage de la Distribution au Sol des Aerosols et des Gaz dans le Vent des Installations Polluantes	R. Rzekiecki	France
25	Variability of the Washout Ratio for Some Fallout Radionuclides	M. de Bortoli and P. Gaglione	Italy
14	Studies on the Improvement of a Composite Dust Sampler and Its Utilization in Environmental Research	H. Kamada, M. Yukawa, and M. Saiki	Japan
26	Effect of Meteorological Variables on Atmospheric Suspended Particulates and Associated Natural Radon and Thoron Daughters	A. Reimer, J. K. Reichert, and A. G. Scott	Canada
Session IV Production and Effects			
9	Tritium, Krypton, Iodine, and Xenon Production in an Advanced Design High-Temperature Gas-Cooled Reactor	J. A. Angelo, Jr., R. G. Post, and F. E. Haskin	United States
22	Helicopter-Borne Measurement of Radiation Exposure at a BWR Nuclear Power Station	W. L. Brinck, W. J. Averett, H. E. Kolde, and B. Kahn	United States
15	Dépôt et Rétention sur l'Herbe de l'Iode Élémentaire et d'Iodure de Méthyle	K. Heinemann, K. J. Vogt, and L. Angeletti	France
30	Production de Gaz Étalons de Radioactivité	H. Goenvec	France
Session V Local Behavior, Theoretical and Modeling			
17	Mesure et Estimation des Doses de Rayonnement Gamma Récusées à la Suite de l'Émission d'Argon-41 dans l'Atmosphère	E. Nagel	Switzerland

Table 1 (Continued)

Paper No. (SM-181/)	Title	Author	Country
Session V (Continued)			
18	Radioactive Pollutants Released in Accidents of LWR Power Plants: A Review and Attempt at Classification	J. P. Hosemann, W. Schikarski, and H. Wild	Germany
19	Estimates of Dry Deposition and Plume Depletion Over Forests and Grassland	R. P. Hosker, Jr.	United States
27	A Numerical Model for the Study of the Dispersion of Radioactive Pollutants in Air	G. Zuccaro-Labellarte	Italy
32	Calculations of Dose and Population Dose in the General Environment Due to Boiling-Water Nuclear Power-Reactor Radionuclide Emissions in the U. S. in 1971	J. A. Martin, Jr., and C. B. Nelson	United States
33	Recent Developments in the Prediction of the Environmental Consequences of Radioactive Releases from Nuclear Power Reactors	H. F. MacDonald, P. J. Darley, and R. H. Clarke	United Kingdom
Session VI Regional and Global Behavior, Experimental			
6	Particulate and Gaseous Atmospheric Iodine Concentrations	F. P. Brauer, H. G. Rieck, Jr., and R. L. Hooper	United States
13	Chemical Properties of Polonium-210 in the Atmosphere	S. Abe and M. Abe	Japan
34	World Distribution of Environmental Tritium	W. R. Schell, G. Sauzay, and B. R. Payne	United States
38	Natural Radium-226 and Thorium-228 in Thyroids of Cattle from Nigeria, West Africa	O. L. V. Ekpechi, L. Van Middlesworth, and G. Cole	Nigeria
Session VII Regional and Global Behavior, Theoretical and Modeling			
7	Regional- and Global-Scale Dispersion of Krypton-85 for Population-Dose Calculations	L. Machta, G. J. Ferber, and J. L. Heffter	United States
8	Recent Analytical and Experimental Efforts on Single-Source Effluent Dispersion to Distances of 100 km	I. Van der Hoven, C. R. Dickson, G. E. Start, and L. L. Wendell	United States
10	Principes de Traitement Numérique Complet des Transferts Physiques dans l'Atmosphère et dans l'Hydrosphère	A. Doury	France
20	Mound Laboratory Air-Surveillance System	J. L. Hebb	United States
21	Mound Laboratory Environmental-Control Program	J. L. Hebb	United States
Session VIII Regional and Global Behavior, Theoretical and Modeling			
24	Artificial Radioactive Material at High Altitudes in the Atmosphere	K. Stewart	United Kingdom
29	La Diffusion d'Effluents Gazeux Radioactifs à Échelle Régionale: Évaluation des Risques	P. Cagnetti and M. Pagliari	Italy
31	Classification of Weather According to Lapse Rate	W. R. Helm and B. C. Winkler	South Africa
37	A Computation of Individual and Population Dose in an Urban Area Under Accident Conditions	Ch. Gyllander, U. Widemo, and S. O. W. Bergström	Sweden
Session IX Panel Discussion on Physical Behavior of Radioactive Contaminants in the Atmosphere and Consequent Environmental Impacts			

der and Widemo computed concentrations for various release times and source heights, using a Gaussian model and locally measured dispersion coefficients. They then compared the results with those obtained by standard U.K. Atomic Energy Authority and U.S. Atomic Energy Commission calculation methods. Brun, Hugon, and Le Quinio discussed the effect of exposure duration on measured concentrations and suggested a power-law dependence. Rzekiecki found that the behavior of an aerosol tracer agrees with that of a gaseous tracer within a factor of 2. De Bortoli and Gaglione presented monthly washout ratios for several radionuclides for periods up to 9 years and discussed their variation. Kamada, Yukawa, and Saiki described a new filter with a collection efficiency of 99% for 10- μ m particles. Finally, the study by Reimer et al. of suspended particulate concentrations and their relation to meteorological conditions indicates a seasonal dependence as well as a cyclical variation of about 4 days, corresponding well to synoptic changes.

The production and possible effects of radioactive effluents were considered in Session IV. Angelo, Post, and Haskin compared the calculated fission products from a high-temperature gas-cooled reactor (HTGR) with those from a light-water reactor (LWR) and found that the activities of certain species (e.g., ^{85}Kr) are much greater for the HTGR. Brinck et al. reported on helicopter-borne and ground-based measurements of radiation exposure due to an elevated release and compared their results with calculated values. Heinemann, Vogt, and Angeletti discussed the deposition and retention of iodine and methyl iodide on vegetation, taking into account both the meteorological conditions and the vegetative characteristics. Goenvec described the production of radioactive-gas standards suitable for calibration use.

Theoretical studies of the local behavior of effluents were presented in Session V. Nagel calculated the gamma dose from release of ^{41}Ar and compared it with measurements obtained with pressurized ionization chambers and various thermoluminescent detectors. Hosemann, Schikarski, and Wild classified the isotopes present in an LWR according to radiotoxicity by calculating the activity inventory of the reactor, estimating the accidental release fractions, and computing the resulting external dose. Hosker estimated, by means of a modified Gaussian model, the ranges of effectiveness of a forest and of a grassy area as collectors of dry deposition. Zuccaro-Labellarte used a plume model, allowing deposition and nonideal ground-plane reflection, to compute normalized concentrations and, from those, the maximum permissible

release rates of certain radionuclides. Martin and Nelson calculated doses due to reactors operating in the United States in 1971 out as far as 80 km, taking into account plume rise, time of travel and consequent decay, and deposition with its attendant cloud depletion. MacDonald, Darley, and Clarke estimated doses from a possible reactor accident, using a computer code that calculates fission-product inventories and describes their behavior within the reactor and outside in the atmosphere.

BEHAVIOR OF EMISSIONS ON REGIONAL AND GLOBAL SCALES

The experimental behavior of emissions on regional and global scales was considered in Session VI. Brauer, Rieck, and Hooper presented data on the seasonal behavior patterns of particulate and gaseous radio-iodine concentrations collected from all parts of the globe over a period of several years. S. Abe and M. Abe's study of the volatility and solubility of the ^{210}Po compounds in atmospheric dust indicates the presence of at least two polonium compounds. Schell, Sauzay, and Payne discussed their measurements of the global distribution of tritium and their estimates of its atmospheric residence time and transit time between global hemispheres.* Ekpechi, Van Middlesworth, and Cole reported in their paper that ^{226}Ra and ^{228}Th are apparently concentrated by the thyroids of certain cattle. These cattle originate in a portion of Nigeria that is known for both its high natural-background radioactivity and its high rate of human goiter; the authors suggested that these phenomena may be related.

Theoretical studies of regional and global effluent behavior made up the last two technical sessions. Machta, Ferber, and Heffter used a model for regional- and global-scale dispersion to compute population doses due to emissions from two hypothetical locations in the United States. They found that early plume behavior is significant only for the local and regional exposures. Van der Hoven et al. utilized puffs diffusing along air trajectories calculated from a large network of meteorological stations to predict concentration isopleths over a 90- by 140-km grid and compared the results with those obtained using only the wind data at the site of the emissions. Within about 30 km of the

*At the beginning of Session VII, S. G. Malakhov of Russia reported orally on measurements of various radionuclides (including tritium) in the USSR; he noted that both seasonal and regional (i.e., coastal vs. midcontinental) differences are observed.

source, they found good agreement over a 1-year period, but substantial disagreement for shorter intervals. Doury reviewed the processes significant for long-range transport and applied the appropriate diffusion equation to puffs traveling along air trajectories to compute concentration isopleths for time-varying meteorological conditions. Hebb described an air-surveillance system, various environmental-protection measures, and a public-information dissemination program being used at a large nuclear research facility. Stewart estimated that nuclear test debris is potentially hazardous to occupants (and possibly maintenance personnel) of high-flying aircraft for up to a few days after formation of the debris cloud. Cagnetti and Pagliari compared the results of an inversion-capped radially spreading diffusion model under both neutral and stable conditions with those of a Gaussian model under highly stable conditions. They also discussed typical European air-mass trajectories governing transport and the synoptic conditions associated with them. Helm and Winkler made diffusion calculations using coefficients chosen according to the measured atmospheric lapse rate. Finally, Gyllander, Widemo, and Bergström presented individual and population doses calculated for a hypothetical reactor accident within an urban area.

DISCUSSION

A panel discussion on the probable behavior and environmental effects of radioactive contaminants in the atmosphere concluded the agenda. Reiter opened

the discussion by urging more detailed experimental studies of plume behavior, a program to establish background radionuclide levels before additional effluents are added, more work on gas and aerosol interaction and removal processes, additional study of whether present dose standards are too strict or not strict enough, and research on efficient energy transmission and gaseous-effluent containment techniques to facilitate the construction of nuclear power plants in locations far from such valuable property as farmland and cities. The panel concluded by considering questions submitted by the audience on a variety of topics, including practical classifications of atmospheric stability, model recommendations, wet- and dry-effluent removal processes, and long-range transport of contaminants.

REFERENCES

1. *Environmental Aspects of Nuclear Power Stations*, Symposium Proceedings, New York, 1970, International Atomic Energy Agency, Vienna, 1971 (STI/PUB/261).
2. *Interaction of Radioactive Contaminants with the Constituents of the Marine Environment*, Symposium Proceedings, Seattle, Wash., 1972, International Atomic Energy Agency, Vienna, 1973 (STI/PUB/313).
3. *Environmental Behavior of Radionuclides Released in the Nuclear Industry*, Symposium Proceedings, Aix-en-Provence, France, 1973, International Atomic Energy Agency, Vienna, 1973 (STI/PUB/345).
4. *Environmental Surveillance Around Nuclear Installations*, Symposium Proceedings, Warsaw, Poland, 1973, International Atomic Energy Agency, Vienna (to be published).

A Comparison of Estimation Procedures for
Over-Water Plume Dispersion
September 1974

R. P. Hosker, Jr.
Air Resources
Atmospheric Turbulence and Diffusion Laboratory
National Oceanic and Atmospheric Administration
Oak Ridge, Tennessee

(Published in the proceedings of the Symposium on Atmospheric Diffusion
and Air Pollution held September 9-13, 1974 in Santa Barbara, California.)

A COMPARISON OF ESTIMATION PROCEDURES FOR
OVER-WATER PLUME DISPERSION

R. P. Hosker, Jr.
Air Resources
Atmospheric Turbulence and Diffusion Laboratory
National Oceanic and Atmospheric Administration
Oak Ridge, Tennessee

1. INTRODUCTION

Effluent transport and diffusion over water is receiving increased study, largely because of the current interest in off-shore nuclear power plants. Dispersion estimations identical to those used over land are open to question because, for given weather conditions (e.g., clear skies, moderate wind), the over-water turbulence will differ greatly from that over land. This paper attempts to assess the predictive capability of techniques similar to those in general use, but which utilize descriptions of turbulence perhaps more appropriate to over-water flows.

2. THEORETICAL DEVELOPMENT

2.1 Gaussian Plume Formulation

The normal or Gaussian distribution function is a fundamental solution of the Fickian diffusion [Sutton (1953)]. As such, it is strictly applicable only for large diffusion time and homogeneous, stationary conditions. However, many studies have verified its practical utility over land [Gifford (1968)]. In view of the horizontally nearly homogeneous and more or less stationary conditions that may be expected over the ocean, the formulation seems to be a reasonable choice for over-water flow as well. The concentration \bar{X} due to a continuous source of strength Q_0 located at the x-y origin at elevation h is [Gifford (1968)]:

$$\frac{\bar{X}}{Q_0} = \frac{1}{2\pi\sigma_y\sigma_z\bar{u}} \exp \left[-\frac{y^2}{2\sigma_y^2} \right] \cdot \left\{ \exp \left[-\frac{(z-h)^2}{2\sigma_z^2} \right] + \right. \\ \left. + \exp \left[-\frac{(z+h)^2}{2\sigma_z^2} \right] \right\} \quad (1)$$

For practical applications, a number of authors [e.g., Gifford (1961), the ASME (1968, 1973), Briggs (1973)] have presented the dispersion coefficients σ_y and σ_z either graphically, or as analytic functions of distance x , for a variety of stability conditions. The choice of stability category is typically made using easily observed variables such as "surface" wind speed, insolation, temperature gradient, and/or fluctuations in wind speed and direction. Nearly all such dispersion coefficients are based on data gathered over open land of modest roughness and, strictly speaking, should be used only for calculations over similar terrain. Within this restriction, the time-averaged

concentration estimates made with this technique can be expected to be accurate within a factor of 2 [Islitzer and Slade (1968)] or 3 [Turner (1969)].

A similar methodology for over-water use is desirable. However, the dispersion parameters obtained over land and classified according to over-land stabilities cannot be expected to be directly applicable over the sea. As Van der Hoven (1967) has pointed out, the smooth water surface results in substantially less mechanically generated turbulence than over land, while the air-water temperature difference will either enhance or hinder convection. Evaporation may also significantly affect atmospheric stability [Lumley and Panofsky (1964)] and the resultant diffusion.

An extensive set of over-water diffusion experiments from which characteristic dispersion coefficients might be deduced is not yet available. The work being done at Brookhaven National Laboratory [Michael, et al. (1973a,b)] should help to remedy this situation. In the meantime, diffusion estimates can only be made by means of expressions, often empirical, for σ_y and σ_z which utilize some sort of observed over-water wind data that can serve to characterize the turbulence. This approach has been adopted here. Its adequacy can be judged by comparing its predictions to the relatively few observations reported thus far in the literature.

2.2 Characterization of Over-water Stability and Roughness Effects.

Detailed simultaneous observations of wind, temperature, and humidity profiles and of sea surface conditions are unlikely to be available at ocean sites for which diffusion estimates are needed. For this study, techniques were therefore chosen which require only data obtainable from quite simple instrumentation.

The standard deviation of the horizontal wind angle, σ_θ , is known to be strongly related to σ_y [Van der Hoven (1967), Islitzer and Slade (1968)]. In fact, for over-land use, Slade (1966) has associated a particular σ_θ value with each Pasquill stability class to provide a quantitative means of choosing the appropriate category. However, σ_θ contains an implicit description of the site roughness as well as the convective activity [Cramer, et al. (1958), Gifford (1972)]. Here, σ_θ is assumed to provide an adequate description of the local turbulence; the problem is then to find σ_y curves based on σ_θ which correctly predict the lateral diffusion. Slade (1962) and Van der Hoven (1967) have used σ_θ in a somewhat similar fashion to estimate coastal region diffusion. They did not attempt

to compare their results to observations, probably because of lack of data.

The connection between σ_θ and the vertical diffusion parameter σ_z is not so well defined. Cramer, et al. (1964) have suggested that σ_z , like σ_y , can be quantitatively related to σ_θ , and the ASME Guide (1968, 1973) also supplies an explicit scheme for this. One other technique seems possible; it is based on a formulation for σ_z in which the roughness and stability effects are considered separately [Smith (1972)].

2.3 Expressions for σ_y and σ_z .

Obvious first choices are the Pasquill-Gifford (P.-G.) curves for σ_y and σ_z as functions of x . These are given in Figures 1 and 2, where the value of σ_θ appropriate to each curve [Slade (1966)] has been indicated. The usual letter-stability classification (e.g., "D" = neutral) has been dropped, since it is incorrect over water. Figures 1 and 2 also show the dispersion parameters suggested by Briggs (1973); these curves were deduced in part from long-range experiments, and so may be somewhat more reliable than their P.-G. counterparts at large distances.

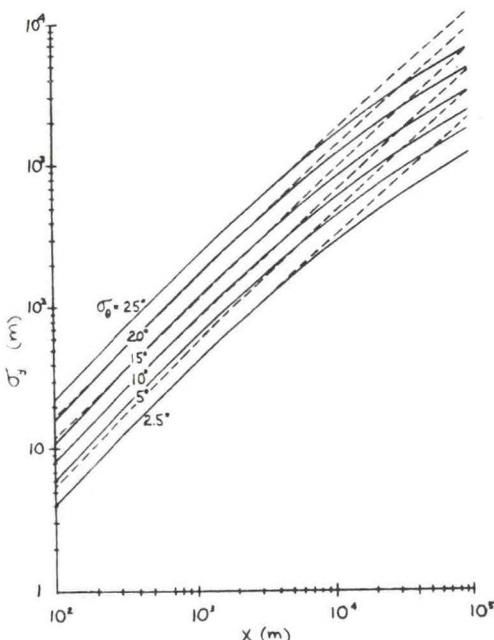


Figure 1. Pasquill-Gifford (broken) and Briggs (solid) curves for lateral dispersion coefficient.

Some expressions for σ_y make explicit use of the local value of σ_θ . For example Cramer, et al. (1964) use a power-law in x :

$$\sigma_y = \sigma_\theta x_r (x/x_r)^p , \quad (2)$$

where p depends on stability and x_r is a reference length. For over-land use, Cramer, et al. (1964) supply the exponents listed in Table I, classified by σ_θ . Similar relations are suggested in the ASME Guide (1968, 1973).

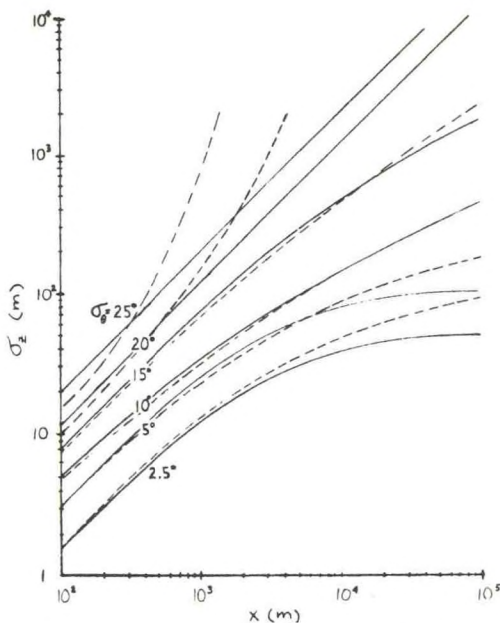


Figure 2. Pasquill-Gifford (broken) and Briggs (solid) curves for vertical dispersion coefficient.

Table 1

Power-law exponents for $\sigma_y = \sigma_\theta x_r (x/x_r)^p$,
 $\sigma_z = \sigma_\theta x_r (x/x_r)^q$, from Cramer, et al.
(1964), for use over land

Stability	σ_θ (deg)	$200 \leq x \leq 800$ m	$50 \leq x \leq 800$ m
↑	3	0.45	0.86
	4	0.56	0.86
	5	0.64	0.88
	6	0.71	0.91
	7	0.80	0.96
	8	0.85	1.13
Neutral	10	0.85	1.29
↓	12	0.85	1.55
	20	0.85	1.74
	25	0.85	1.89

Over land, $\sigma_\theta \approx 10^\circ$ under neutral conditions; in over-water flows, observed values of σ_θ are typically less than 4° or 5° [Cramer, et al. (1965), Smith and Beasmer (1967), Michael, et al. (1973a,b)]. Such values over land would indicate rather stable conditions but this is not true over water. To see this, one can estimate σ_θ for neutral conditions over the sea from

$$\sigma_{\theta, \text{neutral}} = \frac{\sigma}{u^*} \left|_{\text{neutral}} \right. \cdot \frac{k}{\ln z - d} \frac{z_0}{z} \quad (3)$$

For moderate winds z_0 is on the order of a few tenths of a mm. With $z \approx 10$ m, the log-law is then rather insensitive to displacement height d , which can be estimated as a meter or so (wave height). Lumley and Panofsky (1964) cite neutral stability values over land of σ_v/u^* varying between 1.3 and 2.6, with larger values originating at rougher sites; Frenzen and Hart (1973) find $\sigma_v/u^* \approx 1.7$ for neutral

conditions over Lake Michigan. For winds of about 10m/sec, then, $\sigma_\theta/\sigma_{\theta\text{neutral}}$ may be expected to be between 3° and 5° over the ocean. Evidently Cramer, et al.'s (1964) exponents as functions of σ_θ cannot be expected to directly apply over the sea, since σ_θ will be so much smaller there.

In an attempt to side-step this problem, the exponent p was taken from Table 1 as a function of $\sigma_\theta/\sigma_{\theta\text{neutral}}$ (Figure 3); here $\sigma_\theta/\sigma_{\theta\text{neutral}}$ serves as an indicator of relative stability. Equations (3) and (10) were used to compute $\sigma_{\theta\text{neutral}}$ over the sea as a function of wind speed at 10m (Figure 4), assuming $\sigma_v/u^*_{\text{neutral}} = 1.3$. By using observed wind speed, one can estimate $\sigma_{\theta\text{neutral}}$; this, combined with observed σ_θ , allows formation of the relative stability indicator $\sigma_\theta/\sigma_{\theta\text{neutral}}$. The exponent p is then chosen from Figure 3 for use in equation (2). It might be noted that Cramer, et al. (1965) and Smith and Niemann (1969) choose $p = 0.8$ in their discussions of over-water diffusion.

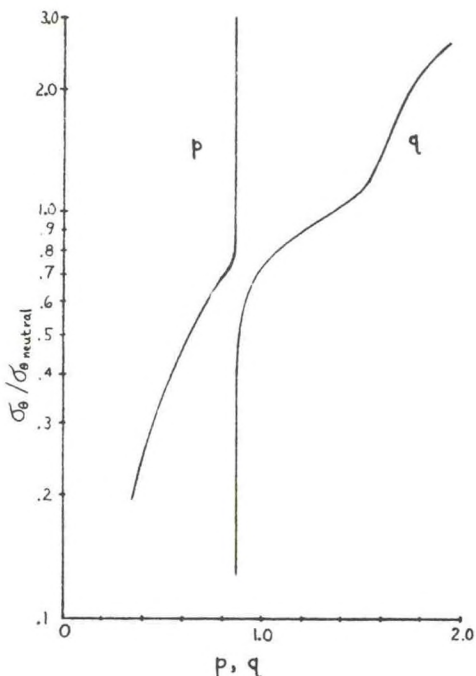


Figure 3. Cramer, et al.'s (1964) exponents as functions of $\sigma_\theta/\sigma_{\theta\text{neutral}}$.

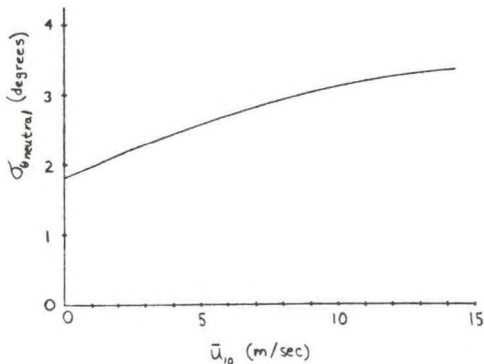


Figure 4. Estimate of $\sigma_{\theta\text{neutral}}$ vs. wind speed over the sea.

Islitzer (1961) gives the relation

$$\sigma_y = \frac{\sigma_\theta}{1.23} x . \quad (4)$$

This equation was deduced from experiments conducted over flat desert terrain in unstable conditions, but has been used by Frenzen and Hart (1973) to estimate σ_y values over Lake Michigan.

Taylor (1921) demonstrated that, for homogeneous isotropic turbulence, an exponential form of the Lagrangian correlation coefficient leads to

$$\sigma_y = \sqrt{At - \frac{A^2}{2(\sigma_\theta \bar{u})^2} \left[1 - \exp \left[- \frac{2(\sigma_\theta \bar{u})^2 t}{A} \right] \right]} , \quad (5a)$$

where t is travel time. The legitimacy of applying this expression to the atmospheric boundary layer is open to some question [see the discussion following Vaughan (1964)], but, as a practical matter, may be permissible for σ_y , which is less affected by inhomogeneities. Fuquay, et al. (1964) suggest the empirical form

$$A = 13 + 232 \sigma_\theta \bar{u} . \quad (5b)$$

Equations (5) have been applied to over-water diffusion by Smith and Beesmer (1967).

When data on the standard deviation of angle of elevation, σ_ϕ , are available, Islitzer (1961) recommends $\sigma_z = (\sigma_\phi / 1.23)x$. Typically, $\sigma_\phi/\sigma_\theta$ ranges between 0.2 (stable conditions) and 0.7 (unstable) [ASME Guide (1968, 1973)], and so

$$\sigma_z = \frac{\sigma_\theta}{B} x , \quad (6)$$

where B is a constant of order 5 or so.

Cramer, et al. (1964) suggest

$$\sigma_z \approx \frac{\sigma_\theta}{3} x_r (x/x_r)^q . \quad (7)$$

Their exponent q is listed for land use in Table 1, and has been plotted as a function of $\sigma_\theta/\sigma_{\theta\text{neutral}}$ in Figure 3. Cramer, et al. (1965) indicate that $q \approx 0.35$ for over-water travel at San Nicholas Island, California. Smith and Niemann (1969) found $q \approx 0.45$ for over-water releases at Oceanside, California.

A fairly elaborate scheme for computing σ_z on the basis of local stability and roughness has been set forth by F. B. Smith (1972). Smith gives a "baseline" curve corresponding to neutral, overland stability and roughness length $z_o \approx 10$ cm. An x -dependent stability correction factor is then selected according to local conditions. Adjustment for local roughness is provided by means of another x -dependent correction factor. The technique is extended here to very small z_o . The vertical dispersion coefficient is given by

$$\sigma_z = F(z_o; x) \cdot G(\sigma_\theta; x) . \quad (8)$$

The dimensionless roughness correction factor F (Figure 5) is obtained by extrapolation from Smith's (1972) work. The set of "baseline" curves $G(\sigma_\theta; x)$ correspond to $z_o \approx 10$ cm, and are labeled in Figure 6 according to Slade's (1966) scheme for σ_θ .

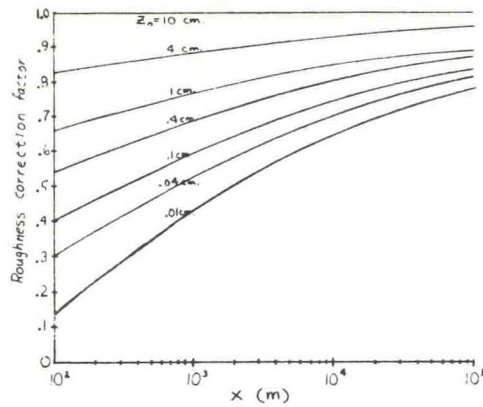


Figure 5. Dimensionless roughness correction factor $F(z_0; x)$ for small values of z_0

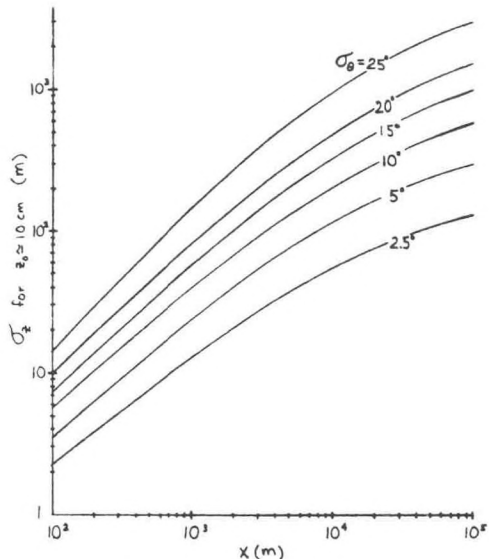


Figure 6. F. B. Smith's (1972) vertical dispersion coefficients for $z_0 = 10 \text{ cm}$.

To use Smith's method, z_0 over the ocean must be estimated. Kitaigorodskii (1973) has hypothesized that z_0 depends on the stage of development of the wind-driven waves, as well as on wind speed. Garratt's (1973) work supports this idea. Hence z_0 will vary with fetch, wave height and phase velocity, and wind speed and duration. A plot of observations of z_0 vs. friction velocity u^* alone will therefore show tremendous scatter. A statistical analysis of such a plot by Kitaigorodskii (1973) indicates, however, that z_0 (in cm) is described, to at least order of magnitude accuracy, by

$$\bar{z}_0 = 0.035 u^{*2}/g. \quad (9)$$

The overbar indicates a mean value for the ensemble of all states of wave development possible for a given u^* . Equation (9) is within a factor of 3 of that suggested by Charnock (1955). Equation (9) may be combined with the logarithmic velocity profile to obtain z_0 as a function of \bar{u}_{10} , the mean wind at 10 m (Figure 7). An excellent approximation to this curve is the simple expression

$$z_0 \approx 2 \times 10^{-4} \bar{u}_{10}^{2.5}, \quad (10)$$

with z_0 in cm and \bar{u}_{10} in m/sec. Equation (10) is also indicated in Figure 7; it, together with Figures 5 and 6, provides a simple means of estimating $\sigma_z(x)$ through equation (8).

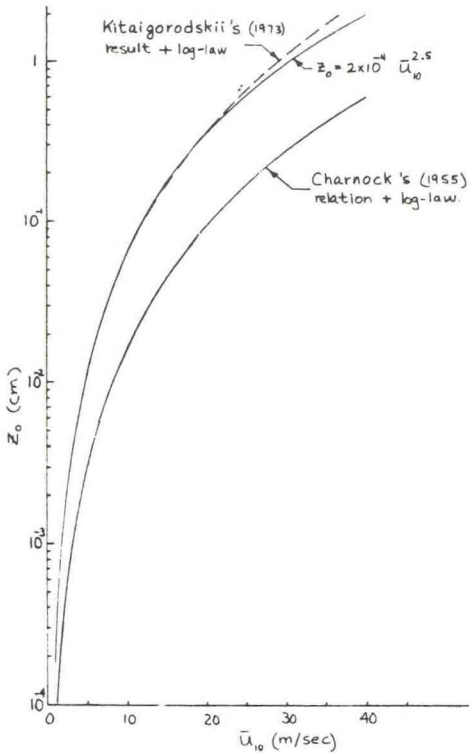


Figure 7. Over-ocean roughness length vs. wind speed by several techniques.

3. COMPARISON WITH DATA

Data from recent over-water oil smoke experiments conducted off Long Island are given in Table 2 [Michael, et al. (1973b), R. M. Brown and S. SethuRaman (private communications)]. Table 3 lists data accumulated from fluorescent particle (FP) releases at Bolsa Island, off California [Smith and Beesmer (1967)].

Table 2

Brookhaven over-water diffusion data [Michael, et al. (1973b), Brown (1974), SethuRaman (1974)]

Run no.	x (m)	$\bar{u} @ 16 \text{ m}$ (m/sec)	σ_y (m)	$\bar{\tau}_{CL}/Q_0$ (sec/m ³)	Time-adjusted [†]	
					σ_y (deg)	σ_y (m)
2.1	1900	4.8	134	2.8×10^{-8}	3.57	130
2.2	5500	5.9	83.5	1.4×10^{-8}	1.64	74.7
3.2	6700	3.9	66.1	3.3×10^{-8}	-3.56	67.5
4.1	2300	6.06	119	0.68×10^{-8}	4.04	112
4.2	2300	6.06	169	0.46×10^{-8}	4.04	169
6.1*	2600	4.68	93.3	7.13×10^{-8}	-1.5	77.7
6.2*	2600	5.91	96.3	8.95×10^{-8}	2.4	85.6
6.3*	460	4.67	35.5		1.37	35.9
6.4*	930	5.18	62.9		2.48	75.6
6.5*	1840	5.91	75.1		2.40	75.9
7	4300	9.96	53.9	4.56×10^{-8}	1.73	49.7
8.1**	1380	8.36	227	1.52×10^{-8}	8.67	177
8.2**	460	8.36	120	5.74×10^{-8}	8.67	111
9.1	4900	5.7	86.7	2.55×10^{-8}	2.12	78.9
10	3400	10.8	140	0.189×10^{-8}	2.62	120

*Rainy day.

**Off-shore winds.

[†]Adj. to time interval of 20 minutes, using $\sigma(T_1) \approx \sigma(T_2) [T_1/T_2]^{1/5}$

Table 3
Bolla Island over-water diffusion data
[Smith and Beesmer (1967)]

Trial no.	x (m)	\bar{u} @ 16 m (m/sec)	σ_y^* (m)	\bar{x}_{CL}^*/Q_0 (sec/m ³)	σ_θ^* (deg)
1	1300	3.2	100	0.43×10^{-5}	3.5
2	1300	6.8	104	1.05×10^{-5}	2.6
3	1280	9.0	65	1.14×10^{-5}	3.5
5	1310	10.0	90	0.53×10^{-5}	5.3
6	1340	9.6	52	1.25×10^{-5}	3.0
7	1230	5.8	97	1.43×10^{-5}	3.0
8	1250	11.2	47	1.31×10^{-5}	2.3
9	1230	9.6	41	2.30×10^{-5}	2.6

*Time interval of 10 minutes.

In Table 2, since it was not always possible to obtain σ_θ measurements for the same time and duration as those of σ_y and \bar{x}_{CL}/Q_0 , the values were adjusted to a common averaging time of 20 minutes via the empirical law [Cramer, et al. (1964)]

$$\sigma(t_1) = \sigma(t_2) \cdot (t_1/t_2)^{1/5}. \quad (11)$$

All calculations are made using these adjusted values except for the computation of σ_z , which is evaluated directly from the observed data. Neither data set has been corrected for depletion due to deposition; this may be particularly important for the FP data in Table 3 [Cramer, et al. (1965)], as discussed below.

3.1 Models of σ_y

The parameter σ_y was estimated for the measured values of σ_θ , x , and \bar{u} corresponding to each field trial. Careful interpolation was used with the P.-G. and Briggs curves. The Cramer formulation, equation (2), was applied with several different values for x and p . From these estimates, the ratio of predicted to observed σ_y was formed for each trial, and the overall mean and standard deviation of this ratio was computed for each model. The correlation of the individually predicted values of σ_y and the observed σ_y 's was also calculated for each model. Examination of preliminary results indicated that the predictability of run 3.2 of Table 2 was very poor. A study of the rough data [R. M. Brown and S. Sethuraman (private communications)] revealed that the wind measurements for that run had been made a few hours before the smoke releases were begun. It seemed quite possible that the character of the wind fluctuations might have changed during that interval, and so run 3.2 was eliminated. The computations were again performed; the results are shown in Table 4.

The Briggs σ_y curves give the best mean value, but also the highest standard deviation (S.D.) and the lowest correlation coefficient.* The Taylor-Fuquay model, on the other hand, is almost as accurate as the Briggs model in predicting the

*Since the data set is small, emphasis should not be placed on the exact value of the correlation coefficient r . Confidence limits (2σ) on r are indicated in Tables 4, 6, and 7; these ranges overlap for many models.

mean, and has the advantage of smaller S.D. and a much better correlation coefficient. Of the ten models considered, five (Briggs, Taylor-Fuquay, P.-G., Islitzer, and Cramer "D") predict the mean within 6%. Of these five, the Cramer "D" model gives by far the smallest S.D. and the highest correlation coefficient. It is also very easy to use. It is interesting that its exponent, p , corresponds to near-neutral conditions over land. The attempts to use stability-adjusted exponents led to high correlation coefficients but considerable underprediction of the mean. Notice that while the Briggs and P.-G. models are both quite accurate in the mean, they both show large S.D.'s (and hence large probable errors) and poor correlation coefficients. Therefore the other models which depend more explicitly on meteorological information are probably preferable.

Table 4

Mean values of ratios of predicted to observed σ_y 's, and correlation of predicted to observed σ_y for several models applied to over-water dispersion*

Model	Type	Mean, pred./obs.	Std. dev., pred./obs.	Corr. coeff., pred. vs obs.	Range (2σ) of corr. coeff.
Pasquill-Gifford	Interpolation between curves	0.957	0.569	0.262	-0.188, 0.621
Briggs (1973)	Interpolation between curves	0.972	0.609	0.213	-0.238, 0.588
Cramer et al. (1964) "A"	$\sigma_y = 100 \sigma_\theta(x/100)^{.80}$	0.641	0.246	0.736	0.449, 0.885
Cramer et al. (1964) "B"	$\sigma_y = 500 \sigma_\theta(x/500)^{.80}$	0.884	0.340	0.736	0.449, 0.885
Cramer et al. (1964) "C"	$\sigma_y = 100 \sigma_\theta(x/100)^{.85}$	0.744	0.303	0.713	0.409, 0.875
Cramer et al. (1964) "D"	$\sigma_y = 500 \sigma_\theta(x/500)^{.85}$	0.947	0.386	0.712	0.407, 0.874
Cramer et al. (1964) "E"	$\sigma_y = 100 \sigma_\theta(x/100)^p$	0.679	0.249	0.783	0.533, 0.907
Cramer et al. (1964) "F"	$\sigma_y = 500 \sigma_\theta(x/500)^p$	0.898	0.322	0.767	0.504, 0.900
Islitzer (1961)	$\sigma_y = (\sigma_\theta/1.23)x$	0.953	0.466	0.630	0.275, 0.834
Taylor (1921); Fuquay et al. (1964)	$\sigma_y = f_n[x/\bar{u}, \sigma_\theta \bar{u}]$	1.033	0.477	0.613	0.250, 0.825

*Uses all data of Tables 2 and 3, except run 3.2 of Table 2.

3.2 Models of σ_z

Similar computations for σ_z were carried out for each field trial except 3.2 of Table 2. Interpolation was used to read σ_z from the P.-G. and Briggs curves. In the Smith technique, z_0 was estimated from equation (10), and used to interpolate a roughness correction factor from Figure 5; this factor was then applied to the interpolated "baseline" value from Figure 6 to yield a roughness-compensated σ_z . Several variations of the Cramer model, equation (6), were also considered. The experimental data from Tables 2 and 3 were used to compute values of σ_z from equation (1), assuming a sea-level source and taking $y = z = 0$.

From these numbers, ratios of predicted to "observed"** σ_z 's were formed for each field test, and the mean values and S.D. were computed for each model, as were the correlations between

**The quotation marks are used because σ_z is not really observed; it is calculated after a number of assumptions from observed results. Its accuracy is as good as the assumptions.

individual σ_z predictions and "observations". Examination of preliminary results indicated that all the Bolsa Island data were underpredicted, typically by a factor of 2 to 4, even when the predictions of the Brookhaven results were reasonably good. This was particularly true of trial 1 (Table 3) at Bolsa Island, for which σ_z was about 5 times larger than all the other Bolsa Island results, and hence a factor of 10 or more larger than predicted. Smith and Beesmer (1967) also noted this difficulty with trial 1, and discarded it as a "bad" point, though the data they present provide no clear indication as to why this should be so.

Now, as mentioned above, Cramer et al. (1965) suggested the possible importance of deposition with regard to the diffusion of FP above the sea. One can estimate the importance of this phenomenon by incorporating Chamberlain's (1953) definition of deposition velocity v_d into the Gaussian plume [e.g., Van der Hoven (1968)]. The net effect is to replace Q_0 in equation (1) by an "effective," source strength $Q(x)$. For a ground-level source, a plume centerline receptor sees the normalized concentration due to the depleting plume as

$$\frac{\bar{x}_{CL}}{Q_0} = \frac{Q(x)/Q_0}{\pi \sigma_y \sigma_z \bar{u}}, \quad (12a)$$

where

$$Q(x)/Q_0 = \exp \left[- \sqrt{\frac{2}{\pi}} \frac{v_d}{\bar{u}} \int_0^x \frac{dx}{\sigma_z(x)} \right]. \quad (12b)$$

Hence

$$\sigma_z = \frac{Q(x)/Q_0}{\pi \bar{u} \sigma_y \frac{\bar{x}_{CL}}{Q_0}} \leq \frac{1}{\pi \bar{u} \sigma_y \frac{\bar{x}_{CL}}{Q_0}}. \quad (13)$$

The right side of this inequality is the value calculated from observed data when deposition is ignored; i.e., neglecting deposition leads to over-estimation of experimental σ_z 's. To evaluate the degree of over-estimation which may be involved in the Bolsa Island data, the procedure and curves published by Van der Hoven (1968) were used. If a deposition velocity of 8 cm/sec is assumed for FP over water, and the near-neutral ("D") curve of Van der Hoven (1968) is adopted as a conservative approximation for a sea-level source, then the deposition-corrected values of σ_z listed in Table 5 are found. Note that the low wind speed during trial 1 leads to strong plume depletion, thus reducing σ_z for trial 1 to a value quite similar to those obtained for the other Bolsa Island trials. These values are also much more in line with the Brookhaven results, and with the predictions of the various σ_z models. A deposition velocity of 8 cm/sec for FP is large, but not entirely unreasonable; Islitzer and Dumbauld (1961) have cited values ranging between 0.2 cm/sec and 9.2 cm/sec for FP over desert terrain. Furthermore, although data for FP over water could not be found, there is some indication [e.g., see data reviewed by Gifford and Pack (1962)] v_d over water may be larger (perhaps a factor of 2 or so) than over dry surfaces such as sand.

Table 5
Sample results of deposition correction applied to σ_z based on Bolsa Island data.
Distance $x \geq 1300$ m, deposition
velocity $v_d \geq 8$ cm/sec, and
near-neutral conditions

Trial no.	Uncorrected σ_z (m)	\bar{u} @ 10 m (m/sec)	$Q(x)$ / Q_0	Dep.-corrected σ_z (m)
1	231	3.1	0.10	23.1
2	42.9	6.5	0.33	14.2
3	47.7	8.6	0.44	21.0
5	66.7	9.5	0.47	31.3
6	51.0	9.2	0.46	23.5
7	39.6	5.5	0.27	10.7
8	46.2	10.7	0.51	23.6
9	35.2	9.2	0.46	16.2

*Computed by power law $\bar{u}_{10}/\bar{u}_{16} = [10/16]^{0.1}$; Davenport (1965).

Since reliable estimates of v_d for FP over the sea could not be found to permit adjustment of the Bolsa Island results, it was decided to drop that data from further consideration. The deposition velocity of oil smoke on water is unknown, and so no correction could be applied to the Brookhaven data. This effect should probably be investigated in future analyses of these data.

The computations of the ratios of predicted to observed and of the correlation between predicted and observed values were repeated for the Brookhaven data alone; the results are indicated in Table 6.

Table 6
Mean values of ratios of predicted to "observed" σ_z 's, and correlation
of predicted to "observed" σ_z , for several models applied
to over-water dispersion*

Model	Type	Mean, pred./obs.	Std. dev., pred./obs.	Corr. coeff., pred. vs obs.	Range (2 σ) of corr. coeff.
Pasquill-Gifford	Interpolation between curves	1.698	1.266	0.239	-0.345, +0.689
Briggs (1973)	Interpolation between curves	1.585	1.272	0.378	-0.202, +0.762
F. B. Smith (1972)	Roughness-corr. interpolation	0.903	0.716	0.514	-0.035, +0.825
Cramer "A"	$\sigma_z = 100 (\sigma_y/2) (x/100)^{-3.5}$	0.658	0.742	-0.062	-0.582, +0.494
Cramer "B"	$\sigma_z = 500 (\sigma_y/2) (x/500)^{-3.5}$	1.872	2.110	-0.062	-0.582, +0.494
Cramer "C"	$\sigma_z = 500 (\sigma_y/2) (x/500)^{-4.5}$	2.071	2.158	0.003	-0.537, +0.541
Cramer "D"	$\sigma_z = 100 (\sigma_y/3) (x/100)^{-9.5}$	2.329	1.768	0.377	-0.204, +0.761
Cramer "E"	$\sigma_z = 500 (\sigma_y/3) (x/500)^9$	4.440	5.221	0.184	-0.394, +0.658
Cramer "F"	$\sigma_z = (\sigma_y/30) x^{1.2}$	1.248	0.882	0.445	-0.124, +0.794
Cramer "G"	$\sigma_z = (\sigma_y/80) x^{1.3}$	1.012	0.706	0.447	-0.121, +0.795
Islitzer "A"	$\sigma_z = (\sigma_y/3) x$	2.704	2.013	0.401	-0.176, +0.773
Islitzer "B"	$\sigma_z = (\sigma_y/8) x$	1.014	0.754	0.400	-0.177, +0.773

*Uses only Brookhaven data (Table 2), except run 3.2.

The Cramer "G" and Islitzer "B" models provide the best mean values, but the Cramer "G" model gives a lower S.D. and somewhat higher correlation coefficient. The exponent of this model is that appropriate for near-neutral conditions over land. The best correlation coefficient is exhibited by the Smith formulation; this model also has a low S.D., and predicts, in the mean, to within about 11%. The P.-G. and Briggs curves seriously overpredict σ_z , have large S.D.'s, and poor correlation with the experimentally derived values. In general, the standard deviations are larger and the correlation coefficients are smaller than for the σ_y models in Table 4, i.e., σ_z seems less predictable than σ_y .

3.3 Models of \bar{x}_{CL}/Q_o

Four σ_y models (P.-G., Briggs, Cramer "D", Taylor-Fuquay) were selected from Table 4, and used with four σ_z formulations (P.-G., Smith, Cramer "G", Islitzer "B") from Table 6 in the sea-level, center-line version of equation (1) to predict \bar{x}_{CL}/Q_o . Observed winds from the Brookhaven experiments were used. Again the means and standard deviations of ratios of predicted to observed, and the correlation of individual pairs were examined; the results appear in Table 7.

Table 7
Mean values of ratios of predicted to observed \bar{x}_{CL}/Q_o 's, and correlation of predicted to observed values, for several models applied to over-water dispersion data from Brookhaven

σ_y model*	σ_z model**	Mean, pred./obs.	Std. dev., pred./obs.	Corr. coeff., pred./obs.	Range (2 σ) of corr. coeff.
Taylor-Fuquay	P.-G.	1.146	1.227	0.697	0.253, 0.899
Cramer "D"	P.-G.	1.248	1.343	0.693	0.246, 0.897
P.-G.	P.-G.	1.356	1.390	0.565	0.037, 0.846
Briggs	P.-G.	1.362	1.389	0.540	0.001, 0.836
Taylor-Fuquay	Cramer "G"	1.695	1.499	0.659	0.186, 0.884
Taylor-Fuquay	Islitzer "B"	1.756	1.643	0.694	0.247, 0.897
Cramer "D"	Cramer "G"	1.824	1.611	0.686	0.233, 0.894
Taylor-Fuquay	Smith	1.895	1.577	0.671	0.207, 0.889
Cramer "D"	Islitzer "B"	1.909	1.786	0.686	0.234, 0.894
Cramer "D"	Smith	2.074	1.726	0.655	0.179, 0.883
P.-G.	Cramer "G"	2.098	1.875	0.484	-0.075, 0.811
P.-G.	Islitzer "B"	2.098	1.944	0.602	0.093, 0.862
Briggs	Islitzer "B"	2.107	1.950	0.581	0.061, 0.853
Briggs	Cramer "G"	2.111	1.891	0.467	-0.096, 0.804
P.-G.	Smith	2.228	1.872	0.642	0.157, 0.877
Briggs	Smith	2.236	1.885	0.624	0.128, 0.870

*Definitions from Table 4.

**Definitions from Table 6.

The combination of the Taylor-Fuquay expression for σ_y [equations (5)], and σ_z as read from the P.-G curves [Slade (1968)] gives the best mean value, lowest standard deviation, and highest correlation coefficient of all the combinations tested. All the models overpredict in the mean, some by a factor of 2 or more, and all exhibit quite large S.D.'s; roughly speaking, the standard deviation increases with the degree of mean overprediction.

4. SUMMARY AND CONCLUSIONS

It has been found that five models can predict σ_y , in the mean, to within about 6%, and with reasonable accuracy (factor of 2 or better, generally) for individual points. The best of these models is that suggested by Taylor (1921) and Fuquay, et al. (1964), and expressed in equations (5). The Pasquill-Gifford curves provide good accuracy in the mean, but the confidence limits of their predictions are somewhat larger.

Only three models can predict σ_z , in the mean, within 11%, and the accuracy for individual predictions is rather poor (factor of 3 or worse). Part of the difficulty may be related to the problem of accurately determining experimental values of σ_z . Indirect evaluations, such as performed above, are subject to substantial errors introduced by deposition. It would be most helpful to have direct measurements of σ_z in future experiments. Deposition estimates should also be reported whenever possible.

The combination of the Taylor-Fuquay expression for σ_y and the Pasquill-Gifford curves for σ_z provides estimates of \bar{x}_{CL}/Q_o , in the mean, to about 15%, but the confidence limits on individual predictions are rather larger (factor of 4 or so). Other model combinations provide worse prediction in the mean, coupled with larger probable errors.

On the whole, the use of observed u and σ_0 seems to provide sufficient information for adequate estimates of lateral diffusion. Prediction of the vertical diffusion and of the centerline concentration is not as satisfactory, but may be acceptable. It should be remarked that these results are largely based on analysis of a rather small data set from a single ocean site, and are subject to revision as more data becomes available. In the meantime, estimation of over-water diffusion should continue to be approached with caution.

ACKNOWLEDGEMENT

My thanks to R. M. Brown, P. Michael, G. S. Raynor, and S. Sethuraman of Brookhaven National Laboratory's Meteorology Group for providing data, and for their helpful discussions. This work was performed under an agreement between NOAA and the U. S. Atomic Energy Commission.

REFERENCES

- A.S.M.E., (1968, 1973), Recommended guide for the prediction of the dispersion of airborne effluents, 1st and 2nd editions, A.S.M.E., New York.
- Briggs, G. A. (1973), Diffusion estimation for small emissions, NOAA-ARL-ATDL- contribution no. 79 (draft), May.
- Chamberlain, A. C. (1953), Aspects of travel and deposition of aerosol and vapour clouds, British report AERE-H.P./R.-1261.
- Charnock, H. (1955), Wind stress on a water surface, *Quart. J. Roy. Meteorol. Soc.* 81, 639-640.
- Cramer, H. E., G. M. DeSanto, K. R. Dumbaugh, P. Morgenstern, and R. N. Swanson, (1964), Meteorological prediction techniques and data system, GCA tech. rep. no. 64-3-G, March.
- , H. L. Hamilton, Jr., and G. M. DeSanto, (1965), Atmospheric transport of rocket motor combustion by-products, vol. I., data analysis and prediction technique, GCA tech. report to Commander, Pacific Missile Range, Pt. Mugu, Calif., December.
- , F. A. Record, and H. C. Vaughan, (1958), The study of the diffusion of gases or aerosols in the lower atmosphere, AFCRC-TR-58-239, ASTIA no. 152582, May 15.
- Davenport, A. G. (1965), The relationship of wind structure to wind loading, in Proc. of Symp. on Wind Effects on Buildings and Structures, Teddington, England, June 26-28, 1963, vol I, 53-102.
- Frenzen, P., and R. L. Hart, (1973), Atmospheric dispersion over water inferred from turbulence statistics, in Radiological and Environmental Research Division Annual Report for 1972, Argonne National Laboratory, ANL-7960, part IV, 74-83.

- Fuquay, J. J., C. L. Simpson, and W. T. Hinds, (1964), Estimates of ground-level air exposures resulting from protracted emissions from 70-m stacks at Hanford, Pacific Northwest Laboratory report HW-80204, January.
- Garratt, J. R. (1973), Studies of turbulence in the surface layer over water (Lough Neagh), III, wave and drag properties of the seasurface in conditions of limited fetch, *Quart. J. Roy. Meteorol. Soc.* 99, 35-47.
- Gifford, F. A. (1961), Use of routine meteorological observations for estimating atmospheric dispersion, *Nucl. Safety* 2(4), 47-51.
- _____, (1968), An outline of theories of diffusion in the lower layers of the atmosphere, ch. 3 of Meteorology and Atomic Energy 1968, ed. by Slade, TID-24190.
- _____, (1972), Transport and dispersion in urban environments, ch. 4 in Dispersion and Forecasting of Air Pollution, WMO tech. note no. 121.
- _____, and D. H. Pack, (1962), Surface deposition of airborne material, *Nucl. Safety* 3(4), 76-86.
- Islitzer, N. F. (1961), Short-range atmospheric dispersion measurements from an elevated source, *J. Meteorol.* 18 (4), 443-450.
- _____, and D. H. Slade, (1968), Diffusion and transport experiments, ch. 4 in Meteorology and Atomic Energy 1968, ed. by Slade, TID-24190.
- Kitaigorodskii, S. A., (1973), The physics of air-sea interaction, Israel program for scientific translations, Jerusalem.
- Lumley, J. L. and H. A. Panofsky, (1964), The structure of atmospheric turbulence, Interscience, New York.
- Michael, P., G. S. Raynor, and R. M. Brown, (1973a), Preliminary measurements of over-ocean atmospheric diffusion, presented at Amer. Nucl. Soc. meeting on The Oceans, Nuclear Energy, and Man, Singer Island, Fla. April 25-27.
- _____, (1973b), Atmospheric diffusion from an off-shore site, presented at IAEA Symp. no. 181 on the Physical Behavior of Radioactive Contaminants in the Atmosphere, Vienna, Austria, Nov. 12-16.
- Slade, D. H., (1962), Atmospheric diffusion over Chesapeake Bay, *Mon. Weather Rev.* 90 (6), 217-224.
- _____, (1966), Estimates of dispersion from pollutant releases of a few seconds to 8 hours in duration, ESSA-TN-39-ARL-3, April.
- _____, (1968), editor, Meteorology and Atomic Energy 1968, TID-24190.
- Smith, F. B., (1972), A scheme for estimating the vertical dispersion of a plume from a source near ground level, in Proc. of 3rd Meeting of the NATO Expert Panel on Air Pollution Modeling, Paris, France, Oct. 2-3, available from U.S.E.P.A. Tech. Info. Ctr., Research Triangle Park, N.C.
- Smith, T. B., and K. M. Beesmer, (1967), Bolsa Island meteorological investigation, MRI-67-FR-650, October 9.
- _____, and B. L. Niemann, (1969), Shoreline diffusion program Oceanside, California, vol I, tech. report., MRI-64-FR-860, November.
- Sutton, O. G., (1953), Micrometeorology, McGraw-Hill, New York.
- Taylor, G. I., (1921), Diffusion by continuous movements, *Proc. of Lond. Math. Soc.*, ser.2, XX, 196-212.
- Turner, D. B., (1969), Workbook of atmospheric dispersion estimates, U. S. Public Health Service publication no. 999-AP-26 (revised).
- Van der Hoven, I., (1967), Atmospheric transport and diffusion at coastal sites, *Nuc. Safety* 8 (5), 490-499.
- _____, (1968), Deposition of particles and gases, ch.5-3 in Meteorology and Atomic Energy 1968, TID-24190.
- Vaughan, L. M., (1964), Fundamental problems on the meso-scale, Conference on AEC Meteorological Activities, May 19-22, at Brookhaven Nat. Lab., BNL-914 (C-42), 103-106.

A Method for Evaluating the Accuracy of Air Pollution
Prediction Models

September 1974

Carmen J. Nappo, Jr.

Air Resources
Atmospheric Turbulence and Diffusion Laboratory
National Oceanic and Atmospheric Administration
Oak Ridge, Tennessee

(Published in the proceedings of the Symposium on Atmospheric Diffusion
and Air Pollution held September 9-13, 1974 in Santa Barbara, California.)

A METHOD FOR EVALUATING THE ACCURACY OF AIR POLLUTION
PREDICTION MODELS

Carmen J. Nappo, Jr.

Air Resources
Atmospheric Turbulence and Diffusion Laboratory
National Oceanic and Atmospheric Administration
Oak Ridge, Tennessee

1. INTRODUCTION

The accuracy of an air pollution prediction model can be evaluated only by measuring its ability to reproduce an air pollution episode. This ability is often measured by comparing the time changes of the predicted with the observed air pollution concentrations at several monitoring stations within the prediction area. Often, the predicted and observed time-average concentrations are compared and/or the temporal correlation coefficients are formed between these quantities at each station. This rather one-dimensional view has resulted in a controversy over which of the current urban air pollution prediction models is best. Table 1 shows a typical result of such an evaluation. The column labeled "Model" lists the references as well as the numerical technique used, i.e. trajectory, particle-in-cell, etc. All of these models predict carbon monoxide, CO, concentration from extended area sources and all but the model by MacCracken, *et al.* (1971) are applied to the Los Angeles basin. The model by MacCracken, *et al.* is applied to the San Francisco Bay area. In the column labeled "Average Temporal Correlation," the station average of the temporal correlation coefficient formed for each model is listed. In cases where several predictions were performed, the average of the correlations from all predictions is used. The column labeled "Computation Time," estimates the computer time, in minutes, required by each model for a 24-hour forecast using an IBM 360/65 machine. Finally under "Computer Cost," the approximate cost for this 24-hour prediction, in dollars, is presented.

One obvious result of such an evaluation is that although many of the models are roughly of equal accuracy, there is a great disparity in their complexity and operating cost. This is the basis for the above mentioned controversy. In this discussion, a more comprehensive method of evaluation is proposed and applied to the CO air pollution models listed in Table 1. The method in essence takes into account the spatial variability as well as the

temporal variability of the prediction. The following are a few of the results observed:
1) models which were previously regarded accurate on the basis of their time correlations, are not so accurate when the comprehensive evaluation is used; 2) the detailed modeling of vertical diffusion is of little significance in determining ground concentrations of CO; and 3) model predictions are sensitive mostly to the source emissions.

TABLE 1
MODEL EVALUATION BASED ON TEMPORAL CHARACTERISTICS

Model	Average Temporal Correlation Coefficient	Computer Time for 24 Hour Prediction (min)	Computer Cost for 24 Hour Prediction (dollars)
MacCracken <i>et al</i> (1971) multi-box	0.37	106	350
24 Hour Persistence	0.47	None	None
Roth <i>et al</i> (1971) primitive equation	0.52	60	200
Hanna (1973) ATDL simple model	0.60	None	None
Sklarew <i>et al</i> (1972) particle-in-cell	0.65	49	160
Pandolfo and Jacobs (1973) primitive equation	0.66	20	70
Reynolds <i>et al</i> (1973) primitive equation	0.73	30	100
Eschenroeder <i>et al</i> (1972) trajectory	0.73	15	50
Lamb and Neiburger (1971) trajectory	0.90	35	115

2. THE METHOD

If a prediction model is to accurately reproduce an air pollution episode, it must reproduce at each monitoring station the observed time-varying pollution concentration, and reproduce at each monitoring time the observed space-varying pollution pattern. The degree with which the observed time-varying concentration is reproduced is measured in part by the station (spatial) average of the temporal correlation coefficient formed at each station, $\bar{R}(t)^s$. This term can be regarded as the measure of the model's ability to reproduce the observed temporal trends of air pollution over the whole network of monitoring stations. In the same manner, the degree with which the observed spatial trends of air pollution are reproduced over the entire prediction period is measured by the time average of the correlation coefficient formed between the predicted and observed patterns of the concentration isopleths at each monitoring time, $\bar{R}(s)^t$. The temporal and spatial correlation coefficients are discussed in the Appendix. Ideally, $\bar{R}(t)^s$ and $\bar{R}(s)^t$ would equal unity. Often, however, there is insufficient spatial resolution of the data to form the isopleths needed to determine $\bar{R}(s)^t$. Instead, at each observation time, a correlation coefficient is formed using the predicted and observed pollution concentrations at all monitoring stations. It is expected that this term in quality, at least, reflects the correlation of the observed and predicted concentration patterns.

As indicated above, $\bar{R}(s)^t$ and $\bar{R}(t)^s$ do not completely measure a model's accuracy. The ability of a model to reproduce the time and space varying amounts of air pollution must also be measured. This can be done in the following way. At each monitoring station, the time average of the ratio of predicted to observed concentration is formed; these time-averaged ratios are then averaged over all stations and called $\bar{r}(t)^s$. Next, at each monitoring time, the space average of the ratio of predicted to observed concentration is formed; these are averaged over all monitoring times and called $\bar{r}(s)^t$. The formation of these averaged ratios is explained in the Appendix. Because of the way these averages are formed, $\bar{r}(t)^s$ equals $\bar{r}(s)^t$ (see Appendix), and this number represents the totally averaged ratio of the predicted to observed air pollution concentration. If a model reproduces exactly the air pollution averaged over space and time (e.g. the 24-hour averaged air pollution in the Los Angeles basin), then for the model $\bar{r}(s)^t = \bar{r}(t)^s = 1$. However, while these averaged ratios are equal, their standard deviations are not, and these deviations represent the error or variance contained in the models prediction of the time-and space-averaged amounts of the air pollution. Let the space average of the variance in the time-averaged prediction be designated by $\sigma(t)^s$, and the time average of

the variance in the space-averaged prediction be designated by $\sigma(s)^t$.

The evaluation of the accuracy of an air pollution prediction model requires the formation of the following quantities:

$$\bar{R}(t)^s, \bar{R}(s)^t, \bar{r}(t)^s + \sigma(t)^s, \text{ and } \bar{r}(s)^t + \sigma(s)^t.$$

The ideal model would have

$$\bar{R}(t)^s = \bar{R}(s)^t = 1$$

and

$$\bar{r}(t)^s + \sigma(t)^s = \bar{r}(s)^t + \sigma(s)^t = 1.$$

3. ILLUSTRATION OF THE METHOD

As an illustration of this evaluation method, the above quantities are formed for each of the CO prediction models listed in Table 1. The plot of the space average of the temporal correlation coefficient, $\bar{R}(t)^s$, versus the time average of the spatial correlation coefficient, $\bar{R}(s)^t$, is shown in Figure 1 for each model. It is seen that the models reproduce the temporal trends better than the spatial

- ROTH *et al.* (1971)
- ▲ REYNOLDS *et al.* (1973)
- HANNA (1973)
- ▼ PANDOLFO AND JACOBS (1973)
- ◊ SKLAREW *et al.* (1972)
- △ LAMB AND NEIBURGER (1971)
- ◆ MacCRACKEN *et al.* (1971)
- ESCHENROEDER *et al.* (1972)
- 24 hr PERSISTENCE

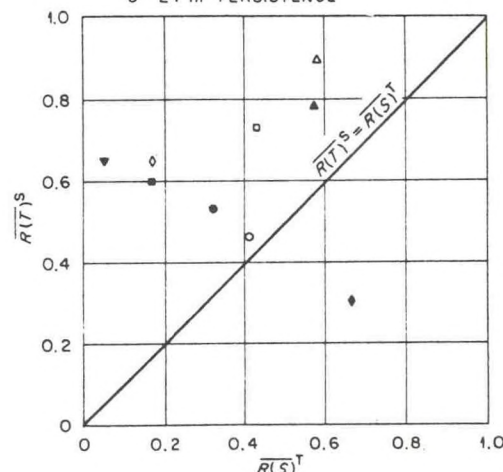


Figure 1. $\bar{R}(t)^s$ versus $\bar{R}(s)^t$
Average result for each model tested.

trends, with the exception of the San Francisco Bay area model (MacCracken, et al.). The differences in the ability of the models to reproduce the spatial trends is also quite obvious. In Figure 2, the space average of the time-averaged ratios of the predicted to observed CO concentration, $\overline{r(t)^s}$, is plotted against the time average of the space-averaged ratios of the predicted to observed concentrations, $\overline{r(s)^t}$, with accompanying error bars representing the standard deviations $\overline{\sigma(t)^s}$ and $\overline{\sigma(s)^t}$. Comparing Figures (1) and (2), several significant features are observed. First of all, while Hanna's application of the ATDL simple air pollution model reproduces the observed trends of pollution as well as the complicated particle-in-cell model (Sklarew, et al.), there is a great difference in their ability to predict the amounts of air pollution, with the ATDL simple model seriously over-estimating the observed concentrations. Secondly, the trajectory model of Lamb and Neiburger which from Table 1 and Figure (1) might be judged the best of the models, seriously underpredicts the observed CO concentration. Finally, while the accuracy of the temporal and spatial trend prediction of the Systems Application 1973 model (Reynolds, et al.) is greatly increased over its original 1971 form (Roth, et al. (1971)), there is no correspondingly large change in ability to predict the amount of CO.

- ROTH et al. (1971)
- ▲ REYNOLDS et al. (1973)
- HANNA (1973)
- ▼ PANDOLFO AND JACOBS (1973)
- ◊ SKLAREW et al. (1972)
- △ LAMB AND NEIBURGER (1971)
- ◆ MacCRACKEN et al. (1971)
- ESCHENROEDER et al. (1972)
- 24 hr PERSISTENCE

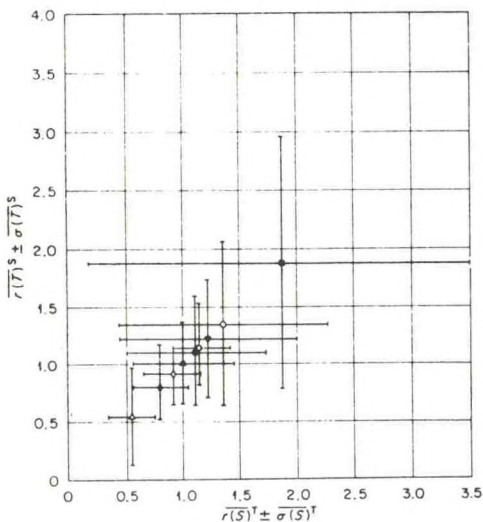


Figure 2. $\overline{r(t)^s} + \overline{\sigma(t)^s}$ versus $\overline{r(s)^t} + \overline{\sigma(s)^t}$
Average result for each model tested.

In Figure (3), $\overline{\sigma(t)^s}$ is plotted against $\overline{\sigma(s)^t}$. Again we see that while Hanna (1973) and Sklarew, et al. (1972) reproduce the trends equally as well, there is a great difference in the variances of the predicted amounts of air pollution. We also see that the primitive equation models have greater error (variance) in their spatial predictions than in their temporal predictions, i.e. $\overline{\sigma(s)^t} > \overline{\sigma(t)^s}$, while the reverse is true for the trajectory, particle-in-cell, and box models.

4. RESULTS OF THE EVALUATION

From the above illustration of the evaluation of the evaluation method, two results follow. First of all, it seems clear that the detail of the vertical diffusion calculations is not very significant in determining a model's accuracy. Note that Lamb and Neiburger's model has no vertical detail in the distribution of pollution concentration. The Systems Application 1971 model had ten levels in the vertical while the 1973 version has only five. The model of Eschenroeder, et al. (1972) also has five levels, while the ATDL simple model assumes a gaussian distribution of pollutants in the vertical. This observation is further confirmed by Reynolds, et al. (1973) who compared a two-dimensional (no vertical diffusion) model with their five-layer model, and found that "differences in prediction were generally (though not always)

- ROTH et al. (1971)
- ▲ REYNOLDS et al. (1973)
- HANNA (1973)
- ▼ PANDOLFO AND JACOBS (1973)
- ◊ SKLAREW et al. (1972)
- △ LAMB AND NEIBURGER (1971)
- ◆ MacCRACKEN et al. (1971)
- ESCHENROEDER et al. (1972)
- 24 hr PERSISTENCE

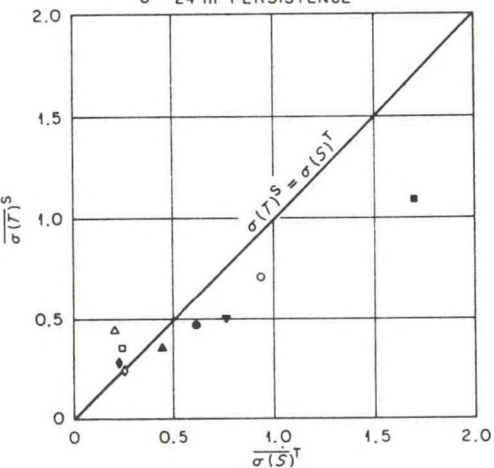


Figure 3. $\overline{\sigma(t)^s}$ versus $\overline{\sigma(s)^t}$
Average result for each model tested.

rather small." They go on to recommend that "the question of dimensionality be further explored in future studies of model sensitivity."

The second result is that model sensitivity and accuracy are dependent mostly on the degree of detail of the source emissions inventory. This is quite evident in comparing the Systems Application 1971 and 1973 models and their respective results. The 1973 meteorological model has been simplified ("detuned") with respect to its 1971 form. For example, the original vertical resolution is halved, and a less accurate finite differencing scheme is used for the horizontal advection together with a less detailed wind field. However, in the 1973 model a much more detailed source emissions inventory is utilized. This appears to have more than compensated for the "detuning" of the earlier meteorological model because the resulting overall accuracy has been improved.

5. CONCLUSION

A method for evaluating the accuracy of air pollution models has been proposed. The method measures a model's ability to reproduce the observed spatial and temporal trends of air pollution, as well as the observed spatial and temporal amounts of air pollution and their respective errors. This method was illustrated by evaluating several models of CO air pollution. Initial results of this evaluation are that: 1) models previously regarded as quite accurate are in fact, less accurate when comprehensively evaluated; 2) the Los Angeles Basin models reproduce the observed temporal trends of air pollution better than observed spatial trends, while the reverse is true for a San Francisco Bay area model; 3) primitive equation models have greater variance in their spatial predictions of air pollution concentrations than in their temporal predictions, while the reverse is true for trajectory, particle-in-cell and box models; 4) the detailed calculation of vertical diffusion does not appear significant in the prediction of air pollution ground concentrations; and 5) a model's accuracy is sensitive mostly to the degree of detail of the source emission inventory.

APPENDIX: FORMATION OF THE STATISTICS

Let the predicted and observed concentrations at the t 'th monitoring time and the s 'th monitoring station be given by $P_{s,t}$ and $O_{s,t}$ respectively. The temporal correlation coefficient is formed at each monitoring station by

$$R_s(\tau) = \frac{\sum_{t=1}^T P_{s,t} O_{s,t}}{\sqrt{\sum_{t=1}^T (P_{s,t})^2} \sqrt{\sum_{t=1}^T (O_{s,t})^2}} \quad (1)$$

where T is the number of monitoring times and

$$\bar{P}_{s,t} = P_{s,t} - \overline{P_{s,t}}^\tau \quad (2)$$

$$\bar{O}_{s,t} = O_{s,t} - \overline{O_{s,t}}^\tau \quad (3)$$

The overbar denotes a time average. The spatial average of the temporal correlation coefficient, $R(\tau)^s$, is given by

$$\overline{R(\tau)} = \frac{1}{N} \sum_{s=1}^N R_s(\tau) \quad (4)$$

where N is the number of monitoring stations.

The spatial correlation coefficient is formed at each monitoring time by

$$R_t(\tau) = \frac{\sum_{s=1}^N \bar{P}'_{s,t} \bar{O}'_{s,t}}{\sqrt{\sum_{s=1}^N (\bar{P}'_{s,t})^2} \sqrt{\sum_{s=1}^N (\bar{O}'_{s,t})^2}} \quad (5)$$

where

$$\bar{P}'_{s,t} = P_{s,t} - \overline{P_{s,t}}^\tau \quad (6)$$

$$\bar{O}'_{s,t} = O_{s,t} - \overline{O_{s,t}}^\tau \quad (7)$$

The overbar denotes a space or station average. The temporal average of the spatial correlation coefficient is given by

$$\overline{R_t(\tau)} = \frac{1}{T} \sum_{\tau=1}^T R_t(\tau) \quad (8)$$

The time average and the space average of the ratio of the predicted to observed concentrations is given respectively by

$$r_t(\tau) = \frac{1}{T} \sum_{\tau=1}^T (P_{s,t}/O_{s,t}) \quad (9)$$

and

$$r_s(\tau) = \frac{1}{N} \sum_{s=1}^N (P_{s,t}/O_{s,t}) \quad (10)$$

The space average of the time-averaged ratios is

$$\overline{r(t)}^s = \frac{1}{N} \sum_{A=1}^N r_A(t) \quad (11)$$

The time average of the space-averaged ratios is given by

$$\overline{r(s)}^t = \frac{1}{T} \sum_{T=1}^T r_t(s) \quad (12)$$

We can easily show that $\overline{r(t)}^s = \overline{r(s)}^t$ by using (9) to (12) as follows.

$$\begin{aligned} \overline{r(t)}^s &= \frac{1}{N} \sum_{A=1}^N r_A(t) \\ &= \frac{1}{N} \frac{1}{T} \sum_{A=1}^N \sum_{T=1}^T \left(P_{A,T} / O_{A,T} \right) \\ &= \frac{1}{T} \sum_{T=1}^T \frac{1}{N} \sum_{A=1}^N \left(P_{A,T} / O_{A,T} \right) \\ &= \frac{1}{T} \sum_{T=1}^T r_T(s) \\ &= \overline{r(s)}^t \end{aligned}$$

ACKNOWLEDGEMENT

This work was performed under an agreement between the National Oceanic and Atmospheric Administration and the U. S. Atomic Energy Commission.

REFERENCES

- Eschenroeder, A. Q., J. R. Martinez and R. A. Nordsieck, 1972: Evaluation of a diffusion model for photochemical smog simulation. Final Rpt. No. 68-02-0336 for the Environmental Protection Agency. General Res. Corp., Santa Barbara, Cal.
- Hanna, S. R., 1973: Urban air pollution models - why? ATDL contribution file no. 83, Atmospheric Turbulence and Diffusion Lab., Oak Ridge, Tennessee.
- Lamb, R. G. and M. Neiburger, 1971: An interim version of a generalized urban air pollution model. *Atmos. Environ.*, No. 4, Vol. 5, pp 239-264.
- MacCracken, M. C., T. V. Crawford, K. R. Peterson, and J. B. Knox, 1971: Development of a multi-box air pollution model and initial verification for the San Francisco Bay area. Lawrence Radiation Lab. No. UCRL-73348, Livermore, Cal.
- Pandolfo, J. P. and C. A. Jacobs, 1973: Tests of an urban meteorological-pollutant model using CO validation data in the Los Angeles metropolitan area. Vol. 1, EPA Rpt. No. R4-730-025A, The Center for the Environ. and Man, Inc., Hartford, Conn.
- Reynolds, S. D., M. K. Liu, T. A. Hecht, P. M. Roth, and J. H. Seinfeld, 1973: Further development and evaluation of a simulation model for estimating ground level concentrations of photochemical pollutants. Final Rpt. EPA Contract 68-02-0339, Systems Applications, Inc., Beverly Hills, Cal.
- Roth, P. M., S. D. Reynolds, P. J. W. Roberts, and J. H. Seinfeld, 1971: Development of a simulation model for estimating ground level concentrations of photochemical pollutants. Final Rpt. 71-SAI-21, Systems Applications, Inc., Beverly Hills, Cal.
- Sklarew, R. C., A. J. Fabrick, and J. E. Prager, 1971: A particle-in-cell method for numerical solution of the atmospheric diffusion equation, and applications to air pollution problems. Final Rpt. 3SR-844, Systems, Science and Software, La Jolla, Cal.

Research Needs Related to Hydrometeorologic Aspects
of Future Energy Production*

by Steven R. Hanna
Air Resources
Atmospheric Turbulence and Diffusion Laboratory
National Oceanic and Atmospheric Administration
Oak Ridge, Tennessee

Abstract

Plans are being made to develop large power parks and energy centers which will dissipate several thousand megawatts of waste heat to the atmosphere. Characteristics of these energy centers are discussed and estimates of environmental impact are made. Research needs are outlined.

1. Introduction

Waste heat is being dissipated to the atmosphere from intense energy centers at a maximum rate of about 3000 MW at a few locations in the United States. In some cases, direct river, lake, or ocean cooling is used, and the waste heat is gradually emitted to the atmosphere in the form of sensible, latent, and radiative heat over a broad area ($\sim 10^{10} \text{ m}^2$). Consequently the waste heat can affect the atmosphere by forming light fog or by increasing temperatures and convection very slightly over this broad area. In other cases, cooling ponds are used to dissipate the waste heat. Since about two acres of water surface is required to dissipate 1 MW of waste heat, the cooling pond area necessary to dissipate 3000 MW is about $3 \times 10^7 \text{ m}^2$. Cooling ponds are observed to cause local fogging and icing, and slight temperature increases in the vicinity of the ponds. The recent trend is towards evaporative cooling towers, which dissipate the waste

Presented at the Workshop on "Research Needs Related to Water for Energy," Indianapolis, Indiana, October 20-22, 1974, sponsored by the Water Resources Center, University of Illinois at Urbana-Champaign.

heat from an area of about 10^4 m^2 . Cooling towers are known to cause the development of small cumulus clouds and can contribute to local intense fog. On the whole, however, we can state that atmospheric effects of waste heat dissipation are currently observed to be of only slight significance.

But it is necessary now to take a new look at environmental modification by cooling towers and ponds, because of the plans of this country to develop large energy centers. Orders of magnitude increases in heat rejection from given areas can be expected. Unfortunately we do not have the research background to properly evaluate these environmental effects.

2. Waste Heat from Coal Gasification

While there are not currently any large coal gasification plants operating in this country, the fuel shortage has inspired many utilities and oil companies to make plans to build many of these plants. Briefly, in a coal gasification plant coal is burned to form a gas, which is usually a combination of methane, hydrogen, and carbon monoxide.¹ The resulting gas is supposedly "cleaner" than the coal. Because this gasification process is only about 50% efficient, there are large quantities of waste heat which must be dissipated.

The Burnham I Coal Gasification Complex of the El Paso National Gas Company is to be constructed near Farmington, New Mexico.² In order to produce $8.15 \times 10^6 \text{ m}^3/\text{day}$ of gas, at an energy rating of 9.87 kw hr./m^3 ,

it will be necessary to use about $.5 \text{ m}^3/\text{sec}$ of water. The total power capability of the gas production will be about 3000 MW, or about three times the capability of the largest currently operating units of fossil or nuclear power plants.

Evaporative cooling towers will consume $.2 \text{ m}^3/\text{sec}$ of water (equivalent to 400 MW). Because of the shortage of water in New Mexico, only 15% of the waste heat is to be dissipated by cooling towers. In the eastern or midwestern United States, a greater percentage of the waste heat would be dissipated by cooling towers and water consumption would be greater.

The Institute for Energy Analysis in Oak Ridge (R. Rotty, private communication) estimates that in 1984 about 10^8 tons per year of coal will be consumed in coal gasification. This figure is obtained on the basis of construction plans furnished by various utilities. Assuming that one ton per year of coal produces .03 megawatts of power, and that the process has a thermal efficiency of 50%, then evaporative cooling must dissipate 3×10^5 MW of waste heat. This amounts to a water consumption of $300 \text{ m}^3/\text{sec}$ in 1984 for the cooling of the coal gasification process.

3. Waste Heat from Power Parks

The Atomic Energy Commission is currently evaluating about a dozen sites for power parks, where 20 to 50 thousand MWe of power will be generated on sites with areas of about 10 to 100 km^2 . The advantages

of power parks are their ease of maintenance, the concentration of nuclear fuel cycle facilities, and safety. The heat disposal problem may be the most important argument against power parks. Since nuclear power plants are only about 33% efficient, it is possible that 100,000 MW of waste heat may be dissipated by cooling towers over a 10 to 100 km^2 area. This heat flux, 1000 to $10,000 \text{ w/m}^2$, is many times greater than the solar energy flux (330 w/m^2) and is spread over an area the size of a small city. Local climate modification has been well documented over small cities, where the man-made energy flux is typically about 100 w/m^2 .

Preliminary evaluations of planned power parks at Hanford, Washington and Riverbend, Louisiana are being made by Battelle Pacific Northwest Laboratory and Oak Ridge National Laboratory, respectively. The Atmospheric Turbulence and Diffusion Laboratory is involved in estimating the meteorological effects of the Riverbend power park, which is planned to dissipate about 72,000 MW of waste heat to the atmosphere from several dozen natural draft cooling towers over an area of 6.3 km^2 . About $40 \text{ m}^3/\text{sec}$ of water, drawn from the Mississippi River, will be evaporated from the cooling towers. This water flux is equivalent to 12 cm/yr. of rain over an area of 10^4 km^2 .

Since there are no currently operating power parks which approach this heat output by even an order of magnitude, there are no data available on the environmental effects of the heat and moisture output. The impact must be estimated using geophysical analogues or computer models.

The only comparable stationary heat sources of this magnitude are large fires and volcanoes. Bourne⁴ describes meteorological phenomena that accompanied the Surtsey volcano, which released an estimated 100,000 MW of heat continuously to the atmosphere from an area less than 1 km². This energy was released in the form of sensible (convective) heat. A permanent cloud extending to heights of 5 to 9 km formed over the volcano. Waterspouts also formed below the bent-over plume from this volcano, indicating that the buoyant motions acted to concentrate local atmospheric vorticity. As another example of the meteorological effects of large energy releases, Taylor et al.⁵ describe their observations of a large, controlled bushfire on an area of 50 km² in Australia. The average heat output over a six hour period was 100,000 MW, causing a cumulus cloud to form which reached to a height of 6 km.

In both the volcano and bushfire, the heat output took the form of sensible (convective) heat and carried many ash particles. The heat output from cooling towers or ponds is mostly in the form of latent heat (water vapor). While these geophysical phenomena and the cooling devices are not strictly analogous, it is still interesting to compare the effects of their heat releases.

Urban heat islands are observed to form over most cities. But the heat flux per unit area (100 w/m²) is less than that from the proposed power parks. Furthermore, the heat is injected much higher into the atmosphere when cooling towers are used. Consequently it is felt that bushfires are more closely related to energy releases from cooling towers than are urban heat islands.

4. Calculations of Atmospheric Effects due to Heat Releases from Large Energy Centers.

Water vapor, heat, and drift droplets are emitted by cooling towers.

Drift drops are drops of circulating water which by accident have been carried away by the air stream. If the circulating water contains salt, the drift is potentially harmful to vegetation surrounding the towers. The following specific calculations are used to determine the environmental impact of these emissions:

a. Plume rise and cloud formation due to a single cooling tower is treated using Briggs'⁶ plume rise theory as modified by Hanna⁷ for cooling tower plumes, and a simple one-dimensional cloud growth model such as that developed by Weinstein.⁸

b. Ground level fog formation is calculated by assuming that the water vapor diffuses in a passive manner. A Gaussian plume model⁹ or the diffusion equation¹⁰ can be used.

c. Drift deposition is calculated for drops with radii greater than 100 μm by assuming that they follow a ballistic trajectory, with their settling speed changing as the drop evaporates.¹¹ Drops with radii less than 100 μm will diffuse as they settle and their deposition is calculated using Chamberlain's theory.¹²

The above calculations are usually all that are considered in environmental impact statements. The AEC sponsored a symposium "Cooling Tower Environment - 1974" in March of this year, in order to discuss these various calculation techniques.¹³ Also, some methods of determining ecological effects of cooling tower drift were presented. It was clear

that there are many models of plume rise, fogging, and drift deposition, but very few observations. A major measurement program at the Chalk Point, Maryland, cooling tower will begin this year¹⁴ and hopefully will provide sufficient data to begin refining models. Much more data is needed, however.

There are many other potential environmental impacts of cooling towers which should be considered but are receiving very little attention:

- e. Thunderstorms may be triggered by the cooling tower.
- f. During overcast, rainy days, the cooling tower may augment rain for several tens of km downwind of the tower.
- g. Vapor and SO₂ plumes may merge to form acid plumes.
- h. Climate may be modified on a regional scale.

Although none of these impacts has been measured sufficiently, casual observations suggest that current cooling towers (about 1000 MW) are not significantly impacting the atmosphere in these ways. But the prospect of power parks and energy centers should change our perspectives, for the total heat output is expected to grow by two orders of magnitude to nearly 100,000 MW. This is approximately the rate of energy production in a severe storm or a Great Lakes snow squall.¹⁵ For example, it was calculated that the cloud from the Riverbend power park would extend 40 km from the park about 50% of the time.

If the heat were released from cooling ponds rather than cooling towers, then our calculations of atmospheric effects are even less

certain. Models of heat exchanges at water surfaces are based on old measurements at lakes and reservoirs. Ryan¹⁶ has recently attempted to model cooling ponds in the laboratory and has suggested improved formulas for heat transfer. These formulas must be tested at operating cooling ponds, where temperatures can be as much as 40°C above the temperatures of natural ponds in the vicinity.

5. Recommended Research

The following items of research are listed in their order of priority:

a. The formation of clouds by multiple cooling tower plumes and their feedback on the atmospheric environment should be studied. One dimensional cloud models⁸ are not adequate. Some work is underway on multiple cloud fields with feedback included.¹⁷ Briggs'¹⁸ has begun a study of multiple plume merging. This research area would require several man years to complete.

b. A cloud growth model should be tested using an operating natural draft cooling tower. Cross-sectional and vertical distributions of liquid and gaseous water, temperature, and air velocity should be made in the plume and its environment. Since the input parameters of a cooling tower are known, the model can be accurately tested. Both wet and dry towers can cause clouds to form. The dry tower plume entrains moist environmental air, which may condense as it is lifted and cooled.

c. In order to calculate the increases in fog due to waste heat rejection, a dispersion theory should be developed which accounts for the effects of latent heat release. The thermodynamic equations should be coupled with the equations of motion and continuity of water. Current models predict fog to occur at the ground when in reality the condensed water forms a stratus deck some distance above the ground.

d. Measurements of drift deposition at a variety of towers should be obtained and used to check the many existing models.¹³

e. Physical modeling of the "lift off" of downwashed buoyant plumes and the effects of cooling tower geometry on the plume trajectory should be undertaken.

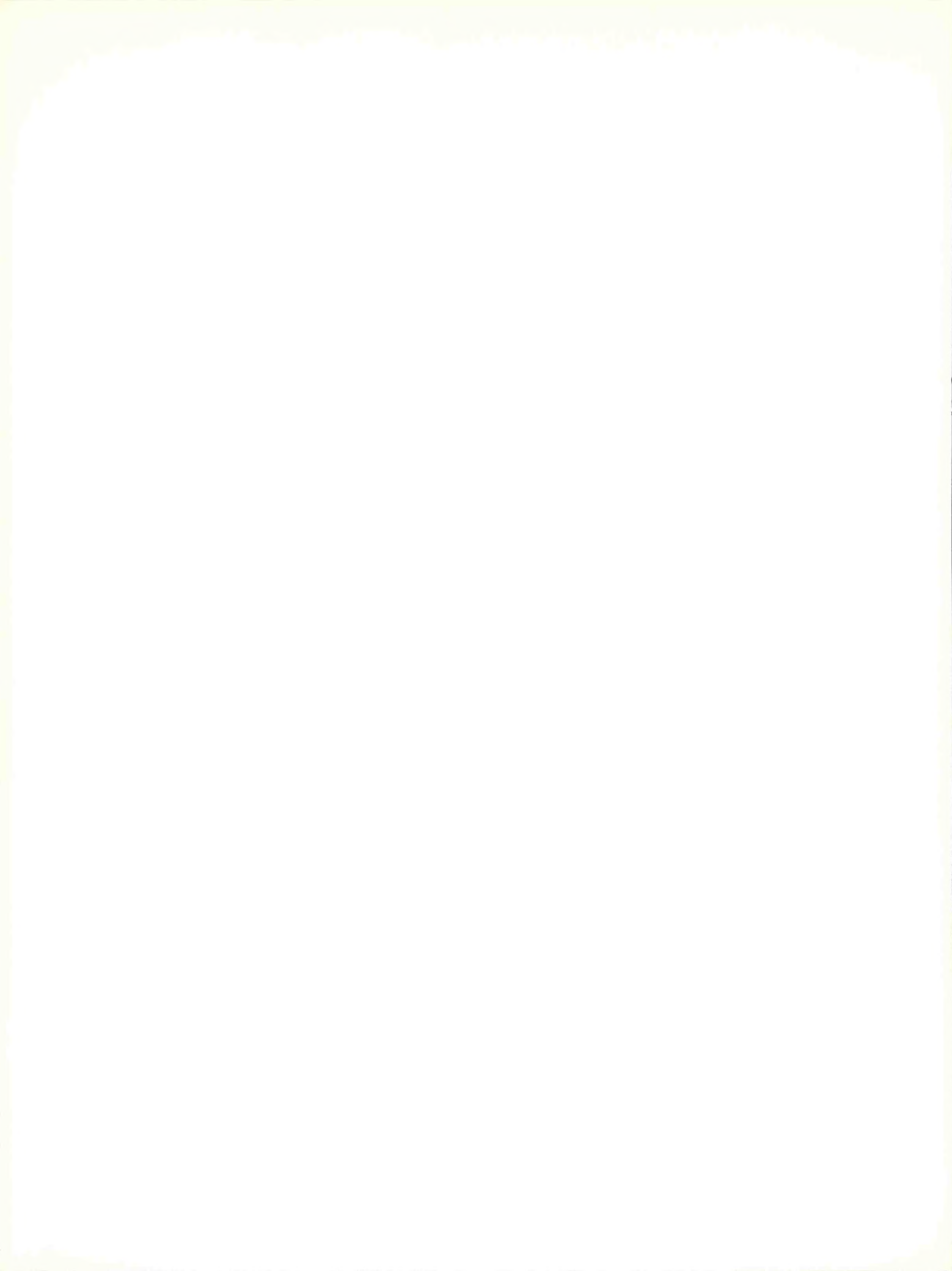
f. Observations of heat budget terms at operating cooling ponds should be used to develop models of heat rejection from these ponds.

Acknowledgements: This research was performed under an agreement between the National Oceanic and Atmospheric Administration and the Atomic Energy Commission.

References

1. Perry, H., 1974: Cool Conversion Technology, Chemical Engineering, July, 1974, 88-102.
2. Davis, G. H. and L. A. Wood, 1974: Water demands for expanding energy development, Geological Survey Circular 703, available from U. S. Geol. Surv. Nat. Center, Reston, Va. 22092.
3. Peterson, J. T., 1969: The Climate of Cities: A Survey of Recent Literature, Raleigh, N.C., Nat. Air Poll. Cont. Adm., U. S. Pub. Health Serv., 48 pp.
4. Bourne, A. G., 1964: Birth of an island, Discovery, 25(4), 16-19.
5. Taylor, R. J., S. T. Evans, N. K. King, E. T. Stephens, D. R. Packham, and R. G. Vines, 1973: Convective activity above a large scale bushfire, J. Appl. Meteorol. 12(7), 1144-1150.
6. Briggs, G. A., 1969: Plume Rise, AEC Critical Review Series, available as TID 25075 (price \$3.00) from Clearinghouse for Fed. Scient. and Tech. Inf., U. S. Dept. Comm. Springfield, Va. 22151, vi + 81 pp.
7. Hanna, S. R., 1972: Rise and condensation of large cooling tower plumes, J. Appl. Meteorol., 11(5), 793-799.
8. Weinstein, A. I., 1970: A numerical model of cumulus dynamics and microphysics, J. Atmos. Sci., 27, 246-255.
9. Gifford, F. A., 1968: An outline of theories of diffusion in the lower layers of the atmosphere," in Meteorology and Atomic Energy - 1968, D. H. Slade (ed.), USAEC Report TID-24190, 65-116.
10. Roffman, A. and R. E. Grimble, 1974: "Drift deposition rates from wet cooling systems," in Cooling Tower Environment - 1974, (see ref. 13).
11. Hanna, S. R., 1974: Fog and drift deposition from evaporative cooling towers, Nucl. Safety, 15(2), 190-196.
12. Van der Hoven, I., 1968: "Deposition of particles and gases," in Meteorology and Atomic Energy - 1968, D. H. Slade (ed.), USAEC Report TID-24190, 202-208.

13. Cooling Tower Environment - 1974, AEC Symposium Series, soon to be available as CONF-74302 (price \$13.60) from Clearinghouse for Fed. Scient. and Tech. Inf., U. S. Dept. of Com.. Springfield, Va. 22151.
14. Pell, J., 1974: "The Chalk Point cooling tower project," in Cooling Tower Environment - 1974 (see ref. 13).
15. Hanna, S. R. and S. D. Swisher, 1971: "Meteorological effects of the heat and moisture produced by man," Nucl. Safety, 12(2), 114-122.
16. Ryan, P. J., 1974: "Surface heat transfer," ch. 4 in Heat Disposal in the Water Environment (D. R. Harleman, ed.), MIT Press.
17. Arakawa, A. and W. H. Schubert, 1974: "Interaction of a cumulus cloud ensemble with the large scale environment, Part I," J. Atmos. Sci., 31(3). 674-701.
18. Briggs, G. A., 1974: "Plume rise from multiple sources," in Cooling Tower Environment - 1974 (see ref. 13).



DISCUSSIONS

A COMPARISON OF THE TRAJECTORIES OF RISING BUOYANT PLUMES WITH THEORETICAL EMPIRICAL MODELS*

In his paper on buoyant plume trajectories, Dr. Moore argues for a lumpy plume instead of a continuous plume model for plume rise and tries to show that the former is in closer agreement with observations (Moore, 1974).

He claims that the essential difference between the two-and three-dimensional model is differing exponents for the power law dependence of plume rise on the heat emission. This is not true, because the result $z \propto Q^{1/4}$ does not come about through the assumption of three-dimensionality, but through the particular assumption made about the rate at which the "puffs" or "lumps" merge and recombine. Moore (1966) assumed that the heat content of a lump increases linearly with *distance*, but no support for the assumption was given. It would seem to me more reasonable to assume that the heat content of a lump increases linearly with *rise*, i.e. with the radius. The ratio of average spacing between lumps to average lump radius would then be constant, while it gets increasingly larger in Moore's model (one wonders how such lumps could continue to "find" each other and merge). The result of this new recombining assumption is that at large distances in neutral stratification

$$z \propto Q^{1/3} x^{2/3}/U,$$

the same " $x^{2/3}$ law" predicted by the two-dimensional model.

In my opinion, the essential difference between these models is that the three-dimensional model requires an additional assumption, i.e. the recombining assumption, to predict plume rise. The resulting prediction varies according to what assumption is made.

My own preference for the two-dimensional model is based on simplicity and common observation. In coning and in stable conditions, plumes from continuous sources usually *appear* to be essentially continuous. Although a sampling of cross-sections by lidar will show that plume concentration does not decrease monotonically with distance from the source, I believe that the "naive" picture given by the human eye is essentially correct. In either theory, the plume motion is assumed to be turbulent. Since turbulence is inherently three-dimensional, the plume entrains "wisps" of outside air into itself causing the concentration to fluctuate in all three dimensions. These "wisps" are of a scale comparable to the plume radius. The two-dimensional theory assumes that they are part of the plume's "effective mass" and are not pockets of "free air" available for the plume to expand into. In the few photographs that I have seen of "lumpy" plumes, the clear spaces between the lumps were somewhat smaller than the plume radius, consistent with this point of view.

The two-dimensional theory definitely does not require a monotonic decrease in instantaneous concentration, as Moore implies; indeed, this is contrary to expectations. The theory only assumes that the *mean* motion of a plume is quasi-two-dimensional. Since the three-dimensional model gives the same asymptotic plume rise predictions as the two-dimensional, if the ratio of puff radius to puff spacing is assumed constant, the difference between these two concepts is more philosophical than practical.

The recombination assumption made by Dr. Moore leads to a slightly different prediction for the rising stage, namely $z \propto Q^{1/4} x^{3/4}/U^{3/4}$. However, $z \propto U^{-1}$ fits most data better than $z \propto U^{-3/4}$ (Briggs, 1969). This could be interpreted as support for plume rise models which predict $z \propto U^{-1}$ directly, such as the " $x^{2/3}$ law." Moore makes his puff model predict $z \propto U^{-1}$ by assuming a variable entrainment parameter depending on wind speed, arguing that the shear of ambient wind velocity with height contributes to the entrainment induced by relative velocity between the plume and its surroundings.

I would like to demonstrate, in a rough way, that this component of relative velocity has negligible effect. To do this, neglect wind direction shear and assume a nearly constant wind speed shear $\partial U/\partial z$ through the layer of plume rise. With conservation of horizontal momentum and $V \propto z^2$ or $V \propto z^3$ (for two- or three-dimensional models, respectively), we find a mean plume horizontal speed equal to the ambient wind speed at $(2/3)z$ or $(3/4)z$, respectively. Since the vertical relative velocity is just dz/dt , the ratio of downwind to vertical relative velocities is simply

$$R = \left(\frac{1}{3} \text{ or } \frac{1}{4} \right) z \frac{\partial U / \partial z}{dz / dt}.$$

From the "2/3" or "3/4" power laws of rise with x (assuming $x \doteq Ut$), $z/(dz/dt) = 3/2$ or $4/3$ times x/U , so

$$R = \left(\frac{1}{2} \text{ or } \frac{1}{3} \right) \frac{x}{U} \frac{\partial U}{\partial z}.$$

Thus, R does not depend on the magnitude of U at all, but only on the variation of $\log U$ with height. Also, $R \propto x$, so the downwind component is bound to have negligible effect at small x .

This ratio can be easily evaluated for the neutral surface layer, where it is well established that $\partial U / \partial z = u^*/kH$ (u^* is the friction velocity, and $k = 0.35$ (Businger *et al.*, 1971)). This gives $R \approx x/(H U/u^*)$. It just so happens that the distance of the maximum ground concentration is also approximately equal to $H U/u^*$, if one assumes a mean downward propagation speed of the plume of the order of u^* . Then, *at the distance of maximum ground concentration*, $R \approx 1$. However, most plume rise theorists have considered that the stage of rise in which relative velocity dominates entrainment ends at a fraction of this distance, so R is small in this stage of rise. Furthermore, considering the experimental conclusion that the "entrainment constant" is about 1/5 as large for velocity shear parallel to the plume axis as for cross-axial shear (Briggs, 1969), it would seem very unlikely that the shear of ambient wind with height could significantly affect the rate of entrainment of a bent-over plume.

The prediction of Moore's model that $z \propto Q^{1/4} x^{3/4}/U$ is so similar to the $x^{2/3}$ law that it is not possible to conclusively prove either formula superior on the basis of data from real sources. The scatter of the data is very

* MOORE D. J. (1974) *Atmospheric Environment* 8, 131-147.

large, for reasons that are well illuminated by Dr. Moore's discussion. Consequently, Q and x need to range over many orders of magnitude to clearly demonstrate a best fit to formulas differing by a factor of only $Q^{1/12}$ or $x^{1/12}$. Also, in comparing predictions with observations of diverse duration, samples per period, type of plume detection, and extraneous local effects, it is impossible to avoid some arbitrary decisions about how to weight the data or "correct" the data (Moore was forced to do this with the Northfleet observations). These decisions do affect the results, as I have shown in a recent paper that compares several different methods of weighting the same plume rise observations (Briggs, 1974).

In his discussion of Table 1, Moore emphasizes the comparative number of effective hours of observation for which $z \propto Q^{1/4}$ or $z \propto Q^{1/3}$ gives the better fit. However, in the great majority of cases the actual difference in the residual scatters about these two equations is very small. The average residual scatters, weighted by the effective hours of observation, are 11.8 and 12.0 per cent, respectively. A 0.2 per cent difference in scatter has no practical significance, and probably has no statistical significance either.

If x_T is a function of Q as suggested by Briggs (1969), this effect should not necessarily be seen in Table 1, since x somewhat exceeds the predicted values of x_T (a conservative prediction) only at Northfleet. This station is definitely subject to a terrain effect. This effect is bound to vary with the initial height of the plume, which will alter the apparent value of any exponent in a power fit to plume rise.

The values of A_0 , A_1 , $\Delta\theta_1$ and H_1 given in Moore's Section 4.3 are puzzling, for how could any real "optimization" of the four parameters describing the neutral component of x_T be achieved when the actual distances of plume rise observation fall considerably short of this distance? Considering the scatter in the plume rise data and considering that the calculated deviation from the simple $z \propto x^{3/4}$ relationship is no more than 10 or 15 per cent at the very greatest observation distances for the neutral category, optimization of A_0 and A_1 to 3 significant digits hardly seems possible. One does wonder what specific technique was used to choose these parameters; surely this display of accuracy is misleading.

The values of \bar{Z}/\bar{Z}_c given in Table 2 show no obvious trend with distance, as long as the first distance category is ignored. If it is not, a smaller exponent than 3/4 would give a better fit to $z \propto x^e$. The author claims that the high average values of \bar{Z}/\bar{Z}_c for $x < 400$ m "is almost certainly due to the effect of efflux velocity," but this is not an adequate explanation. Referring to the author's own theoretical development we can integrate equation (4) of Moore's 1966 paper using either $V \propto z^2$ or $V \propto z^3$ (for two- or three-dimensional plume growth, respectively). We then find the buoyant plume rise augmented by a momentum enhancement factor

$$\left| 1 + 2 \frac{F_m U}{F_x} \right|^a,$$

where F_m is the initial momentum flux, F is the buoyancy flux (for most sources, $F \propto Q$) and $a = 1/3$ or $1/4$, depending on the type of growth assumed. The quantity F_m/F is equal to the efflux velocity divided by gravity and the relative density difference between the effluent and the ambient. It is relatively independent of plant size, and averages less than 4 s. Using $F_m/F = 4$ s, $a = 1/3$, $U = \bar{U}^*$ and $x = \bar{x}^*$, we conclude that *at most* the increase in rise due to efflux velocity is 5.1 per cent in the $x < 400$ m category and 1.4 per cent in the $x > 2000$ m category. Thus, this explanation can account for no more than 4 per cent of the increase in \bar{Z}/\bar{Z}_c observed for $x < 400$ m.

A more likely explanation for such irregularities in \bar{Z}/\bar{Z}_c is the shift in source weighting with different ranges of stability and distance. Table 4 shows that values of \bar{Z}/\bar{Z}_c (with fixed A) can range over a factor of 3 for different data sources and stability classes, and also that the effective number of observations in some stability classes come mostly from just one or two sources. Although it is not shown, a similar situation probably exists for the different distance categories, particularly since near-in plume rises were not measured in some experiments and some experiments did not go as far downwind as others. For instance, the $x > 2000$ m category is likely dominated by Northfleet data. This makes it very difficult to specify the best fit exponent to $z \propto x^e$.

The basic shortcoming of the approach suggested by Dr. Moore is that it is unnecessarily complicated. While it is partly based on sound physical ideas, several empiricisms have been introduced without adequate theoretical support (for instance, an entrainment parameter that is proportional to a power of the wind speed, and a plume rise correction factor based only on the source height). These kind of empirical assumptions may be expedient, but they make extrapolation of the results less certain. While I agree that refinement of simple plume rise prediction equations will not improve the fit with real data, I do not agree that the suggested equations are the most pessimistic or (especially at the same time) the most realistic, particularly in the case of extrapolation to small sources.

In my opinion the " $x^{2/3}$ law" has been proven reliable over a much greater range of source sizes (Briggs, 1972):

$$\begin{aligned} \Delta h &= 1.6 F^{1/3} U^{-1} x^{2/3} \\ &= 3.3 Q^{1/3} U^{-1} x^{2/3}. \end{aligned}$$

(For sources where mean molecular weight or latent heat do not contribute significantly to the buoyancy (most hot sources), the buoyancy parameter $F = 8.9 Q$ in mks units, if Q is in MW.) A good estimate of final rise can be obtained simply by terminating this rise at

$$x = x_T = \text{Minimum } \{A_2 U / \Delta\theta^{1/2}, 2.0 H \log_{10}(1.6 h/z_0)\}.$$

The notation is the same as Moore's except that z_0 is an average roughness length for the surrounding terrain (about 1 m in cities and forests, 0.3 m in mixed open and covered terrain, 0.1 m in open, tall grassland, and 0.01 m or less on flat, arid land nearly devoid of vegetation). I have suggested $A_2 = 130$ as optimum (Briggs, 1969), which is very close to Moore's optimized value for the $x^{3/4}$ relationship. Briggs (1972) cites a number of recent experiments which support this formulation for final rise in stable conditions. Some of these suggest smaller values of A_2 ; a fairly conservative value is $A_2 = 100$.

In neutral conditions, it is still quite difficult to say anything conclusive about x_T . This is due to the lack of observations at distances clearly greater than x_T , as close scrutiny of the data will show. The above suggestion for x_T is based on a fraction of the estimated distance of maximum ground concentration, namely, $x_T \approx 0.3 H(U/u^*)$. This is intuitively satisfactory and gives the same prediction for the maximum ground concentration at the "critical wind speed" as several other approaches (Briggs, 1968). These predictions are consistent with observed maximum concentrations (Briggs, 1965) and suggest required stack heights proportional to $Q^{0.4}$, which is quite

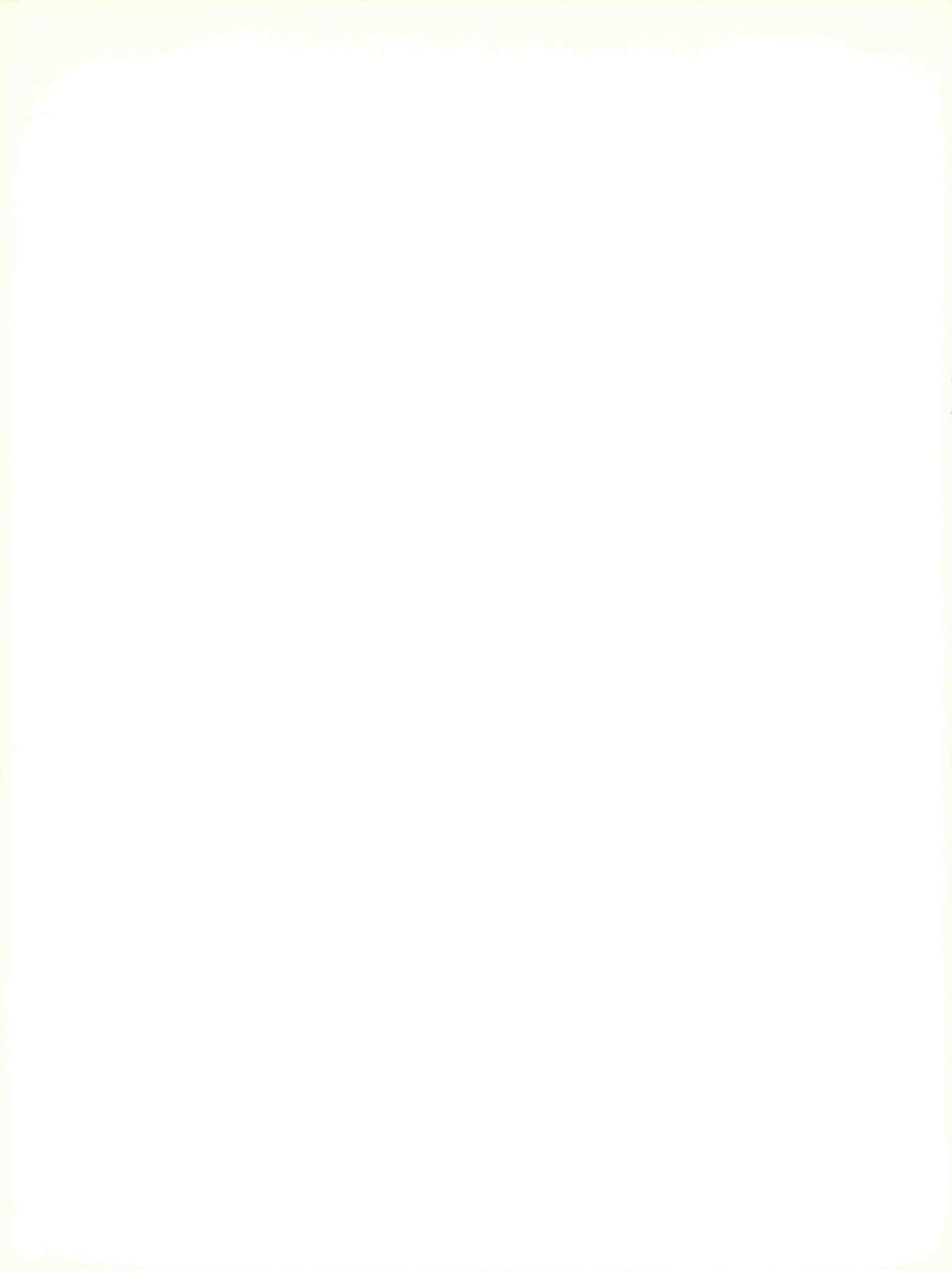
consistent with past experience (Briggs, 1968; Moore, 1968). The estimate of U/u^* is based on the logarithmic variation of U with height in neutral conditions applied at the plume height at critical wind speed ($H = 1.6 h$). An alternative formulation for neutral conditions that is simpler to compute is $x_T \approx 0.5 h(U/u^*) \doteq 3.5 h \log_{10}(2 h/z_0)$. This gives the same prediction for maximum ground concentration at the critical wind speed (at which $H = 2 h$ in this case), but probably gives too low a rise at lower wind speeds. However, it is more generally applicable than my earlier suggestion that $x_T = 10 h$ (Briggs, 1969) which did not account for the effects of ground roughness on ambient turbulence intensity at plume height.

*Atmospheric Turbulence and
Diffusion Laboratory,
NOAA, Oak Ridge, Tennessee 37830, U.S.A.*

G. A. BRIGGS

REFERENCES

- Briggs G. A. (1965) A plume rise model compared with observations. *J. Air. Pollut. Control Ass.* **15**, 433-438.
Briggs G. A. (1968) Contribution to the round table discussion on plume rise and dispersion. *Atmospheric Environment* **2**, 228-232.
Briggs G. A. (1969) *Plume rise*. TID 25075, Clearinghouse for Federal Scientific and Technical Information, Springfield, Va.
Briggs G. A. (1972) Discussion of: Chimney plumes in neutral and stable surroundings. *Atmospheric Environment* **6**, 507-510.
Briggs G. A. (1974) Plume rise from multiple sources. *Proceedings of Cooling Tower Environment—1974 Symposium*, University of Maryland.
Businger J. A., Wyngaard J. C., Izumi Y. and Bradley E. F. (1971) Flux-profile relationships in the atmospheric surface layer. *J. Atmos. Sci.* **28**, 181-189.
Moore D. J. (1968) Contribution to the round table discussion on plume rise and dispersion. *Atmospheric Environment* **2**, 247-250.
Moore D. J. (1974) A comparison of the trajectories of rising buoyant plumes with theoretical empirical models. *Atmospheric Environment* **8**, 131-147.



Description of the Eastern Tennessee Trajectory
Experiment (ETTEX)

December 1974

S. R. Hanna, C. J. Nappo, R. P. Hosker, and G. A. Briggs
Air Resources
Atmospheric Turbulence and Diffusion Laboratory
National Oceanic and Atmospheric Administration
Oak Ridge, Tennessee

(Presented orally at the First AMS Conference on Regional and Mesoscale
Modeling, Analysis, and Prediction, Las Vegas, Nevada, May 6-9, 1975.)

Description of the Eastern Tennessee Trajectory
Experiment (ETTEX)

S. R. Hanna, C. J. Nappo, R. P. Hosker, and G. A. Briggs
ARATDL, NOAA, Oak Ridge, Tennessee

Abstract

The eastern Tennessee trajectory experiment was conducted during July and August, 1974. Its primary purpose was to measure certain aspects of mesoscale transport and diffusion over rather complex terrain. The trajectories of radar-tracked tetroons were determined for several different launch times under a variety of weather conditions. These results are to be compared with trajectories computed using vertical wind profiles and surface measurements obtained concurrently over a grid of five single-theodolite pibal stations. Observed relative diffusion of tetroon pairs will be used in refining prediction techniques based on diffusion theory.

In addition, the aerial and ground level SO₂ concentrations due to convective afternoon conditions were studied. Helicopter traverses of the plume from a tall stack were used to determine SO₂ distribution within the plume. Concurrent vertical profiles of eddy dissipation rate and temperature and vertical velocities induced by convection in the mixing layer were obtained with an instrumented airplane. Frequent double-theodolite pibal ascents provided vertical wind profiles. These results will be used in an effort to predict ground-level effluent concentrations in convective conditions.

This report describes the overall design of the experiment and the schedule of its execution. More complete analyses will appear in subsequent reports.

I. Introduction

Knowledge of atmospheric transport and diffusion over distances of 10 to 100 km (the so-called "mesoscale") is quite deficient, particularly with regard to observational data. Yet such information is essential for reliable estimation of air parcel trajectories and air pollutant concentrations over mesoscale distances. Our Atmospheric Turbulence and Diffusion Laboratory (ATDL), for example, is currently attempting to estimate regional transport and diffusion from nuclear reactors and fossil fuel power plants located along the Tennessee River valley, from lead smelters in Missouri, and from a proposed power park in Louisiana. At present, only rather crude guesses can be made about the probable air motions and diffusion coefficients over these regions.

Most previous workers have not attempted to observe simultaneously a three-dimensional mesoscale wind field and its resultant air parcel trajectories and relative diffusion. For example, wind observations have been made by Bornstein (1968) and by Ackerman (1973, 1974) near urban areas, by Wendell (1970, 1972) over open country, and by Egami, et al. (1974) and Kao, et al. (1974) over fairly rough terrain. These experiments obtained the wind field either from surface stations or from pilot balloon ("pibal") ascents; air parcel trajectories were not explicitly measured. Over flat terrain it may be possible to construct fairly realistic trajectories from limited measurements of the regional wind field (e.g., Wendell, 1970, 1972), but it has not yet been demonstrated that such a technique is feasible over rough terrain. Similarly, observations of the trajectories of "tagged" air parcels have been reported by numerous authors including Angell, et al. (1971, 1973), Hall, et al. (1973), Leahey and Hicklin (1973), and Leahey and Rowe (1974). In almost all cases the three-dimensional wind field was not determined; hence models cannot be constructed to reliably predict these trajectories.

The Eastern Tennessee Trajectory Experiment (ETTEX) described below represents an attempt to simultaneously obtain all of the meteorological parameters required to develop techniques for prediction of atmospheric transport and diffusion over the fairly rugged terrain of the eastern Tennessee River valley. A separate experiment to investigate convective fumigation from tall stacks was carried out concurrently; this effort was conducted near the Tennessee Valley Authority (TVA)'s Bull Run steam plant, near Oak Ridge. The data from these studies are intended to be complementary.

2. Experimental Design and Procedure.

Our experiments were centered about Oak Ridge, Tennessee, located some 30 km west of Knoxville, within the great valley which separates the Cumberland mountains and plateau on the northwest and west and the Great Smoky mountains on the southeast (Figure 1). This valley is about 100 km wide in our area. Elevations above the valley floor are up to 850 m within the Cumberland chain, and as much as 1800 m within the Great Smokies. Both mountain ranges run roughly southwest to northeast. The valley between them is corrugated by broken ridges rising 75 m to 100 m above the floor; these ridges are oriented parallel to each other and to the mountains. The ridge spacing is typically 2 or 3 km. This topography has been found (U.S. Weather Bureau, 1953) to influence our local climate; in particular, the surface winds are often parallel to the ridge-valley structure, suggesting a strong channeling effect.

During the period of July 15-August 8, 1974, three more or less independent mesoscale experiments were conducted over this region.

2.1 Trajectory experiment.

The ultimate objective of our interest in mesoscale trajectories is the development of a realistic predictive trajectory model to be used for estimates of transport and diffusion over large distances and over non-ideal terrain. The technique presently contemplated is similar to that discussed by Heffter (1973), using vertically averaged winds within a layer, weighted according to distance from the air parcel of interest, to predict the path of that air parcel within that layer of the atmosphere. Vertical wind profiles, to be used as input data, must therefore be obtained from several stations scattered over the locale of interest. Validation of the model developed using this information requires a comparison of the predicted air parcel trajectories to those observed by following a "tagged" parcel-- e.g., a radar-tracked constant-level tetrahedral balloon ("tetroon").

To provide such data, a network of pibal stations was set up, (Figure 2), roughly centered about a radar unit loaned by NOAA's ARL Field Laboratory of Idaho Falls. Each station's wind profile was envisioned as being, for computational purposes, more or less representative of the winds within a 50 km radius of that station. The station locations were chosen to provide a degree of overlap of these representative regions, while covering fairly completely the area encompassed by the maximum range of the radar (about 100 km). Interpolation to any point within the radar range should thus be feasible.

The central pibal station was located in an open field to the southwest of Oak Ridge, about 3.5 km from Oak Ridge National Laboratory

(ORNL). The other pibal stations were located at airports to insure relatively open fetches and ease of access. Each station was equipped with a single optical theodolite, a Thorntwaite low-threshold anemometer for "surface" (i.e. 2 m) wind speed, and a standard shelter for temperature and humidity instrumentation (Figure 3). Surface wind direction was obtained from Thorntwaite low-threshold vanes at all stations but Crossville, where the FAA Flight Service Office records surface winds. Observations of the ascent of 30 gm pibals were made at 30 second intervals after launch for a period of 10 minutes. Half-hourly launches were made at each site during the "transition" periods of the day (i.e., sunrise, sunset), with hourly launches at other times.

The M-33 precision tracking radar (Figure 4) was placed near the summit (1030 m, MSL; about 750 m above the valley floor) of Buffalo Mountain, a peak in the Cumberland range about 15 km northwest of Oak Ridge. A road maintained by the Oliver Springs Mining Company leads to the mountain top. Commercial power (440v., 3Ø) was installed at the radar site so that generators were not required.

The tetroons and tracking technique used are similar to those described by Moses, et al. (1968). The balloon is a tetrahedron of about 1 m^3 volume, constructed of DuPont Mylar (Figure 5). The physical characteristics of this envelope are such that the tetroon volume is virtually constant for superpressurization of less than 70 mb or so. This type of balloon thus floats, in the absence of vertical air motions, along isopynic surfaces. The inflation and launch procedures required to attain a particular flight altitude have been recently summarized by

Hoecker (1974). A tetroon is tracked by means of a radar-triggered transponder carried beneath the balloon (Figure 5). The radar signal actuates this transponder, which then emits a slightly tuneable 403 MHz signal, indicating that the radar unit's transmitting antenna is pointed more or less toward the transponder. As the broadcast power (and hence the radar beam width) is slowly reduced, the transmitting antenna must be pointed more and more accurately toward the transponder in order to trigger it. It is by this method that the transponder location may be ultimately determined to within about 20 m. A number of other experimenters have developed and used this same radar-tetroon-transponder system (eg., Pack, 1962; Angell et al., 1968).

During our experiments, tetroons were launched from the ATDL offices, from our central pibal site near ORNL, from the Bull Run steam plant, or from the Oak Ridge municipal water treatment plant (on a ridge just above ATDL), depending on the prevailing wind direction and the specific purpose of the individual experiment. Most of these launches were made by W. H. Hoecker of ARL, Silver Spring, Md. Radiosondes to provide the vertical temperature profile required for tetroon inflation and for subsequent meteorological information were launched from the first three of these sites. Because local topography frequently obscured the transponders from the radar signal before launch, it was found advisable to first carry each transponder aloft with a tethered 100 gm pibal, so that transponder operation could be checked just before launching the tetroons. This also permitted adjustment of the transponders to be used in any given experiment to slightly different frequencies, thus allowing the radar to

easily distinguish among the balloons.

In our trajectory experiments, three tetroons were released sequentially at 15 minute intervals. Flight altitudes were found to range between 300 m and 1000 m above the ground. At the radar, the receiver was tuned to the frequency of one of the transponders, and the range, elevation angle, and azimuth angle of that transponder were read and manually recorded. The receiver was then tuned to another frequency, and the process repeated. Readings were taken once each minute, so that the interval between successive observations of any given tetroon was typically three minutes. An automatic plotboard provided a visual indication of the location of the balloons.

We had originally planned to follow the tetroons for 12 hour periods covering both night and day. Lack of personnel forced us to cut the experiments to 6 hours in duration, but we were nevertheless able to obtain measurements during most times of the day (sunrise, mid-day, sunset, and mid-night). Most of the tetroons never wandered very far from the center of our observational grid; the light winds experienced during most of these experiments are quite characteristic of eastern Tennessee in summertime (U. S. Weather Bureau, 1953). As expected, most of the tetroons travelled along a SW-NE axis, roughly parallel to the local ridge-valley structure described above. A few tetroons were prematurely lost because of transponder malfunctions, topographic interference, and rain. A total of seven trajectory experiments was completed.

2.2 Convective Diffusion Experiment.

It is believed that, on convective summer afternoons, downdrafts may bring the effluent from most stacks quickly to the ground, with

relatively high surface concentrations of effluent resulting. To study this phenomenon, concentrations of SO_2 in the plume and at the ground were determined together with the associated meteorological conditions near the TVA's Bull Run steam plant (244 m stack),

Cross-sections of the elevated plume were obtained during helicopter traverses using a specially-designed SO_2 sensor loaned and operated by the Kennecott Copper Corporation (Figure 6). Surface SO_2 measurements were made by the West-Gaeke method at four roving stations at distances out to 4 km from the stack. Vertical temperature gradients and eddy dissipation rates were measured near the plume from an airplane equipped with an aspirated thermistor and an MRI Universal Indicated Turbulence Meter borrowed from the TVA (Figure 7). The airplane, a Cessna 172, also carried a vertical accelerometer for a crude measure of convective scale vertical velocities in the mixing layer. Since indicated air speed was also recorded, the vertical acceleration can be corrected for the plane's response to horizontal gusts. Data were recorded on a Teac R-70 4 channel cassette tape recorder. Vertical temperature and humidity profiles were also determined by radiosondes. Mixing heights were detected by the ATDL lidar and by acoustic sounders located at Kingston (unit loaned by the TVA) and at our pibal station southwest of ORNL (unit loaned by the Savannah River Laboratory). Tetroons pairs were simultaneously released near the steam plant (Figure 8); radar tracking provided information on the wind velocity and vertical velocities in the mixing layer. Vertical wind profiles were obtained from double-theodolite pibal ascents near the Bull Run site.

A total of five experiments, each lasting from roughly 1 p.m. to 4 or 5 p. m. (EDT), was completed. It was found that the point of initial

plume contact with the ground frequently missed the network of roving surface SO₂ stations; this was primarily due to the large, erratic fluctuations in wind direction (and hence plume path) experienced during these afternoon runs with low wind speed. Most other aspects of this experiment were satisfactory, however.

2.3. Relative Diffusion Experiment.

On each of the days that a smoke plume experiment was carried out, and on several other days, tetroon pairs were released simultaneously and tracked by the radar for times up to two hours, and distances up to 40 km from the launch site. It is planned to relate the measured relative displacement of each tetroon pair to theoretical diffusion calculations based on the observed wind and temperature gradients and turbulence in the atmospheric boundary layer. These tetroon launches were made from either the ATDL offices or from the Bull Run site. Vertical wind profiles were obtained from either half-hourly double theodolite or rapid sequence (launches every 15 minutes; readings every 30 seconds for 10 minutes) single theodolite pibal observations. Radiosonde ascents were completed during all but one of these experiments. In many cases, data such as eddy dissipation rate and vertical temperature profile were also available from the airplane measurements associated with the smoke plume study. A total of nine relative diffusion experiments was completed, most of these between noon and 4 p.m. (EDT).

3. Schedule of Experiments.

As indicated above, seven trajectory experiments, five convective diffusion experiments, and nine relative diffusion experiments were

completed. Table 1 summarizes the dates and times, experiment types, and meteorological information available for each run.

4. Schedule of Analysis

Many of the data are still in raw form. Computer programs to analyze the pibal, radiosonde, and tetroon data were obtained from ARL's Field Laboratory in Idaho Falls, and are being modified to suit our needs. The chemical analysis required for the surface SO_2 measurements was performed by the Analytical Chemistry Division of ORNL. The airborne measurements of SO_2 concentrations, eddy dissipation rates, vertical accelerations, and vertical temperature profiles are being reduced by hand and by analogue computer. A tentative schedule for the various stages of the analyses is given in Table 2.

Additional meteorological data for the experimental period have been obtained from the TVA and the National Weather Service (NWS). These include "surface" wind, temperature, and humidity information from TVA sites at the Bull Run, Kingston, Watts Bar, and John Sevier steam plants, and from the Clinch River Breeder Reactor (LMFBR) site near Oak Ridge. Hourly SO_2 concentrations from TVA monitors near these plants were also provided, together with data on coal quantity and sulfur content to permit source strength assessment. NWS data on winds and temperature aloft at all reporting stations surrounding eastern Tennessee were procured from the National Climatic Center in Asheville, N. C. . Synoptic maps were also obtained.

TABLE 1.
SUMMARY OF ETTEX EXPERIMENTS, JULY-AUGUST, 1974.

Date (1974)	Approx. Time (EDT)	Experiments Conducted*	Tetroons; Launch Site	Pibal Obs.**; Launch Sites	Radiosondes; Launch Site	Aircraft Measurements***	Ground SO ₂	Acoustic Sounder Site
7/15	1000-1600	"TRJ"	—	ST; All Sites	—	—	—	0800
7/16	1000-1400	TRJ	1; 0800	ST; All Sites	—	—	—	0800
7/17	1000-1600	TRJ	3; ATDL	ST; All Sites	—	T, E	—	0800
7/18	1600-2100	TRJ; GS	3; ATDL	ST; All Sites	—	—	2 Samplers	0800; Kingstor
7/19	1600-2130	TRJ	3; 0800	ST; All Sites	—	—	—	0800; Kingstor
7/22	1000-1510	RD	2; ATDL 2; ATDL	DT; 0800	—	—	—	0800; Kingstor
7/25	1200-1700	RD; CD; GS	2; Bull Run 2; Bull Run	DT; Bull Run	5; Bull Run	T, E, SO ₂	5 Samplers	0800
7/26	1500-1640	RD	2; ATDL	ST; ATDL (rapid)	1; ATDL	—	—	0800
7/27	1200-1600	RD	2; Bull Run 2; Bull Run	DT; Bull Run	4; Bull Run	T, E	—	0800
7/29	1200-1540	RD; GS	2; ATDL 2; ATDL	ST; ATDL (rapid)	2; ATDL	—	2 Samplers	0800
7/30	1100-1430	RD; GS	2; ATDL 2; ATDL	ST; ATDL (rapid)	1; ATDL	—	2 Samplers	0800
7/31	1300-1700	RD; CD; GS	2; ATDL 2; ATDL	DT; Bull Run	4; ATDL	T, E, SO ₂	5 Samplers	0800
8/1	1300-1620	RD; CD; GS	2; ATDL 2; ATDL	DT; Bull Run	5; ATDL	T, E, SO ₂	5 Samplers	0800
8/2	1300-1630	RD; CD; GS	2; Bull Run 2; Bull Run	DT; Bull Run	4; ATDL	T, E, SO ₂	4 Samplers	0800
8/5	1130-1600	CD; GS	—	DT; Bull Run	4; 0800	T, E, SO ₂	3 Samplers	0800
8/6	0400-1000	TRJ; GS	3; 0800	ST; All Sites but Crossville	6; 0800	—	1 Sampler	0800
8/7	0400-1000	TRJ	3; O. R. Water Works	ST; All Sites	7; 0800	—	—	0800
8/8	0400-0830 (rain)	TRJ; GS	3; Water Works 2; ATDL	ST; All Sites	5; 0800	—	1 Sampler	0800

*TRJ = Trajectory, CD = Convective Diffusion, RD = Relative Diffusion, GS = Ground SO₂

**ST or DT = Single or Double Theodolite

***T = Temperature Profile, E = Eddy Dissipation Rate, SO₂ = Plume SO₂ Concentration

TABLE 2
Analysis schedule for ETTEX and related data.

Experiments	ATDL Personnel	Tentative Reporting Date
Wind field	Nappo, Pollock	May 1975
Trajectories	Hanna, Nappo, Hosker, Pollock	December 1975
Relative diffusion	Hanna, Pollock	May 1975
Convective diffusion	Briggs, Pollock	June 1975

5. Acknowledgements

The people who assisted this study are legion, and it is unfortunately impossible to thank them all by name. However, the experiment would have been impossible without the aid of the following persons. We are particularly grateful to C. R. Dickson of the A.R.L. Field Office in Idaho Falls for providing the M-33 radar unit and the men to set it up and maintain it. G. White and D. Forsythe of Idaho Falls were in charge of the radar's operation. Dickson also loaned us his mobile radiosonde unit, an enormous collection of routine but essential equipment, and assisted us in procuring a long list of expendable items.

The Coal Creek Mining and Manufacturing Corporation and the Oliver Springs Mining Company (specifically, C. H. Smith and C. Owens) were very cooperative in helping us select and travel to and from the radar site.

We thank the managers of the following airports for allowing us to use their facilities for our pibal observations: Crossville Municipal (E. Donnelly), McMinn County (J. Scruggs), New Tazewell (W. Coffee), and Sevierville (P. Roberts).

The Tennessee Valley Authority permitted us to use their Bull Run and Kingston steam plants for portions of the study. T. L. Montgomery and J. H. Coleman of the TVA's Air Quality Branch loaned several crucial pieces of equipment.

S. Taylor of Kennecott Copper Corporation of Utah traveled here to operate his sensitive SO₂ sampler during the convective diffusion experiments. W. H. Hoecker of ARL's Silver Spring, Md. office supervised the inflation and launching of our tetroons. D. R. Matt of ATDL and A. W. Andren and his associates of ORNL's Environmental Sciences Division carried out the design and operation of the surface SO₂ monitors. J. Schubert of the Savannah River Laboratory (SRL) loaned and set up an acoustic sounder; M. Pendergast of the same laboratory provided data collected from SRL's instrumented TV tower during a "fly-by" of our airplane in order to calibrate the indicated turbulence meter.

Finally, thanks are certainly due to our regular staff, to our summer research assistants from Oak Ridge Associated Universities and to our part-time student employees for their good-natured acceptance of long working hours at unusual times of the day and night. Without their efforts, these experiments could never have been carried out.

This research was performed under an agreement between the National Oceanic and Atmospheric Administration and the U. S. Atomic Energy Commission.

6. References.

- Ackerman, B., 1973: The airflow program in Metromex, in Summary Report of Metromex Studies, 1971-1972, ed. by F. A. Huff, Rept. of Invest. 74, State of Illinois, p 113-124.
- _____, 1974: Wind profiles and their variability in the planetary boundary layer, in preprints of AMS Symposium on Atmospheric Diffusion and Air Pollution, Santa Barbara, Cal., Sept. 9-13, p 19-22.
- Angell, J. K., D. H. Pack, and C. R. Dickson, 1968: A Lagrangian study of helical circulations in the planetary boundary layer, J. Atmos. Sci. 25 (5), 707-717.
- _____, P. W. Allen, and E. A. Jessup, 1971: Mesoscale relative diffusion estimates from tetroon flights, J. Appl. Meteorol. 10 (1), 43-46.
- _____, W. H. Hoecker, C. R. Dickson, and D. H. Pack, 1973: Urban influence on a strong daytime air flow as determined from tetroon flights, J. Appl. Meteorol. 12 (6), 924-936.
- Bornstein, R. D., 1968: Observations of the urban heat island effect in New York City, J. Appl. Meteorol. 7(), 575-582.
- Egami, R. T., V. Sharma, and R. L. Steele, 1974: Diffusion study in the vicinity of Mohave Generating Plant, in preprints of AMS Symposium on Atmospheric Diffusion and Air Pollution, Santa Barbara, Cal., Sept. 9-13, p 209-213.
- Hass, W. A., W. H. Hoecker, D. H. Pack, and J. K. Angell, 1967: Analysis of low-level constant volume balloon (tetroon) flights over New York City, Quart. J. Roy. Meteorol. Soc. 93, 483-493.
- Heffter, J. L., 1973: Atmospheric Transport and Dispersion of Pollutants and Related Meteorological Studies, Trajectory Programs, July 1971-June 1972, ed. by R. J. List, NOAA Tech. Memo. ERL-ARL-40, p 21-46.
- Hoecker, W. H., 1974: A universal simplified procedure for weighing off small constant-volume balloons for low-level flight, and for estimating vertical air speeds from vertical balloon speeds, submitted to J. Appl. Meteorol.

Kao, S. K., H. N. Lee, and K. I. Smidy, 1974: A preliminary analysis of the effect of mountain-valley terrains on turbulence and diffusion, in preprints of AMS Symposium on Atmospheric Diffusion and Air Pollution, Santa Barbara, Cal., Sept. 9-13, p 59-63.

Leahy, D. M., and H. S. Hicklin, 1973: Tetroon studies of diffusion potential in the airshed surrounding the Crowsnest Pass area, Atmosphere 11(3), 77-87.

_____, and R. D. Rowe, 1974: Observational studies of atmospheric diffusion processes over irregular terrain, paper 74-67, 67th Air Pollution Control Assoc. (APCA) Annual Meeting, Denver, Col., June 9-13.

Moses, H., E. Robinson, M. E. Smith, G. C. Gill, E. M. Wilkins, and C. R. Dickson, 1968: Meteorological instruments for use in the atomic energy industry, ch. 6-12 of Meteorology and Atomic Energy, ed. by D. H. Slade, TID-24190, p 298-300.

Pack, D. H., 1962: Air trajectories and turbulence statistics from weather radar using tetroons and radar transponders, Mon. Wea. Rev. 90(12), 491-506.

U. S. Weather Bureau, 1953: A Meteorological Survey of the Oak Ridge Area: Final Report Covering the Period 1948-52, USAEC Rpt. ORO-99, Oak Ridge, Tenn.

Wendell, L. L., 1970: A preliminary examination of mesoscale wind fields and transport determined from a network of wind towers, NOAA Tech. Memo. ERL-ARL-25.

_____, 1972: Mesoscale wind fields and transport estimates determined from a network of wind towers, Mon. Wea. Rev. 100(7), 565-578.

Appendix

One piece of equipment used during ETTEX is unique enough, we believe, to merit a separate description. This item is a battery-powered, variable time interval pilot balloon observation timer designed by D. H. Turner of ATDL for use at remote field sites. It is unusual in its use of a regulated power supply and an integrated circuit timer to provide a combination of good accuracy and low battery drain.

The circuit is shown in Figure 9a. Power is supplied by 5 "D" cell batteries. The supply voltage is maintained at 5.10 volts by IC-1, a μ A723C precision voltage regulator. This stabilized power is then supplied to the heart of the system, IC-2, a Signetics 555 timer and its associated RC network. At the end of the switch-selected (and adjustable) time interval of 30 or 60 seconds, the timer switches on transistor Q1 to activate a Mallory "Sonalert," which emits a continuous tone for five seconds. The pilot balloon observation is made when the Sonalert shuts off. A battery check is provided by a pushbutton which applies full battery voltage to a 110Ω load resistor and to the Sonalert through Z1; zener Z1 provides a lower threshold (battery voltage \approx 7.0 volts) below which the Sonalert is not energized. The absence of the tone thus denotes the need for a battery change. This threshold voltage is still in excess of the minimum requirements of IC1 and IC2, so that accurate operation of the device is insured at least until a battery change is indicated. Diode D1 serves to block current from the load resistor during normal, timer-triggered operation of the Sonalert, thus minimizing battery drain. The operating circuit requires only about 4 ma until the Sonalert is activated, when the

current jumps to about 8 ma. This drain is small enough that several work-weeks of operation are obtained from a single set of batteries.

All resistors are 1% wire-wound or metal film high-stability types (unless otherwise indicated). The solid-state components are all mounted in sockets to facilitate servicing. The circuit and batteries are housed in a metal box 23cm L x 13cm D x 15cm H for protection (Figure 9b). The power switch, time-interval selector, and battery check button are front-panel mounted, as are the Sonalert and its volume control. Five such units were used extensively in the field during July-August, 1974, and were found to be quite rugged and reliable.

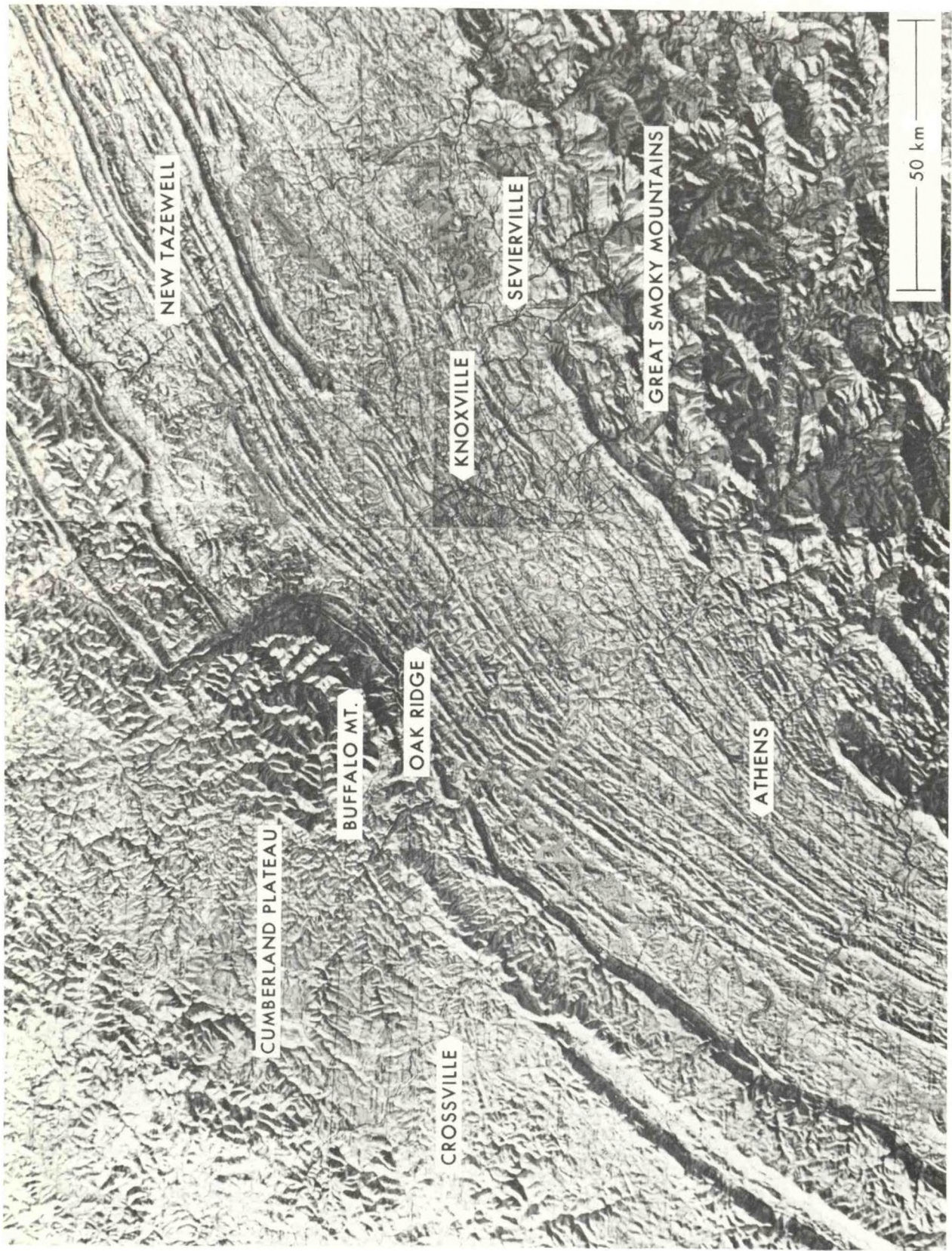


FIGURE 1 Topography of Eastern Tennessee, Vicinity of Oak Ridge.

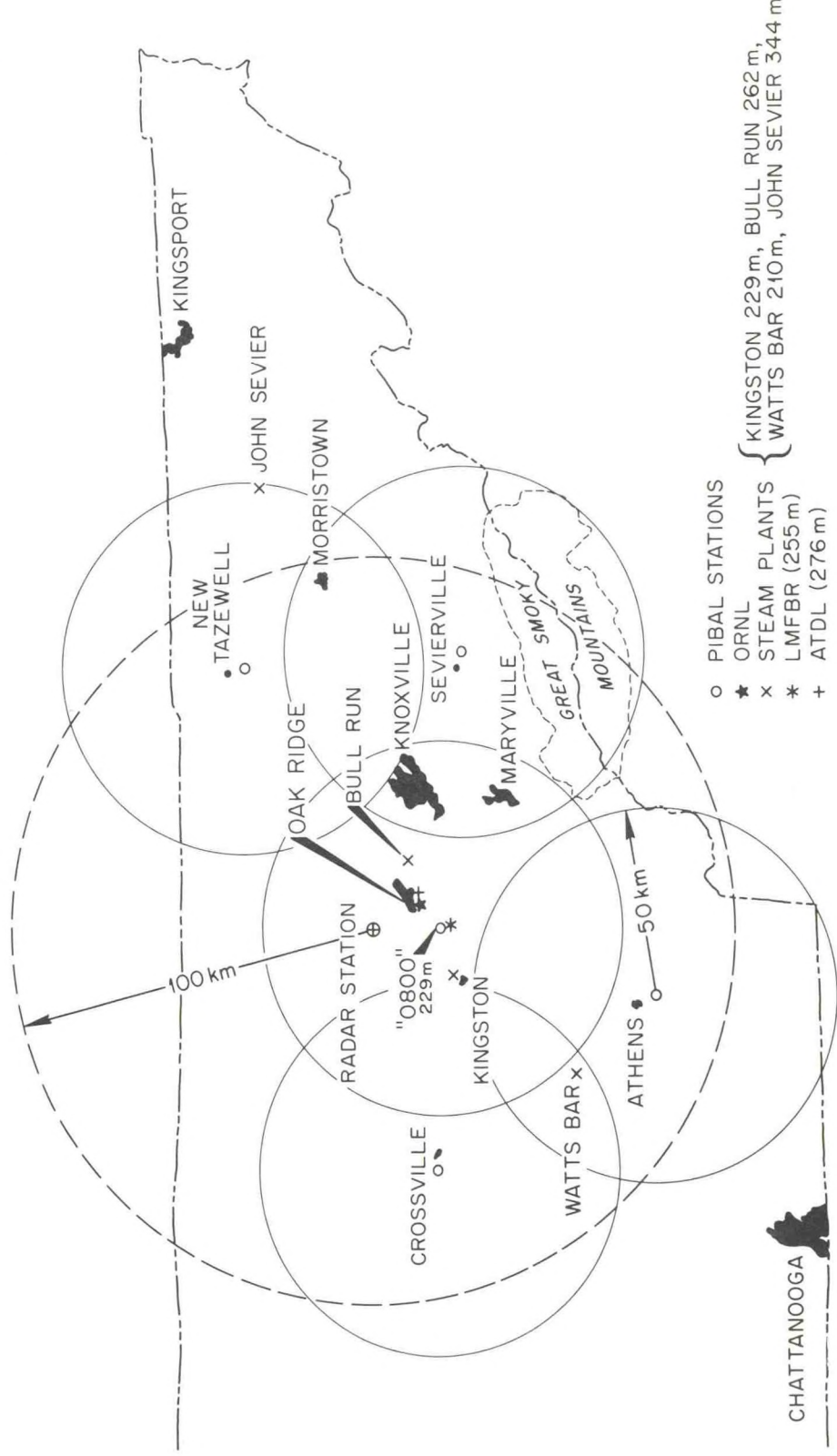


FIGURE 2
ETTEX Map, Indicating Locations, Elevations (MSL), and Effective Observing Ranges of Radar Unit and Pibal Stations. Tetroon Launch Sites are also Shown.

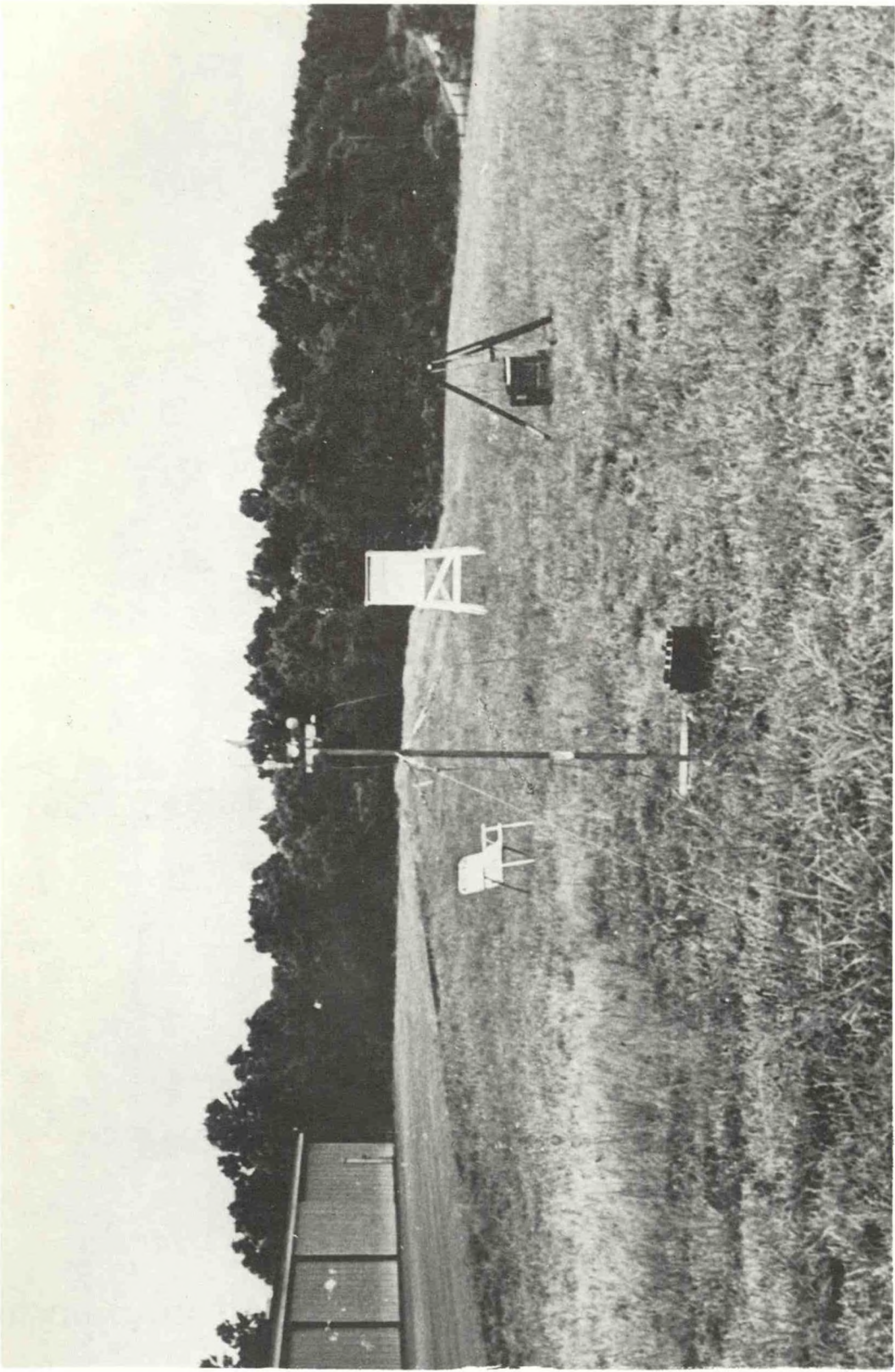


FIGURE 3
Typical Pilot Balloon Site, with Low-Threshold Anemometer and
Vane, Single Optical Theodolite, and Standard Shelter for Tem-
perature and Humidity Instruments.

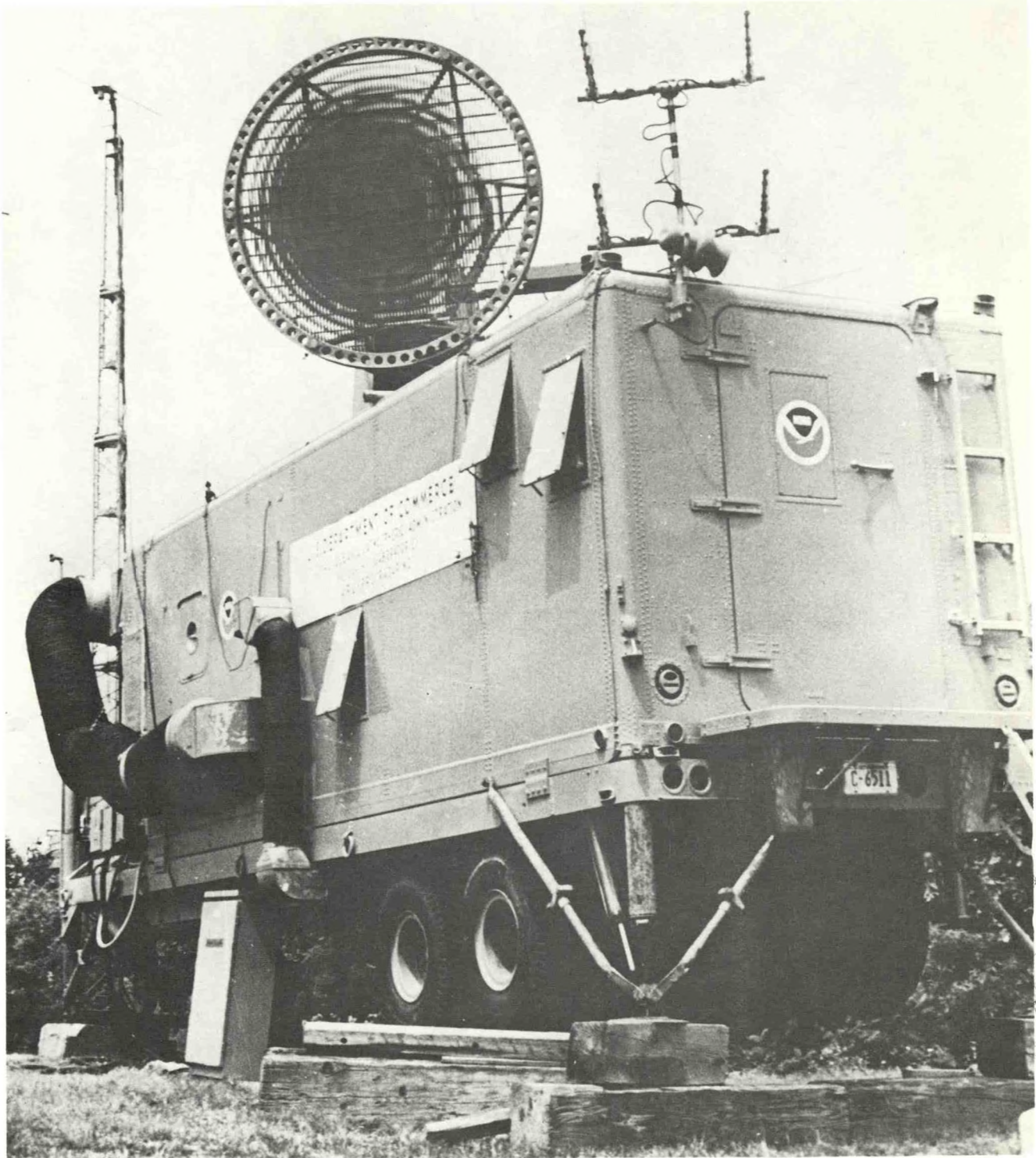


FIGURE 4

M-33 Precision Tracking Radar, Installed on Summit of Buffalo Mt. (750m Above Oak Ridge).

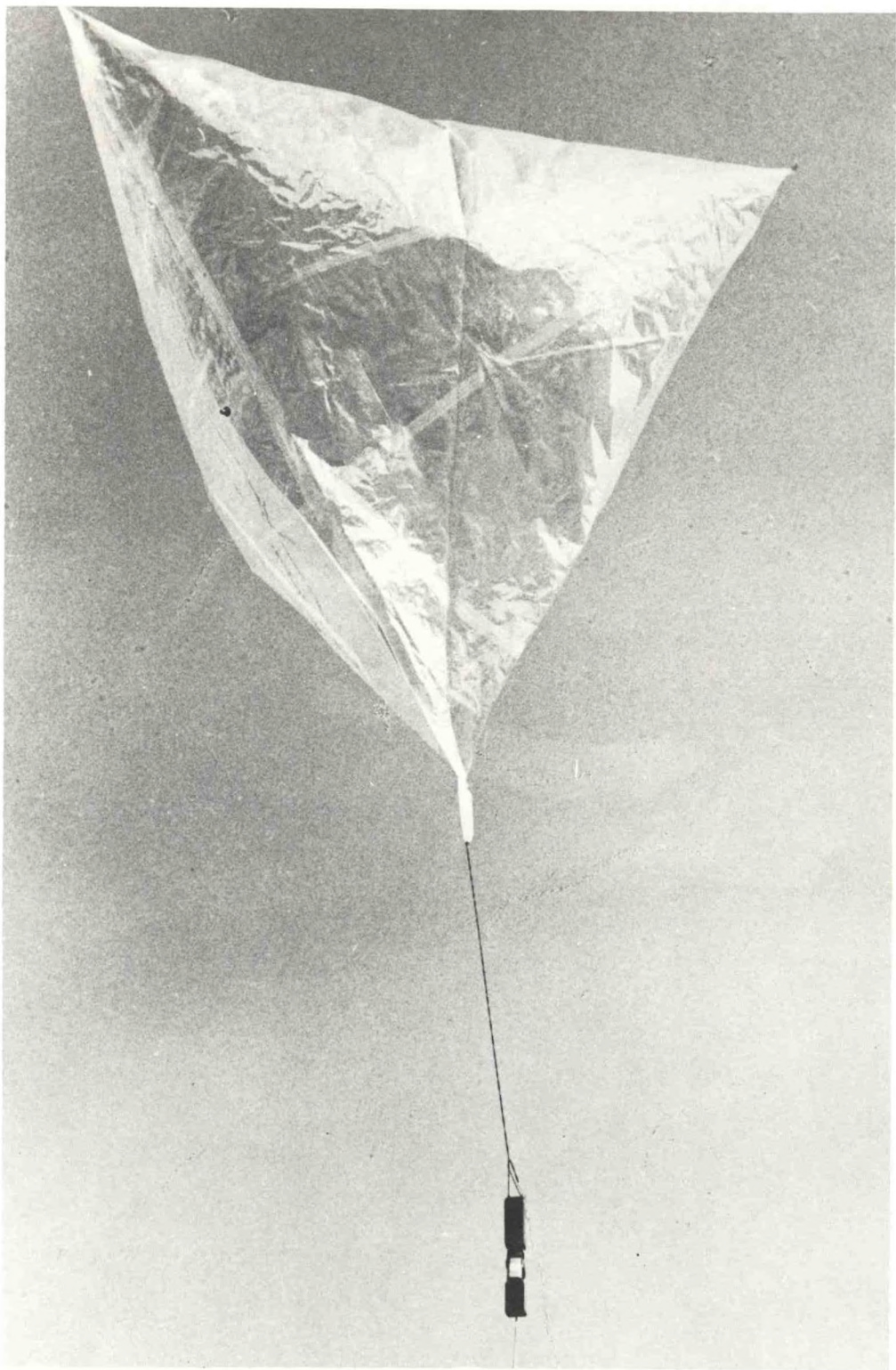


FIGURE 5 Tetroon and 403 MHz Transponder.

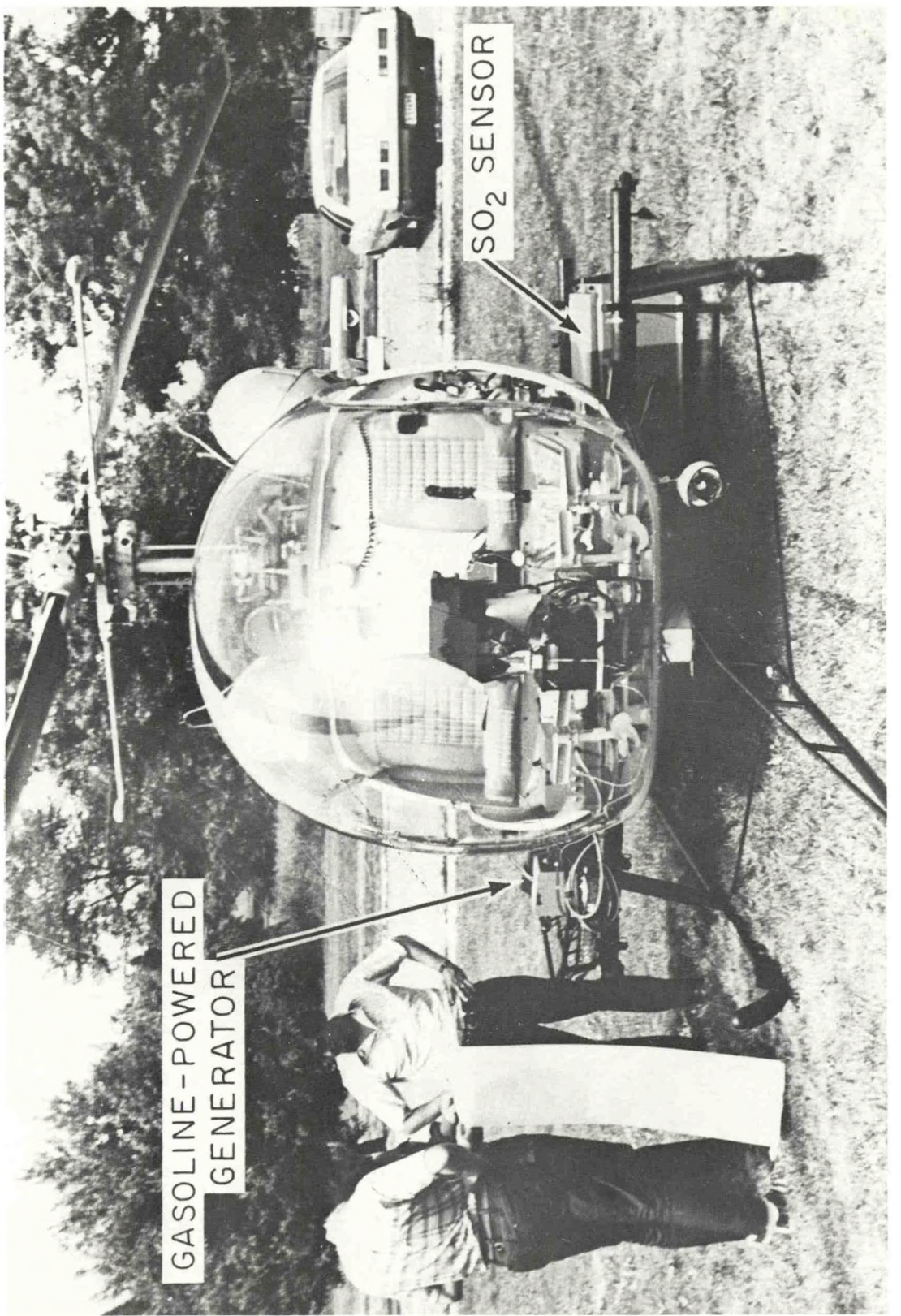


FIGURE D
Helicopter Equipped with SO₂ Sensor and Power Generator.

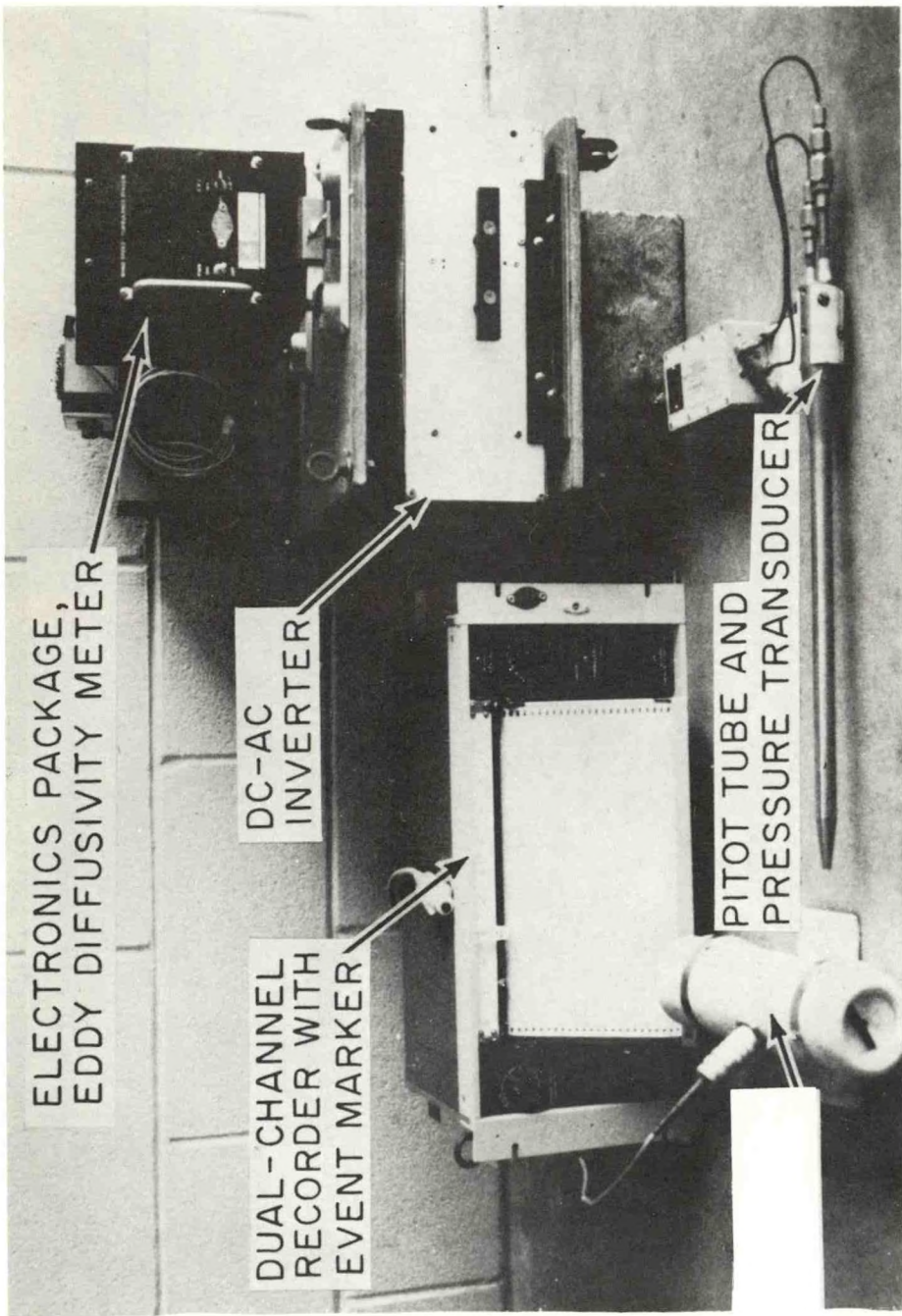


FIGURE 7
Airplane-Borne Instrumentation for Temperature, Airspeed,
Eddy Diffusivity (ϵ), and Altitude (Recorder's Event Marker
is Triggered for Each 200 feet of Altitude Change Indicated
by Airplane's Altimeter). Vertical Accelerometer and
4-Channel Tape Recorder are Not Shown.

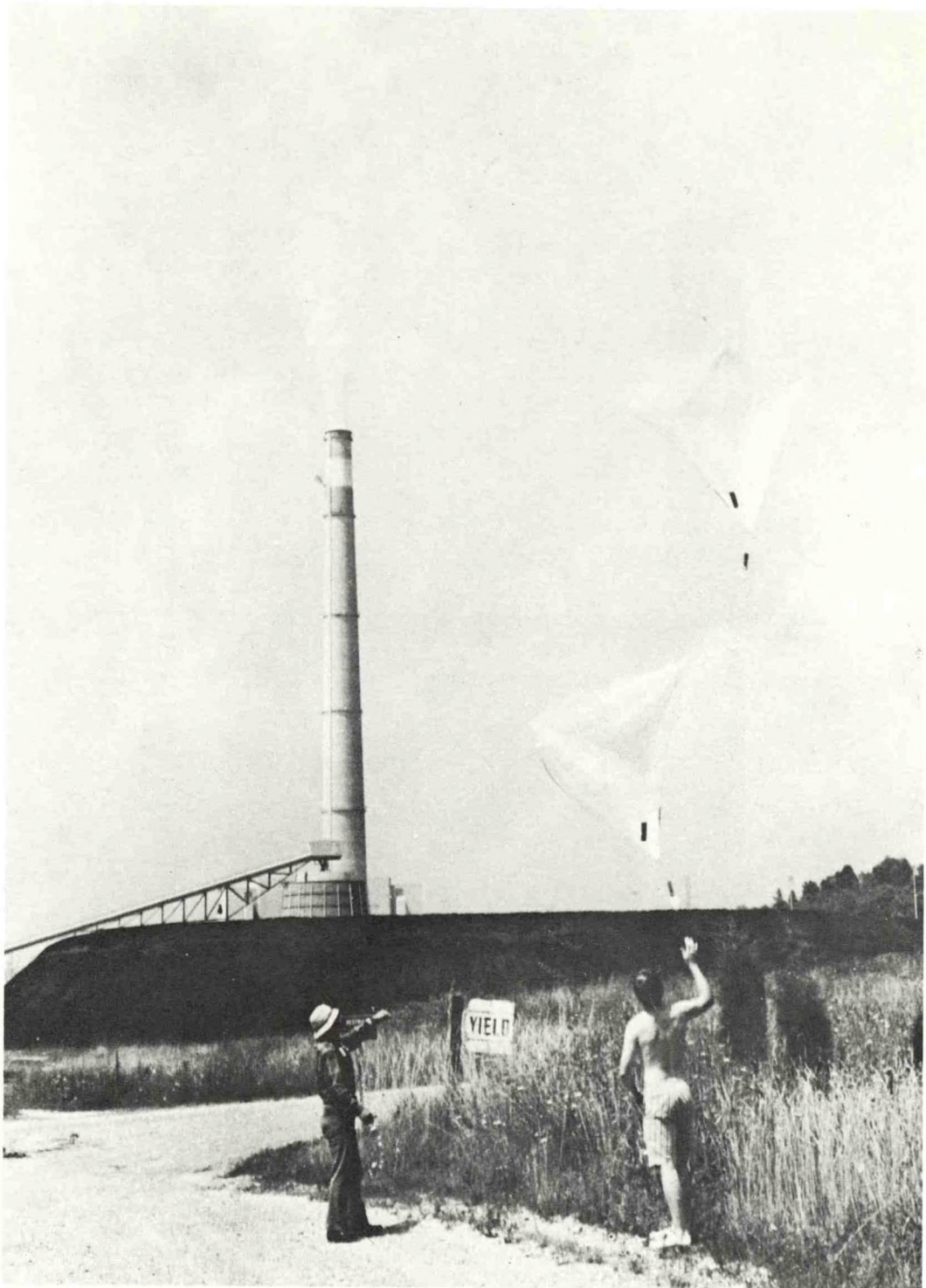
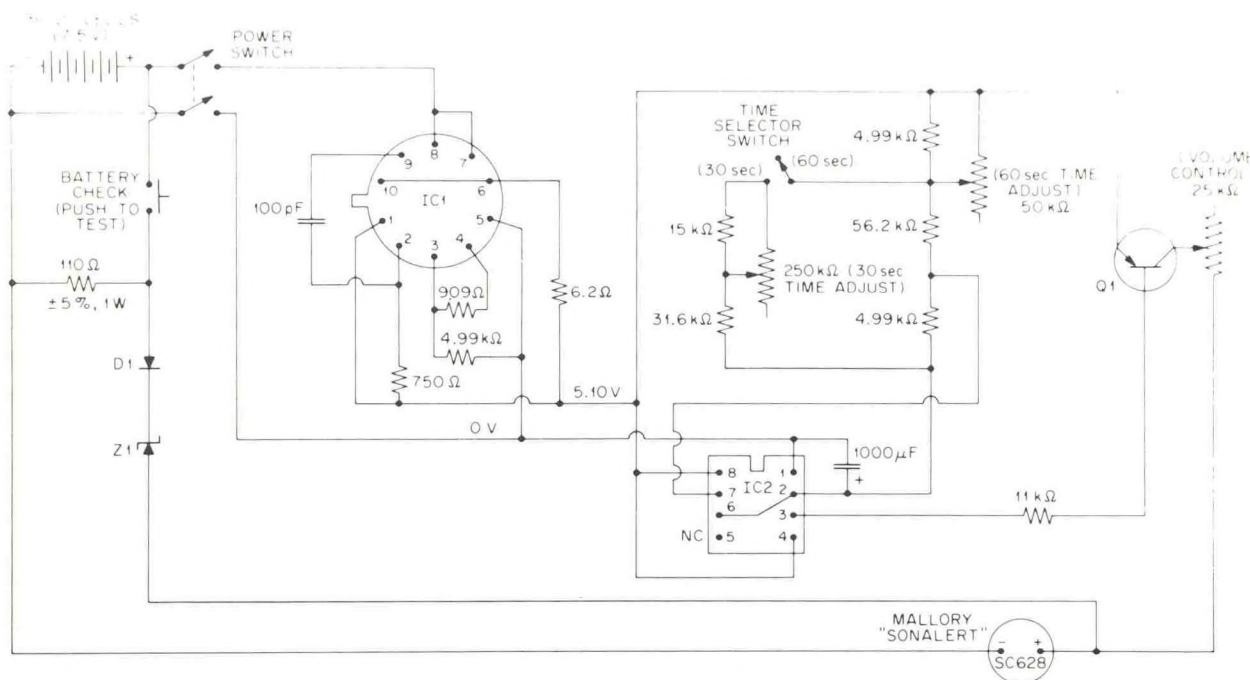


FIGURE 8

Launch of Tetroon Pair Near Steam Plant for Combined Convective-Diffusion and Relative-Diffusion Experiments.



ALL RESISTORS AND POTS ARE WIRE-WOUND OR METAL FILM HIGH-STABILITY TYPES,
1/2 watt MAXIMUM, UNLESS NOTED

IC1- μ A 723C VOLTAGE REGULATOR

IC2-SIGNETICS 555 TIMER

Q1-2N4036

Z1-1N753A, 6.1V ZENER

D1-1N4004

FIGURE 9a SCHEMATIC (DESIGNED BY D.H.TURNER, NOAA, ARATDL, JUNE 1974)

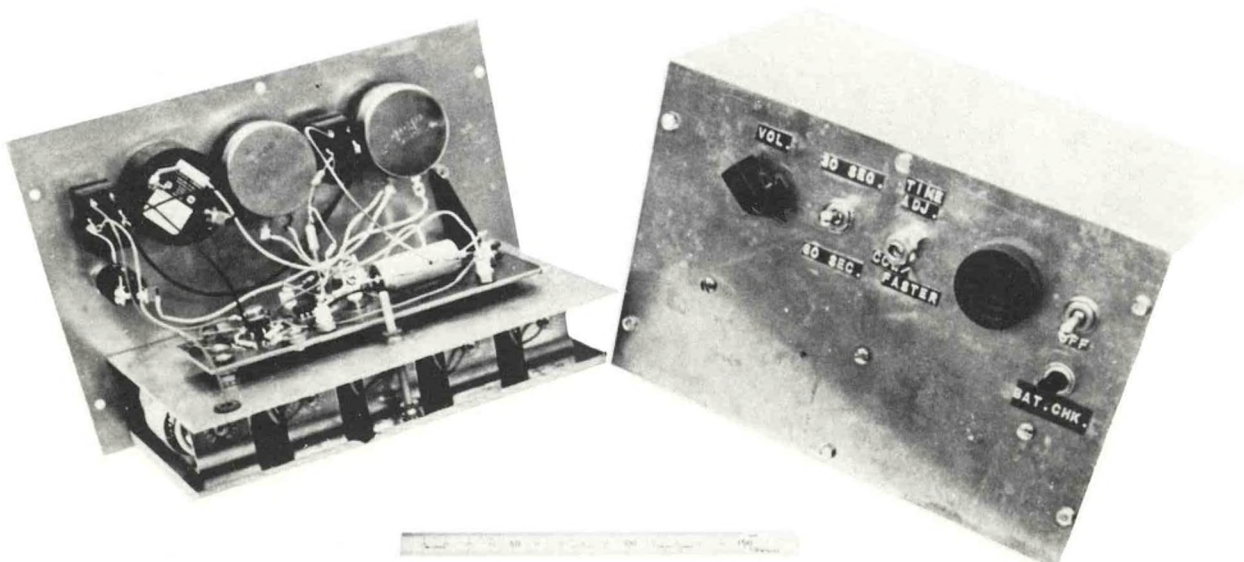


FIGURE 9b

ASSEMBLED TIMERS

Battery-Powered, Variable Time-Interval Pilot Balloon Observation Timer.

AVERAGE AEROSOL SCALE HEIGHTS OVER OAK RIDGE, TENNESSEE

Walter M. Culkowski and Searle D. Swisher
Air Resources
Atmospheric Turbulence and Diffusion Laboratory
National Oceanic and Atmospheric Administration
Oak Ridge, Tennessee, U.S.A.
September 1974

Paper presented at the 1974 International Laser Radar Conference,
6th Conference on Laser Atmospheric Studies, Sendai, Japan, Sept.,
1974.

AVERAGE AEROSOL SCALE HEIGHTS OVER OAK RIDGE, TENNESSEE

Walter M. Culkowski and Searle D. Swisher,
Atmospheric Turbulence and Diffusion Laboratory, NOAA
Oak Ridge, Tennessee, U.S.A.

ABSTRACT

The results of 19 months of routine lidar shots are presented. The aerosol scale height is a function of both time of day and month of the year. Average scale heights correlate well ($r = 0.87$) with average daily solar radiation.

Location and Equipment

Our equipment has been described at these conferences previously (1), (2), so there is no need to dwell on details. Briefly we fire a Holobeam neodymium-type lidar at approximately one to one and one-half joules. The beam is deflected from the horizontal to a vertical mode by a prism, and the return signal is reflected by a conventional plate glass mirror into the usual collector system.

We feel the bulk of the aerosol material we see is of natural, and therefore surface origin. Although the region around Oak Ridge is not exactly rural, with Tennessee Valley Authority steam plants 12 km to the east and 22 km to the southwest, the lidar shows that only occasionally does the plume from one of these plants

make a noticeable trace below the 800 meter level. The city of Oak Ridge heats with electricity or natural gas. As Table I shows, the atmospheric turbidity levels are definitely seasonal and follow the vegetative growth cycle. Turbidity was measured with a sun photometer provided by the Environmental Protection Agency.

TABLE I

Average Turbidity by Months in the Oak Ridge Area. $\lambda = 500 \text{ nm}$

Month	Jan	Feb	Mar	Apr	May	June	July	Aug	Sept	Oct	Nov	Dec
Initial	.059	.071	.092	.130	.144	.193	.291	.413	.279	.203	.069	.049
Final	.054	.070	.094	.129	.162	.203	.305	.393	.280	.174	.076	.046

Table I shows average turbidities, by months, for days when two or more readings were possible. It is evident that the integrated aerosol content, as measured by optical methods, remains constant throughout the day.

Computations

As Table II implies, lidar probes were taken at regular intervals throughout the day, excluding hours with rainfall, low clouds, or anomalous intrusive elements such as a plume from a power plant. The height interval measured at the laser powers we used was from 50 meters to 800 meters, the lower part of the Ekman layer. Probing only the lower part of the troposphere assured

long life to the laser components as a result of operating at only 1/3 of their capability, and avoided the anomalies of cumulus behavior near the lifting condensation level. The lidar return, corrected for absorption, was fitted to the well known exponential distribution.

$$N = N_0 e^{-z/H}$$

where N = number density of aerosols at height z ; N_0 = number of aerosols at the surface. H = scale height.

The correlations of experimental to fitted curves ran generally from above $r = 0.95$ for the morning hours to about $r = 0.80$ for the afternoon hours. Some of the degradation of correlation was undoubtedly due to increased light from the sky inducing noise in the photomultiplier tube.

Results

Average aerosol scale heights for the Oak Ridge, Tennessee, area are listed in Table II. There are several methods of averaging, but we chose the simplest, merely summing the hourly scale heights and dividing by the appropriate number. For those hours in the afternoon where the scale height approached infinity, the average of the finite scale heights was multiplied by the total number of observations and divided by the number of finite observations. This permitted the averages to be affected by the extreme values but more strongly weighted by the finite values.

TABLE II

Average Aerosol Scale Heights in Meters for Oak Ridge, Tennessee.
(November 1973-May 1974)

Month/hr	0730	0900	1030	1200	1330	1500	1600	Notes
Nov 72	510	550	560	770	670	920		1
Dec 72	270	290	410	425	450	570		
Jan 73	320	580	500	520	765	655		
Feb 73	770	1390	915	1550	1810	1245		2
Mar 73	475	540	665	1645	1405	1340		
Apr 73	705	875	1210	1310	1785	1625		
May 73	575	605	1290	2125	1815	2025		
June 73	485	620	675	1255	1950	910	895	
July 73	630	690	1130	1530	1930	1885	1920	
Aug 73	480	620	1130	1935	1785	2120	3135	3
Sept 73	370	440	625	1020	1360	1165	885	
Oct 73	410	595	525	850	1420	1575	1260	
Nov 73	350	605	570	875	1165	1120	910	
Dec 73	575	350	400	525	735	1120	970	
Jan 74	495	480	765	415	990	1540	1475	4
Feb 74	525	440	370	500	1105	1285	1425	
Mar 74	720	555	850	965	1635	1635		
Apr 74	560	490	575	1040	1410	1150	1055	
May 74	715	844	1230	1295	1015	1570	930	

Note 1. Standard time November 72-April 72, November 1973..
All other times daylight saving.

Note 2. February data rejected due to warped mirror.

Note 3. 1600 hours of August considered non-representative with
only 6 observations compared to 18 observations at 1500.

Note 4. January 1974 data rejected, afternoon data appears anomalous.

Dependence of Scale Height on Solar Radiation.

After averaging the highest and lowest heights for each month listed in Table II, and excluding observations mentioned in the notes, the correlation between average scale heights and solar radiation for the 17 remaining months was found to be $r = + 0.87$.

Comparison with other Studies

Those of you familiar with the mixing depth approach to air pollution problems may have noticed a similarity between the maximum and minimum scale heights and the corresponding average mixing depths as computed by Holzworth (3).

Table III shows the similarities in detail.

TABLE III

Mean Morning and Afternoon Mixing Depths Compared with Aerosol Scale Heights (Meters)

	Winter	Spring	Summer	Fall
Morning m.d.	500	550	430	350
Morning s.h.	345	595	530	410
Afternoon m.d.	1100	1800	1800	1500
Afternoon s.h.	1060	1700	2000	1255

The average seasonal scale heights are generally within 10% of the expected mixing depths.

Many such relationships can be expected of course, since the vertical diffusivity, K_z , which is largely a function of solar radiation, controls all vertical distributions in the mixing layer. An excellent illustration of this

is seen in Table IV, a comparison of the average monthly vertical diffusivity above Oak Ridge with the average diffusivity over Paris from the period 1890-1894, derived by G. I. Taylor(4) from temperature measurements by M. Angot at various levels of the Eiffel Tower. Also included in Table IV are the average daily solar radiation values for Oak Ridge. The value of K_z for Oak Ridge was obtained from the steady state equation

$$H = (K_z T)^{1/2}$$

where T = "residence time" of an aerosol. In this case T was taken as 24 hours.

Solar radiation is given in Langleys per day.

TABLE IV

Comparison of Average Monthly Vertical Diffusivities over Oak Ridge, Tennessee (November 1972-May 1974) with Those over Paris, France (1890-1894)

Month	O.R. H	O.R. S.R.	O.R. K_z	Paris K_z
Jan	540	201	3.4	4.3
Feb	660	264	5.0	6.4
Mar	1060	311	12.9	10.5
Apr	1040	425	12.5	10.2
May	1220	465	17.3	12.9
June	1215	515	17.1	18.3
July	1280	482	19.0	16.7
Aug	1300	456	19.6	14.6
Sept	865	371	8.7	8.0
Oct	990	379	11.3	5.9
Nov	735	217	6.3	5.4
Dec	590	137	4.0	6.5

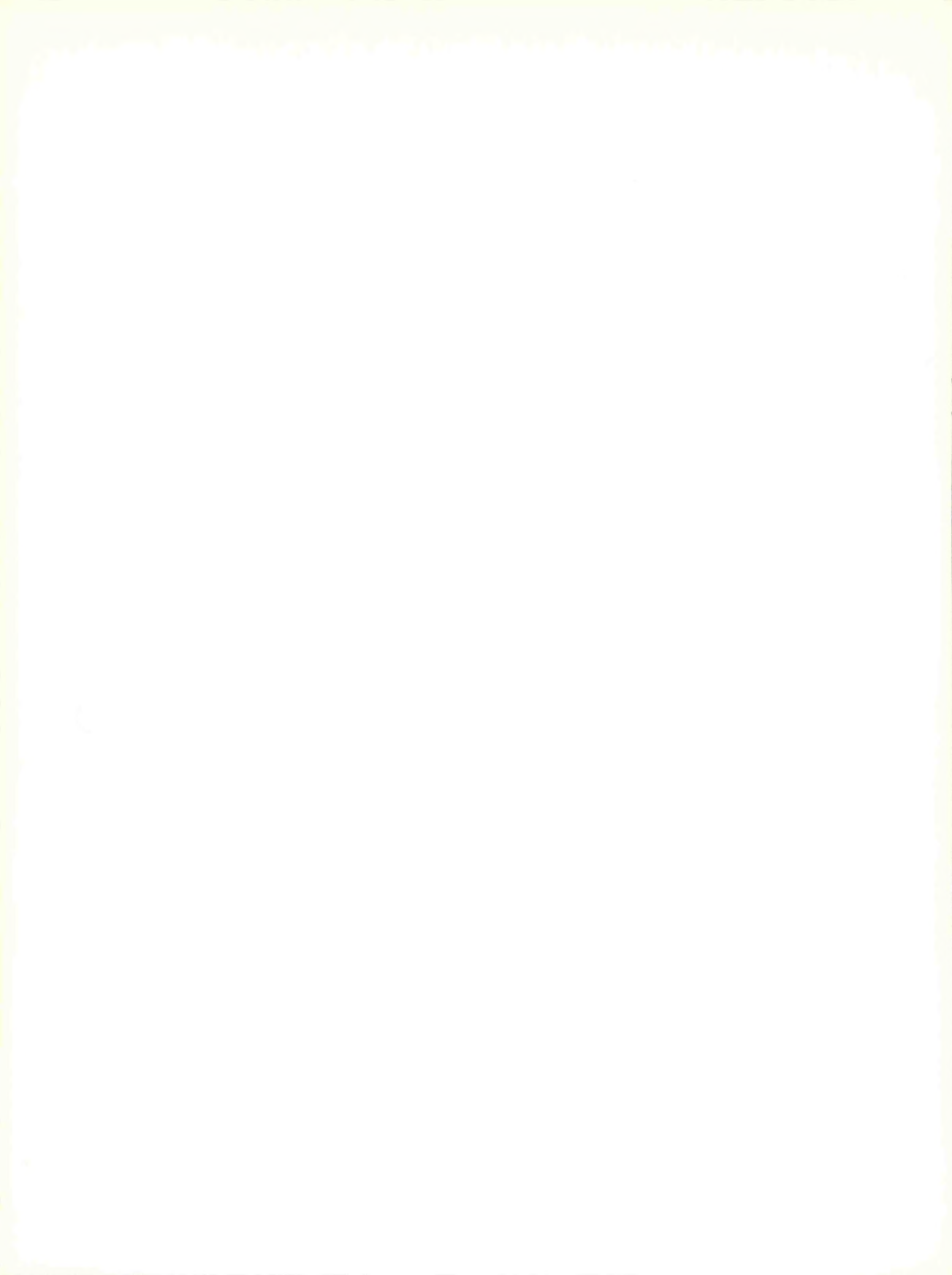
Of course, one need not accept an aerosol residence time of 24 hours; a shorter residence time may be more realistic. But from Table IV one may argue that some constant residence time may be acceptable throughout the year. Since the residence time is not related to turbidity, i.e. particle number density, the role of coaguation, which depends on N^2 , in particle removal cannot be considered a dominant mechanism.

Acknowledgement

This research was performed under an agreement between the U. S. Atomic Energy Commission and the National Oceanic and Atmospheric Administration.

References

1. Second Conference on Lasar Radar Studies of the Atmosphere, April 15-16, 1969, Brookhaven National Lab., L. I., N. Y.
2. Fifth Conference on Lasar Studies of the Atmosphere, June 4-6, 1973, Williamsburg, Va.
3. Holzworth, G. C., 1972, Mixing Heights, Wind speeds, and Potential for Urban Air Pollution Throughout the Contiguous United States. Office of Air Programs Pub. No. AP-101, 118 pages.
4. Taylor, G. I., 1917, Phenomena Connected with Turbulence in the Lower Atmosphere. Proc. of the Royal Society, A, Vol. XCIV, pp 137-55.



Comments on "Study of Atmospheric Transport over Area Sources by an Integral Method," by S. Lebedeff and S. Hameed

F. A. Gifford

Air Resources
Atmospheric Turbulence and Diffusion Laboratory
National Oceanic and Atmospheric Administration
Oak Ridge, Tennessee

December 1974

ATDL Contribution File No. 105
(Withdrawn)

Environmental Research Laboratories

Air Resources

Atmospheric Turbulence and Diffusion Laboratory

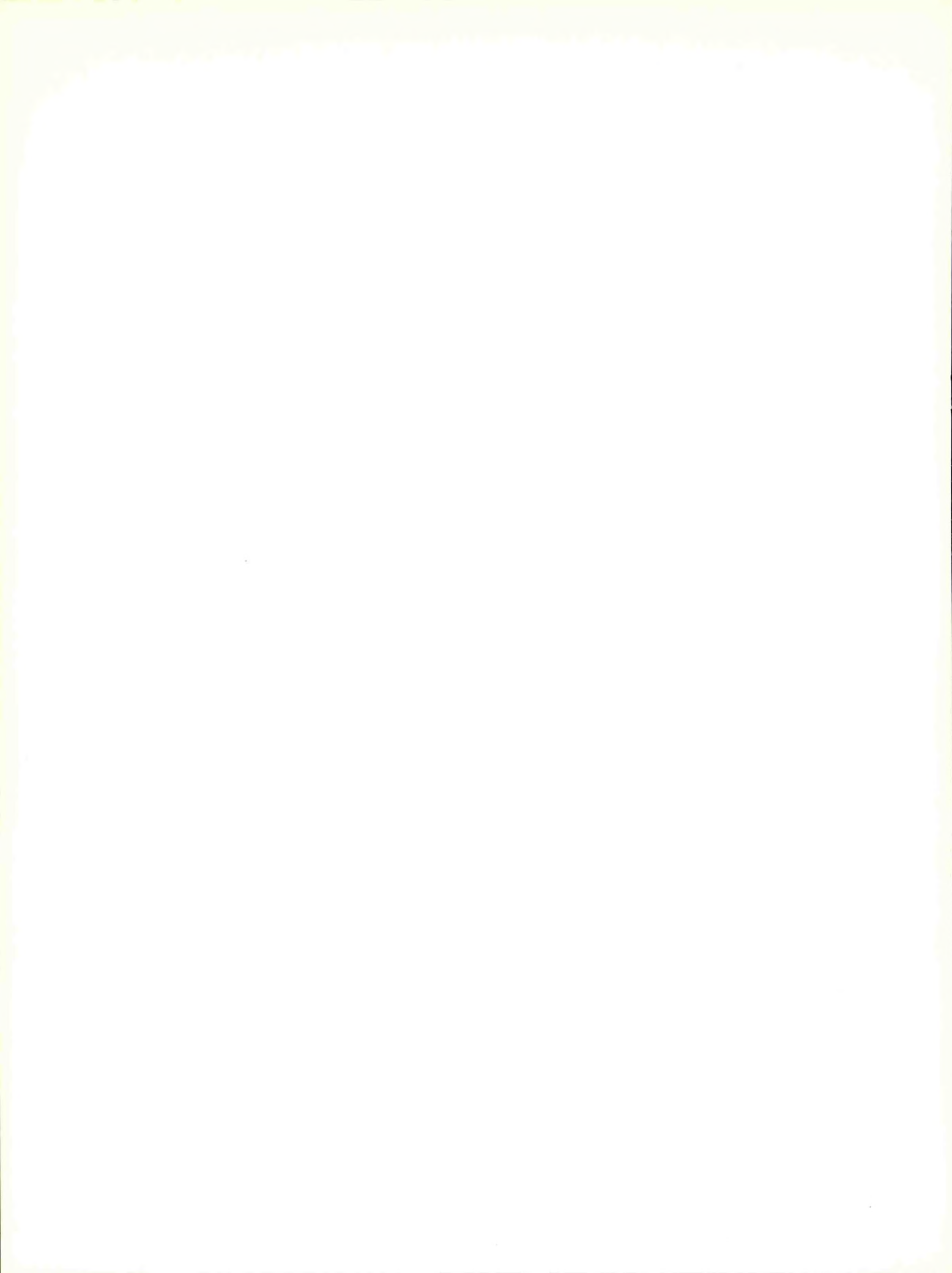
Oak Ridge, Tennessee

December 1974

1973 ANNUAL REPORT

**U. S. DEPARTMENT OF COMMERCE
NATIONAL OCEANIC AND ATMOSPHERIC ADMINISTRATION**

ATDL Contribution File Number 106



EASTERN DECIDUOUS
FOREST BIOME
MEMO REPORT 74-1

Response of Lintronic Dome Solarimeters to Varying
Solar Radiation Flux Densities

D. R. Matt

and

B. A. Hutchison

Air Resources
Atmospheric Turbulence and Diffusion Laboratory
National Oceanic and Atmospheric Administration
Oak Ridge, Tennessee

May 1974

NOTICE: This memo report contains information of a preliminary nature, prepared primarily for internal use in the US-IBP Eastern Deciduous Forest Biome program. This information is not for use prior to publication unless permission is obtained in writing from the authors.

Research supported by the AEC (Division of Biomedical and Environmental Research) and by the Eastern Deciduous Forest Biome, International Biological Program, funded by the National Science Foundation under Interagency Agreement AG-199, 40-193-69 with the U. S. Atomic Energy Commission, Oak Ridge National Laboratory.

(Paper given at Third Joint National Conference on Fire and Forest Meteorology of the American Meteorology Society, Lake Tahoe, California/Nevada, April 2, 1974).

Report printed on recycled paper

Abstract

Solar radiation has been measured in a Liriodendron tulipifera forest for the past year as part of the US-IBP Eastern Deciduous Forest Biome effort at Oak Ridge, Tennessee. During our collection and analysis of these data, the calibration coefficients of Lintronic Dome Solarimeters were compared to a shelf standard Eppley precision pyranometer. Large variation from manufacturer's supplied calibration coefficients was noted at low-intensity radiation levels resulting in non-linear response. This variation is of significance since it is largest precisely in the flux density regime present within fully leafed, mature forests. An empirical relationship for each Lintronic Dome solarimeter was determined to better approximate the calibration coefficients for low-flux density levels.

Introduction

In experimental micrometeorology it is often necessary to measure a variable in several locations at the same time. Research projects are limited in funds so it is often necessary to limit either quantity or quality of equipment. Thus it is of importance that the investigator be aware of instrument limitations when using them in experiments.

Lintronic Dome Solarimeters exhibit non-linearity of response at low-level incident radiant flux density. This non-linearity can be quite consequential in fully leafed, mature forests. In this paper an empirical relationship will be presented that changes the solarimeter's calibration coefficient so that the reduced flux densities more closely approximate values one would obtain from a precision Eppley pyranometer.

Solar radiation has been measured in a Liriodendron tulipifera forest for the last several years as part of the US-IBP Eastern Deciduous Forest Biome effort at Oak Ridge, Tennessee (Hutchison, 1972). The research project consisted in part of measuring the incoming solar short-wave radiation ($.3 \leq \lambda \leq 3\mu$) above, in, and below the forest canopy. The solar radiation flux density was measured using thermopile solarimeters of the type first developed by Monteith (1959) and manufactured by Lintronic Agromet Data System.

According to the manufacturer's specifications, the Lintronic Dome Solarimeter is a multi-junction thermopile bonded to a thin fiber-glass substrate mounted on a circular molded pedestal. The solarimeter measures the incident short-wave solar radiation by producing an emf proportional to the temperature difference between a central black spot and a surrounding white annulus. The thermopile element is protected from the environment by a thin-walled frosted glass dome which also diffuses the incoming radiation.

Monteith-type solarimeters were studied extensively by several investigators including Monteith (1959), Anderson (1967), and Bringman (1968). Anderson and Bringman built their own version of the Monteith solarimeter and, additionally, Anderson compared her versions with the commercially available model built by Lintronic.

Monteith theoretically predicted a temperature coefficient of $-0.12\% ({}^{\circ}\text{C})^{-1}$ and a non-linearity of $-0.8\% \text{ ly/min}$. In her study of the commercial model, Anderson measured a temperature coefficient of $-0.21\% ({}^{\circ}\text{C})^{-1}$ and observed a non-linearity of -35% for incident intensity ranges $\Delta I = 0.1 - 0.2 \text{ ly/min}$. For higher levels of radiation

(i.e., $\Delta I = 0.5 - 0.6 \text{ ly/min}$) the non-linearity was -3%. At low solar angles the Monteith solarimeter output was lower relative to a Moll-Gorczyński solarimeter than when compared to the same instrument at higher solar angles. Anderson also noted variation in response due to azimuthal rotation of the sensor. Investigators using Monteith-type solarimeters should be aware of deviations from normal cosine response as well as differences in linearity of response at low incident flux density levels when using the sensors in the field.

By comparing the output from Lintronic Dome Solarimeters to an Eppley precision pyranometer, we derived curvilinear calibration functions for each of the Lintronic Dome Solarimeters used in our study which serve to minimize the effects of these deviations.

Methods

During the data collection phase of our research program, forty-two Lintronic Dome Solarimeters were used to measure incident radiant flux densities in a tulip poplar (Liriodendron tulipifera) forest having a secondary canopy of red bud (Cercis canadensis) and flowering dogwood (Cornus florida). The sensors were randomly located in horizontal space at three levels within the forest, twelve at the base of the overstory canopy (at about 16 m), fourteen at the base of the secondary canopy (at about 3 m), and fourteen on the forest floor. The flux density of solar radiation incident upon the top of the forest was measured with two solarimeters situated on the top of a walkup tower (33 m). Output signals from all sensors were converted to digital form and recorded on punch paper tape by a Novatronics Model SP 1000 data logging system. All sensors were usually scanned once every ten minutes.

During the calibration phase of our program, the output signals from all the solarimeters were compared to an Eppley precision pyranometer used as a shelf standard. Sensors were mounted on a 1 m x 3 m platform on top of the 33 m walkup tower, and the output of each sensor was scanned sequentially by the data logger. This procedure was continued for several days, obtaining comparisions for various sky cover conditions.

Results

Figure 1 shows the calibration coefficient of one dome solarimeter (sensor M-319) plotted as a function of incident radiant flux density for September 29, 1972. The incident radiant flux density was determined by the shelf standard Eppley precision pyranometer; and the calibration coefficient was determined by assuming that the output of the sensor should indicate the same radiant flux density as the Eppley, that is,

$$E_S = V_S / C_S , \quad (1)$$

where

E_S = flux density measured by sensor,

V_S = output voltage by sensor, and

C_S = calibration coef. of sensor;

and similarly

$$E_E = V_E / C_E , \quad (2)$$

where

E_E = flux density measured by Eppley,

V_E = output voltage by Eppley, and

C_E = calibration coef. of Eppley.

Solving for C_s yields

$$C_s = V_s/E_E \quad (3)$$

From Fig. 1 it can be seen that V_s varies linearly with E_E at the higher flux density values but at lower values this relationship is no longer valid, and as $E_E \rightarrow 0$, since $V_s > 0$, $C_s \rightarrow \infty$. In order to correct for this effect, C_s was plotted as a function of V_s of the solarimeter (Fig. 2). It was then assumed that C_s could be represented in the form

$$C_s = A/V_s + B + C \cdot V_s \quad , \quad (4)$$

where A, B, and C are constants. The A parameter determines the location of the upward bending of the curve, B determines the vertical displacement from zero, and C yields the slope of the asymptote. A least-squares routine was used to fit the parameters to the curve; the solid line represents the best fit for sensor number M-319.

Figure 3 shows the incident radiant flux density as measured by the Eppley as a function of time on September 29, 1972. As can be seen from Fig. 3, the day was partly cloudy with some fog early in the day. Figure 4 again shows the Eppley measurements as well as the flux density determined by M-319 using the factory calibration coefficient.

Substituting Eq. (4) into Eq. (1) and recalculating incident radiant flux density, one obtains the values shown in Fig. 5. The incident radiant flux density determined from the output signal from M-319 now more closely approximates that measured by the precision Eppley. The values very closely approximate one another at the lower flux density values where previously they often differed by as much as 50%. There

is still some difference in readings at noon due to the differences in response time of the instruments. The most significant differences occurred during times of highly fluctuating incident flux densities.

Conclusion

The output from a Lintronic Dome Solarimeter can be corrected to the extent that it approximates the readings from an Eppley pyranometer by assuming the calibration coefficient of the instrument is a function of the flux density. The error introduced by azimuthal asymmetry can be corrected for by this technique by using care in sensor orientation during calibration as well as during data acquisition. The error due to improper cosine response is decreased somewhat, but as yet we are not ready to quantify the amount.

All in all, the small size, weight, and relatively low cost make the Monteith-type solarimeter desirable for use in experimental micrometeorology. The apparent disadvantages of hardware design can be overcome to some extent by software utilization and this appears to be a necessity at the low flux density values observed in fully leafed mature forests.

References

- Anderson, M. C. 1967. The role of heat transfer in the design and performance of solarimeters. J. Appl. Met., 6, 941-947.
- Bringman, M., and N. Rodskjer. 1968. A small thermoelectric pyranometer for measurements of solar radiation in field crops. Arch. Met. Geoph. Biokl., Ser. B, 16, 418-433.
- Hutchison, B. A., and D. R. Matt. 1972. Distribution of solar radiation within a deciduous forest. Eastern Deciduous Forest Biome Memo Rpt. 72-170.
- Monteith, J. L. 1959. Solarimeter for field use. J. Scientific Inst., 36, 341-346.

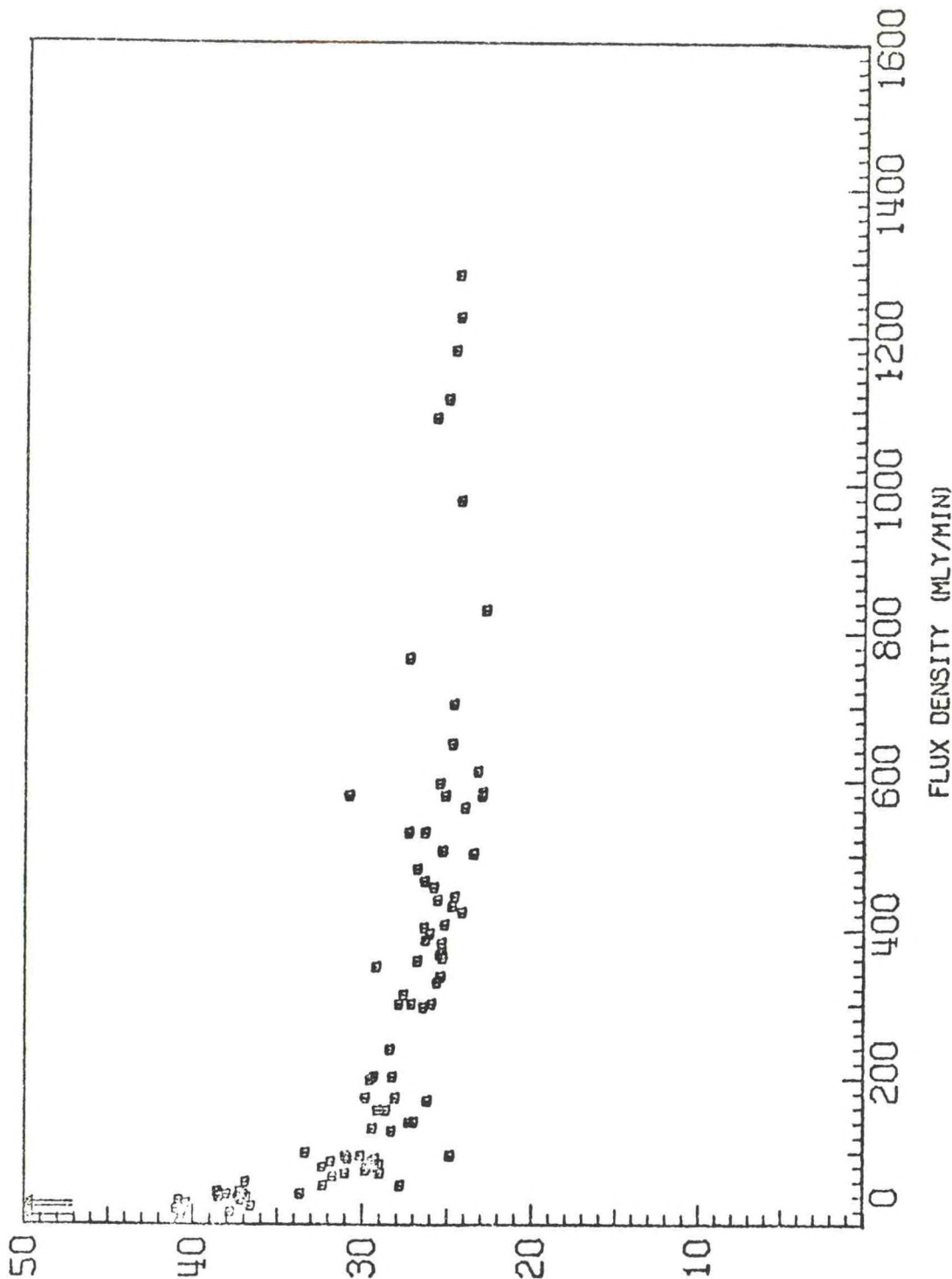
List of Figures

- Figure 1. M-319 Calibration Coefficient. The calibration coefficient for sensor M-319 is shown as a function of incident radiant flux density measured by an Eppley precision pyranometer on September 29, 1972.
- Figure 2. Sensor Calibration Coefficient. The calibration coefficient for sensor M-319 is shown as a function of output voltage from M-319. The solid line represents the least squares fit to the data for the equation
- $$C_s = A/V_s + B + C \cdot V_s .$$
- Figure 3. Incident Flux Density F^n (time). The incident radiant flux density measured by the Eppley pyranometer is shown as a function of time (EST) on September 29, 1972.
- Figure 4. Flux Density Before Correction. The incident radiant flux density measured by M-319 before correction is shown plotted with the value measured by the pyranometer as a function of time for September 29, 1972.
- Figure 5. Flux Density After Correction. The incident radiant flux density as measured by M-319 after correction of calibration coefficient is plotted together with the Eppley pyranometer measurements as of function of time on September 29, 1972.

FIGURE 1

SEPT 29, 1972

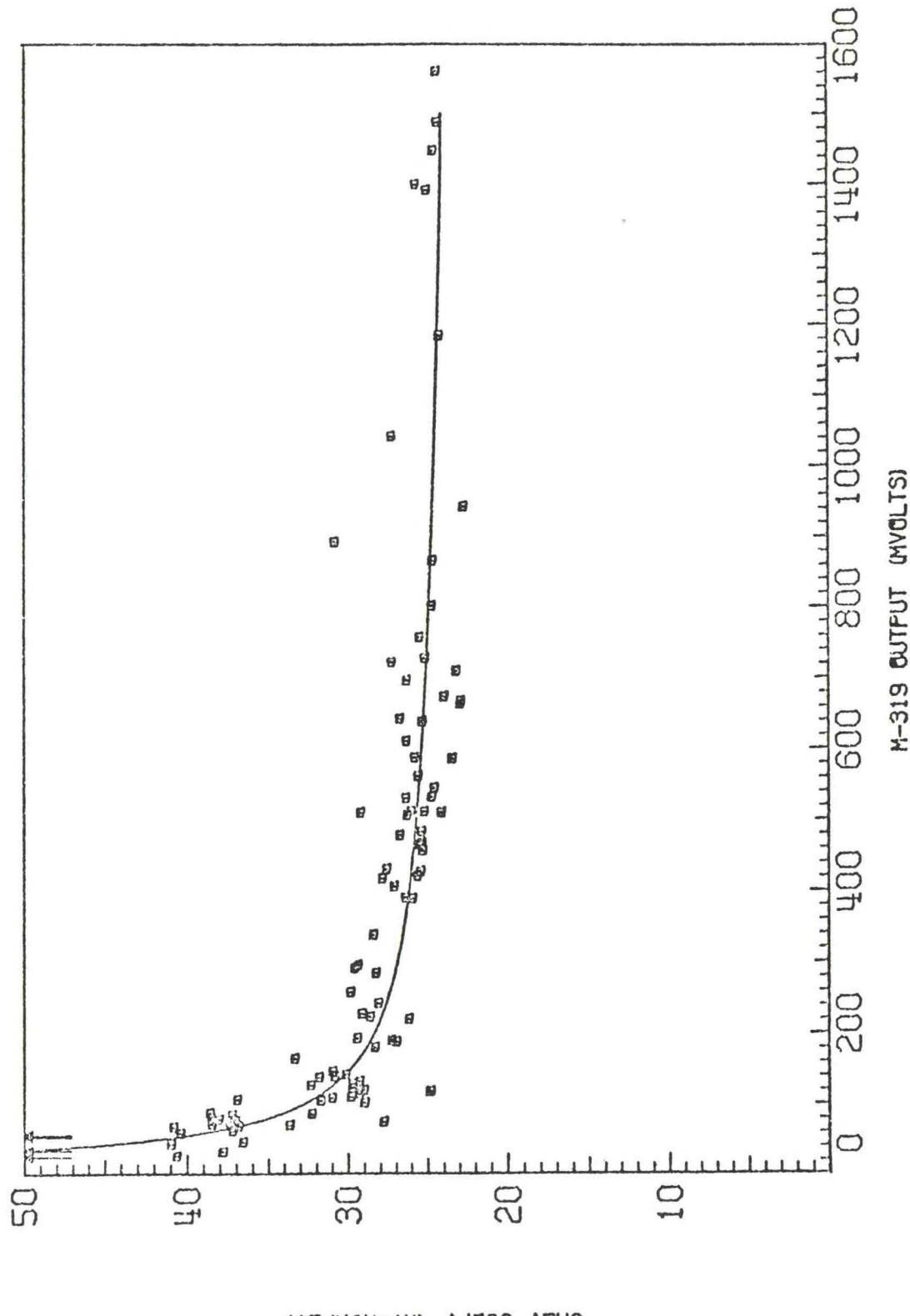
M-319 CALIBRATION COEF.



CAL. COEF. (MV MIN/LY)

FIGURE 2

SEPT 29, 1972
SENSOR CALIBRATION COEF.



CRL, COEF. (MV*MJ/N/LY)

FIGURE 3 SEPT 29, 1972
INCIDENT FLUX DENSITY FN (TIME)

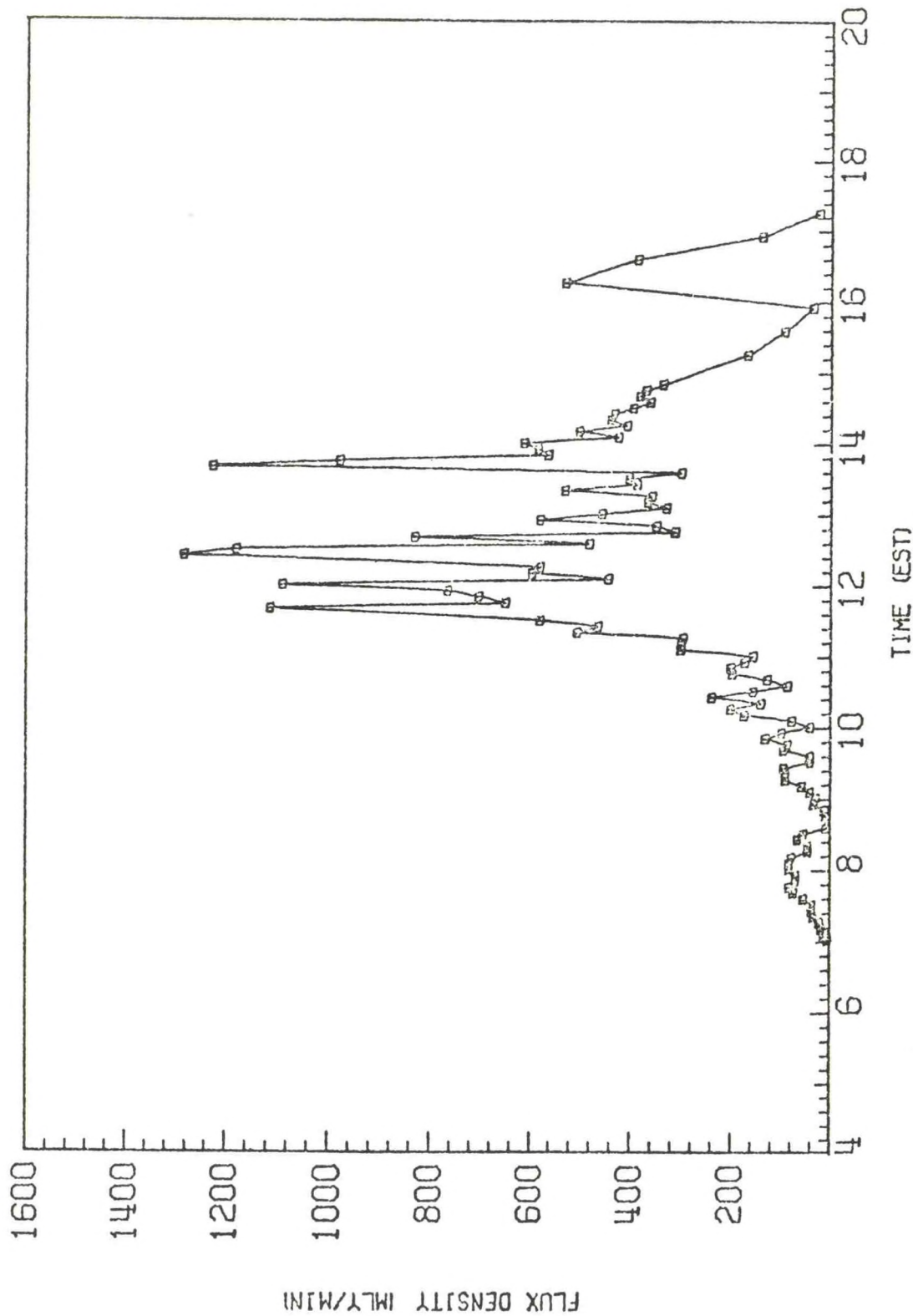


FIGURE 4 SEPT 29, 1972
FLUX DENSITY BEFORE CORRECTION

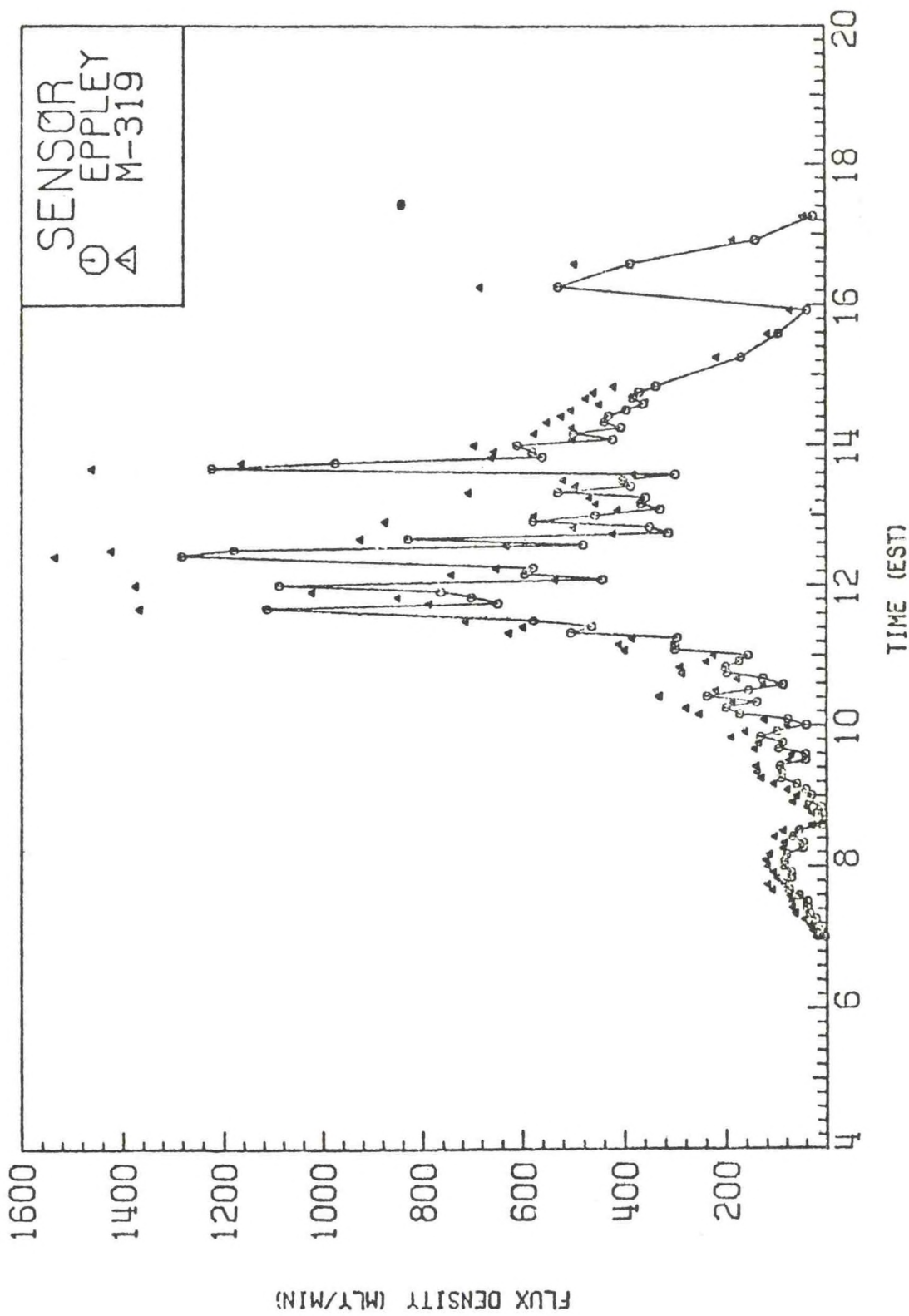


FIGURE 5

